THE UNIVERSITY *of* EDINBURGH

Investigating the role of eEF1A2 in motor neuron degeneration

Lowri Ann Griffiths

A thesis submitted for the degree of Doctor of Philosophy

The University of Edinburgh

2011

I dedicate this thesis to my greatest fan, my Dad.

Gone but never forgotten.

Declaration

I declare that this thesis was composed entirely by myself and that the work presented therein is entirely my own unless clearly indicated. All sources of information and other individuals contributions have been appropriately acknowledged. This work has not been previously submitted for any other degree or professional qualification except as specified.

Lowri Griffiths

Table of Contents

List of figures

List of tables

Acknowledgements

There are just so many people who contributed to this project and to my PhD survival. Firstly a huge thank you to my main supervisor Prof. Cathy Abbott who has always supported me and has been a true provider of guidance and understanding throughout the last 4 years, she is all I could have asked for in a supervisor. I would also like to thank my second supervisor Dr Colin Smith who not only provided access to his clinical samples but also shared his much needed neuropathology expertise. Thank you also to my additional thesis committee members Dr Kathy Evans and Prof. Bob Hill for their intellectual contributions and useful discussions.

I would like to thank all members of the Abbott group both past and present; Julia, Helen, Jennifer, Miriam, Mariam, Justyna & Cheryl for all your help with experiments, in answering my often dim questions and in making working in the lab so much fun. I especially would like to thank Helen for her antibody advice and Jennifer who not only taught me a great deal about cloning and of course the joys of transgenics but also helped hugely in my final months with last minute experiments. To all the students I have helped to supervise: Antonia, Charlotte, Sam, Lucy and James for their experimental contributions to the project. For technical and experimental support I'd like to thank the following; Frances Carnie in Neuropathology, Laura Lettice in the HGU for help with creating the transgenic constructs, Dawn Lister and Helen Caldwell for their histology support, Emma Murdoch for generating the transgenics, Alan Hart for his transgenic expertise, Abraham Acevedo for providing the SOD1 tissue samples and David Brownstein for his pathology services and expertise. A massive thank you goes out to all BRF staff especially to Bill, Davey and Chris for their help and advice over the years. For insightful discussions about mouse behavioural testing and analyses I wish to thank Steve Clapcote.

Thanks to my fellow Wellcome students Cat, Jan, Ekin and Paula, it wouldn't have been the same without you, its been a blast. Thanks especially to Paula for all the fun science communication activities and frequent therapy sessions/pub trips. Thanks also to the Wellcome trust for the funding and also the course organisers here in Edinburgh for giving me this fantastic opportunity.

Surviving a PhD is not only about working hard but also playing hard. To that end I owe a huge thank you to my fellow students Gareth Briggs (for organising weekly pubnights), Rosie Walker, John Logan, Manu Coste, Dave Collins and Miriam Portella for providing much entertainment and distraction from work, I will miss you all. I would also like to thank all PhD students in the MMC and the new friends I have made across the IGMM (especially within the POGS committee) who have made the PhD experience such a great one, and I wish you all the best with your projects. Thanks also to all medgenners who throughout the years have been ever supporting and great fun to work alongside. I'd also like to thank my fantastic friends Nic, Adam, Emma, Haz and Ed for all their help and support over the years.

I wouldn't have got through the last 4 years without the love and support of my amazing family, both old and new. A massive thanks to my parents for always believing in me (even when I didn't believe in myself), for always encouraging me to shoot for the stars and for teaching me that a job worth doing is worth doing well, I hope I've done you proud here. Thanks to my amazing sisters Cari and Eleri, its been a tough few years for us all but together we have supported each other and become far closer as a result, so I thank you for your constant support and comfort through the tough times.

Finally the biggest thanks goes to my amazing husband Chris, who has always been my pillar of hope and understanding. For always forcing me to keep going when I was down and for listening to my endless excited ramblings when things were going well. I never would have survived the last 4 years without your constant love and support.

Abstract

Abnormal expression of the eukaryotic translation elongation factor 1A (eEF1A) has been implicated in disease states such as motor neuron degeneration and cancer. Two variants of eEF1A are found in mammals, named eEF1A1 and eEF1A2. These two variants are encoded by different genes, produce proteins which are 92% identical but have very different patterns of expression. eEF1A1 is almost ubiquitously expressed while eEF1A2 is expressed only in specialised cell types such as motor neurons and muscle.

A spontaneous mutation in eEF1A2 results in the wasted mouse phenotype which shows similar characteristics in the mouse to those seen in human motor neuron degeneration. This mutation has been shown to be a 15.8kb deletion resulting in the complete loss of the promoter region and first non coding exon of eEF1A2 which completely abolishes protein expression.

The main aim of this project was to further investigate the role of eEF1A2 in motor neuron degeneration.

Firstly, although the wasted phenotype is considered to be caused by a recessive mutation, I established a cohort of aged heterozygote mice to evaluate whether any changes are seen later in life that might model late onset motor neuron degeneration. A combination of behavioural tests and pathology was used to compare wild type and heterozygous mice up to 21 months of age. Whilst results indicate that there is no significant difference between ageing heterozygotes and wildtype controls, there is an indication that female heterozygote mice perform slightly worse that wildtype controls on the rotarod (a behavioural test for motor function).

Secondly, I aimed to investigate the primary cause of the wasted pathology by generating transgenic wasted mice expressing neuronal eEF1A2 only. This would complement previous experiments in the lab which studied transgenic wasted mice expressing eEF1A2 in muscle only. Unfortunately the expression of eEF1A2 in the transgenic animals was not neuronal specific. However a transgenic line with

expression of eEF1A2 in neurons and skeletal muscle but not cardiac muscle has been generated which clearly warrants further investigation.

Thirdly, I wished to assess whether eEF1A2 has any role in human motor neuron degeneration. To achieve this, eEF1A2 expression was investigated in spinal cords from human motor neuron disease (MND) patients. Preliminary data suggests that motor neurons from some MND patients express significantly less eEF1A2 than motor neurons of control samples. Further work is required to confirm these findings.

Finally, I investigated the individual roles of eEF1A1 and eEF1A2 in the heat shock response. I used RNAi to ablate each variant separately in cells and subsequently measured the ability of each variant individually to mount a heat shock response. Results indicate a clear role for eEF1A1 but not eEF1A2 in the induction of heat shock. This may explain in part why motor neurons exhibit a poor heat shock response as they express eEF1A2 and not eEF1A1.

These experiments shed light on our understanding of the role of eEF1A2 in motor neuron degeneration and uncover many new avenues of future investigation.

Abbreviations

ALS	Amyotrophic lateral sclerosis
ALS2	Alsin
AMPS	Ammonium persulphate
BHK	Baby hamster kidney
BSA	Bovine serum albumin
cDNA	Complementary DNA
CNS	Central nervous system
CO_2	Carbon dioxide
DAB	Diaminobenzidene
DAPI	4'6-diamidino-2-phenylindole
dATP	Deoxyadenosine triphosphate
dCTP	Deoxycytidine triphosphate
dGTP	Deoxyguanosine triphosphate
dH_2O	Distilled water
DMEM	Dulbecco's modified eagle medium
DMSO	Dimethyl sulphoxide
DNA	Deoxyribonucleic acid
dNTP	Deoxynucleotide triphosphates
dTTP	Deoxythymidine triphosphate
ECL	Enhanced chemiluminesence
EDTA	Ethylenediamenetetraacetic acid
eEF1A	Eukaryotic elongation factor 1A
Eef1a1	Eukaryotic elongation factor 1A1 (mouse gene)

eEF1A1	Eukaryotic elongation factor 1A1 (protein)
Eef1a2	Eukaryotic elongation factor 1A2 (mouse gene)
EEF1A2	Eukaryotic elongation factor 1A2 (human gene)
eEF1A2	Eukaryotic elongation factor 1A2 (protein)
eEF1B	Eukaryotic elongation factor 1B
eEF2	Eukaryotic elongation factor 2
eIF2B	Eukaryotic inititation factor 2B
FALS	Familial amyotrophic lateral sclerosis
FTD	Frontotemporal dementia
FUS	Fused in sarcoma
GAPDH	Glyceraldehyde-3-phosphate dehydrogenase
gDNA	Genomic DNA
GDP	Guanosine diphosphate
GFAP	Glial fibriallary acidic protein
GRP78	Glucose regulated protein 78
GTP	Guanosine triphosphate
H_2O_2	Hydrogen peroxide
HCG	Human chorionic gonadotrophin
HCl	Hydrogen chloride
HeLa	Henrietta Lacks (deceased patient from where they came)
HRP	Horse radish peroxidase
HSA	Human specific actin
HSF1	Heat shock factor 1
HSP	Heat shock protein
HSR	Heat shock RNA

IHC	Immunohistochemistry
kb	kilobase pair
kDa	kilodalton
LB	Luria-Bertani
MND	Motor neuron(e) disease
mRNA	Messenger ribonucleic acid
NaOH	Sodium hydroxide
NBF	Neutral buffered formalin
NCBI	National Centre for Biotechnology Information
NeuN	Neuronal nuclei
NSC	Neuroblastoma spinal cord
NSE	Neuron specific enolase
PBS	Phosphate-buffered saline
PCR	Polymerase chain reaction
RIPA	Radioimmunoprecipitaion assay
RNA	Ribonucleic Acid
RNAi	RNA interference
RPM	Rotations per minute
RPMI	Roswell Park Memorial Institute
RT	Reverse transcriptase
SALS	Sporadic amyotrophic lateral sclerosis
SD	Standard deviation
SDS	Sodium dodecyl sulphate
SEM	Standard error of the mean
siRNA	Small interfering RNA

SMA	Spinal muscular atrophy
SMN	Survival motor neuron
SOD1	Superoxide dismutase
Taq	Thermus Aquaticus
TAE	Tris-Acetate-EDTA
TBE	Tris-Borate-EDTA
TDP-43	Tar DNA binding protein 43
TE	Tris-EDTA
TEMED	N,N,N',N'-tetramethylethylenediamine
Tg	Transgenic/ Transgene
TLS	Translated in liposarcoma
VAPB	VAMP (vesicle-associated membrane protein) – associated protein B
VEGF	Vascular endothelial growth factor
VWM	Vanishing white matter
W/V	Weight/volume
Wr	Wobbler gene
wst	Wasted
WT	Wildtype
ZPR1	Zinc finger protein 1

1. Chapter 1: Introduction

1.1. Eukaryotic Elongation Factor 1A (eEF1A)

1.1.1. Translation

Each stage of protein synthesis is precisely regulated, to produce the correct protein in the correct amounts at the correct time. The translation of mRNA into protein occurs in three main stages: 1. initiation, which involves the correct placement of the RNA within a ribosome, 2. elongation where peptides are sequentially added to a growing peptide chain in accordance with the sequence of codons of the mRNA, 3.termination; denoted by the presence of a stop codon in the mRNA sequence being positioned in the peptidyl (P) site of the ribosome thus resulting in the release of the mRNA from the ribosome. The reactions at all three stages are promoted by protein factors i.e. initiation factors (IFs), elongation factors (EFs) and release factors (RFs).

1.1.2. The elongation factors

There are known to be three main players in the translation elongation process in eukaryotes; eukaryotic elongation factor 1A (eEF1A), eukaryotic elongation factor 1B (eEF1B) and eukaryotic elongation factor 2 (eEF2). The roles of each have been investigated, however eEF1A has been the most heavily studied. Diagramatic representation of the role of eEF1A in translation can be seen in figure 1.1. It is thought that eEF1A is responsible for the recruitment of amino acyl tRNAs to the ribosome acceptor (A) site (Hershey 1991). eEF1A binds guanosine triphosphate (GTP) and in this GTP-bound state, interacts with amino acyl transfer RNA (tRNA) to recruit it to the ribosome A site (Merrick 2000). The interaction between the mRNA codon and anticodon on the tRNA triggers hydrolysis of GTP by the ribosome, resulting in eEF1A bound to guanosine diphosphate (GDP) being released from the ribosome (Pape *et al.,* 1998). eEF1A-GDP is incapable of binding another tRNA molecule and so requires a guanine nucleotide exchange factor, which exchanges GDP for GTP to regenerate the active eEF1A-GTP. This role is undertaken by the elongation factor eEF1B which consists of three subunits: alpha

(α), delta (δ) and gamma (γ) (Le Sourd *et al.,* 2006). eEF1Bα and eEF1Bδ are thought to fulfil the GTP exchange role while eEF1Bγ is usually considered a structural subunit. Following the release of GDP bound eEF1A from the ribosome, eEF2 translocates the peptidyl tRNA from the ribosome A-site to the ribosome P-site by one codon. The GTP-dependent step results in the movement of the ribosome along the mRNA strand. Like eEF1A, eEF2 bound to GDP is released from the ribosome in the inactive state following hydrolysis at the ribosome (Rodnina *et al.,* 1997).

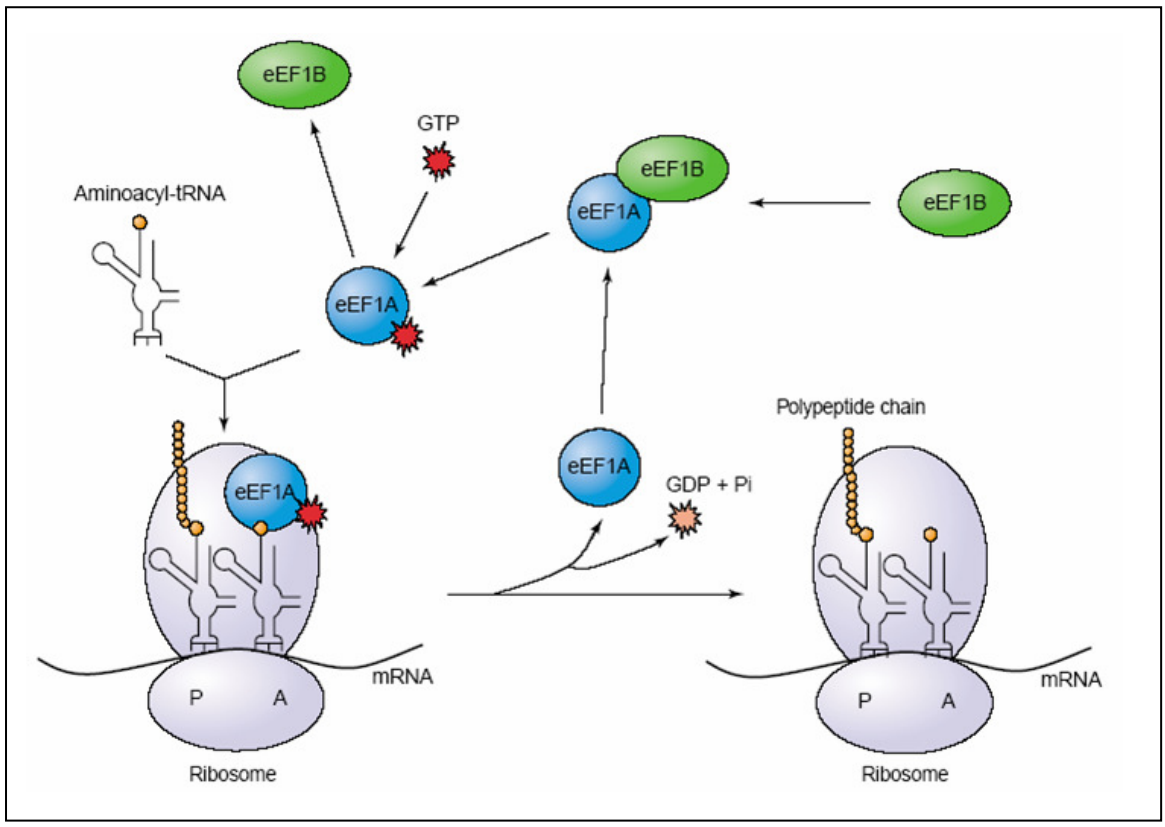

Figure 1.1. Diagramatic representation of the role of eEF1A in translation.

This image is taken from Abbott and Proud 2004 (Abbott and Proud 2004). In brief, eEF1A recruits tRNAs to the ribosome in a GTP dependent reaction. eEF1B acts as the guanine exchange factor recycling inactive GDP bound eEF1A to its active GTP bound state.

1.1.3. eEF1A: a tale of two variants

Eukaryotic elongation factor 1A (eEF1A, previously called eEF-1α) is the second most abundant protein in the cell after actin (Slobin 1980; Derventzi *et al.,* 1993; Condeelis 1995), accounting for 3-5% of the cell's total protein (Lee *et al.,* 1993). The crucial role of this elongation factor is highlighted in yeast, where deletion of eEF1A is thought to be lethal (Cottrelle *et al.,* 1985). It is therefore assumed that a lack of eEF1A would be incompatible with life in higher organisms.

eEF1A exists in two variant forms in mammals named eEF1A1 and eEF1A2 (originally referred to as S1 after its antigenic similarity to statin (Ann *et al.,* 1991)). These variants are encoded by different genes on completely separate chromosomes. In human, *EEF1A1* is found on chromosome 6 at 6p14 while human *EEF1A2* is found on chromosome 20 at 20q13.3. In mouse *Eef1a1* is located on chromosome 9 while *Eef1a2* is located on chromosome 2 (Lund *et al.,* 1996). While multiple pseudogenes exist for *EEF1A1*, *EEF1A2* appears to exist as a single copy (Lund *et al.,* 1996). Both proteins are highly conserved among mammalian species with mouse and human eEF1A2 only differing by 1 amino acid (Lee *et al.,* 1994). eEF1A2 does however appear to be a specific variant in vertebrates as it has been found in all mammals investigated and also in chicken and xenopus but not in Drosophila (Lund *et al.,* 1996).

The separate genes give rise to similar transcript length (1.8-1.9Kb) and encode proteins of the same molecular weight (50KDa) that are 92% identical at the amino acid level and 98% similar (Knudsen *et al.,* 1993). While the amino acid sequences display a large amount of homology, the same cannot be said for the 5' and 3' untranslated regions which only share 20% homology (Ann *et al.,* 1991; Lee *et al.,* 1992). This observation led to the idea that these two genes are differentially regulated which was quickly confirmed by mRNA and protein analysis

At the whole tissue level eEF1A1, which is present throughout development is expressed almost ubiquitously with the exception of adult muscle. eEF1A2 in contrast is developmentally controlled and is expressed only in the brain, spinal cord and in muscle (Lee *et al.,* 1992; Knudsen *et al.,* 1993; Lee *et al.,* 1995). Additionally,

in those tissues where eEF1A2 is expressed, eEF1A1 is downregulated postnatally (Lee *et al.,* 1993; Lee *et al.,* 1995). It has been shown that in skeletal muscle and heart eEF1A1 expression begins to decline around 7 days postnatal until it is undetectable by 21 days. In contrast eEF1A2 expression is minimal at birth but increases steadily until at 21 days it is the sole eEF1A variant detectable in muscle (Chambers *et al.,* 1998; Khalyfa *et al.,* 2001). eEF1A1 levels remain constant throughout development in tissues that don't express eEF1A2 e.g. liver (Lee *et al.,* 1993).

This variant switch can also been seen at the cellular level. In brain tissue a subtle decrease in total eEF1A1 is seen following birth, however expression does not totally disappear (Pan *et al.,* 2004). This is due to the variety of cell types within the brain, as different cells within the central nervous system express different eEF1A variants. Motor neurons and Purkinjie cells for example express eEF1A2 while glial cells express eEF1A1 (Khalyfa *et al.,* 2001; Newbery *et al.,* 2007). eEF1A2 expression in the brain is restricted to mature, terminally differentiated neurons following a switch in eEF1A variants (as seen in muscle and heart) (Pan *et al.,* 2004). Prior to postnatal day 7, eEF1A1 is the primary variant expressed in neurons however by postnatal day 20 eEF1A2 is the primary variant present. eEF1A2 has also more recently been found to be expressed in specific cells within other tissues (where expression at the whole tissue level is not detected by western blot) e.g. ganglion cells in the retina, glucagon expressing cells in the Islets of Langerhaans and enteroendocrine cells in the crypts of the small intestine (Newbery *et al.,* 2007). However, the expression of eEF1A1 has yet to be investigated in these cells thus the effect of the loss of eEF1A2 in these cells cannot yet be determined.

At the cellular level the two eEF1A variants are almost always exclusively expressed. The only occasions when both have been observed within the same cell type is during tumorgenesis and in cultured cells.

1.1.4. Why two variants?

The reason for the existence of two variants and the developmental switch in some cells is as yet undetermined. The only known difference in their roles in translation elongation is that eEF1A2 has a lower GDP disassociation rate than eEF1A1 (Kahns *et al.,* 1998) which may slow translation down, resulting in increased translational fidelity. Yeast-2-hybrid experiments suggest that while eEF1B binds eEF1A1, eEF1A2 has no detectable affinity for eEF1B (Mansilla *et al.,* 2002) and as such eEF1B may not in fact be the guanine exchange factor for eEF1A2. However, to our knowledge, this has not been tested in other experimental systems.

While they have almost indistinguishable roles in elongation, the two isoforms may have varying roles in other cellular mechanisms. The observation that the presence of eEF1A2 in addition to eEF1A1 can transform cells and give rise to tumours supports different functional properties of the two variants (Tomlinson *et al.,* 2005). In addition to its role in translation eEF1A1 has been implicated in numerous other cellular processes such as cytoskeletal rearrangement (Murray *et al.,* 1996), apoptosis (Duttaroy *et al.,* 1998), nuclear transport (Chuang *et al.,* 2005; Khacho *et al.,* 2008), proteasomal-mediated degradation (Chuang *et al.,* 2005) and the heat shock response (Shamovsky *et al.,* 2006). Whether eEF1A2 has a role in any of these processes has yet to be fully established, as many studies don't distinguish between the two variants. This is largely because many commercially available antibodies recognise both variants equally.

The separate roles of eEF1A1 and eEF1A2 in apoptosis however, have been investigated. While eEF1A1 has been shown to be pro-apoptotic in cultured myotubes, eEF1A2 which is shown to be upregulated during differentiation acts in the opposite way by protecting cells from apoptosis (Ruest *et al.,* 2002). Differences in their non-canonical functions may therefore account for the presence of two variant forms.

While brain, heart and muscle are very different tissues with different functions, they all contain cells with similar properties, which may account for the expression of eEF1A2 and not eEF1A1. eEF1A2 mRNA accumulation correlates with the

formation of terminally differentiated (i.e. post mitotic) neurons and myocytes during *in vivo* neurogenesis and myogenesis respectively (Lee *et al.,* 1993). It is therefore believed that eEF1A2 is switched on once cells complete the terminal differentiation process. The requirement for enhanced translational fidelity in these terminally differentiated cells (Lee *et al.,* 1992) may be one reason for the specific expression of eEF1A2 and not eEF1A1. It has also been shown that eEF1A2 is highly expressed in serum starved NIH3T3 cells (which don't normally express eEF1A2), in the G_o stage of the cell cycle but on serum stimulation expression of eEF1A2 declines (Ann *et al.,* 1991). Thus a quiescent state appears also to be a factor for eEF1A2 expression. It should also be noted that muscle cells have been shown to express eEF1A1 following injury and then revert back to eEF1A2 expression once the repair process is complete (Carlson *et al.,* 2002; Khalyfa *et al.,* 2003).

All three tissues (brain, muscle and heart) contain cells which are fully differentiated and non-proliferating, with large cytoplasmic volume and a stable shape. An attractive hypothesis would be that eEF1A2 is required in terminally differentiated, quiescent cells such as myocytes and motor neurons, to undertake its translational role (like eEF1A1) without the additional roles undertaken by eEF1A1 which may be detrimental to such cells such as apoptosis or cytoskeletal rearrangement.

1.1.5. Translation factors in disease

Translation factors have been implicated in a variety of diseases. Mutations in the eukaryotic inititation factor 2B (eIF2B) for example have been found to be a causative in the neurological condition Leukoenphalopathy with vanishing white matter (VWM) (Leegwater *et al.,* 2001). While no mutations of eEF1A1 have been implicated in disease, it is overexpressed in some cancers. eEF1A2 has been shown to be a proto-oncogene with high levels of eEF1A2 protein being observed in approximately 63% of breast tumours (Tomlinson *et al.,* 2005) and 30% of ovarian tumors (Anand *et al.,* 2002), tissues that would otherwise show no expression of eEF1A2. Interestingly while overexpression is linked to tumorgenesis, a deletion of the promoter of eEF1A2 has been shown to cause the wasted phenotype in mice (details below) which are studied as a model of motor neuron degeneration.

Mutations in mitochondrial elongation factors have also been shown to cause disease such as fatal mitochondrial encephalomyopathy (Smeitink *et al.,* 2006). To our knowledge no release factors have been found to have a causative effect in disease.

1.1.6. The wasted mouse

In 1972 the Jackson lab published information on a spontaneous mutation which arose in their HRS/J stock. This mutation was named wasted (*wst*) and was originally thought to be a model for ataxia telangiectasia (Shultz *et al.,* 1982). Further investigation however has led to the belief that it is in fact a more useful model for the early stages of human motor neuron disease (Lutsep and Rodriguez 1989; Newbery *et al.,* 2005).

It has been shown by our lab and others that the mutation is a 15.8kb deletion in the promoter region of the gene for the translation elongation factor eEF1A2 (Chambers *et al.,* 1998). The deletion completely removes the promoter region and the non coding first exon which results in complete loss of eEF1A2 protein. No other gene is present in the deleted region, and transgenic experiments have concluded that the wasted phenotype is caused purely by the loss of the gene encoding eEF1A2 (Newbery *et al.,* 2007).

Mice homozygous for the deletion develop normally until around 21 days of age where they start to show progressive neuromuscular decline, including tremors, un-coordinated gait and severe weight loss (largely attributed to loss of muscle bulk (Newbery *et al.,* 2005)) and usually die by 28 days (Shultz *et al.,* 1982). This timing is thought to be unaffected by genetic background or environmental changes (Abbott *et al.,* 1994). A photo of a wasted mouse can be seen in figure 1.2.

From a neuropathological perspective, motor neurons in the spinal cord of wasted mice show numerous similarities to motor neurons from the early onset stages of human motor neuron disease (often referred to as amyotrophic lateral sclerosis (ALS)) patients. As in ALS, neurons in the spinal cord of wasted mice show signs of vacuolation, which is accompanied by increased gliosis (indicated by an increase in

reactive astrocytes) and neurofilament accumulation in the neuronal cell body. Seventeen day old wasted mice show progressive retraction of neurons from motor endplates at the thoracic level, extending to the lumbrical level by 23 days of age (Newbery *et al.,* 2005). This observation in addition to the weak synaptic transmission at 23 days at the thoracic level and 25 days at the lumbrical level shows that disease progresses along a rostrocaudal gradient in the spinal cord. In addition, a decline in performance on the rotarod is observed from 21 days (Newbery *et al.,* 2005). In contrast to human disease no motor neuron loss was initially observed in wasted mice (Lutsep and Rodriguez 1989), however our lab have demonstrated that vacuolation of motor neurons is common at disease end stage (Newbery *et al.,* 2005). As disease progression in wasted mice occurs over a much shorter period of time to that of human disease, many later pathological findings of human disease may not have manifested in this short time. Wasted mice are therefore a useful model for the early pathological stages of motor neuron degeneration.

Wasted mice also exhibit immunological defects not normally seen in other models of motor neuron degeneration such as atrophy of the spleen, thymus and lymph nodes (Shultz *et al.,* 1982). The spleen to body weight ratio of wasted mice is less than half that of wildtype animals by 28 days (Shultz *et al.,* 1982). No expression of eEF1A2 is observed in either rat or mouse spleen (Lee *et al.,* 1992; Chambers *et al.,* 1998) suggesting that atrophy is likely to be a secondary characteristic of the disease in these animals possibly due to stress.

Symptom onset coincides with the developmental switch in the eEF1A variants. At birth muscle tissue expresses high levels of eEF1A1. This declines over time until eEF1A1 is eventually replaced by eEF1A2 which gradually increases from 7 days postnatal. By approximately 21 days eEF1A2 has taken over from eEF1A1. In wasted mice however eEF1A2 is not expressed. Wasted mice retain the genetic regulation of eEF1A1 and thus once the levels of eEF1A1 have disappeared there is no eEF1A2 to take over, which is presumed to result in no protein synthesis in these tissues, although this hasn't been investigated to our knowledge. This pattern in expression is closely linked to the timing of synaptogenesis in the rat (Aghajanian and Bloom 1967). It was therefore possible that eEF1A2 either has a role in

synaptogenesis or is only required following synaptogenesis. It has recently been shown that eEF1A2 is essential for the prevention of pre-synaptic degeneration (Murray *et al.,* 2008).

Investigation of the wasted mouse has therefore improved our understanding of the biology of eEF1A and also has highlighted important aspects of motor neuron degeneration.

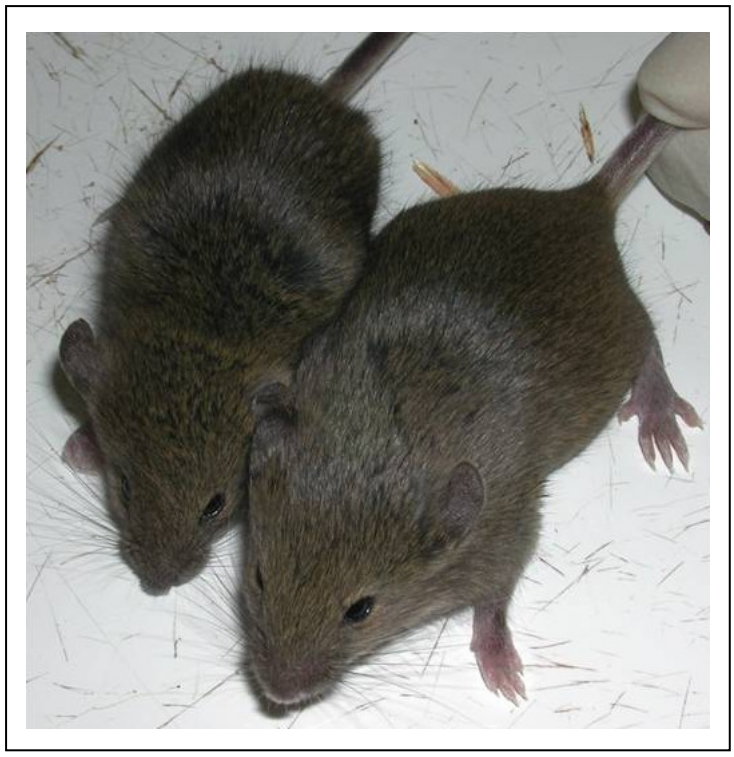

Figure 1.2. Photograph of a wasted (*wst/wst*) and wildtype (+/+) mouse.

A wasted mouse (*wst/wst,* left) with a wildtype littermate control (+/+, right). Photo courtesy of Dr Helen Newbery.

1.1.7. A role for eEF1A in spinal muscular atrophy (SMA)

Spinal Muscular Atrophies (SMA) are characterised by degeneration of lower motor neurons in the anterior horn (Markowitz *et al.,* 2004). Proximal- SMA (usually referred to as SMA) is an autosomal recessive condition, caused by deletion of, or mutations in the *Survival Motor Neuron-1* (*SMN1*) gene on human chromosome 5q13 resulting in low level expression of the full length SMN protein (Lefebvre *et al.,* 1995; Lefebvre *et al.,* 1997). The *SMN1* gene encodes a ubiquitously expressed 38kDa protein with highest levels of expression found in brain, spinal cord and liver (Coovert *et al.,* 1997). While the major cause of SMA is the loss of expression of full length SMN, potential modifiers such as the zinc finger protein ZPR1 may also play an important role in disease.

ZPR1, which is expressed at low levels in SMA patients (Helmken *et al.,* 2003), may affect the severity of the disease. ZPR1 was identified as a zinc finger protein necessary for translocation of SMN to the nucleus (Gangwani *et al.,* 2001). Reduced expression of ZPR1 in mice heterozygous for $ZPR1^{-/+}$ (generated by disrupting one ZPR1 allele) show signs of neurodegeneration including motor neuron degeneration and loss in addition to axonal defects (Doran *et al.,* 2006). Another gene located in the same region as *SMN1* is *SMN2* which expresses a truncated form of SMN protein that does not interact with as many factors as the full length protein including ZPR1 (Gangwani *et al.,* 2001). It is the loss of the full length SMN protein that is the major cause of SMA.

eEF1A has been found in a complex with ZPRI and SMN, however the specific variant involved has yet to be determined. It is thought that the interaction of ZPR1 with eEF1A is essential for cell proliferation (Gangwani *et al.,* 1998). Upon mitogen treatment ZPR1 binds directly to eEF1A (Gangwani *et al.,* 1998) and assembles into multi protein complexes with SMN (Gangwani *et al.,* 2001). It has also been demonstrated that axonal degeneration in wasted mice correlates with a decrease in ZPR1 expression (Murray *et al.,* 2008). Investigating the role of this complex and the interactions between the proteins within it are therefore potentially important for our understanding the role of eEF1A in motor neuron degeneration.

1.2. Motor neuron disease

1.2.1. Introduction

Due to their complex nature, neurodegenerative diseases are often poorly understood. A classic example of this is the motor neuron (or neurone) diseases, the most common of which is amyotrophic lateral sclerosis (ALS) otherwise known as Lou Gehrig's disease (named after a famous baseball player who suffered from the condition). ALS, first described by neurologist Jean-Martin Charcot in 1869, is a highly complex disorder with a variety of symptoms, age of onset and disease progression. The complexity and heterogeneity of ALS has resulted in little progress being made in both understanding the disease and in its prevention and treatment. The primary hallmark of ALS is the selective degeneration of both upper and lower motor neurons, leading to muscle atrophy, weakness and paralysis (Pasinelli and Brown 2006). Respiratory failure is typically the cause of death, which usually occurs within 5 years of symptom onset. The mean age of onset is between 50 and 65 years of age, although juvenile forms are also seen. The incidence of disease is around 1-2 per 100,000 (Boillee *et al.,* 2006; Pasinelli and Brown 2006) and at any given time, approximately 5,000 individuals in the UK and 30,000 in the US are affected by the condition (Bruijn *et al.,* 2004). The cause of most cases of ALS is unknown and no effective treatments are currently available.

1.2.2. Pathology

ALS is a progressive neurodegenerative disease involving mainly motor neurons in the cerebral cortex, brain stem and spinal cord. The common distinguishing feature of ALS is the selective vulnerability of motor neurons, which involves both upper motor neurons (run from the brain to the spinal cord) and lower motor neurons (run from the spinal cord to muscle). In some motor neuron diseases, such as the childhood motor neuron disease spinal musclular atrophy (SMA), only loss of lower motor neurons is observed. In ALS loss of motor neurons is accompanied by reactive gliosis (Nagy *et al.,* 1994; Fujita *et al.,* 1998), neurofilament accumulation (Munoz *et al.,* 1988) in the neuronal cell body and ubiquitinated inclusion within motor neurons

(Leigh *et al.,* 1988; Leigh *et al.,* 1991), features often seen in mouse models of the disease (discussed below).

Understanding the selective vulnerability of motor neurons in these diseases is one of the great challenges facing researchers in neurodegenerative conditions, especially given that many of the genes (described below) involved in ALS are often ubiquitously expressed. Distinguishing features of motor neurons include their large somatic diameter (approx 50-60μm) and very long axonal processes (some up to a meter in length). These features of motor neurons would suggest high energy demand and metabolic rate, which may be a contributing factor to their vulnerability (Shaw and Eggett 2000).

Understanding the reason for the selective vulnerability of motor neurons is key to improving our understanding of the disease and to uncover potential therapeutic interventions.

1.2.3. Genetics

Approximately 10% of ALS cases are inherited (often referred to as FALS (Familial amyotrophic lateral sclerosis)) and the remaining 90% are of unknown cause (often referred to as SALS (Sporadic amyotrophic lateral sclerosis)). In terms of clinical and pathological features FALS and SALS are largely indistinguishable.

Of those cases presenting with FALS, approximately 20% are due to a dominant mutation in the Superoxide dismutase 1 (*SOD1*) gene (Rosen *et al.,* 1993). Until recently much of the research on ALS has focused on understanding the pathology of *SOD1* mutations and developing and analysing transgenic *SOD1* models. *SOD1* mutations may only account for a small proportion (approximately 2%) of all ALS cases, however given the pathological similarities between FALS and SALS it was hypothesised that studying models of FALS may identify pathological mechanisms common to both FALS and SALS. In addition to *SOD1,* family-based linkage studies have identified 12 loci and 8 genes for ALS alone, and three loci for ALS with frontotemporal dementia (FTD, reviewed by Dion *et al* (Dion *et al.,* 2009)). Defects in genes such as angiogenin (Greenway *et al.,* 2006), alsin (Hadano *et al.,* 2001;

Yang *et al.,* 2001) dynactin (Puls *et al.,* 2003), synataxin (Chen *et al.,* 2004) and VAPB (VAMP (vesicle-associated membrane protein) – associated protein B) (Nishimura *et al.,* 2004) have been identified as being causative of various forms of ALS, but for many years investigating the pathology of *SOD1* mutations has dominated the motor neuron disease research field. This all changed in 2006 with the identification of a new candidate gene in ALS: *TDP-43*.

In 2006 the 43kDa Tar (Transactive response) DNA-binding protein TDP-43 was found to be a major constituent of ubiquitinated inclusions in patients with FTD and ALS (Arai *et al.,* 2006; Neumann *et al.,* 2006). Ubiquitination of misfolded proteins, forming aggregates within cells of the central nervous system, is a key hallmark of neurodegenerative disease. TDP-43 is a highly conserved, ubiquitously expressed, predominantly nuclear protein. It is believed to be involved in RNA processing through the repression of transcription and regulation of splicing (Buratti *et al.,* 2001; Buratti *et al.,* 2004; Mercado *et al.,* 2005).

In patients with ALS, TDP-43 is depleted from the nucleus and is instead found redistributed in the cytoplasm of affected cells, where it is sequestered in a phosphorylated form into insoluble aggregates (Neumann *et al.,* 2006). While TDP-43 is predominantly expressed in the nucleus, some shuttling between the nucleus and cytoplasm has been shown (Ayala *et al.,* 2008). Recent evidence suggests that the cytosolic localisation of TDP-43 observed may represent a response to neuronal injury, with nuclear localisation being restored following recovery (Moisse *et al.,* 2009a; Moisse *et al.,* 2009b).

The discovery of TDP-43 in ubiquitinated inclusions has led to the identification of more than 30 dominantly inherited mutations in TDP-43 that so far account for 1-3% of all ALS cases (Reviewed in Lagier-Tourenne and Cleaveland (Lagier-Tourenne and Cleveland 2009)). The identification of mutations in TDP-43 that result in neuronal toxicity supports a pathophysiological role for TDP-43 aggregation in ALS. However, abnormal TDP-43 pathology is not observed in all ALS patients. It appears that FALS associated with mutant *SOD1* do not show abnormal distribution of TDP-43 (Mackenzie *et al.,* 2007). Consistently with this finding, SOD1 transgenic mice also fail to show TDP-43 positive inclusions (Robertson *et al.,* 2007). It is as yet

unclear whether it is the loss of normal function of TDP-43, or gain of a toxic function, that is causative of disease pathology.

The discovery of TDP-43 as a major player in ALS led in quick succession to the identification of another DNA/RNA binding protein implicated in ALS; FUS (fused in sarcoma) or TLS (translocated in liposarcoma) (Kwiatkowski *et al.,* 2009; Vance *et al.,* 2009). Normally expressed in the nucleus, FUS/TLS (like TDP-43) is thought to be involved in the regulation of transcription and RNA splicing (Ou *et al.,* 1995; Yang *et al.,* 1998). Mutations in the gene encoding FUS/TLS results in the mislocalisation of FUS/TLS in the cytoplasm, and as with mislocalisation of TDP-43, FUS/TLS protein is also found to be sequestered into cytoplasmic aggregates (Kwiatkowski *et al.,* 2009; Vance *et al.,* 2009). While the similarities between the abnormal expression of TDP-43 and FUS/TLS are clear, FUS/TLS positive inclusions are in fact negative for TDP-43 (Vance *et al.,* 2009), implying that the FUS/TLS disease pathway may be independent of that of TDP-43.

Together, the discovery of these key factors in neuronal degeneration highlights common pathways in the pathogenesis of ALS, despite the involvement of potentially different genes and proteins. The importance of the role of protein localisation, aggregate formation and RNA processing have become clear not only in ALS but also in other neurodegenerative conditions. The SMN protein, for example, has also been shown to have a role in mRNA splicing (Pellizzoni *et al.,* 1998). The generation of cellular and animal model systems to identify the precise roles of these newly identified players in ALS, will provide further insight into disease progression, and may identify possible pathways for therapeutic intervention in the future.

1.2.4. Models of MND

In additional to the wasted mouse model (described previously in section 1.1.5.1), numerous other models of motor neuron degeneration are under investigation, including both spontaneous models and those generated by genetic manipulation. Investigating multiple models is crucial for understanding common, and often fundamental, disease processes. The oldest spontaneous model is the wobbler (*wr*)

mouse where homozygous expression of the mutant wobbler gene *wr* causes motor neuron death in the cervical section of the spinal cord (Mitsumoto and Bradley 1982). Genetically modified models have been developed for many of the genes implicated in ALS, such as *ALS2* (Cai *et al.,* 2005) and dynactin (Laird *et al.,* 2008). The most heavily studied animal models for ALS are the transgenic superoxide dismutase 1 (SOD1) models. Numerous transgenic *SOD1* models have been generated by the expression of mutant human SOD1. These include the most commonly studied G93A (substitution of glycine at position 93 for an alanine) (Gurney *et al.,* 1994), A4V (Gurney *et al.,* 1994), G37R (Wong *et al.,* 1995) and G85R (Bruijn *et al.,* 1997) mutations. The pathogenesis of each line is subtly different (due to different mutations and the level of mutant SOD1 expression), however common pathological features include vacuolar degeneration of motor neurons, followed by motor neuron loss and gliosis (Dal Canto and Gurney 1995). These pathogical features coincide with hind limb weakness, developing to complete limb paralysis. Pathology in these mice closely mimics human disease.

To date, the majority of ALS research has been focused on the *SOD1* transgenic models, under the assumption that SALS and SOD1-mutant ALS are pathologically similar. However, given the biochemical distinction of mutant SOD1 and non-SOD1 cases, as highlighted by TDP-43, this now needs to be re-addressed. This may explain in part the so far ineffective transfer of therapeutic strategies from ALS mouse models to human disease (Ludolph and Sperfeld 2005; DiBernardo and Cudkowicz 2006). While mutations in *SOD1* and *TDP-43* show similar clinical phenotypes, different pathways may be being disrupted, but with the same conclusion – motor neuron degeneration. Both spontaneous and genetically modified models of neurodegeneration should continue to be fully investigated to attempt to identify the common pathological pathways in human disease. While not all models will be ideal, each may provide new information on common mechanisms that, when disrupted, cause damage to motor neurons. Utilising information from multiple models will therefore improve our overall understanding of motor neuron biology, which is crucial to understanding the pathogenesis of motor neuron disease.

1.2.5. Pathogenesis: A role for RNA processing

Following the identification of *SOD1* as the first familial ALS gene to be identified (Rosen *et al.,* 1993), much research has been dedicated to understanding the disease mechanisms caused by *SOD1* mutations. As a result much of what we know about pathogenesis of ALS has stemmed from research on SOD1 models. Many diverse processes have now been implicated in ALS, and given the highly variable nature of the disease, it is likely that multiple factors and pathways influence disease. Possible pathogenic causes include oxidative stress excitotoxicity, disruption in axonal transport and mitochondrial dysfunction (reviewed in (Bruijn *et al.,* 2004; Boillee *et al.,* 2006; Cozzolino *et al.,* 2008; Tovar *et al.,* 2009)). The identification of disrupted TDP-43 and FUS/TLS expression in ALS has now highlighted the important role of disrupted RNA processing in ALS. Investigations have shown that many of the genes so far implicated in ALS appear to have some role in one or more stages of RNA processing, including splicing (TDP-43 (Buratti *et al.,* 2001; Mercado *et al.,* 2005) and FUS/TLS (Yang *et al.,* 1998)), RNA transport and stability (*TDP-43* (Strong *et al.,* 2007), *FUS/TLS* (Zinszner *et al.,* 1997), *SOD1 (Lu et al., 2007; Li et al., 2009)*) and both transcription (*FUS/TLS* (Wang *et al.,* 2008b), *ANG* (Xu *et al.,* 2002), *TDP-43* (Ou *et al.,* 1995)) and translation (*ANG (Saxena et al., 1992)* , *TDP-43(Wang et al., 2008a)*). It is possible that the vulnerability of motor neurons is therefore partly due to susceptibility to RNA processing defects as the central nervous system (CNS) is thought to contain more alternatively spliced variants than other tissues (Yeo *et al.,* 2004).

1.2.6. Heat Shock in motor neuron degeneration

The heat shock response is simply a defence mechanism adopted by cells in response to a wide variety of cellular insults. Stress stimuli such as significant temperature changes or infection result in varying degrees of protein misfolding. The cells respond to these stresses by upregulating molecular chaperones known as heat shock proteins (HSPs) or stress proteins to try and reduce toxicity. These HSPs act as molecular chaperones and are responsible for the refolding of damaged proteins or the targeting of severely damaged proteins for degradation (Reviewed by Muchowski

and Wacker 2005 (Muchowski and Wacker 2005). The HSP family is a large collection of chaperones, some of which are constitutively expressed while others are inducible and thus only detectable following stress. HSPs are simply named, based on their mass in kilodaltons (KDa) e.g. HSP70 is 70kDa, and have been classified into 6 main families HSP100, HSP90, HSP70, HSP60, HSP40 and the small HSPs e.g, HSP27.

The reason for the selective vulnerability of motor neurons to stress is one of the great unanswered questions in neurodegenerative disease research. One possible cause of their vulnerability could be that motor neurons have a high threshold for induction of the heat shock response (Batulan *et al.,* 2003). The exposure of primary spinal cord cultures to heat shock, glutamate excitotoxicity or expression of mutant SOD1 does not result in the upregulation of HSP70. Other neuronal cells such as cortical neurons and astrocytes however do upregulate HSP70 in response to stress (Lowenstein *et al.,* 1991; Bechtold *et al.,* 2000; Batulan *et al.,* 2003). The impaired ability of motor neurons to activate HSPs may lead to an increase in misfolded protein. Terminally differentiated neurons are particularly vulnerable to accumulation of misfolded proteins as they are unable to dilute the toxic effect by cell division. Therefore the disruption of the stress response pathway may lead to aggregation of misfolded proteins within cells, a hallmark of some neurodegenerative diseases including intracellular neurofibrillary tangles in Alzheimers (Selkoe 2001), intracellular α-synuclein positive Lewy bodies in Parkinson's disease (Spillantini *et al.,* 1997), and TDP-43 positive inclusion in FTD and ALS (Neumann *et al.,* 2006).

The accumulation of HSPs, such as HSC70, in mutant SOD1 inclusions in ALS and in transgenic models has been demonstrated and is thought to contribute to disease (Watanabe *et al.,* 2001). Mutations in HSPs have also been implicated in neurodegenerative disease e.g. a mutations in the gene encoding HSP27 have been shown to cause Charcot-Marie-Tooth (CMT) (Evgrafov *et al.,* 2004) and distal motor neuropathy (Irobi *et al.,* 2004).

Research into HSPs could therefore increase our understanding of the role of misfolded proteins in neurodegenerative disease and also may prove a valuable resource for therapeutic intervention.

1.3. Project aims

The main aim of this project was to increase our understanding of the role of eEF1A, particularly the muscle and motor neuron specific variant eEF1A2, in motor neuron degeneration. To achieve this, four separate avenues of research were conducted. Firstly, to investigate whether there is a gene dosage effect of eEF1A2, an ageing cohort of wasted heterozygotes (*+/wst*) were examined for signs of motor neuron degeneration. Secondly, to further investigate the primary cause of the pathology observed in wasted mice, transgenic animals expressing eEF1A2 under the control of tissue specific promoters were generated and studied. Thirdly, to observe whether eEF1A2 has a role in human motor neuron disease, eEF1A2 expression in spinal cords of patients with motor neuron disease were compared to spinal cords from control patients. Finally the role of eEF1A1 and eEF1A2 in the heat shock response was investigated to address whether they have similar or different roles in the heat shock response, which could potentially identify an important functional difference between the two variants. Together these projects will improve our understanding of the role of eEF1A2 in motor neuron degeneration.

Recent studies have shifted the research of neurodegenerative disease toward factors involved in RNA processing, where eEF1A2 clearly has a role. Its function in translation combined with its role in the pathology of a mouse model for motor neuron disease, makes it an ideal candidate for further investigation. Understanding the biology of eEF1A and the pathogenesis of the wasted mouse will thus improve our understanding of motor neuron degeneration.

2. Chapter 2: Materials and Methods

2.1. Materials

Unless otherwise stated, all general laboratory chemicals were obtained from Sigma-Aldrich Ltd or Fisher Scientific Ltd. All polymerase chain reaction (PCR) primers were ordered from Sigma-Aldrich and all cell culture reagents were obtained from Invitrogen. Unless otherwise stated all dilutions were performed using distilled water (dH_2O). Recipes for buffers and solutions can be found in table 2.1.

25% AMPS	Working stock: 25g of Ammonium Persulphate (AMPS) was dissolved in 100mls of dH_2O. Stored at 4^oC.
5.5M Betaine	Working stock: 7.43g dissolved in 10mls dH_20. Stored at -20^oC
Cell freezing media	90% FBS (v/v) and 10% DMSO (v/v), made fresh immediately before use.
Citric Acid	Working solution: 2.1g of citric acid dissolved in 1L dH_2O. pH to 6.0.
Deoxyribonucleoside triphosphates (dNTPs)	Working mix: was prepared by diluting dATP, dCTP,dGTP, dTTPs in equal measure to 2.5mM in dH_2O.
10x DNA sample loading buffer	Glycerol (Invitrogen) was diluted to 30% (v/v) in dH_2O. 100mg of Orange g powder was added per 50ml of 30% glycerol.
EDTA 0.5M	186.1g Ethylenediaminetetraacetic acid (BDH laboratories) diluted in 1L of dH_2O (pH8.0)
Lithium Carbonate	5g of lithium carbonate dissolved in 1L of dH_2O.
LB (Luria-Bertani) medium	1.0% (w/v) Tryptone, 0.5%(w/v) Yeast Extract, 1.0% (w/v) NaCl dissolved in dH_2O (pH 7.0). Autoclaved and stored at 4^oC.
LB (Luria-Bertani) agar plates	LB was prepared as above but 15g/L of agar was added before autoclaving and subsequent storage at 4^oC.
Microinjection Buffer	10mM Tris (pH8) and 0.1mM EDTA. Buffer was filter sterilised before use.

4% Neutral Buffered Formalin (NBF)	For 1 litre of NBF: 108ml 37% formaldehyde diluted in 892ml of dH_2O. 4g of monobasic sodium phosphate (NaH_2PO_4) and 6.5g disodium hydrogen phosphate (Na_2HPO_4) was then added.
Peroxidase blocking solution	2ml 30% H_2O_2, 10% sodium azide, up to 400ml dH_2O.
Phosphate Buffered Saline (PBS)	1 Phosphate Buffered Saline (PBS) tablet was dissolved in 100mls of distilled water and autoclaved.
Radioimmunoprecipitaion assay (RIPA) Buffer	150mM NaCl, 1% (v/v) NP-40, 0.5% (w/v) sodium deoxycholate, 0.1% SDS (v/v), 50mM Tris-HCL in dH_2O (pH8.0) 1 tablet of complete protease inhibitors (Roche) per 10ml aliquot. Store at -20^oC.
0.32M Sucrose	10.9g in 100mls dH_2O. Separated into 10ml aliquots and stored at -20^oC.
50x TAE (Tris-Acetate-EDTA) buffer	242g Tris, 57.1ml glacial acetic acid, 37.22g EDTA in 1L dH_2O (pH8.0)
10x TBE (Tris-Borate-EDTA) buffer	108g Tris, 55g Boric acid and 9.3g of EDTA in 1L of dH_2O (pH8.0).
Tris-EDTA (TE)	10mM Tris-HCl, 1mM EDTA dissolved in dH_2O (pH8.0).
0.5M Tris-HCl	3g Tris-HCl, 50ml dH_2O (pH 6.8). Stored at 4^oC.
1.5M Tris-HCl	9g Tris-HCl, 50ml dH_2O, (pH 8.8). Stored at 4^oC.
Western Blocking Buffer	5% (w/v) marvel milk powder, 0.2% (v/v) Tween 20 in PBS.
Western Running buffer	10x tris-glycine-SDS buffer (Bio-Rad) diluted 1:10 in dH_2O.
Western Transfer buffer	10x stock: 30g Tris-HCl, 144g Glycine dissolved in 1L dH_2O. Working stock: 100mls 10x stock, 200mls Methanol, up to 1L dH_2O.

Table 2.1. Buffer and solution recipes

2.2. Animal work

2.2.1. Wasted mice

Mice were housed in the Biomedical Research Facility (BRF) at the University of Edinburgh. All mice were maintained in accordance with Home office regulations. They were exposed to 12 hour light/12 hour dark cycles with *ad libitum* access to food and water. Their diet consisted of a standard chow diet. Wasted mice are on a mixed although predominantly C3H/HeH and C57BL/6J background.

2.2.2. Generating transgenic mice

Transgenic mice were generated by Emma Murdoch in the Transgenic unit at the MRC Genetics Unit, Edinburgh. In brief 4-5 week old female B6CBAF1/J mice were superovulated by injection of 5iu (international units) of Pregnant Mare Serum (PMS) between 12-2pm, 2 days prior to mating. This was followed by a further injection of 2.5iu of human chorionic gonadotrophin (HCG) 48 hours later. Following HCG injection the females were placed with B6CBAF1/J stud males for mating. The following morning, successful mating was confirmed by the presence of a vaginal plug and the female mice were sacrificed. The 0.5dpc (day post coitum) fertilised embryos were flushed from the oviducts into a 37^{o}C FHM (Hepes Medium). The DNA construct (2ng/μl) was then microinjected into a pronucleus (usually the male pronucleus) of the embryos until they swelled. Injected embryos were cultured overnight in equilibrated KSOM (Potassium Simple Optomized Medium) at 37^{o}C, 5% CO_2. Healthy 2 cell stage embryos were then selected for implantation and implanted into the oviduct of 0.5dpc pseudo-pregnant (by mating with vasectomised males) CD1 recipient females of around 6 weeks of age (23-30g of weight).

2.2.3. Rotarod testing

The Rotarod (Bioseb) is a rotating wheel where the time taken for a mouse to fall from the wheel is recorded. The time to fall is sensed by magnetic switches and recorded immediately on impact by the machine and shown on the display. There are

two options with the rotarod; constant speed and acceleration. To achieve constant speed the switch is set to "Run" and the speed adjusted to the appropriate speed using the speed dial. The rotarod will begin to turn immediately following the switch to "run". This rotarod can achieve between 4-40rpm. If acceleration is required: the switch on the left must first be switched to accelerate (at which point the spindle will begin to turn at 4rpm), then the time over which the rotarod is required to reach a maximum speed is set using the speed dial (in this study, tests were undertaken at an acceleration of 4-40rpm over 5 minutes). To begin acceleration the start button was pressed. The rotarod has 5 separate compartments thus 5 mice can be tested at the same time. For training the rotarod was set at a constant speed of 4 rpm. Mice are trained for 5 minutes. If testing was to follow training, a 30 minute rest period was allowed between training and testing. Mice were tested 3 times in every session with a 15 minute rest period in between each test. To conduct the test, the rotarod was set to stop and the mice placed on the stationary central spindle. The levers that stop the timers when the mouse lands on them were raised. The switch was moved to "accelerate" and the start button hit immediately to initiate acceleration.

2.2.4. Grip strength analysis

A grip strength meter (Bioseb) was used to measure limb muscle strength. For each test readings for front limbs only as well as for all four limbs combined were recorded. For forelimbs only mice were raised by the tail and lowered vertically onto a wire grid until they grasped the metal grid with both front paws. Once gripping, the tail was lowered steadily so mice were in a horizontal position and pulled steadily from the grid in one fluid movement until the mouse released its grip. For a four limb reading mice were again raised by the tail then placed on the grid so that all four paws gripped the grid, before the tail was steadily and horizontally pulled away from the grid. The maximum force (Newtons (N)) required for the mouse to relinquish its grip was recorded. The readings were normalised to body weight (g). Each mouse was subjected to three trials of forelimbs only and three trials for all four limbs (thus 6 trials in all) with a 1 minute break in between each trial.

2.3. RNAi

2.3.1. Cell culture

Cells were grown in 37°C incubators, at 5% CO_2. Cells were generally cultured in T75 flasks and split every 2-5 days when cells were approximately 70-80% confluent. Baby Hamster Kidney (BHK) cells were cultured in a 1:1 mixture of Dulbecco's Modified Eagle Medium (DMEM) and Ham's F12 media supplemented with 10% Foetal Bovine Serum (FBS). NSC-34 cells (a hybrid: motor neuron/neuroblastoma cell line (Cashman *et al.,* 1992) were cultured in DMEM supplemented with 10% FBS. To passage cells, media was first aspirated from the cells before washing briefly with PBS. TrypLE (a trypsin-like enzyme) was added (5 mls for a T75 flask) and cells returned to 37°C for 5 minutes or until cells had dissociated from the flask. Following complete cell disassociation, prewarmed growth media (equal to the volume of TrypLE used) was added to the cells. The cell suspensions were then removed from the flask and centrifuged at 1200rpm for 5 minutes. The supernatant was removed and the cell pellets were resuspended in fresh pre-warmed (37°C) cell culture media. An appropriate volume was then removed and added to a fresh flask of pre-warmed media. Cells were moved to larger flasks (T175) when large numbers of cells were required e.g. for RNAi. Cells were tested for mycoplasma infection on a monthly basis. Cells were cultured (as required) until passage 15 at which point cells were discarded.

2.3.2. Cryostat preservation of cell lines

Cell stocks were stored long term in liquid nitrogen. To freeze cells for storage they were first disassociated from the flasks and centrifuged, as described for passaging cells (section 2.3.1). Following centrifugation, supernatant was removed and discarded. Cell pellets were resuspended in cell freezing media (Table 2.1) and dispensed into 1ml aliquots for freezing. The volume of freezing media used to resuspend the pellet was dependent on the size of the flask. For a T75 flask 10ml of freezing media was used i.e. 10x1ml stocks could be stored. Samples were then kept overnight at -80°C before transfer to liquid nitrogen for storage.

2.3.3. siRNAs

All small interfering RNAs (siRNAs) were custom made by Invitrogen. siRNAs were designed by copying the relevant eEF1A1 and eEF1A2 sequence into the BLOCK-iT RNAi designer software (Invitrogen) and were ranked based on likely effectiveness. siRNAs were selected based on their ranking and also on the number of base pair differences between eEF1A1 and eEF1A2 at the target site (to ensure specificity for one variant). A table of siRNAs used in this study can be seen below (Table 2.2). siRNAs were resuspended to a concentration of 100µM and aliquoted before storage at -20^{o}C, to avoid repeat freeze-thaw cycles. Three different controls were used in each experiment; a mock transfection (no siRNA), a non-targetting scrambled siRNA (Stealth RNAi negative control duplexes (Invitrogen)) and untreated cells.

Target	siRNA name	Sequence (sense)
Hamster eEF1A1	Ha1A1-1	UUUACUUCUGUUACGUUGACUG
Hamster eEF1A1	Ha1A1-2	AAGAAGCUGGAAGAUGGCCCUAAAU
Mouse eEF1A1	m1A1-a	UGACAAUCCAGAACAGGAGCGUAGC
Mouse eEF1A1	m1A1-b	AAGUGGAGGGUAGUCAGAGAAGCUC
Mouse eEF1A2	m1A2-a	UUAACGGACACAUUCUUCACAUUGA
Mouse eEF1A2	m1A2-b	CAAUCUUGUACACAUCCUGCAGAGG

Table 2.2. siRNAs used in this study.

2.3.4. Nucleofection

A nucleofector system (Amaxa) was used to transfect the cells with siRNAs. Kit V (Amaxa/Lonzo) was used for NSC-34 cells and Kit L for BHK cells, following the manufacturer's instructions. In brief, cells were cultured in flasks to around 80% confluency on the day of transfection. 100µl of cell suspension was added to 9.9 mls of Isotone before counting cells using a Coulter Counter Z (Beckman coulter). 1x10^{6} cells per well were centrifuged at 1200rpm for 5 minutes. Cell pellets were then resuspended in nucleofector reagent (100µl per well). 100µl of cell suspension

together with 2µg of siRNA were moved to a cuvette (supplied with the kit). The cuvette was placed in the nucleofector and the selected programme was initiated. The programme used for BHK cells was A031. Multiple programmes were tested for NSC-34 cells, none of which were deemed effective. Immediately following electroporation the cuvette was removed from the machine, and 500µl of pre-warmed (37^{o}C) media was added to the cells. The entire cell suspension was then moved to the appropriate well on a 6 well plate, containing 2.5ml of pre-warmed media. Plates were mixed by gentle rocking and then incubated at 37^{o}C overnight before heat shock was performed.

2.3.5. siLentFect

siLentFect (Bio-Rad) reagent was used for the transfection of siRNAs into NSC-34 cells, following the manufacturer's instructions. Unlike nucleofection, siLentFect transfection was performed in the plates the cells were grown in. In brief cells were plated in 12 well plates to approximately 50-70% on the day of transfection. Growth media was aspirated, and replaced with fresh media prior to transfection. siRNAs were diluted in serum free media and mixed with siLentFect (also diluted in serum free media) so that the final concentration of siRNA in each well would be 10nM. Following a 20 minute incubation at room temperature the siRNA/siLentFect mixture was added directly to the cells and mixed by gentle rocking. Cells were incubated overnight at 37^{o}C before heat shock.

2.3.6. Heat Shock

Prior to heat shock, growth media was aspirated and replaced with fresh media. All cells were moved to a separate incubator for heat shock, followed by a recovery period in a 37^{o}C incubator for 16 hours (overnight). BHK cells were heat shocked for 2hrs at 42^{o}C and NSC-34 cells for 2 hrs at 43^{o}C unless otherwise stated. Following recovery, cells were disassociated from the wells as previously described (section 2.3.1) and centrifuged at 1200rpm for 5 minutes. The pellets were then stored at –20^{o}C until required for Western blotting.

2.4. Western Blotting

2.4.1. Protein extraction from cells

Protein was either extracted from cell pellets immediately following centrifugation of the cells (section 2.3.1) or, pellets were stored at -20^{o}C and protein was extracted at a later time. Cell pellets were resuspended in RIPA buffer (table 2.1) containing protease inhibitors. For a sample from a 6 well plate 80µl of RIPA was used for pellet resuspension. Volumes were adjusted according to well size. The samples were then placed on a rotating wheel at 4^{o}C for 30 minutes to completely resuspend the pellets. Samples were then centrifuged for 30 minutes at 13,000 rpm at 4^{o}C. Supernatants (containing the protein) were transferred to a fresh tube and stored at -20^{o}C.

2.4.2. Protein extraction from tissue

Mouse tissues were dissected, and immediately flash frozen in liquid nitrogen before storage at -70^{o}C. For protein extraction, the appropriate amount of tissue was excised and weighed before being placed in a homogenisation tube (Peqlab) with 0.32M Sucrose (table 2.1, 100µl per 10µg of tissue). Tissues were homogenised in a Precellys 24 Homogeniser (Precellys). Tubes were then briefly centrifuged to gather all the sample at the bottom of the tube and the homogenised tissue was moved into a fresh tube for storage at -20^{o}C.

2.4.3. Protein quantification

The concentration of protein samples were quantified using the DC Protein Assay (Bio-Rad), following the manufacturer's instructions. Samples were measured against a standard curve produced by serial dilution of BSA (between 4mg/ml – 0.1mg/ml) in RIPA buffer (for measuring protein from cell pellets) of 0.32M sucrose (for measuring protein from tissue). The absorbance (at 750nM) of the standard curve samples and protein samples were measured simultaneously on a microplate. 5µl of each sample was added to an appropriate well on a 96 well plate in triplicate. An appropriate volume of solution A1 was made by adding 20µl of solution S per ml

of solution A required. 20µl of solution A1 was then added to each well, followed by 200µl of solution B. Plates were incubated for 15 minutes at room temperature before absorbance was measured using a Microplate reader (BioTek) and the Gen5 software (BioTek). The absorbance of each BSA standard sample was plotted against the known protein concentration to generate a standard curve. The concentration of the protein samples in each well was then calculated against the standard curve on that plate. Once proteins were quantified they were diluted to a concentration of 2µg/µl with the appropriate solution (RIPA for cells and 0.32M sucrose for tissue). 10µl of protein was then added to 10µl of Laemmli loading dye (Bio-Rad) with added β-mercaptoethanol, resulting in a final concentration of 1µg/µl. Proteins were denatured by heating to 100^{o}C for 10minutes before cooling on ice. Samples were then ready for loading on a Western blot.

2.4.4. Protein separation

Proteins were separated on a SDS-PAGE gel using the BioRad Mini PROTEAN 3 gel apparatus, following the manufacturer's instructions. Firstly a 10% separating gel comprised of the following reagents was made (volumes shown are sufficient for 2 gels).

30% Acrylamide	5.2 ml
1.5M Tris pH 8.8	4 ml
dH_2O	6.68 ml
20% SDS	80 µl
TEMED	10 µl
25% AMPS	40 µl

The reagents were mixed briefly and poured between 2 glass plates (BioRad) to set, leaving a 1-2cm gap for the subsequent stacking gel. The gels were then covered in dH_2O while they set (to prevent them drying out). Once the separating gels had set (approximately 45 minutes) a 4.3% stacking gel was prepared as shown below. The water covering the separating gel was poured off before the stacking gel solution was

added. Combs (BioRad) of the required size were placed in the stacking gel once poured.

30% Acrylamide	1.45 ml
0.5M Tris-HCl pH 6.8	2.5 ml
dH_2O	5.95 ml
20% SDS	50 µl
TEMED	10 µl
25% AMPS	50 µl

Once the stacking gel was set (approximately 30 minutes), gels were removed from the apparatus and moved to a mini TransBlot cell (BioRad) which was then filled with Western running buffer (table 2.1). The combs were removed and the wells were flushed gently with running buffer using a syringe and needle to remove any residual acrylamide that could block the wells. Protein samples (with added loading dye) were then added to the wells. The protein samples were run through the gels at 100v until the loading dye had migrated completely through the gel (approximately 90 minutes). A protein full range ladder (GE healthcare) was used as a size marker. Once the loading dye had run off the bottom of the gel the current was stopped and the gels could be removed.

2.4.5. Membrane transfer

To prepare for membrane transfer, the gels were removed from the tank and placed in a container filled with Western transfer buffer (table 2.1). Also placed in this buffer were pieces of filter paper (4 per gel (Whatman)), sponges (2 per gel) and a piece of Hybond P PVDF membrane (Amersham) per gel of the required size to cover the area of interest. Membranes required brief pre-soaking in 100% methanol to allow them to absorb the transfer buffer. Following 15 minutes of soaking in transfer buffer the gels, membrane, filter paper and sponges were stacked (following the manufacturer's guidelines) and moved to the transfer apparatus filled with transfer buffer. Proteins were transferred at 100v (no more than 400mA) for 1 hour at 4^oC. Following sufficient protein transfer (indicated by the visible transfer of the

ladder on to the membrane) the membranes were removed from the transfer apparatus and placed in Western blocking buffer (table 2.1) overnight on a shaker at 4^{o}C.

2.4.6. Immunoblotting

Following blocking, membranes were incubated at room temperature in primary antibody, diluted in freshly made Western blocking buffer (optimal concentration of antibody and length of incubation can be found in table 2.3). Membranes were then washed in PBS (4 x 5minutes) before incubation in the appropriate Horse Radish Peroxidase (HRP) conjugated secondary antibody for 1 hour (optimal concentration of antibody can be found in table 2.4). Following the secondary antibody incubation, membranes were again washed in PBS (4x 5 minutes). Proteins were detected using the enhanced chemiluminescence (ECL) detection kit (Amersham Biosciences) and exposed to X-ray film (Scientific laboratory supplies) which was developed using a Curix 60 developer (AGFA).

Primary antibody	Species	Supplier	Dilution	Incubation time
eEF1A1-1	Sheep	Helen Newbery (Newbery 2003)	1:1000	2 hours
eEF1A2-3	Sheep	Helen Newbery (Newbery 2003)	1:2000	2 hours
HSP70 (HSP72)	Mouse	Stressgen SPA-810	1:1000	1.5 hours
GAPDH	Mouse	Chemicon MAB374	1:30,000	1 hour

Table 2.3. Optimal dilution and incubation times of primary antibodies used for Western blot.

Secondary Antibody	Supplier	Dilution
Polyclonal Rabbit anti goat immunoglobulins/HRP	DAKO	1:500
Polyclonal Rabbit anti mouse immunoglobulins/HRP	DAKO	1:1000

Table 2.4. Optimal dilution of secondary antibodies used for Western Blot.

2.4.7. Re-probing membranes

Following detection of the protein of interest, GAPDH antibody was almost always used on the same membrane as a loading control Prior to addition of another antibody, membranes were blocked again overnight in blocking buffer and then blotted as previously described (section 2.4.6). eEF1A1 and eEF1A2 antibodies were sensitive to re-probing and as such were always probed first on a membrane. GAPDH was always probed last.

2.4.8. Quantification of Westerns

If quantification was required this was measured using a GeneGnome (Syngene Bio Imaging) system. The films resulting from shortest exposure for a given experiment were scanned using GeneSnap software (Syngene) and the signal intensity of the bands measured using GeneTools software. Readings from the bands of the antibody of interest were normalised to readings from the bands of the GAPDH antibody (loading control) from the same blot.

2.5. Immunohistochemistry

2.5.1. Human tissue

Slides mounted with paraffin embedded human spinal cord sections (4μm thick) were received from the Edinburgh Brain bank (courtesy of Dr Colin Smith).

2.5.2. Mouse tissue

Tissue sections were dissected from mice and transferred to 10x volume of 4% neutral buffered formalin (NBF, Table 2.1). All tissues excluding spinal columns were stored in NBF for 2-3 days before processing by the Pathology Histology service. Following 2 days in NBF, spinal columns were decalcified by placing in 0.5M EDTA for 5 days, with movement to fresh EDTA being conducted every day.

Columns were then moved into fresh NBF for a minimum of 3 days before sending for processing by the Pathology Histology service (University of Edinburgh), using a Leica tissue processor ASP 300S. Paraffin embedded tissue were then sectioned by the Pathology Histology service into 4μm sections and mounted on Superfrost plus slides in preparation for immunohistochemistry. Whole brains and spinal columns from SOD1 mice were received in NBF (Dr Abraham Acevedo, MRC Mammalian Genetics Unit, Hawell.) and treated as above.

2.5.3. Paraffin removal and rehydration of sections

All paraffin embedded mouse and human tissues were first deparaffinised with xylene (2 x 5 minutes) and then rehydrated through an ethanol series: 2 x 5 minutes in absolute ethanol followed by 2 x 5 minutes in 70% ethanol. Samples were then treated with picric acid (for further removal of residual paraffin) for 15 minutes and washed gently in running water for a minimum of 5 minutes.

2.5.4. Antigen retrival

Antigen retrival was performed by microwave treatment of slides in citric acid (table 2.1). A single rack of slides would be placed in 1 litre of citric acid and placed in the designated microwave. The samples were heated in a microwave for 15 minutes on high power. Following this period samples remained in the microwave for another 15 minutes to cool. Samples were then washed in running water for 5 minutes.

2.5.5. Antibody incubations

Two methods for the next stages of immunhistochemistry are described below. The EnVision system and the Polink system were both used in this project. The method used is indicated in the appropriate figure legends in the results chapters. The reason for the use of two methods is simply that at the start of the project the EnVision system was the system in use in the laboratory. However later in the project the EnVision system had been replaced by the Polink system.

2.5.6. The EnVision method: DAKO EnVision detection kit

Following antigen retrival, samples were washed in cold water and loaded with Sequenza cover plates into the Sequenza apparatus (Thermo Shandon). Samples were washed in PBS for 5 minutes, incubated with 100µl peroxidise blocking solution (table 2.1) for 10 minutes to block endogenous peroxidise activity and washed again in PBS for 5 minutes. Samples were then treated with goat serum (diluted 1:5 with PBS) and incubated in primary antibody diluted in PBS (optimal concentration and incubation period for each antibody can be found in table 2.5). Samples were then washed in PBS and incubated in 3 drops (100µl) of EnVision Reagent (HRP Rabbit & Mouse (DAKO)) before a final wash in PBS (5 minutes).

2.5.7. The Polink method: POLINK-2 HRP detection system

Following antigen retrieval, samples were washed in cold water and incubated in 3% hydrogen peroxide for 10 minutes on a rocker. Samples were then washed again in running water and loaded with Sequenza cover plates into the Sequenza apparatus (Thermo Shandon). Samples were then treated with goat serum (diluted 1:5 with PBS) for 10 minutes and incubated in primary antibody diluted in PBS (optimal concentration and incubation period for each antibody can be found in table 2.5). Samples were then washed in PBS (2x 5minutes) and incubated in 100µl of Polink Broad Antibody Enhancer (GBI-inc) for 10 minutes. Samples were washed again in PBS (2x 5 minutes) before a 10 minute incubation in POLINK Polymer-HRP for rabbit and mouse. This final incubation was followed by 2 x 5 minute washes in PBS, before visualisation.

Antibody	Species	Supplier	Dilution	Incubation time
eEF1A2-3	Rabbit	Helen Newbery (Newbery 2003)	1:10	Overnight
eEF1B-Delta	Rabbit	Proteintech (10630-1-AP)	1:100	30 minutes
eEF2	Rabbit	Epitomics EP880Y	1:00 (Human) 1:50 (Mouse)	30 minutes
GFAP	Rabbit	Dako Z0334	1:1000	30 minutes
GRP78	Rabbit	Santa Cruz SC-13968	1:50	30 minutes
Neurofilament	Mouse	Dako M0762	1:80	30 minutes
NeuN	Mouse	Milipore MAB360	1:100 (Human) 1:1000 (Mouse)	30 minutes.
TDP-43	Rabbit	Proteintech (10782-2-AP)	1:200	30 minutes

Table 2.5. Optimal concentration and incubation times of primary antibodies used for immunohistochemistry

2.5.8. Visualisation of staining

For antibody visualisation, a Diaminobenzidne (DAB) kit (Vector) was used. Samples were removed from the Sequenza apparatus, sections were covered and treated for 2 minutes with DAB and washed in running water. Samples were counterstained in haematoxylin for 20 seconds, washed in running water and differentiated in lithium carbonate for 10 seconds. A final wash step in water was performed before dehydrating slides through an ethanol series (10 seconds in 70% ethanol, 10 seconds in absolute ethanol) followed by 3 x 10 second incubations in xylene. Slides were mounted with coverslips using pertex and allowed to dry before visualisation under a Olympus BX60 light microscope. Images were captured using the Cell^D software (Olympus).

2.6. Molecular Biology

2.6.1. Genomic DNA extraction from ear notches

For identification and genotyping, mice were ear notched at no earlier than 14 days of age. Two methods were used for the extraction of genomic DNA from ear notches: the sodium hydroxide method and the DNeasy kit (Qiagen) method.

2.6.1.1. Sodium Hydroxide (NaOH) method

This method was preferred for extraction in non-transgenic studies i.e. for genotyping of the *Eef1a2* alleles only. Ear notches were immersed in 300µl of 50mM Sodium hydroxide (NaOH) and heated at 95^{o}C for 10 minutes. 50µl of 1M Tris-HCl was then added and the samples were centrifuged at 13,000rpm for 6 minutes. The supernatant was removed and stored at -20^{o}C. 1µl of supernatant was used in the genotyping PCR (shown below).

2.6.1.2. Qiagen DNeasy Blood and Tissue kit method

For identification of the transgenes, DNA extraction using the DNeasy Blood and Tissue kit (Qiagen), was performed following the manufacturer's instructions. In brief samples were lysed overnight in lysis buffer (Buffer ATL) and proteinase K at 56^{o}C. The following day, DNA was mixed with buffer AL (with Ethanol) to optimise binding conditions before centrifugation and binding to a column. Remaining contaminants were removed by two wash steps (buffers AW1 and AW2 containing ethanol). DNA was eluted in 100µl of elution buffer (AE buffer). 1µl of each sample was used in subsequence PCRs.

2.6.2. Genotyping PCR

Genotyping PCRs were set up as shown below. For the *Eef1a2* alleles, two sets of primers were used to target the wildtype (Khalyfa *et al.,* 2001) and wasted (Newbery 2003) alleles separately. For transgenic studies, two additional sets of primers were

designed to target the transgene and used separately for each sample (TG1 and TG2). PCR products were visualised on a 2% (w/v) agarose gel.

Target	Primer Sequence (5'-3')	Product size
Wildtype *Eef1a2*	Forward:TAGTGGCTCCTTGGAACAG Reverse: CTACTCTCCCTGAATGCCTT	452bp
Wasted *Eef1a2*	Forward:ATAAGCTCCCCAATGGTAGAGAA Reverse: CGCGCCATTCTTGTATTGTT	200bp
NSE-EEF1A2 (TG1)	Forward: GTGGGCTTCTCCATCTGTCT Reverse: AGTTGGGGTTCCTTCTCAG	671bp
NSE-EEF1A2 (TG2)	Forward: GCCTGCAGCTCTTGACTCAT Reverse: TGTCAATACCTCCGCATTTG	387bp

Table 2.6. Genotyping primers and expected product sizes.

50mM Forward primer	2.5µl
50mM Reverse primer	2.5µl
2.5 mM dNTPs	2.0µl
Sigma taq buffer	2.5µl
5.5M Betaine	6.75µl
dH_20	7.25µl
Sigma Taq	0.5µl
DNA	1.0µl

The thermal cycler programme was as follows: Initial denaturation of DNA at 95^{o}C for 3 minutes followed by 30 cycles of 94^{o}C for 1 minute, 57^{o}C for 1 minute, and 72^{o}C for 1 minute, followed by a final extension step at 72^{o}C for 10 minutes.

2.6.3. Genomic DNA extraction from cell pellets

Genomic DNA (gDNA) was extracted from RAT2 cell pellets (kindly donated by Dr Justyna Janikiewicz) using the Qiagen DNeasy blood and tissue kit (Qiagen) following the manufacturers instructions (previously described in section 2.6.3 above). The optional Ribonuclease A (RNAse A) step was completed to increase the purity of the sample. Samples were eluted in 100µl of elution buffer and 1µl of this was used in subsequent PCRs.

2.6.4. Phusion PCR

For amplification of the NSE promoter region (from RAT2 cells) for insertion into the transgenic construct, and also for colony PCR for the construct the Phusion PCR kit (Finnzymes) was used, following the manufacturers instructions. The Phusion kit contained all required elements excluding the primers. Primer sequences can be found in table 2.6. PCRs were set up as outlined below and run on a thermocylcer.

Master mix	10µl
DMSO	0.6µl
H_2O	6.4µl
Forward primer	1µl
Reverse primer	1µl
DNA	1µl

The thermocycler programme was as follows; Initial denaturation of DNA at 98^{o}C for 30 seconds followed by 30 cycles of 94^{o}C for 1 minute, 60^{o}C for 1 minute, and 72^{o}C for 1 minute, followed by a final extension step at 72^{o}C for 10 minutes.

Primer Target	Sequence 5'-3'
5' end of NSE promoter	ATCGTAAGCTTGAAACCACAGAGTTTTGGAA
3' end of NSE promoter	ATCGTACCGGTTCGAGGACTGCAGACTCAG
5'end of NSE promoter with flanking *Hind*III site	CTGATGCACAATCGTAAGCTTGAAACCA
3' end of NSE promoter with flanking *AgeI* site	CTGATGCACAATCGTACCGGTTCGAGG

Table 2.7. Primer sequences for amplifying the NSE promoter.

Red sequence indicates the restriction site (*Hind*III: AAGCTT, *Age*I: ACCGGT), green sequence indictates the NSE sequence, blue sequence indicates the additional random nucleotides added.

2.6.5. PCR Purification

To purify PCR products and to remove residual PCR components that may interfere with future applications, the Qiagen QIAquick Spin protocol (Qiagen) was used, following the manufacturers instructions. In brief the binding buffer PB was added to the PCR reaction (5x the volume of the PCR reaction) and mixed. The mixture was then added to a QIAquick column and centrifuged for 1 minute at 13,000rpm to bind the DNA to the column. The flow through was discarded and the column washed with buffer PE (containing ethanol) and centrifuged for 1 minute at 13,000rpm to remove residual contaminants. The DNA was then eluted with 30µl of elution buffer (Buffer EB: 10mM Tris-HCl pH8.5) and stored at -20^{o}C until required.

2.6.6. Agarose gel electrophoresis

0.6-2.5% w/v agarose (Invitrogen) was melted in 1xTBE buffer in a microwave. Gels were cooled slightly before SYBR Safe (Invitrogen) was added (diluted 1:10,000). Gels were then cast into gel trays and combs inserted to create wells in which to load the DNA. Once set, gels were moved to an electrophoresis tank and immersed in 1xTBE buffer before removing the combs. DNA loading dye was added to samples (10% of the final volume to be loaded) before loading. The volume loaded into the

gel was dependent on the size of the well. Voltage and time required for electrophoresis is dependent on expected product size and gel percentage. Product sizes were estimated using either a lambda DNA ladder (Invitrogen) or a 1Kb DNA ladder (Bioline).

2.6.7. Sequencing

Prior to sequencing, 5µl of PCR product was purified with 1µl of ExoSap (Affymetrix). The samples were then incubated at 37^{o}C for 15minutes followed by 80^{o}C for 15 minutes. This was done immediately prior to sequencing and thus only the required volume of PCR product for the sequencing reaction was treated with ExoSap at any one time. To confirm the sequencing of the NSE-EEF1A2 construct, the promoter region and each of the exons were first amplified by Phusion PCR before sequencing. The primers used to amplify and sequence regions of interest can be found in table 2.8. Primers were designed with the aid of Primer 3 software (www.frodo.wi.mit.edu/primer3/).

Primer name	Primer target	Primer sequence 5'-3'
pUC19/NSE F1	Puc19 → NSE	ATGCTTCCGGCTCGTAT
pUC19/NSE F2	Puc19 → NSE	TGTGGAATTGTGAGCGGATA
pUC19/NSE F3	Puc19 → NSE	GAGTCAGTGAGCGAGGAAGC
NSE/Puc19 R1	NSE → Puc19	TAAATGCCGTGCAATGTGTT
NSE/Puc19 R2	NSE → Puc19	TGTGTCAGCCATACCACCAT
NSE/Puc19 R3	NSE → Puc19	AGGGGTTAACGCAGGAAAAT
NSE FA	NSE	TGCAGATGGCACACCTAGAG
NSE FB	NSE	ATCTGAAGCTGGGGAGAACA
NSE FC	NSE	GGCTGGTGGTATAGGAGGA
NSE FD	NSE	CTGCAGCTCTTGACTCATCG
NSE RA	NSE	CCTTCCTGCCATCACCTTT
NSE RB	NSE	CCAGTCTGGGACAAAAAGGA
NSE RC	NSE	ACCTCCTCGGCTCTTCTCTC
NSE RD	NSE	GAGCAGAGGAGGAGCTCAGA

eEF1A2/NSE R1	eEF1A2 → NSE	ACCACGATGTTGATGTG
eEF1A2/NSE R2	eEF1A2 → NSE	TTTTGCTGGGAGTGTGAGG
eEF1A2/NSE R3	eEF1A2 → NSE	CTCAACATGGCAGAGTTCCA
NSE/eEF1A2 F1	NSE → eEF1A2	CTGCAGCTCTTGACTCATCG
NSE/eEF1A2 F2	NSE → eEF1A2	GGCTGGACAAGGTTATGAGC
NSE/eEF1A2 F3	NSE → eEF1A2	GAGAGAAGAGCCGAGGAGGT
eEF1A2 Exon 2 F	eEF1A2 intron 1	CCTCACACTCCCAGCAAAAT
eEF1A2 Exon 2 R	eEF1A2 intron 2	AGTTGGGGGTTCCTTCTCAG
* eEF1A2 Exon 3 F	eEF1A2 intron 2	CTGTAACAAGCAGCTCGCAC
* eEF1A2 Exon 3 R	eEF1A2 intron 3	GAGCCAGACTGGGTGAGGG
* eEF1A2 Exon 4 F	eEF1A2 intron 3	GGAGAGGCCTGGAGTGAG
* eEF1A2 Exon 4 R	eEF1A2 intron 4	GTGCCACCTGCCGGTGCCTCG
* eEF1A2 Exon 5 F	eEF1A2 intron 4	AGCAGTACTCCTGGAAGCA
* eEF1A2 Exon 5 R	eEF1A2 intron 5	AGAGATTGGAGACAGCCC
* eEF1A2 Exon 6 F	eEF1A2 intron 5	CTTTGTTGGTTTCCAGGCTC
* eEF1A2 Exon 6 R	eEF1A2 intron 6	GACAGTCCTGCTGCTGTCC
* eEF1A2 Exon 7 F	eEF1A2 intron 6	CCTCCAGTCAGCACTCCGG
* eEF1A2 Exon 7 R	eEF1A2 intron 7	CTGCCATGCTCTGGGCCAAGC

Table 2.8. Primers for sequencing the NSE-EEF1A2 transgenic construct.

* Indicates primers as used in Dr Permphan Dharmasaroja's thesis (Dharmasaroja 2007).

The sequencing reagent used was the BigDye terminator ready reaction mix v3.1 system (Applied Biosciences). Reactions were set up in 96 well plates as follows:

Template DNA	3µl
Primer (forward or reverse)	1.µl
Big Dye	1.0µl
5x Big Dye Buffer	1.5µl
H_2O	3µl

Pre-sequencing PCRs were placed in a thermocycler and run on the following programme: 96°C for 1 minute followed by 24 cycles of 96°C for 30 seconds, 50°C for 15 seconds, and 64°C for 4 minutes. Following the sequencing reaction, samples were allowed to cool to 10°C before removing from the thermocycler. 2.5µl of 125mM EDTA and 30µl absolute ethanol was added to each well. Plates were sealed and inverted 4 times to mix before a 15 minute incubation at room temperature. Plates were then centrifuged at 3000rpm for 30 minutes then removed from the centrifuge. Seals were removed and the plates were then inverted over a paper towel and placed (with the paper towel) in a centrifuge and briefly spun at 1000rpm to remove all traces of liquid. 30µl of 70% ethanol was then added to each well. Sealed plates were centrifuged again at 3000rpm for 15 minutes. Plates were once again inverted over a paper towel and centrifuged (while inverted over a paper towel) to remove all traces of ethanol. Once ensuring the wells were dry, plates were sealed with adhesive film before being stored at -20°C. The samples were then taken to the sequencing service at the MRC Human Genetics Unit, University of Edinburgh where the process was completed. Sequencing was analysed using the BioEdit (Hall 1999) software and alignments checked using ClustalW (Thompson *et al.,* 1994).

2.6.8. Cloning

Plasmids and constructs were stored in glycerol at -80°C. This included the pUC19-eEF1A2 plasmid (kindly provided by Julia Boyd) and the HSA-eEF1A2 transgenic construct prepared by Dr Permphan Dharmasaroja.

2.6.9. Preparation of LB plates

LB agar (table 2.1) stored at 4°C was melted in a microwave until no residual solid agar could be seen. The bottle was then cooled to 56°C for 30 minutes. Once cooled ampicillin was added (100µg/ml) and the LB poured into petri dishes and allowed to set at room temperature. A final drying stage in a 37°C incubator for 20 minutes was performed before plates were ready for use (or storage at 4°C). Stored plates were pre-warmed for an hour at 37°C before use.

2.6.10. Bacterial culture

For production of large quantities of DNA, constructs were taken from already transformed *E.Coli* stored in glycerol at -80^{o}C. A spreading loop was flamed, dipped into the glycerol stock and streaked on a LB plate with ampicillin (100µg/ml). The plate was placed at 37^{o}C for approximately 16 hours (overnight) to allow colonies to grow. Plates with colonies were stored at 4^{o}C for up to 1 month.

2.6.11. Minipreps

If small quantities of DNA were required e.g. to test the construct, a mini-prep was conducted using the Sigma Gene-elute kit (Sigma). Colonies were picked from the appropriate plate and grown in 5mls of LB media overnight in a shaker at 200rpm and 37^{o}C. The following morning the mini-prep could then be conducted following the manufacturers instructions. In brief cultures were centrifuged at 13,000rpm for 1 minute and the supernatant discarded. The pellets were resuspended (resuspension solution, with added RNAseA) and mixed well. Cells were then lysed (lysis buffer) for up to 5 minutes. Cell debris was precipitated (Neutralisation buffer) and pelleted by centrifugation at 13,000rpm for 10 minutes. The DNA (supernatant) was then centrifuged through a column (at 13,000rpm for 1 minute), washed (Wash solution to remove residual contaminants) and eluted (100µl of Elution Solution). DNA concentration (µg/µl) was measured using a Nanodrop (Thermo Scientific). If required storing transformed bacterial colonies was achieved by mixing 500µl of bacterial culture (from the overnight incubation) with 500µl of 80% glycerol. Samples were moved immediately to -80^{o}C for storage.

2.6.12. Maxipreps

If larger volumes of DNA was required e.g. in preparation for microinjection, a Qiagen plasmid Maxi-prep kit was used. Colonies were picked from the appropriate plate and grown for 5-6 hrs in 5mls of LB media containing ampicillin (100µg/ml) in a shaker at 200rpm at 37^{o}C. Following this initial incubation, the samples were then

diluted 1:1000 into a larger volume, typically 200 mls and left to shake overnight (~16hrs) at 200rpm at 37°C. The following morning the samples were removed from the shaker and the maxi-prep could then be conducted following the manufacturer's instructions. In brief, bacterial cultures were centrifuged at 8000rpm for 15 minutes at 4°C and the supernatant discarded. Pellets were resuspended (Buffer P1: 50mM Tris-HCl (pH8.0) and lysed (Buffer P2: 200mM NaOH, 1% SDS). The sample was then neutralized and cell debris precipitated (chilled buffer P3: 3.0M potassium acetate pH5.0). Lysates were then purified through a Qiafilter cartridge and bound to resin in a Maxi tip. The resin bound DNA was then washed (Buffer QC; 1.0MNaCl, 50mM MOPS pH7.0, 15%(v/v) isopropanol) and eluted (Buffer QF; 1.25M NaCl, 50mM Tris-HCl pH8.5, 15% (v/v) isopropanol). DNA was concentrated by precipitation with isopropanol and filtered through a Qiaprecipitator. A final wash of the Qiaprecipitator with 70% ethanol was conducted before final elution of the purified DNA in TE buffer. DNA concentration (µg/µl) was measured using a Nanodrop (Thermo Scientific). If required storing transformed bacterial colonies was achieved by mixing 500µl of bacterial culture (from the overnight incubation) with 500µl of 80% glycerol. Samples were moved immediately to -80°C for storage.

2.6.13. Restriction enzyme digests

DNA digests were carried out at 37°C using site specific restriction enzymes. 1 unit of each enzyme was used to digest 1µg of DNA for 1 hour with the appropriate enzyme buffer (as designated by the supplier). *Hind*III, *Kpn*I, *Age*I (NEB) were used in varying combinations. Single enzyme digests were incubated for 1 hour at 37°C. For double digests, the appropriate buffer was selected based on its compatibility with both enzymes. A one hour digest at 37°C was conducted initially with one enzyme followed by the addition of the second enzyme (and additional buffer and dH_2O as required) and incubation for another hour at 37°C. Enzymes were heat inactivated at 72°C for 20 minutes immediately following digestion. DNA loading dye was added to samples before running on a 0.6% (w/v) agarose gel to assess whether the correct products were present. For preparation of the transgenic

constructs for microinjection, 50µg of DNA was required. As this is a large volume, on this occasion the digest was incubated overnight at 37°C.

2.6.14. Ligation

Ligation was achieved using T4 DNA ligase (Invitrogen) following the manufacturer's instructions. In brief, a ligation reaction was set up which comprised of the digested eEF1A2 vector, the digested NSE promoter, T4 DNA ligase (0.1unit) and 1X reaction buffer. It was found that the optimal conditions for the ligation reaction was to incubate the reaction at 4°C overnight using a 4:1 promoter:vector ratio. Ligation reactions were then diluted 1:5 in TE buffer prior to transformation.

2.6.15. Transforming competent cells

DNA constructs were transformed into OneShot TOP10 cells (Invitrogen) following the manufacturer's instructions. In brief 50µl aliquots of competent cells were thawed on ice. 4µl of ligation reaction was added directly to the cells and mixed gently. Cells were then incubated on ice for 30minutes followed by heat shock at 42°C for 30 seconds. Following heat shock samples were immediately transferred to ice for 2 minutes. 250µl of room temperature SOC medium was added to each vial and the vials were moved to a shaker set at 37°C, 225rpm for 2 hours. Following transformation, the cells were plated on LB plates in varying volumes and incubated at 37°C overnight to allow colonies to grow. Colonies were then screened for the presence of the insert.

2.6.16. Colony screening

To test for the presence of the correct construct in the correct orientation, colony PCRs were performed. Colonies were picked from the appropriate plate using a non-filtered gilson pipette tip, streaked onto a gridded new plate (so that the colony is maintained) and then the pipette tip was placed into a PCR in a 96 well plate. Its position in the 96 well plate corresponded to its position on the new gridded plate (thus each PCR can be easily traced back to its original colony). The primers used to

identify colonies containing the entire construct in the correct orientation were designed so that they crossed the promoter/gene boundary thus eliminating any non-ligated products (the same as used for identifying the presence of the transgene – table 2.6). Colony screens were performed using the Phusion PCR method (section 2.6.6).

2.6.17. Construct purification

To purify constructs for microinjection, the digested 50µg of construct was purified by electroelution using the Elutrap apparatus (Whatman) following the manufacturers instructions. Following restriction digest, a small amount of construct was run on an agarose gel (0.6%) to confirm the digest had worked effectively. A 1% Seakem GTG agarose gel (Cambrex bio-science) was then set using 1xTAE buffer (diluted with miliQ water) and ethidium bromide (final concentration 0.5µg/ml) for visualisation under ultra violet (UV) light. All the remaining construct from the 50µg digest was loaded into a single well on the gel and the gel was run at 100V for 2-3 hours. The gel was viewed by UV light to confirm the construct had separated from the plasmid backbone. The construct was then excised from the gel with a scalpel and loaded into the elutrap apparatus following the manufacturers instructions. In brief, gel slices are placed in the centre of the apparatus, which is then placed horizontally in a standard electrophoresis chamber and covered in 1xTAE buffer so that the gel slice is completely immersed. On electrophoresis the DNA migrates from the gel into a trap area formed by two membranes. Electrophoresis was performed overnight at 60V. Following electrophoresis the buffer from the trap area now containing the DNA was removed to a fresh tube. The DNA was precipitated in sodium acetate (10% of the total volume of the buffer containing the DNA) and absolute ethanol (twice the volume of the buffer containing the DNA) on dry ice for 2 hours. The DNA was then centrifuged at 13,000rpm for 30 minutes at 4^{o}C. The supernatant was discarded and the pellet washed with 70% ethanol before centrifugation for another 5 minutes. The pellet was then resuspended with microinjection buffer (table 2.1) and the concentration checked by nanodrop and confirmed on an agarose gel. The construct was then diluted to 2ng/µl in

microinjection buffer and purified through a column (Spinex). The construct was then ready for microinjection. The preparation of the constructs was completed with the aid of Dr Laura Lettice at the MRC Human Genetics Unit (HGU), University of Edinburgh.

3. Aim Chapter 3: Investigating ageing wasted heterozygotes (+/*wst*) as a possible model for motor neuron degeneration.

3.1. Aim

The aim of this project was to determine if there is a gene dosage effect of eEF1A2 in ageing heterozygote wasted mice and whether wasted heterozygote mice develop any signs of age related motor neuron degeneration. To assess if wasted heterozygotes could be a model for late onset motor neuron degeneration, a combination of behavioural testing and pathological analysis was conducted to look for any differences between wildtype and heterozygote animals of greater than one year old. These experiments are important for increasing our understanding of the wasted mutation and have clear implications for our understanding of the role of eEF1A2 in motor neurons, as well as the possibility of providing a new model for late onset motor neuron degeneration.

3.2. Introduction

3.2.1. Why wasted heterozygotes?

In 2006, Doran *et al* (Doran *et al.,* 2006) published a study in which they investigated 1 year old ZPR1 heterozygous mice for signs of neurodegeneration. The results showed that ageing heterozygous mice displayed gradual loss of ZPR1 in the brain and degeneration of motor neurons at 12 months of age, indicating that ZPR1 deficiency causes motor neuron degeneration in ZPR1 heterozygous mice. This suggests that these animals could be used as a model for late onset motor neuron disease. This coupled with the knowledge that ZPR1 has been shown to interact with eEF1A (Gangwani *et al.,* 1998) and survival motor neuron (SMN) proteins (Gangwani *et al.,* 2001) (mutations of which are the major cause of spinal muscular atrophy) led us to believe that older wasted heterozygote (+/*wst*) mice should also be investigated as a possible model for late onset motor neuron degeneration.

To date, wasted heterozygotes have generally been characterised as phenotypically normal and have often been used as littermate controls in experiments characterizing wasted mice. Due to the early death of wasted mice the eldest wasted and heterozygous mice that have been studied are generally less than 1 month old.

Shown here is the first study examining differences both in behaviour and in pathology between wasted heterozygote mice and wild type control mice of greater than 1 year old to assess whether wasted heterozygotes may be useful as a model of late onset motor neuron disease.

3.2.2. Wasted mice: Behavioural analysis

A paper published by our group in 2005 (Newbery *et al.,* 2005) involved in-depth characterization of the wasted model which included analysis of motor impairment in wasted (*wst/wst*) mice using the accelerating rotarod. Results showed that wasted mice performed significantly worse on the rotarod than their littermate controls from 21 days of age. This coincides with the timing of the developmental switch in eEF1A variants and is the age at which symptoms of neuromuscular disease become evident. This combined with the fact that the rotarod is viewed as the gold standard for detecting motor function deficiencies made it the primary candidate assay for assessing behavioural differences between older heterozygote animals and wildtype controls. Whereas the rotarod is a test of motor co-ordination another significant symptom of wasted mice (and also human motor neuron disease) is progressive skeletal muscle atrophy. A test of limb-strength was therefore investigated in this study. Although there are multiple ways to measure limb-strength the mechanical grip strength meter provides ease of use and no training of mice is required. At the beginning of this study grip strength data was collected from wasted mice and littermate controls using a grip strength meter to assess the time-point at which any difference between wasted mice and controls could first be detected.

3.2.3. Wasted mice: Pathological analysis

The choice of markers to investigate the pathology of wasted heterozygotes came from current knowledge of the pathology of wasted mice and more importantly from knowledge of pathological changes seen in ALS. Newbery *et al* (Newbery *et al.,* 2005) describe the upregulation of glial fibrillary acidic protein (GFAP) in glial cells and also the accumulation of neurofilaments in neuronal cell bodies as hallmarks of the pathology in wasted mice. Reactive gliosis, which is characterised by the upregulation of GFAP is generally seen in response to neurological disease and has been observed in brain and spinal cord of ALS patients (Nagy *et al.,* 1994; Fujita *et al.,* 1998). Accumulation of phosphorylated neurofilaments in the perikarya of motor neurons has also been reported in ALS patients (Munoz *et al.,* 1988). Antibodies to GFAP and neurofilament show distinguishable staining patterns between wasted mice and controls therefore these two markers were used in this study to look for any signs of motor neuron degeneration in ageing heterozygous mice.

3.3. Results

3.3.1. Wasted limb strength

Mice were tested for muscle strength in forelimbs only and then in all four limbs. Mice were tested on 1 day only, thus eliminating any potential disadvantage from multiple testing. Body weight has to be considered when measuring grip strength. To account for this variable all grip strength readings (measured in Newtons) were normalised to body weight (measured in grams). Results show that a significant difference between wasted mice and controls is observable from 20 days in the forelimbs only (figure 3.1 and table 3.1) and in all four limbs (figure 3.2 and table 3.2). These results validate the grip strength meter as a useful test for distinguishing wasted mice from their littermate controls and thus it was considered a valuable test to look for differences between older heterozygotes and wildtypes in the ageing cohort.

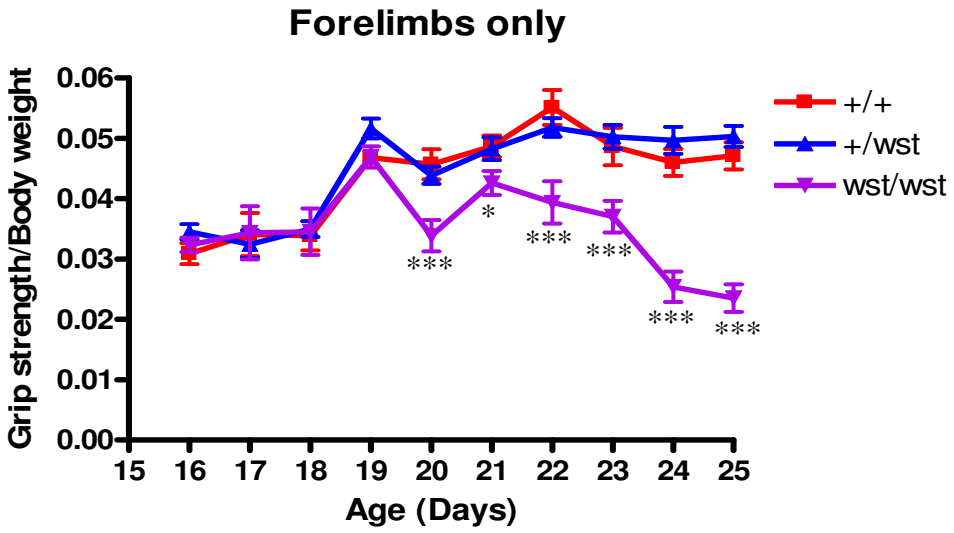

Figure 3.1. Forelimb grip strength analysis of wasted mice

Mean forelimb grip strength of wasted mice (*wst/wst*) and both wildtype (+/+) and heterozygote (+/*wst*) littermate controls between 16-25 days old. The daily grip strength reading of 3 tests (measured in Newtons) were normalised to body weight (grams). P values were calculated comparing wasted mice with controls (+/+ and +/*wst* combined). * indicates a P value<0.05, *** indicates a P value <0.001.

Age	Mean +/+	Mean +/*wst*	Mean *wst/wst*	P value
16 days	0.031 (n=8)	0.034 (n=13)	0.032 (n=3)	0.7737
17 days	0.034 (n=5)	0.032 (n=9)	0.034 (n=3)	0.7726
18 days	0.034 (n=6)	0.035 (n=22)	0.035 (n=6)	0.9526
19 days	0.047 (n=4)	0.052 (n=10)	0.04689 (n=9)	0.1364
20 days	0.046 (n=13)	0.044 (n=26)	0.034 (n=11)	0.0003
21 days	0.049 (n=10)	0.048 (n=13)	0.043 (n=9)	0.0221
22 days	0.055 (n=11)	0.052 (n=25)	0.039 (n=9)	0.0002
23 days	0.049 (n=13)	0.050 (n=18)	0.037 (n=15)	0.0002
24 days	0.046 (n=10)	0.050 (n=17)	0.025 (n=8)	<0.001
25 days	0.047 (n=14)	0.050 (n=14)	0.024 (n=10)	<0.001

Table 3.1. Forelimb grip strength analysis of wasted mice.

Mean forelimb grip strength of wasted mice (*wst/wst*) and both wildtype (+/+) and heterozygote (+/*wst*) littermate controls between 16-25 days old. The daily grip strength reading of 3 tests (measured in Newtons) were normalised to body weight (measured in grams). P values were calculated between the wasted group and controls (+/+ and +/*wst* combined) using a t-test.

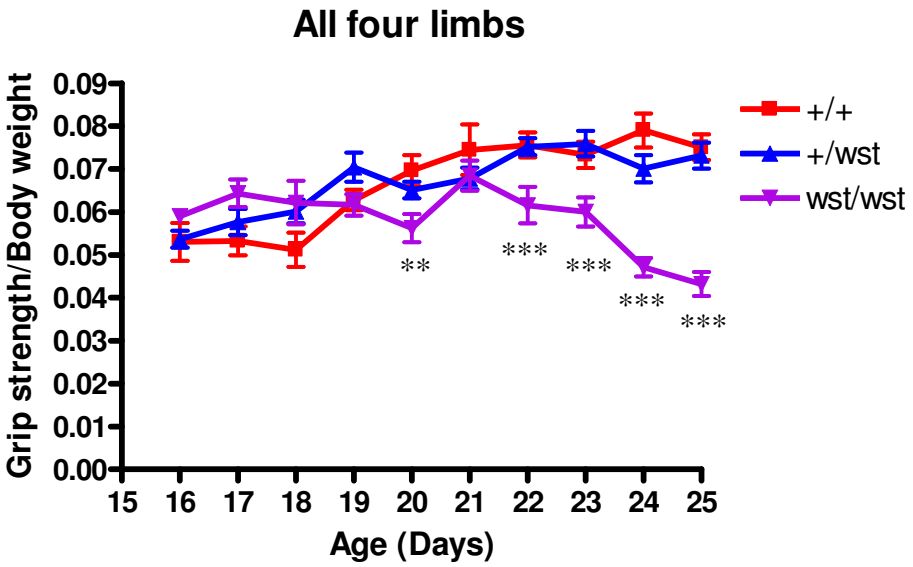

Figure 3.2. Four limb grip strength analysis of wasted mice.

Mean grip strength from all four limbs of wasted mice (*wst/wst*) and both wildtype (+/+) and heterozygote (*+/wst*) littermate controls between 16-25 days old. The daily grip strength reading of 3 tests (measured in Newtons) were normalised to body weight (grams). P values were calculated comparing wasted mice with controls (+/+ and *+/wst* combined). ** indicates a P value<0.01, *** indicates a P value <0.001

Age	Mean +/+	Mean *+/wst*	Mean *wst/wst*	P value
16 days	0.053 (n=8)	0.054 (n=13)	0.059 (n=3)	0.3153
17 days	0.053 (n=5)	0.058 (n=9)	0.064 (n=3)	0.1383
18 days	0.051 (n=6)	0.060 (n=22)	0.062 (n=6)	0.4943
19 days	0.063 (n=4)	0.070 (n=10)	0.062 (n=9)	0.1079
20 days	0.070 (n=13)	0.065 (n=26)	0.056 (n=11)	0.0080
21 days	0.074 (n=10)	0.068 (n=13)	0.068 (n=9)	0.6720
22 days	0.076 (n=11)	0.075 (n=25)	0.062 (n=9)	0.0009
23 days	0.073 (n=13)	0.076 (n=18)	0.060 (n=15)	0.0004
24 days	0.079 (n=10)	0.070 (n=17)	0.047 (n=8)	<0.0001
25 days	0.075 (n=14)	0.073 (n=14)	0.043 (n=10)	<0.0001

Table 3.2. Four limb grip strength analysis of wasted mice.
Mean grip strength of all four limbs of wasted mice (*wst/wst*) and both wildtype (+/+) and heterozygote (*+/wst*) littermate controls between 16-25 days old. The daily grip strength reading of 3 tests (measured in Newtons) were normalised to body weight (measured in grams). P values were calculated between the wasted group and controls (+/+ and *+/wst* combined) using a t-test.

3.3.2. The ageing study

3.3.2.1. Pilot studies

This project was initially started by Antonia Churchhouse in our laboratory. Antonia tested groups of 1 year old heterozygote males and females (*+/wst*) and female wildtype control mice (+/+) for differences in rotarod performance as an indicator of loss of motor function. She showed that at 12 months of age, female heterozygotes demonstrated a significant decrease in rotarod performance compared to both wildtype females and heterozygote males (data not shown). Unfortunately at the time of Antonias project no male wildtype controls were available. Therefore at the start of this project, male heterozygote mice and male wildtype mice were tested following the same protocol as the previous study. These two data sets combined showed that while female heterozygotes showed a significant decrease in rotarod performance at 12 months of age when compared to wildtype females, male heterozygotes did not differ from wildtype males in rotarod performance at this age. The males were then tested again at 15 months of age and at this time, a significant difference was observed between male heterozygotes and wild types (data not shown). Although poor rotarod performance can be attributable to many factors, preliminary immunohistochemistry data (conducted by Antonia) of motor neuron numbers in the anterior horn of the spinal cord of these same animals showed a decrease in the number of motor neurons in the female *+/wst* compared to both male *+/wst* and female controls at 12 months of age. This is the first account of any observable abnormality in wasted heterozygous mice and therefore warranted further investigation.

3.3.2.2. The ageing cohort

As there was never a complete set of suitable mice (male wildtypes, male heterozygotes, female wildtypes and female heterozygotes) at any one time, a new cohort of ageing male and female heterozygous mice as well as both male and female wildtype controls were established. Four groups of 8 animals were bred (male wildtype, female wildtype, male heterozygotes, female heterozygotes) from 3 breeding pairs. Genotyping data can be seen in figure 3.3. Mice were selected from the first two litters of each breeding pair, thus there were slight differences in age of some of the litters but this was no greater than 1 month. For testing purposes the tests were conducted when the youngest mice were of the required age. All animals were housed in single sex cages but all cages were a mixture of both wildtypes and heterozygotes with 2-3 animals in each cage. This was to eliminate any stress that may occur in single housed animals. The entire cohort was tested on the same days and all tests were carried out in the morning to eliminate any variables that may be caused by time of day. Initially these animals were to be tested at tri-monthly intervals for motor function using an accelerating rotarod and also for limb strength using the grip strength meter. The tri-monthly intervals (at 3,6,9,12,15 and 18 months of age) would allow identification of the starting point of any difference between wildtypes and heterozygotes.

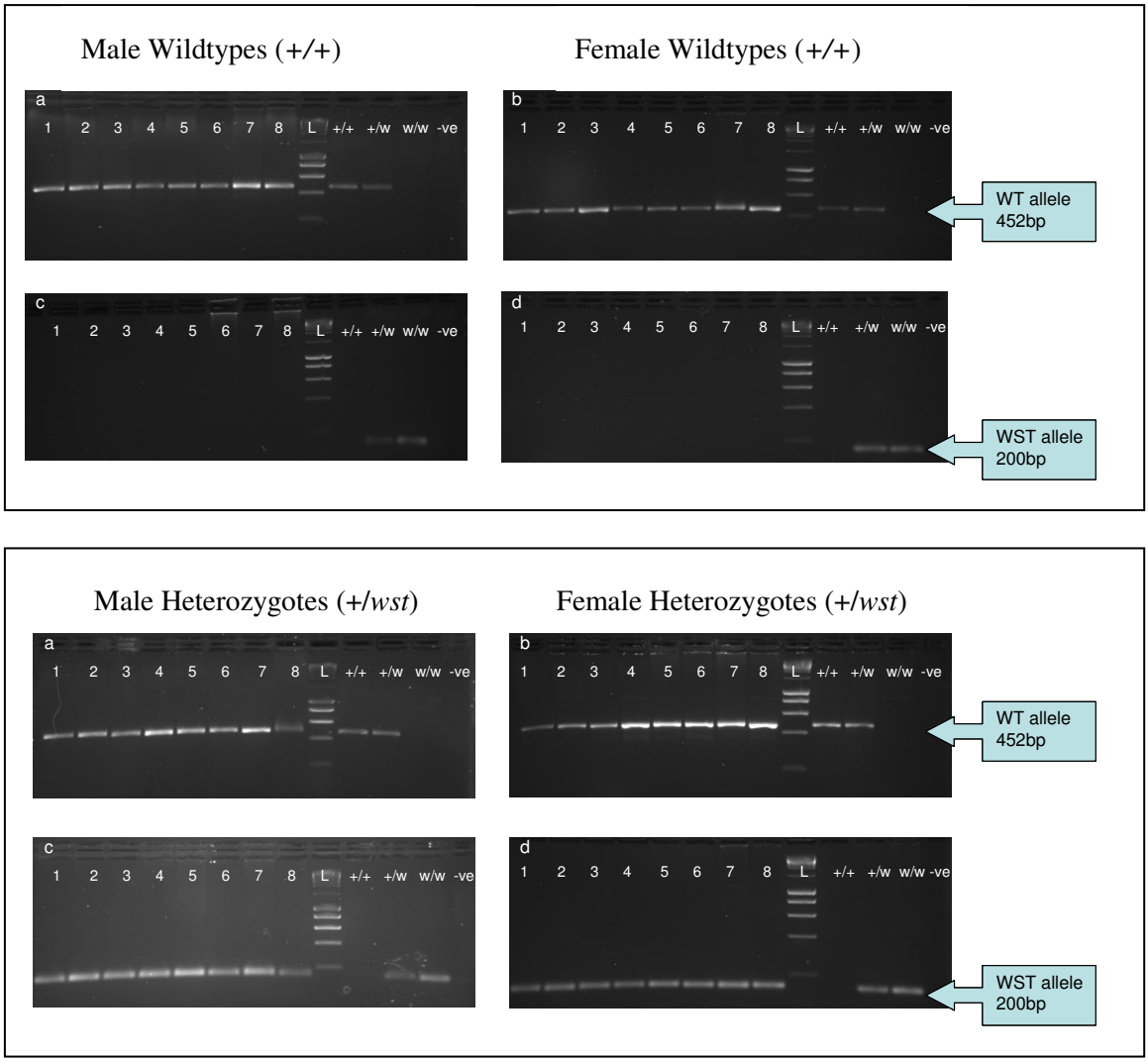

Figure 3.3. Ageing study mouse genotypes.

Agarose gels (2%) showing genotyping PCR results from all mice in the ageing cohort. The top panel shows wildtype animals (+/+) while the bottom panel shows heterozygote animals (*+/wst*). Gels (a) and (b) in both panels show results from PCRs of the wildtype (WT) allele (expected size of product: 452bp). Gels (c) and (d) in both panels show results from PCRs of the wasted (WST) allele (expected size 200bp). L indicates a size ladder, +/+ indicates a wildtype control sample, *+/wst* indicates a heterozygous control sample, *wst/wst* indicates a wasted control sample and –ve indicates a PCR reaction with water added in place of any DNA.

3.3.2.3. Rotarod testing strategy

The rotarod is one of the most commonly used tests for motor co-ordination in mice. Mice are placed on a rotating beam and their latency in falling from the beam is recorded. The rotarod may rotate at a fixed speed or at an accelerating speed. For this study, mice were trained for 5 minutes at a constant speed of 4rpm, followed by a 30 minute rest period, followed by 3 tests at accelerating speed (4-40rpm over 5 minutes) with 15 minute recovery periods in between each test. Mice were tested on alternate days over a fortnight. Test days were Monday, Wednesday and Friday during week one then Monday and Wednesday during week two. Thus mice had at least 1 day to recover between test days. On purchase of a new rotarod at the beginning of this study all mice were unable to walk for even a few seconds without slipping from the beam. This is believed to be due to the material from which the beam was made having little grip and not due to any neuromuscular problem as our mice had no problem performing the task on the previous rotarod. To counteract this problem it was deemed necessary to coat the rod in dolls house carpet (kindly donated by Prof. Cathy Abbott, purchased from Hamleys). Thus all tests on all animals in this study were conducted on the carpeted rotarod. To ensure animals did not require extensive re-training at the start of each testing month, between testing periods mice were trained once a week for 5 minutes on the rotarod set to a constant speed of 4rpm to maintain familiarity with the procedure. To eliminate problems with reproducibility between investigators, all rotarod data was collected blind by myself however weekly training session were conducted by our technician Jennifer Doig. At the start of each testing session mice were monitored for several minutes and weighted to check for any obvious mobility or other health problems. Once mice were deemed healthy the training could commence. If however a mouse showed any signs of illness they were immediately removed from the study and all data for that animal for that given month was excluded.

3.3.2.4. Ageing Rotarod Results

The results on the following pages show all data collected at each of the tri-monthly time points up until 15 months of age. As males and females perform differently in some behavioural tasks such as the rotarod, and given the data from the pilot study it was deemed necessary to separate the data by genotype and also by gender. Figure 3.4 displays the mean daily fall times for each group while figure 3.5 shows the mean monthly fall times for the groups at each tri-monthly time point. As can be seen from the graphs in figure 3.5 no significant difference was observed between wildtypes and heterozygotes of either gender between the ages of 3-15 months of age. The Students t-test was used to confirm this. As the body weight of the animals could potentially affect their rotarod performance, the data were also analysed by normalising the mean daily times to body weight (data not shown) although these data also showed no significant difference between groups.

To summarise, no statistically significant difference was observed on the rotarod in any of these groups by 15 months of age. However as can be observed from both the 12 month and 15 month time point graph in figure 3.5 it appears that female heterozygotes perform slightly worse than the other 3 groups.

All data from the first 15 months of the study combined to show overall rotarod performance of the group over the initial 15 month period is shown in figure 3.6. As can be seen in the graphs, the performance of all four groups appears to decline with age over this 15 month period.

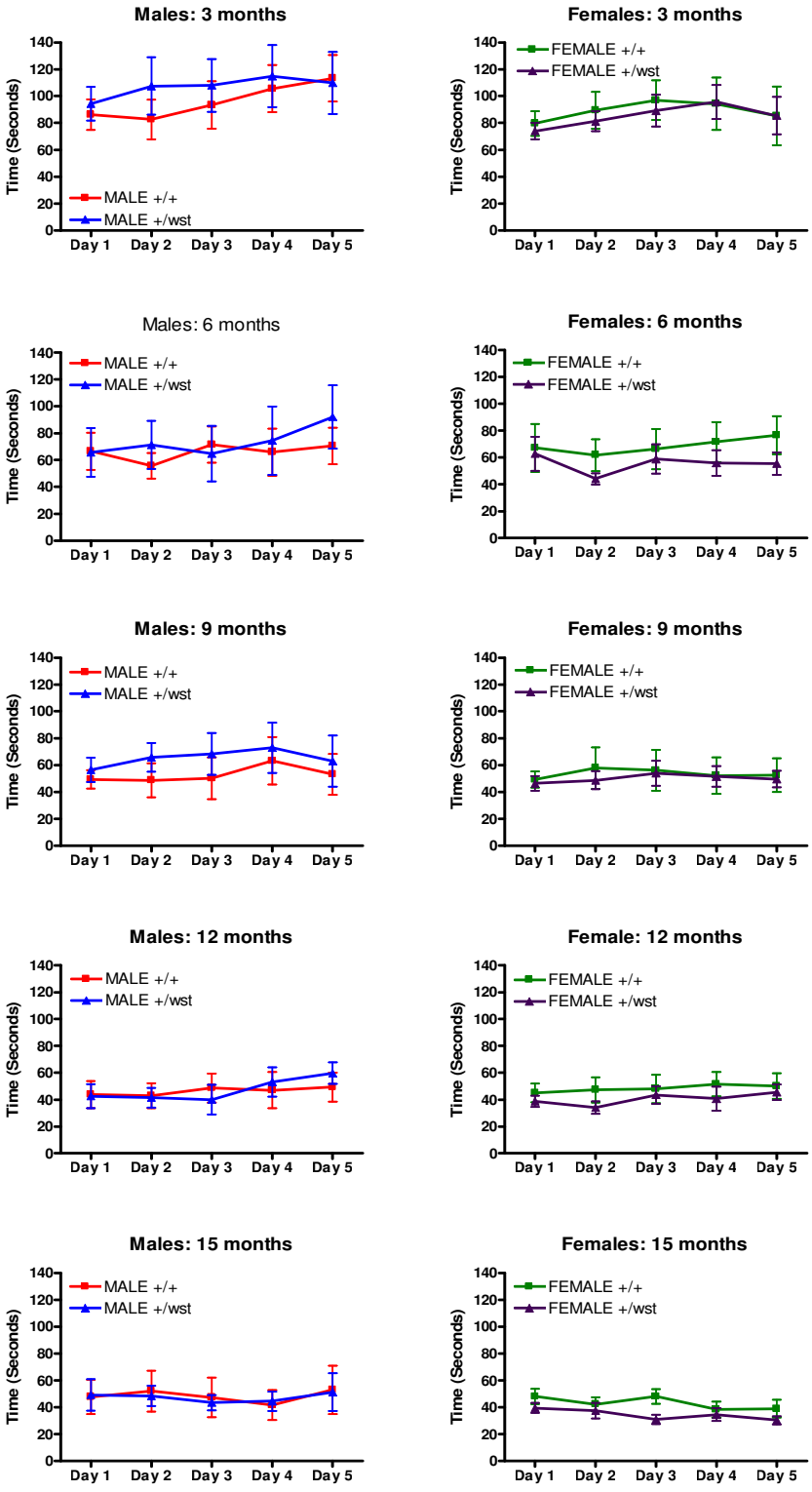

Figure 3.4. Daily rotarod data from the ageing study.
Mean daily times of latency to fall from the rotarod. Left panels show male data while right panels show female data. +/+ indicates wildtype animals, *+/wst* indicates heterozygote animals. Error bars represent the standard error of the mean.

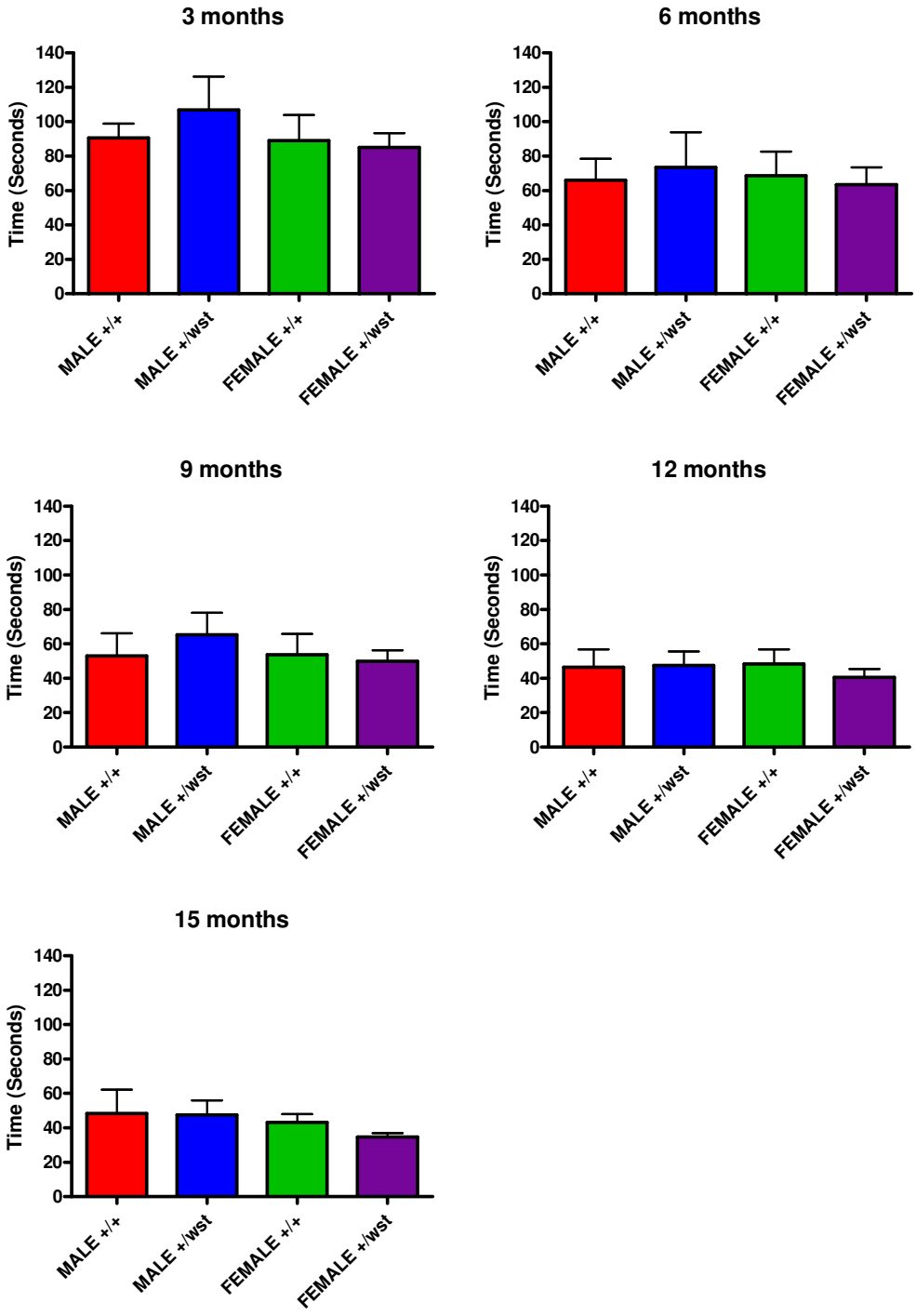

Figure 3.5. Tri-monthly rotarod data from the ageing study.

Mean monthly times of latency to fall from the rotarod for each group in the ageing study. +/+ indicates wildtype animals, *+/wst* indicates heterozygote animals. Error bars represent the standard error of the mean.

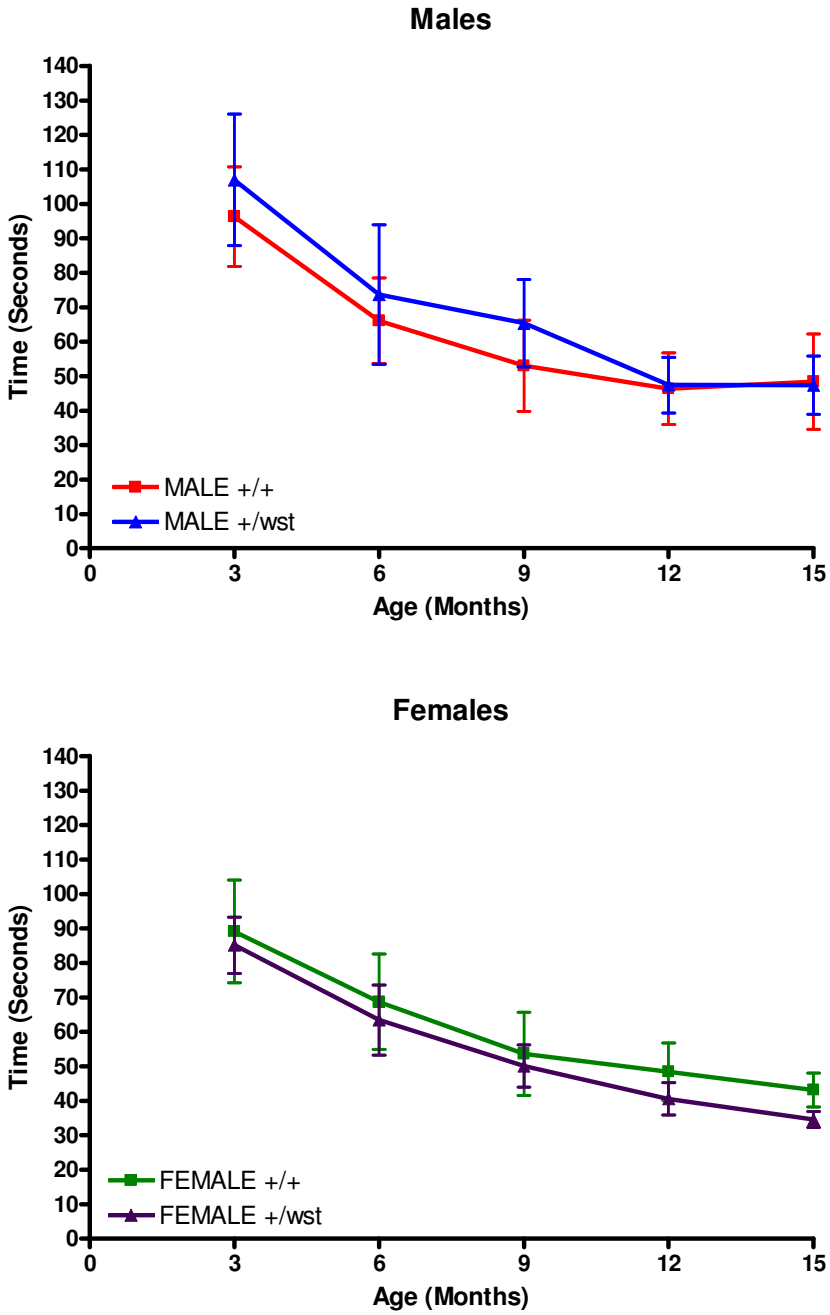

Figure 3.6. Rotarod data between 3-15 months of the ageing study.

Mean times of latency to fall from the rotarod over the first 15 months of the ageing study. +/+ indicates wildtype animals, *+/wst* indicates heterozygote animals. The upper graph shows data from the male groups and the lower graph shows data from the female groups. Error bars represent the standard error of the mean.

Due to the nature of animal work, some mice died over the course of the study from non-motor neuron related conditions such as cervical prolapse, fighting and tumours. This appeared to occur at random in both wildtypes and heterozygotes and thus was not considered to be caused directly by differences in eEF1A2 expression. By 15 months of age only 7 wildtype males, 7 heterozygous males, 5 wild type females and 5 heterozygous females remained.

At this stage it had to be decided whether to terminate all animals immediately and carry out the histological analysis or to continue the behavioural experiments for another few months. To address this issue the spinal cords of the mice that had already been removed from the study were analysed to examine whether there was any evidence of a difference between groups at the histological level. Given the limited number of samples available this analysis was unfortunately inconclusive (data not shown).

As female heterozygotes were beginning to show a decrease in performance compared to the other groups at 12 months of age it was decided behavioural analysis should continue and that the mice would be kept alive for a few more months and analysed on a monthly basis instead of tri-monthly. This would ensure that the number of animals in each group would remain sufficient for accurate pathological analysis i.e. to minimize the risk of reaching the 18 month time point and not having enough animals in any given group for sufficient pathological analysis. If the number of animals in any group had fallen to 3 the study would have been terminated and pathological analysis undertaken at that time point. This was not the case and sufficient numbers survived to 18months. Rotarod analysis was therefore carried out at 16, 17 and 18 months of age on the remaining mice. The mean daily performance of each group can be seen in figure 3.7 while the mean monthly data can be seen in figure 3.8.

As can be observed in figure 3.8. the rotarod data from 16, 17 and 18 months of age showed no statistically significant difference between heterozygotes and wildtypes of either gender. However once again it does appear that female heterozygotes perform worse than the other three groups at 18 and 21 months, but as before this is not statistically significant.

Interestingly, when the data for the entire study is combined (figure 3.9) the data indicates that during the tri-monthly testing period mice generally perform worse with age. However when the behavioural testing becomes more frequent (monthly) rotarod performance in all four groups improves (figure 3.9). Learning behaviour and/or exercise clearly plays a role in the mice's performance on the rotarod. The weekly five minute training session between the tri-monthly tests are clearly not as effective as monthly testing for maintaining the mouse's ability to perform to their maximum ability on the rotarod. This interesting observation combined with the fact that female heterozygotes were continuing to perform slightly worse than the controls led to the decision to keep the animals alive (under close observation) for another three months for one more testing period at 21 months of age. As can be seen in figure 3.8 at 21 months, female heterozygotes appear to be performing worse than the other groups but similarly this is not statistically significant. Interestingly the 3 month break from the rotarod halted the increase in rotarod performance seen between 15-18 months. In fact it appears that this break has now caused a decline in the animals performance (figure 3.9). The mean monthly data for each group at each time point can be seen in table 3.3 and 3.4.

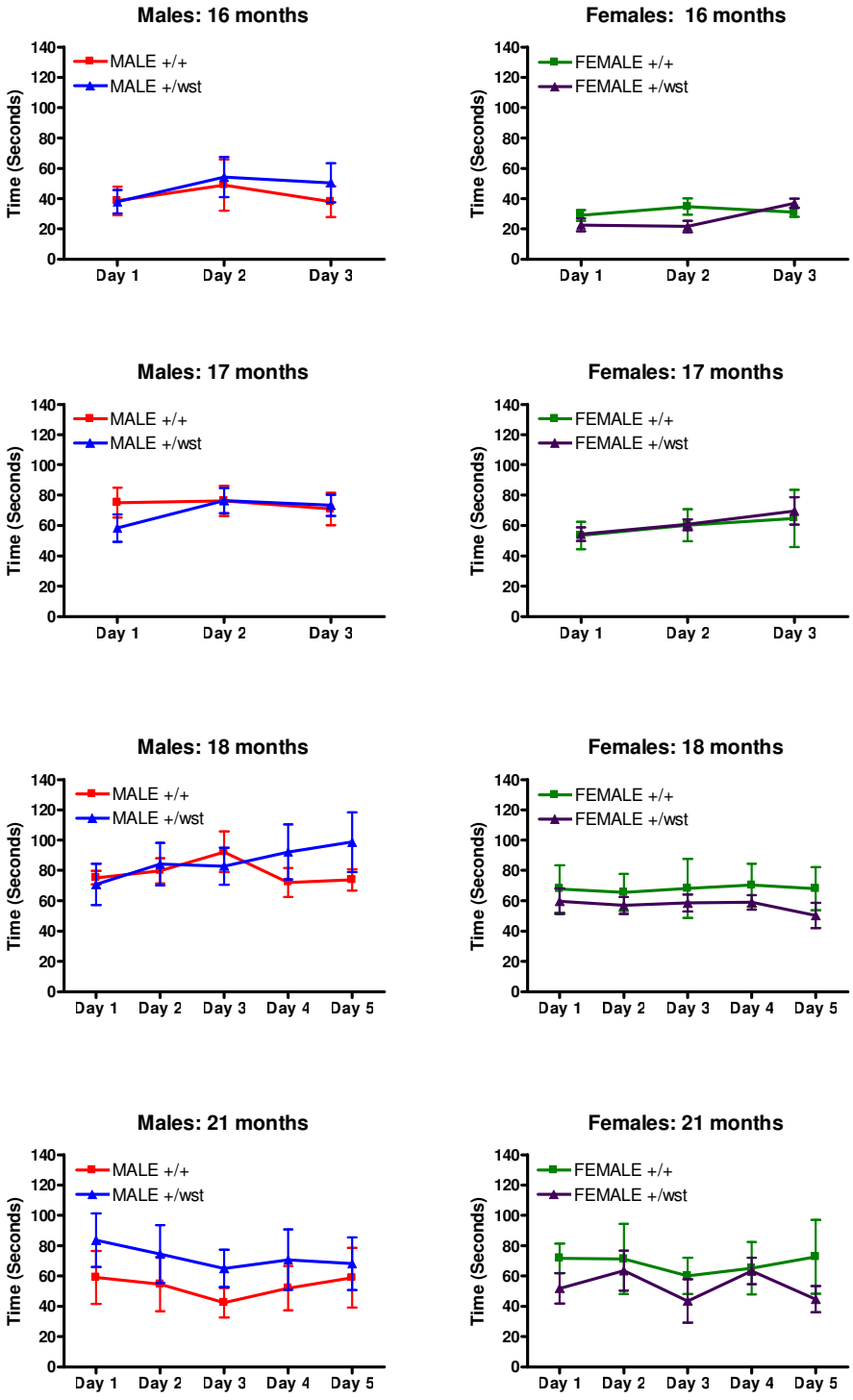

Figure 3.7. Daily rotarod data from the ageing study at 16-21 months of age.

Mean daily times of latency to fall from the rotarod. Left panels show male data while right panels show female data. +/+ indicates wildtype animals, +/*wst* indicates heterozygote animals. Error bars represent the standard error of the mean.

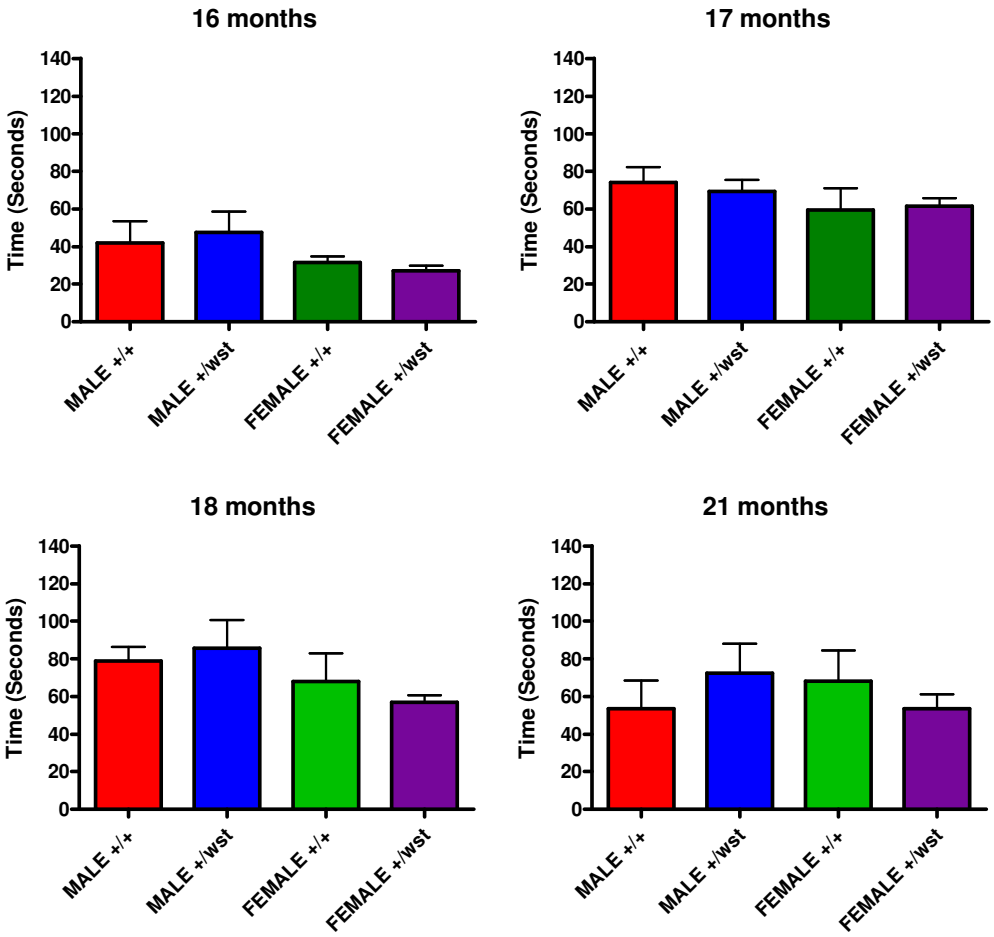

Figure 3.8. Monthly rotarod data from 16-21 months of the ageing study.

Mean monthly fall times from the rotarod for each group in the ageing study between 16 and 21 months of age. +/+ indicates wildtype animals, *+/wst* indicates heterozygote animals. Error bars represent the standard error of the mean.

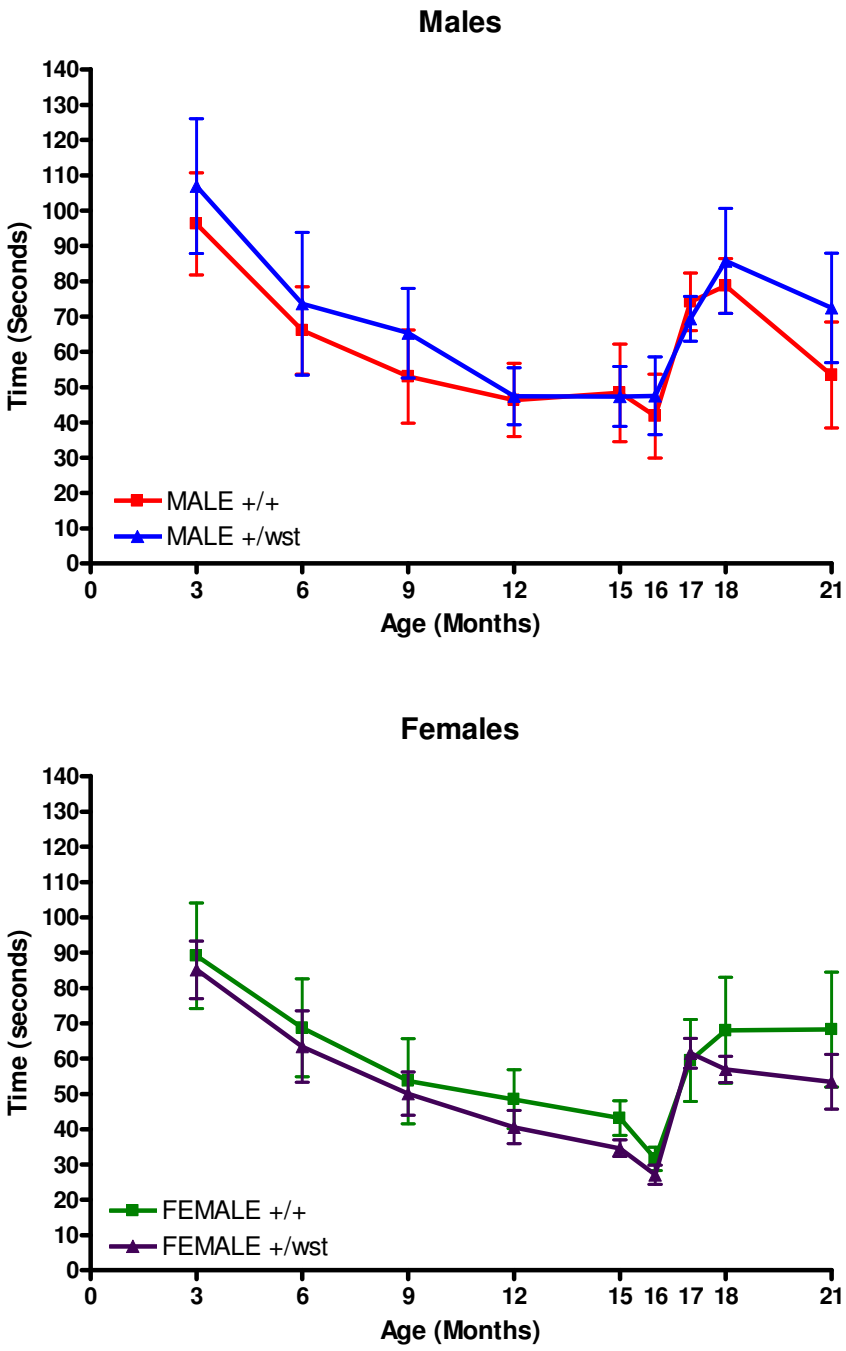

Figure 3.9. Rotarod data over the entire course of the ageing study.

Mean times of latency to fall from the rotarod over the whole 21 months of the ageing study. +/+ indicates wildtype animals, *+/wst* indicates heterozygote animals. The upper graph shows data from the male groups and the lower graph shows data from the female groups. Error bars represent the standard error of the mean.

a. Male wildtype data

Age	N	Mean	Min	Max	S.D	S.E.M
3 months	8	96.23	35.73	160.20	40.89	14.46
6 months	8	66.01	29.20	140.27	35.06	12.39
9 months	8	52.93	19.60	133.47	37.38	13.22
12 months	8	46.32	18.47	109.20	29.40	10.40
15 months	7	48.37	25.93	128.33	36.48	13.79
16 months	7	41.78	20.78	109.56	31.40	11.87
17 months	7	74.13	38.78	97.00	21.58	8.16
18 months	7	78.63	60.47	112.27	20.52	7.76
21 months	5	53.40	28.80	110.27	33.54	15.00

b. Male heterozygote data

Age	N	Mean	Min	Max	S.D	S.E.M
3 months	8	106.92	41.00	184.87	54.05	19.11
6 months	8	73.60	26.47	187.27	57.24	20.24
9 months	8	65.31	25.40	130.73	35.87	12.68
12 months	8	47.38	19.07	91.00	22.86	8.08
15 months	8	47.36	21.67	87.13	23.98	8.48
16 months	8	47.53	19.00	118.00	31.22	11.04
17 months	7	69.37	49.11	93.78	16.67	6.30
18 months	7	85.73	39.53	146.33	39.46	14.91
21 months	6	72.39	37.40	125.60	38.00	15.51

Table 3.3. Male rotarod data from the ageing study.

Mean latency to fall (seconds) from the rotarod for both male groups (wildtypes (table a) and heterozygotes (table b)) from all time points of the ageing study. N indicates the number of animals in the group at any given timepoint, Mean is the average fall time of the group over the month, Min is the minimum fall time of an individual in the group, Max is the maximum fall time for an individual in the group, S.D indicates the standard deviation across the group and S.E.M is a measure of the standard error of the mean.

a. Female wildtype data

Age	N	Mean	Min	Max	S.D	S.E.M
3 months	8	89.12	53.87	179.73	42.21	14.92
6 months	8	68.67	33.67	153.13	39.15	13.84
9 months	8	53.61	25.07	133.40	34.17	12.08
12 months	8	48.40	19.27	90.80	23.54	8.32
15 months	8	43.13	28.67	65.33	13.92	4.92
16 months	7	31.57	22.22	48.67	8.65	3.27
17 months	6	59.44	35.67	112.11	28.47	11.62
18 months	5	67.95	45.93	126.13	33.48	14.97
21 months	4	68.18	40.53	115.47	32.66	16.33

b. Female heterozygote data

Age	N	Mean	Min	Max	S.D	S.E.M
3 months	8	85.13	54.80	123.47	23.00	8.13
6 months	8	63.41	40.33	125.07	28.70	10.15
9 months	8	50.06	24.13	76.27	17.33	6.13
12 months	7	40.52	25.27	64.00	12.58	4.76
15 months	5	34.57	30.20	43.27	5.27	2.36
16 months	5	27.07	19.00	36.22	6.11	2.73
17 months	5	61.51	51.22	75.56	9.49	4.25
18 months	5	56.88	46.53	67.67	8.29	3.71
21 months	3	53.42	42.20	68.33	13.45	7.77

Table 3.4. Female rotarod data from the ageing study.

Mean latency to fall (seconds) from the rotarod for both female groups (Wildtypes (table a) and Heterozygotes (table b)) from all time points of the ageing study. N indicates the number of animals in the group at any given timepoint, Mean is the average fall time of the group over the month, Min is the minimum fall time of an individual in the group, Max is the maximum fall time for an individual in the group, S.D indicates the standard deviation across the group and S.E.M is a measure of the standard error of the mean.

3.3.2.5. Grip strength

As a grip strength meter is thought to provide accurate readings of limb strength and is also able to accurately detect difference between wasted animals and wildtype controls, it was selected as another test for this ageing cohort.

Mice were tested tri-monthly from 3 months of age to 21 months of age. Readings from forelimbs only were taken as well as for all four limbs combined. On a single test day three readings were taken from forelimbs only and 3 readings were taken from all four limbs. In any given testing month these tests were carried out on the Friday of week two of the rotarod test period i.e. two days after the last rotarod test day.

Figure 3.10 (forelimbs only) and 3.11 (all four limbs combined) show the grip strength test results of each testing month separately. Mean data for each animal was normalised to its body weight before combining the group data. There was no significant difference between any of the groups at any time point over the course of the study. This was confirmed statistically using the Students t-test. However at 21 months it appears that female heterozygotes are performing slightly worse than the other 3 groups in the forelimb test only. As can be observed from the combined data in figure 3.12 (and also in tables 3.5 and 3.6) up until 15 months age appears to have no effect on performance. Between 16-18 months of age however there appears to be an increase in performance in all groups. This is most likely due to the increase in exercise the animals received during this time period when the frequency of rotarod testing was increased.

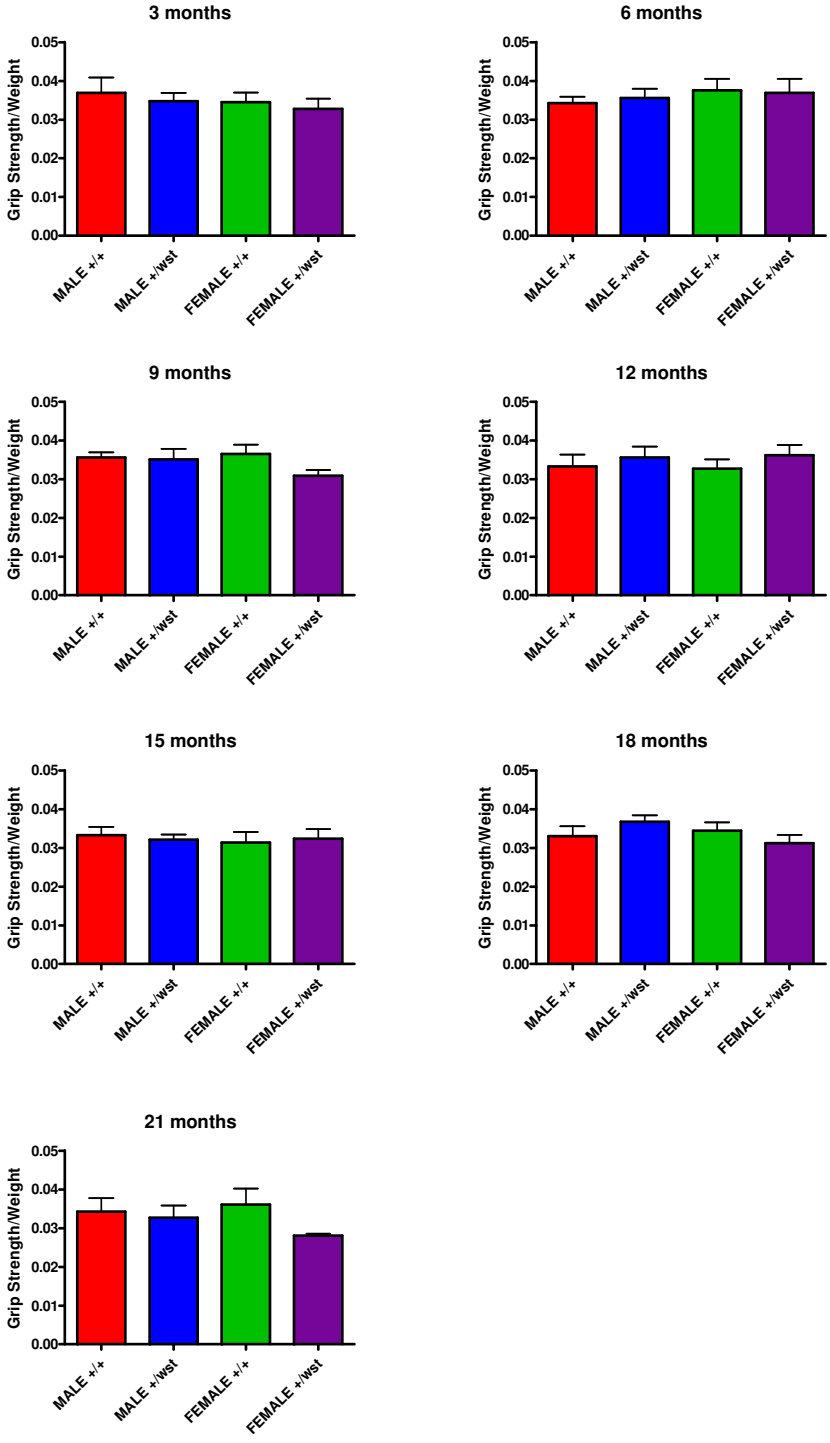

Figure 3.10. Monthly forelimb grip strength data from the ageing study.

Mean monthly grip strength from the forelimbs only of the animals in the ageing study between 3 and 21 months of age. +/+ indicates wildtype animals, *+/wst* indicates heterozygote animals. Error bars represent the standard error of the mean.

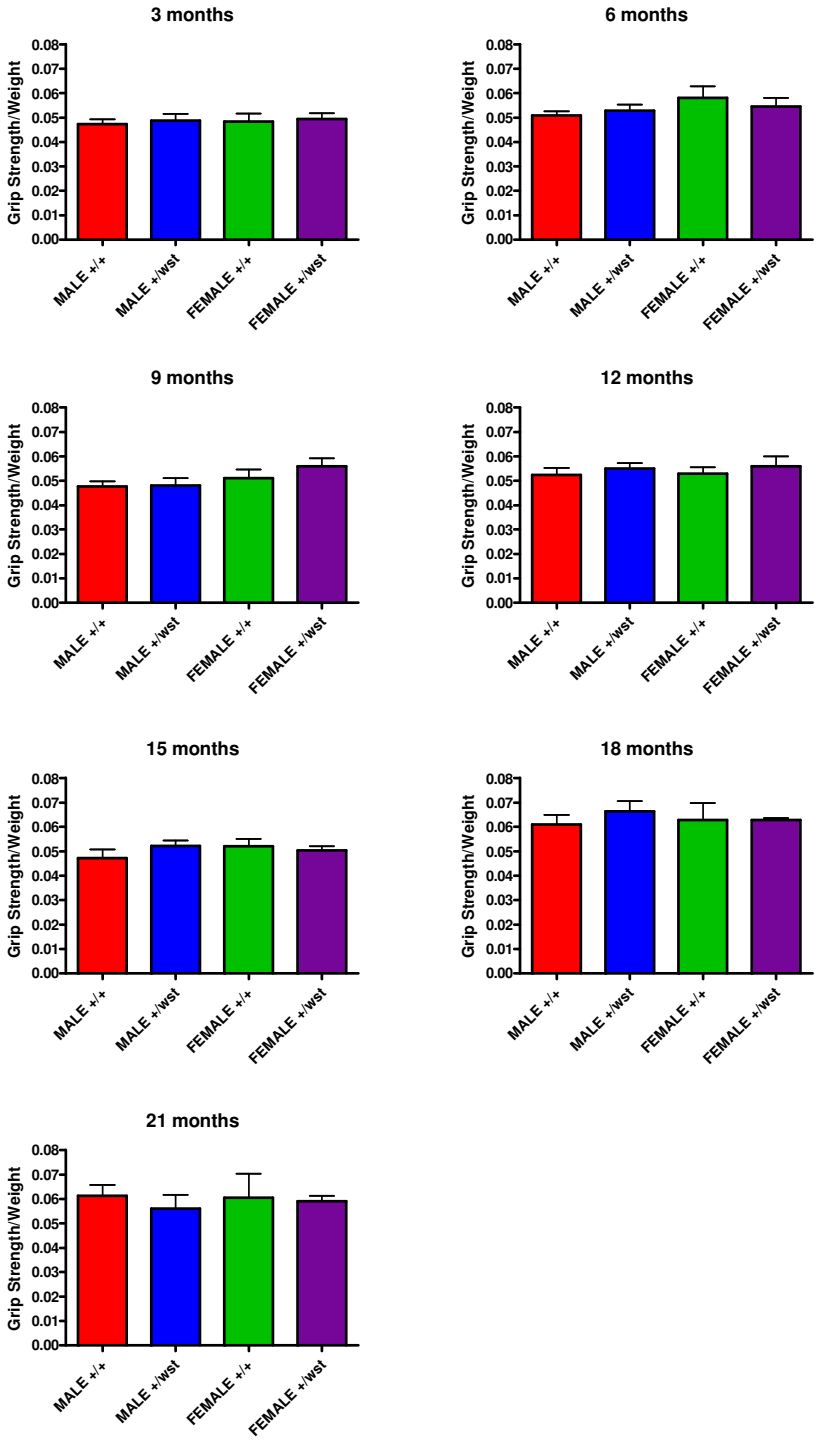

Figure 3.11. Monthly grip strength data from all four limbs combined from the ageing study.

Mean monthly grip strength from the forelimbs only of the animals in the ageing study between 3 and 21 months of age. +/+ indicates wildtype animals, *+/wst* indicates heterozygote animals. Error bars represent the standard error of the mean.

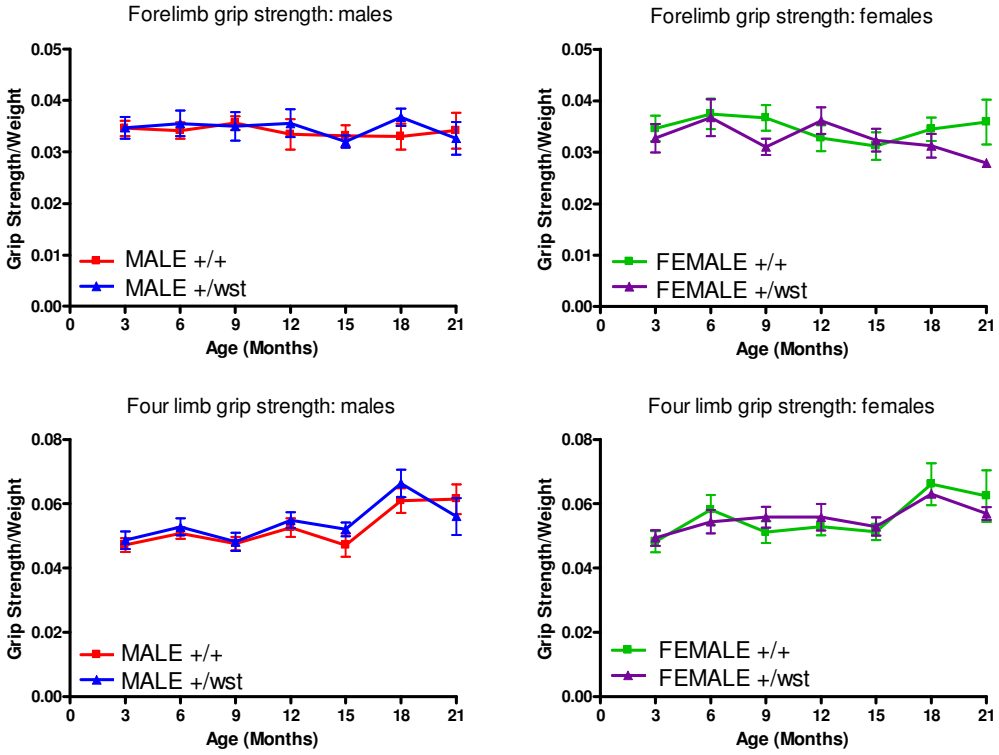

Figure 3.12. All grip strength data from the ageing study.

Collated grip strength data for the entire ageing study. Graphs on the left display male data and graphs on the right display female data. Top graphs display forelimb data only and the bottom 2 graphs display data from all four limbs. +/+ indicates wildtype animals, *+/wst* indicates heterozygote animals. Error bars represent the standard error of the mean.

a	Male Wildtypes +/+						Male Heterozygotes *+/wst*					
Age	**N**	**Mean**	**Min**	**Max**	**S.D**	**S.E.M**	**N**	**Mean**	**Min**	**Max**	**S.D**	**S.E.M**
3	8	0.035	0.031	0.044	0.004	0.001	8	0.035	0.028	0.047	0.006	0.002
6	8	0.034	0.028	0.040	0.004	0.002	8	0.036	0.028	0.046	0.007	0.003
9	8	0.036	0.030	0.042	0.004	0.001	8	0.035	0.024	0.045	0.008	0.003
12	8	0.033	0.025	0.047	0.008	0.003	8	0.036	0.029	0.046	0.008	0.003
15	7	0.033	0.023	0.040	0.006	0.002	8	0.032	0.027	0.038	0.003	0.001
18	7	0.033	0.027	0.041	0.007	0.003	7	0.037	0.032	0.042	0.005	0.002
21	5	0.034	0.026	0.046	0.008	0.004	6	0.033	0.024	0.044	0.008	0.003

b	Female Wildtypes +/+						Female Heterozygotes *+/wst*					
Age	**N**	**Mean**	**Min**	**Max**	**S.D**	**S.E.M**	**N**	**Mean**	**Min**	**Max**	**S.D**	**S.E.M**
3	8	0.035	0.028	0.046	0.007	0.002	8	0.033	0.019	0.042	0.008	0.003
6	8	0.037	0.029	0.056	0.008	0.003	8	0.037	0.024	0.057	0.010	0.004
9	8	0.037	0.029	0.049	0.007	0.002	8	0.031	0.025	0.036	0.004	0.002
12	8	0.033	0.023	0.045	0.007	0.003	7	0.036	0.023	0.043	0.007	0.003
15	8	0.031	0.025	0.049	0.008	0.003	5	0.032	0.025	0.038	0.005	0.002
18	5	0.034	0.030	0.041	0.005	0.002	5	0.031	0.026	0.036	0.005	0.002
21	4	0.036	0.028	0.048	0.009	0.004	3	0.028	0.027	0.029	0.001	0.001

Table 3.5. Forelimb grip strength data from the ageing study normalised to body weight.

Forelimb grip strength data from all time points of the ageing study normalised to body weight. Table (a) shows data from male groups and table (b) shows data from female groups. N= number of animals in the group, Mean = average of group, Min = minimum reading of group, max= maximum reading of group, S.D = standard deviation, S.E.M = standard error of the mean.

a	Male Wildtypes +/+						Male Heterozygotes *+/wst*					
	N	Mean	Min	Max	S.D	S.E.M	N	Mean	Min	Max	S.D	S.E.M
3	8	0.047	0.040	0.060	0.006	0.002	8	0.049	0.036	0.063	0.008	0.003
6	8	0.051	0.036	0.058	0.005	0.002	8	0.053	0.035	0.063	0.007	0.003
9	8	0.048	0.040	0.060	0.006	0.002	8	0.048	0.040	0.066	0.008	0.003
12	8	0.053	0.042	0.067	0.008	0.003	8	0.055	0.038	0.063	0.007	0.002
15	7	0.047	0.040	0.061	0.010	0.004	7	0.047	0.040	0.061	0.010	0.004
18	7	0.061	0.054	0.077	0.010	0.004	7	0.066	0.046	0.082	0.011	0.004
21	5	0.061	0.051	0.075	0.010	0.005	6	0.056	0.042	0.076	0.014	0.006

b	Female Wildtypes +/+						Female Heterozygotes *+/wst*					
	N	Mean	Min	Max	S.D	S.E.M	N	Mean	Min	Max	S.D	S.E.M
3	8	0.048	0.035	0.060	0.009	0.003	8	0.049	0.043	0.062	0.007	0.002
6	8	0.058	0.044	0.082	0.013	0.005	8	0.054	0.041	0.074	0.010	0.004
9	8	0.051	0.038	0.067	0.010	0.003	8	0.056	0.045	0.073	0.009	0.003
12	8	0.053	0.045	0.068	0.008	0.003	7	0.056	0.046	0.079	0.011	0.004
15	8	0.052	0.040	0.060	0.006	0.002	8	0.052	0.043	0.066	0.008	0.003
18	5	0.063	0.052	0.089	0.016	0.007	5	0.063	0.061	0.065	0.002	0.001
21	4	0.061	0.049	0.090	0.020	0.010	3	0.059	0.055	0.063	0.004	0.002

Table 3.6. Four limb grip strength data from the ageing study normalised to body weight.

All four limb grip strength data from all time points of the ageing study normalised to body weight. Table (a) shows data from male groups and table (b) shows data from female groups. N= number of animals in the group, Mean = average of group, Min = minimum reading of group, max= maximum reading of group, S.D = standard deviation, S.E.M = standard error of the mean.

3.3.2.6. Pathology

At 21 months the behavioural study was terminated and pathological analysis was undertaken on the animals.

Western Blotting

Protein levels of eEF1A2 in brain, spinal cord and muscle were examined by Western blot as seen in figure 3.13. Three examples of each of the four groups were selected at random for analysis. All of these animals were from the end stage of the study i.e. 21 months of age. As can be seen in figure 3.13 expression of eEF1A2 is decreased in heterozygote animals (both males and females) compared to the wildtype controls in all three tissue types. The graphs in figure 3.14 show this decrease normalised to GAPDH protein as a loading control. In brain male heteozygotes express 7.5% of eEF1A2 compared to wildtype males and female heterozygotes express 36% compared to wildtype females. In spinal cord males express 45.5% of the level of wildtype males, while female heterozygotes express 38% of wildtype females. Finally in muscle male heterozygotes express 59% of wildtype eEF1A2 and female heterozygotes express 26% of wildtype female eEF1A2.

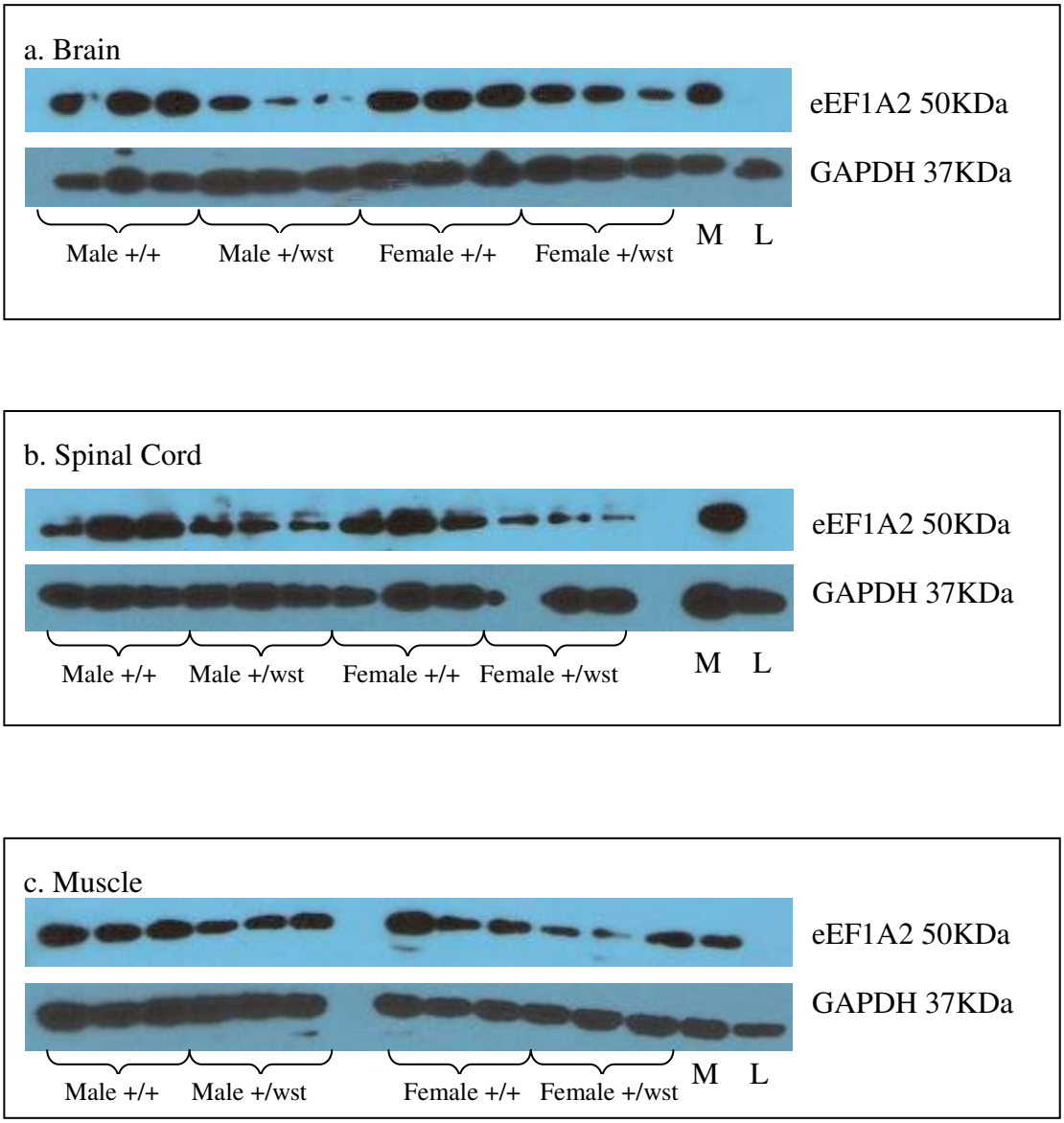

Figure 3.13. eEF1A2 protein expression in tissues from the ageing cohort.

Western blots showing protein expression of eEF1A2 and GAPDH (as a loading control) of animals from the ageing cohort. Three 21month old animals from each group are shown. +/+ indicates wildtype animals, *+/wst* indicates heterozygous animals, M indicates a muscle sample (as an eEF1A2 positive control) and L indicates a liver sample (an eEF1A2 negative control).

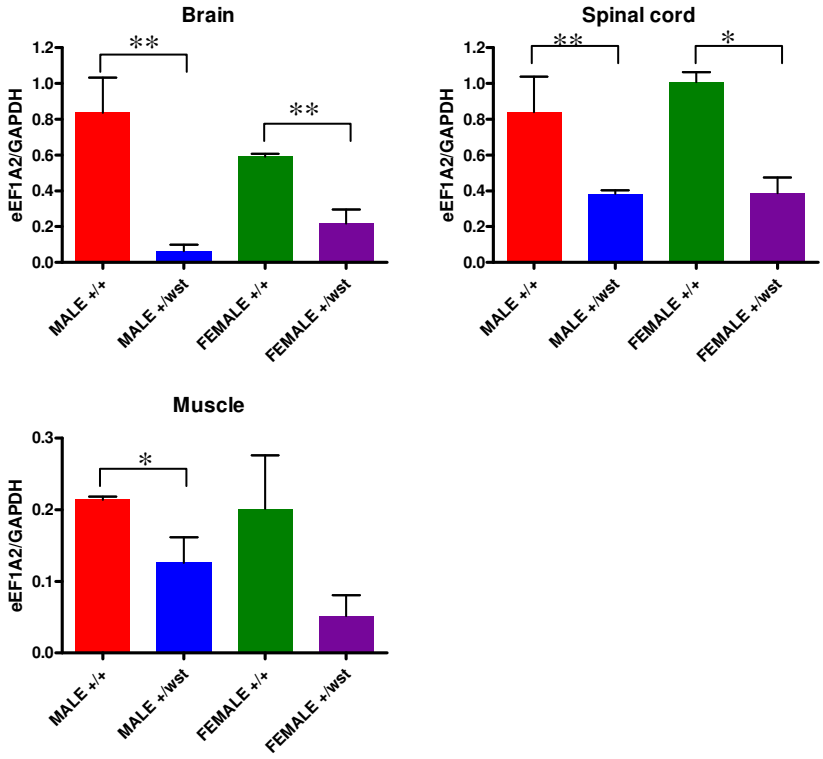

Figure 3.14. eEF1A2 protein expression in tissues from the ageing cohort. Expression of eEF1A2 protein normalised to GAPDH. +/+ indicates wildtype animals, *+/wst* indicates heterozygote animals. Error bars represent the standard error of the mean. * indicates a p value <0.05, ** indicates a p value<0.01.

Immunohistochemistry

To address whether there may be any differences in the pathology of the spinal cord between heterozygotes and wildtype controls, spinal cord sections were examined by immunohistochemistry. These experiments were undertaken by James Ding under my supervision.

Sections were stained with an antibody for glial fibrillary acidic protein (GFAP) as a marker of gliosis. In wasted mice reactive gliosis is the earliest observable abnormality in the spinal cord (Newbery *et al.,* 2005) and an example is shown in figure 3.15 panel b. No observable differences were seen in GFAP staining between wildtypes and heterozygotes of the ageing study. Examples of each of the 4 groups can be seen in figure 3.15 (panels c-f). Unlike younger wildtype animals (figure 3.15 panel a), these older wildtypes display a significant level of reactive gliosis characterised by numerous GFAP positive foci in the grey matter of the spinal cord (figure 3.14 c and d). In wasted mice there is a rostrocaudal gradient of gliosis within the spinal cord. The cervical region displays increased gliosis compared to the thoracic and lumbar levels. Cervical, thoracic and lumbar regions of the spinal cord were all examined in this study. However due to the heavy staining in all sections it proved difficult to establish any difference between regions of the spinal cord.

Sections were also stained with an antibody that recognises phosphorylated neurofilaments (both light and heavy chain). Typically young wildtype mice show little or no staining in neuronal cytoplasm (figure 3.16 panel a), whereas 64-100% of motor neurons in the spinal cord of wasted animals show staining of neuronal cytoplasm (Newbery *et al.,* 2005) (figure 3.16 panel b). The same level of staining was not observed in the heterozygote animals from the ageing study. Occasionally 1 or 2 neurons were observed that had neurofilament staining (as seen in the female heteozygote section in figure 3.16 panel f) but this occurred in both wildtypes and heterozygotes. This supports the findings of Newberry *et al* (Newbery *et al.,* 2005) which showed occasional staining of neuronal cytoplasm in control animals. In conclusion, no significant differences were observed in the pathology of the spinal cords from wildtype and heterozygote animals from the ageing study.

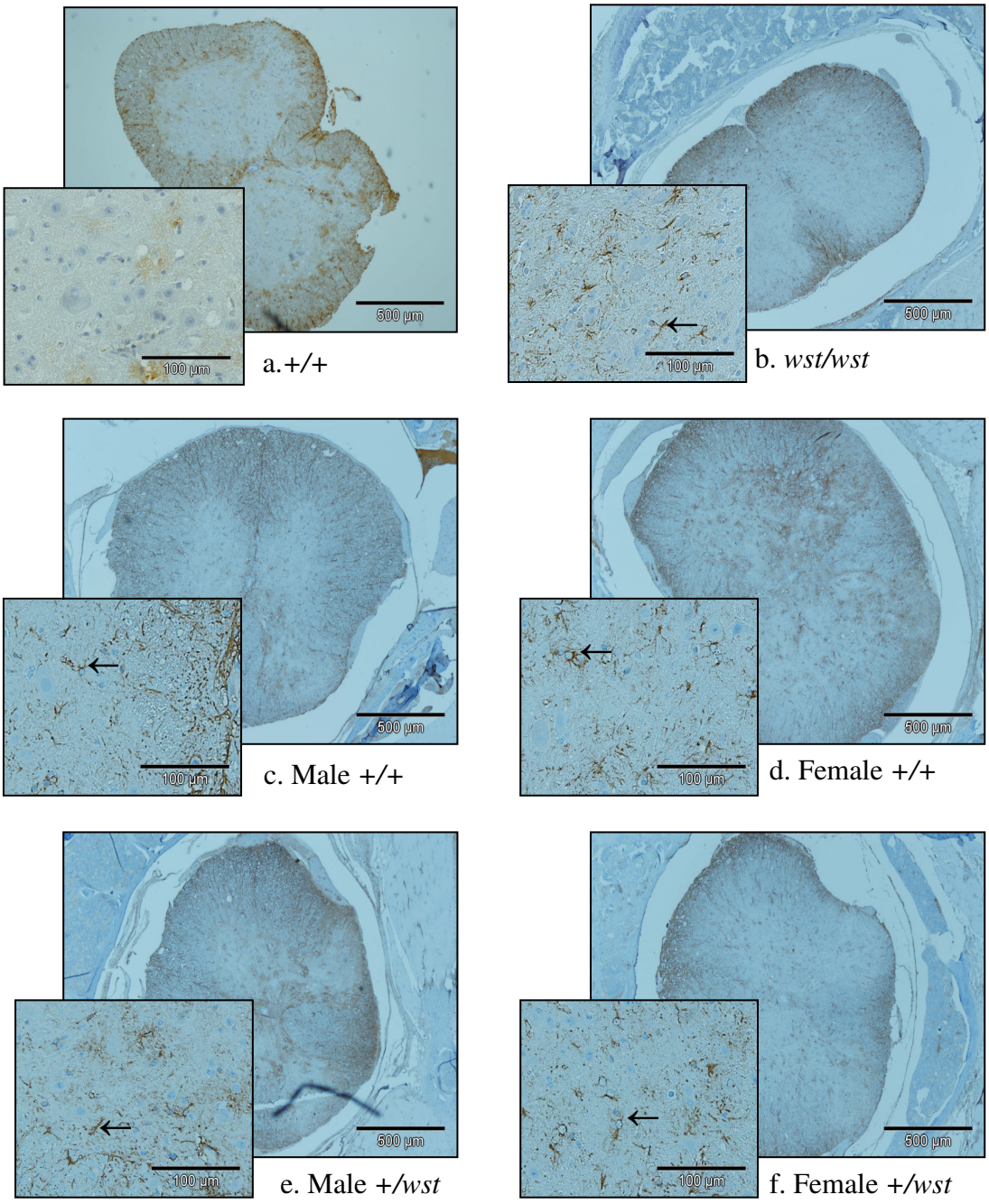

Figure 3.15. GFAP expression in the spinal cord of animals from the ageing study. Cervical spinal cord sections from animals from the ageing study stained with an antibody recognising glial fibrillary acidic protein (GFAP). Section (a) is a section from a 24 day old wildtype animal, (b) is a section from a 24 day old wasted animal as a positive control. (c-e) show examples of each of the four groups of the ageing study all of which show characteristic staining of reactive astrocytes throughout the grey matter of the spinal cord (arrowed) The larger panels are at 4x magnification showing the entire spinal cord section while the smaller panels are a x20 magnification of anterior horn section. These results were obtained using the POLINK method.

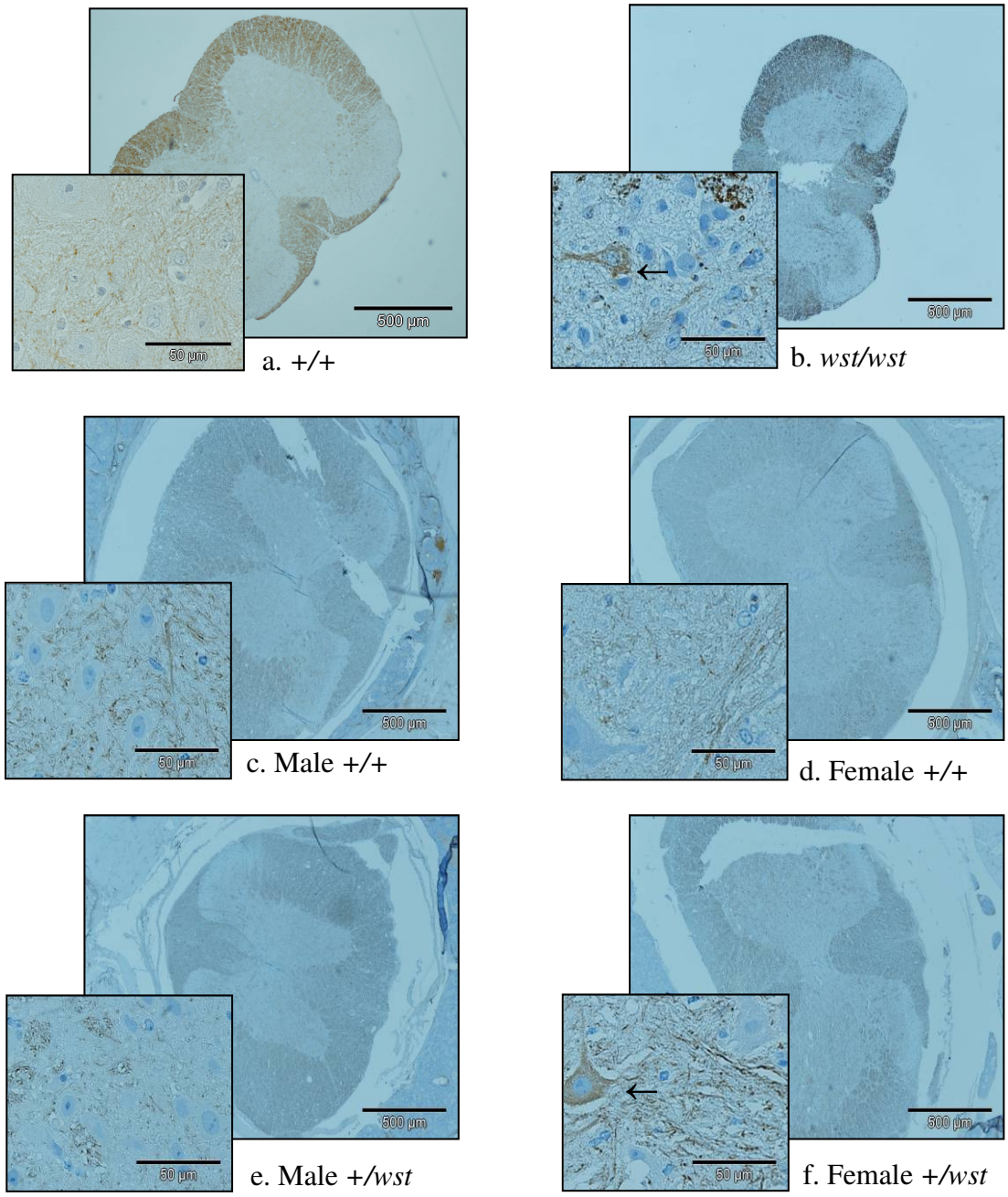

Figure 3.16. Phosphorylated neurofilament expression in the spinal cord of animals from the ageing study.

Cervical spinal cord sections from animals from the ageing study stained with an antibody recognising phosphorylated neurofilaments. Section (a) is from a 24 day old wildtype (+/+), (b) is a section from a 24 day old wasted (*wst/wst*) animal as a positive control. (c-e) show examples of each of the four groups of the ageing cohorts. The larger panels are at 4x magnification showing the entire spinal cord section while the smaller panels are at x40 magnification of anterior horn section. These results were obtained using the POLINK method.

Spinal cord sections were stained with an antibody recognising eEF1A2 to crudely count the motor neurons of the anterior horn section of the spinal cord. Figure 3.17 shows examples of spinal cord staining with the eEF1A2 specific antibody. No significant difference was observed in eEF1A2 staining between wildtypes and heterozygotes of either sex in these sections.

The motor neuron counts were conducted blind by 2 separate individuals each with some experience of examining sections of spinal cord. When counting, the investigators marked on images which cells were counted as motor neurons so any discrepancies could be checked. An example of one such image is shown in figure 3.18. The anterior horn section was divided by drawing a straight line from the central canal to the most central anterior point of the spinal cord. Another line was then drawn perpendicular to this. Motor neurons were counted in the area between these lines as shown in figure 3.18. This region is defined as in Fischer *et al* (Fischer *et al.,* 2004). The images for this analysis were prepared by James Ding under my supervision. No significant differences were observed in motor neuron numbers between wildtypes and heterozygotes at any region of the spinal cord (table 3.7). The graphs (figure 3.19) do show however that heterozygotes (both male and female) show slightly reduced numbers of motor neurons in the thoracic and lumbar regions of the spinal cord.

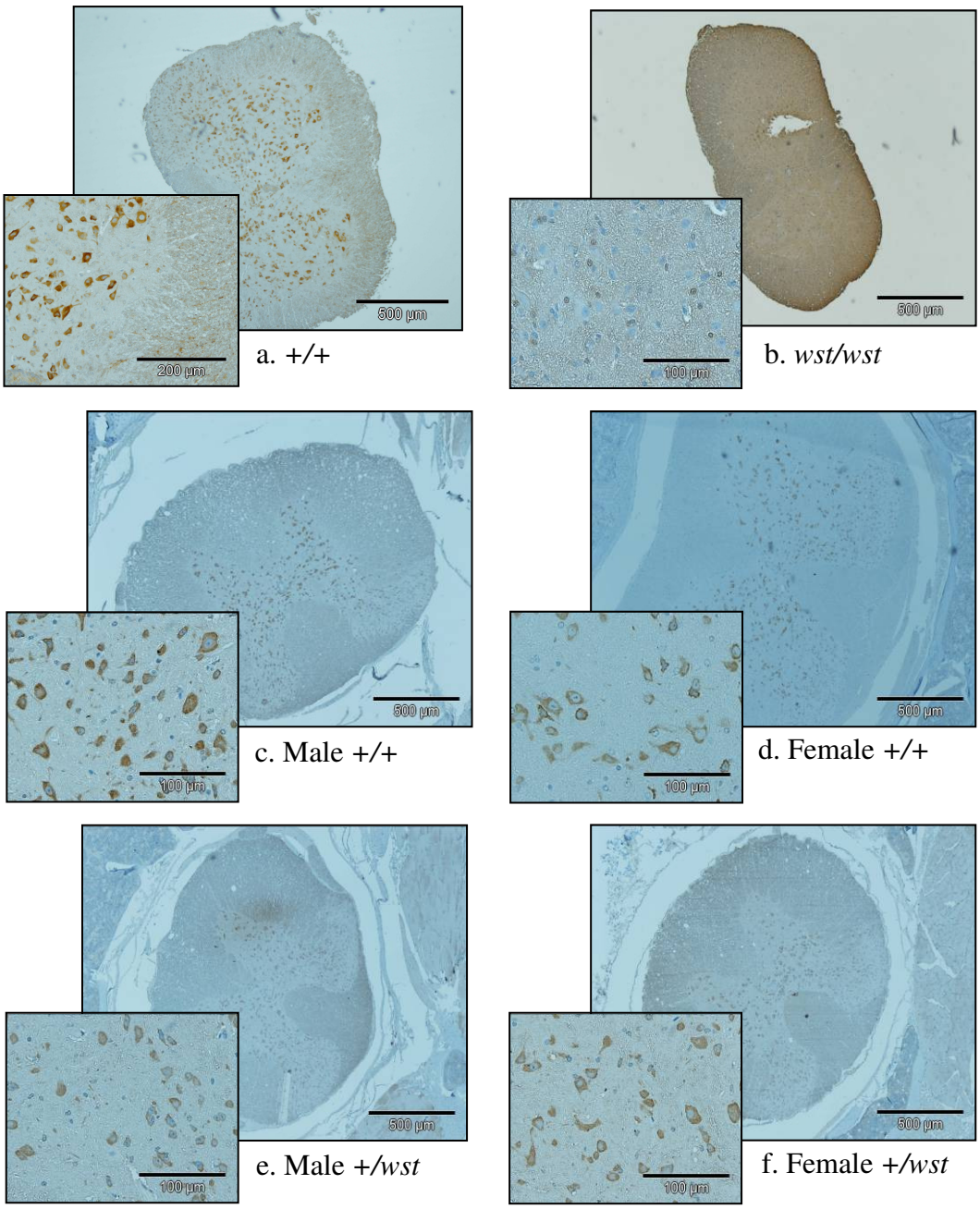

Figure 3.17. eEF1A2 expression in the spinal cord of animals from the ageing study.

Cervical spinal cord sections from animals from the ageing study stained with an antibody recognising eEF1A2. Section (a) is a section from a 24 day old wildtype animal, (b) is a section from a 24 day old wasted animal as a negative control. (c-f) show examples of each of the four groups of the ageing study. The larger panels are at 4x magnification showing the entire spinal cord section while the smaller panels are a x20 magnification of anterior horn section (except for sample (a) where the smaller panel is at x10). These results were obtained using the EnVision method.

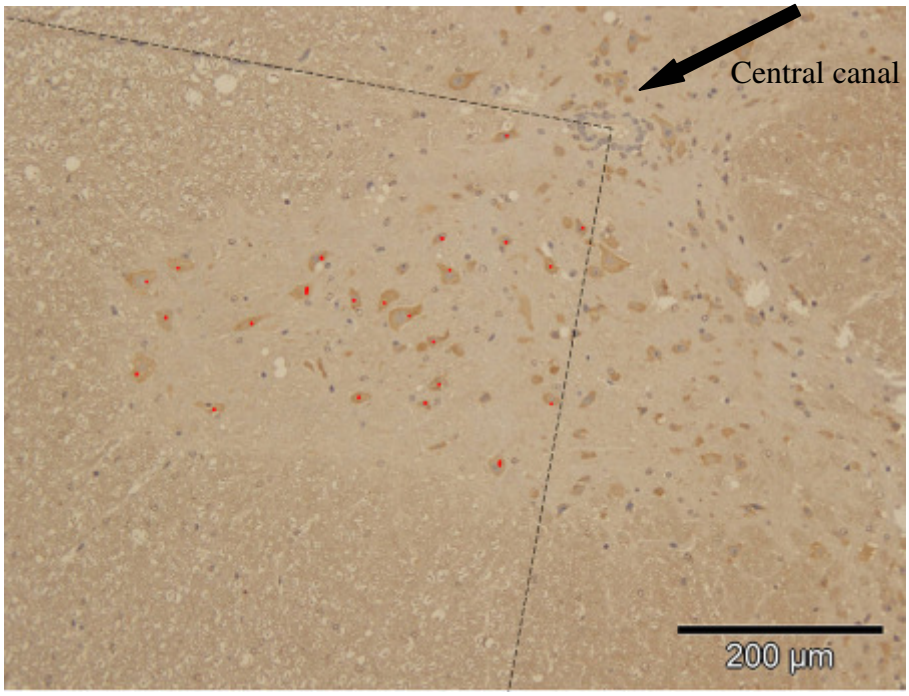

Figure 3.18. An example of a motor neuron count.

An example of how counts were conducted for the motor neuron counts. Counts were conducted in one anterior horn of each section. Each motor neuron was marked with a red dot as seen in the image. The black arrow shows the position of the central canal.

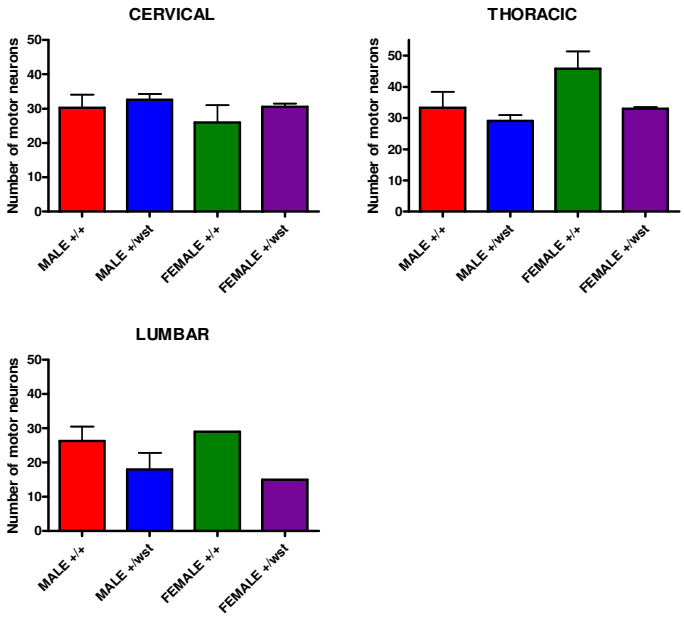

Figure 3.19. Motor neuron numbers from the spinal cords of the ageing cohort. Mean motor neuron counts from spinal cord sections from the ageing cohort. +/+ indicates wildtype animals, *+/wst* indicates heterozygote animals, Error bars represent the standard error of the mean.

Group	Section	N	Mean	Min	Max	SD	SEM
MALE +/+	Cervical	6	30.25	17	45	9.42	3.85
	Thoracic	6	33.25	16	49	12.62	5.15
	Lumbar	4	26.25	19	38	8.43	4.22
MALE *+/wst*	Cervical	5	32.6	29	37	3.83	1.71
	Thoracic	6	29.1	25.5	37.5	4.55	1.86
	Lumbar	4	14.4	10	32	9.64	4.82
FEMALE +/+	Cervical	2	26	21	31	7.07	5.00
	Thoracic	3	36.7	38	56.5	9.57	5.53
	Lumbar	1	29	29	29	N/A	N/A
FEMALE *+/wst*	Cervical	2	30.5	29.5	31.5	1.41	1.00
	Thoracic	2	33	32.5	33.5	0.71	0.50
	Lumbar	1	15	15	15	N/A	N/A

Table 3.7: Motor neuron numbers from the spinal cords of the ageing cohort. Mean motor neuron counts from spinal cord sections from the ageing cohort. +/+ indicates wildtype animals, *+/wst* indicates heterozygote animals N= number of animals in the group, Mean = average of group, Min = minimum reading of group, max= maximum reading of group, S.D = standard deviation, S.E.M = standard error of the mean.

3.3.3. The second ageing study

A possible explanation for the fact that no significant difference was observed in the ageing cohort could be that the repeated exposure to the behavioural test was somehow masking any difference. This is discussed further in the discussion section of this chapter.

A second cohort of animals was therefore tested. These animals had not been exposed to the any tests in the past. An 18 month old cohort consisting of 3 wildtype males, 3 heterozygous males, 3 wildtype females and 4 heterozygote females were tested on the rotarod and with the grip strength meter. These animals were tested as in the ageing study with 5 rotarod tests over a fortnight, with tests being conducted on alternate days.

Female heterozygote animals appear to perform worse than the controls on both the rotarod (figure 3.20) and the grip strength meter (figure 3.21). This difference however, is not statistically significant.

A 12 month old cohort of females was also tested (no males of the correct age were available). This cohort consisted of 2 wildtype females and 5 heterozygote females.

Heterozygote females again appear to perform worse than wildtype females on the rotarod (figure 3.22) and on the grip strength meter (figure 3.23) but once again this difference is not statistically significant.

The rotarod data from this most recent 12 month old female cohort was combined with the data from Antonia's pilot study. As different rotarod were used in these 2 studies the data was initially expressed as the mean difference between wildtypes and heterozygotes before combining the two data sets (figure 3.24). These combined results show that heterozygote females at 12 months show a 33% decreased performance compared to wildtype females.

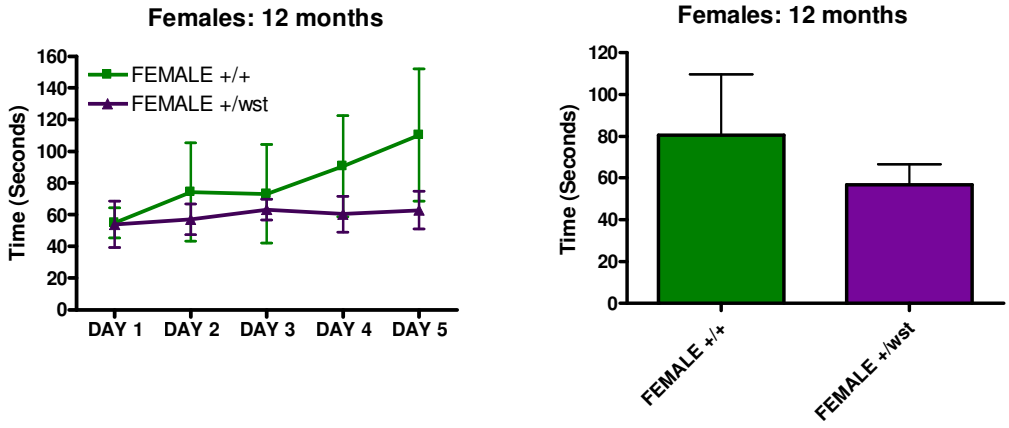

Figure 3.20. Rotarod data from 12 month old cohort.

Left graph shows mean daily times of latency to fall from the rotarod. Right graph shows mean monthly latency to fall times. +/+ indicates wildtype animals, *+/wst* indicates heterozygote animals. Error bars represent the standard error of the mean.

Group	N	Mean	Min	Max	S.D	S.E.M
Female +/+	2	80.67	51.6	109.7	41.11	29.07
Female *+/wst*	5	56.87	38.8	95.07	21.96	9.821

Table 3.8. Rotarod data from the 12 month old cohort.

Number of animals (N), average latency to fall time (Mean), group minimum (Min) and maximum (Max) latency to fall, standard deviation (S.D) and standard error of the mean (SEM) are shown. +/+ indicates wildtype animals, *+/wst* indicates heterozygote animals group

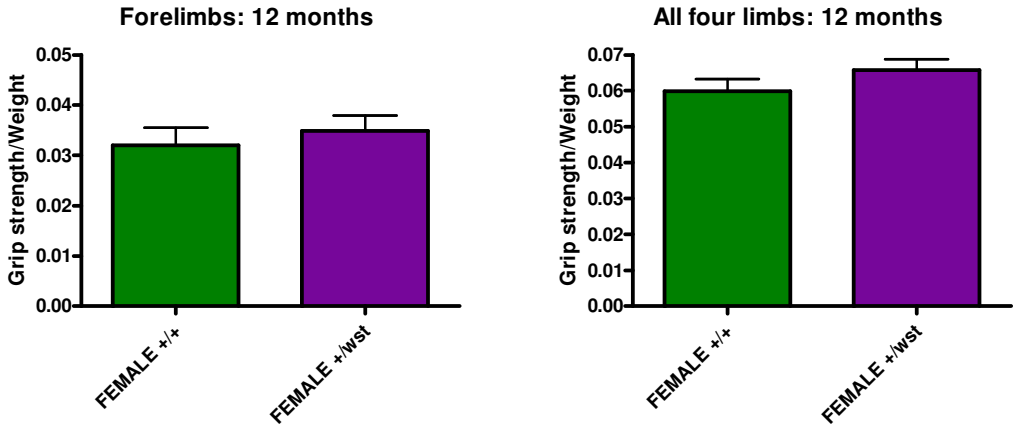

Figure 3.21. Grip strength data from the 12 month old cohort.

Left graph shows mean forelimb grip strength of cohort. Right graph shows mean grip strength for all four limbs. +/+ indicates wildtype animals, *+/wst* indicates heterozygote animals. Error bars represent the standard error of the mean.

a. Forelimbs

Group	N	Mean	Min	Max	S.D	S.E.M
Female +/+	2	0.032	0.029	0.036	0.005	0.004
Female *+/wst*	5	0.035	0.026	0.044	0.007	0.003

b. All four limbs

Group	N	Mean	Min	Max	S.D	S.E.M
Female +/+	2	0.060	0.056	0.063	0.005	0.003
Female *+/wst*	5	0.066	0.058	0.076	0.007	0.003

Table 3.9: Grip strength data from the 12 month old cohort.

Table (a) shows forelimb grip strength only and table (b) shows grip strength data from all four limbs. Number of animals (N), average latency to fall time (Mean), group minimum (Min) and maximum (Max) latency to fall, standard deviation (S.D) and standard error of the mean (SEM) are shown. +/+ indicates wildtype animals, *+/wst* indicates heterozygote animals group.

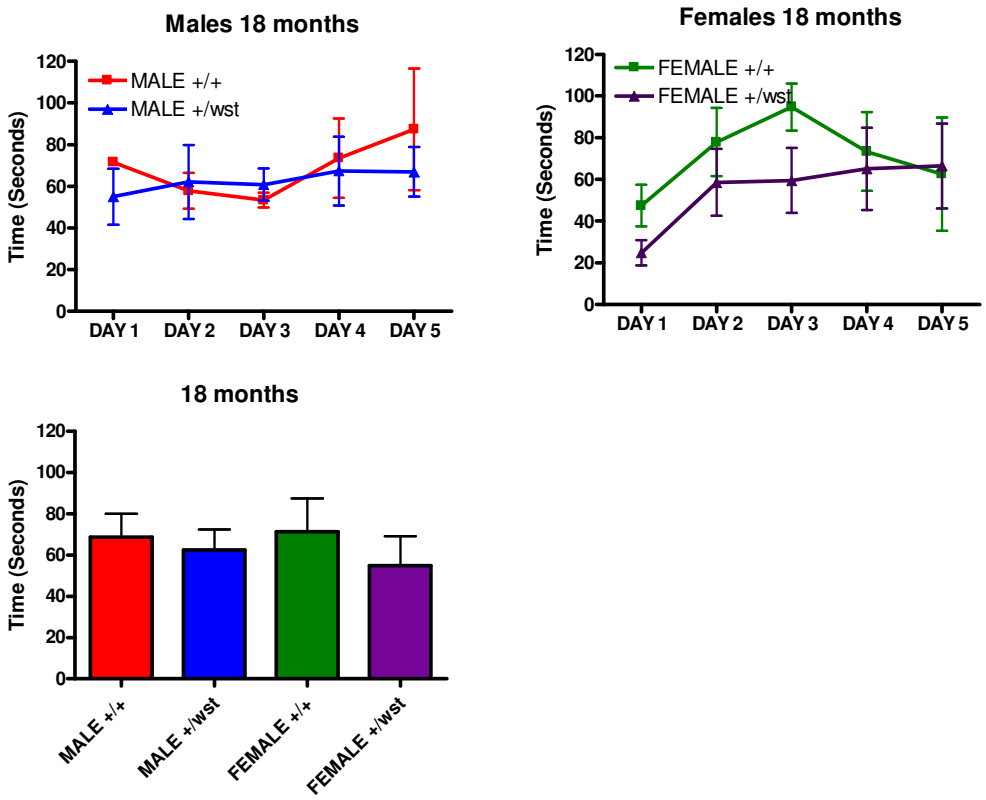

Figure 3.22. Rotarod data from the 18 month old cohort.

Upper graphs shows mean daily times of latency to fall from the rotarod. Lower graph shows mean monthly latency to fall times. +/+ indicates wildtype animals, *+/wst* indicates heterozygote animals. Error bars represent the standard error of the mean.

Group	N	Mean	Min	Max	S.D	S.E.M
Male +/+	3	60.89	54	65.56	6.09	3.516
Male *+/wst*	3	59.33	40.89	82.78	21.39	12.35
Female +/+	3	73.37	58.56	97.56	21.12	12.19
Female *+/wst*	4	47.61	23.78	79.67	24.05	12.03

Table 3.10. Rotarod data from the 18 month old cohort.

Number of animals (N), average latency to fall time (Mean), group minimum (Min) and maximum (Max) latency to fall, standard deviation (S.D) and standard error of the mean (SEM) are shown. +/+ indicates wildtype animals, *+/wst* indicates heterozygote animals.

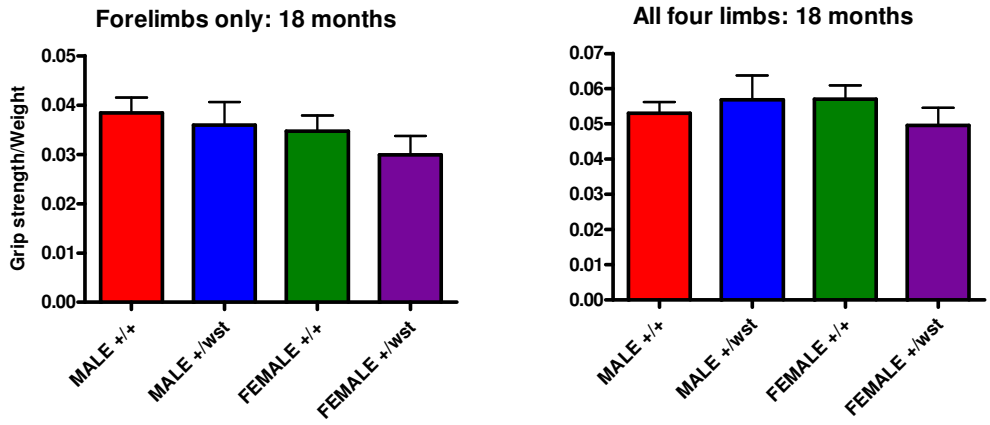

Figure 3.23. Grip strength data from the 18 month old cohort.

Left graph shows mean daily forelimb grip strength of cohort. Right graph shows mean grip strength for all four limbs. +/+ indicates wildtype animals, +/*wst* indicates heterozygote animals. Error bars represent the standard error of the mean.

a. Forelimbs

Group	N	Mean	Min	Max	S.D	S.E.M
Male +/+	3	0.038	0.032	0.042	0.005	0.003
Male +/*wst*	3	0.036	0.027	0.042	0.008	0.005
Female +/+	3	0.035	0.028	0.039	0.006	0.003
Female +/*wst*	3	0.026	0.023	0.031	0.004	0.003

b. All four limbs

Group	N	Mean	Min	Max	S.D	S.E.M
Male +/+	3	0.053	0.049	0.059	0.005	0.003
Male +/*wst*	3	0.057	0.045	0.069	0.012	0.007
Female +/+	3	0.057	0.050	0.064	0.007	0.004
Female +/*wst*	3	0.049	0.039	0.063	0.012	0.007

Table 3.11. Grip strength data from the 18 month old cohort.

Table (a) shows forelimb grip strength data only and table (b) shows grip strength data from all four limbs. Number of animals (N), average latency to fall time (Mean), group minimum (Min) and maximum (Max) latency to fall, standard deviation (S.D) and standard error of the mean (SEM) are shown. +/+ indicates wildtype animals, +/*wst* indicates heterozygote animals.

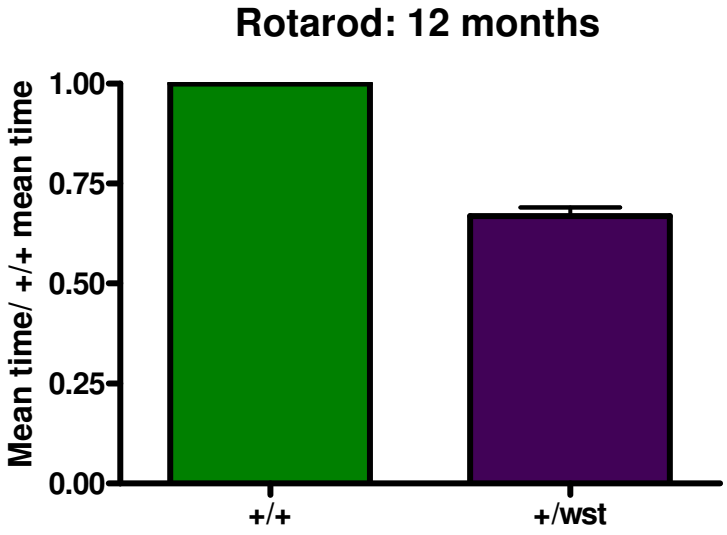

Figure 3.24. Rotarod data from the 12 month old cohort combined with the 12 month old pilot study.

Mean times of latency to fall from the rotarod of wildtype and heterozygote animals normalised to wildtypes. +/+ indicates wildtype animals, *+/wst* indicates heterozygote animals. Error bars represent the standard error of the mean.

3.4. Discussion

In this project, ageing wasted heterozygote (*+/wst*) animals were investigated for signs of late onset motor neuron degeneration.

The rotarod was used as the primary behavioural test in this study. This easily quantifiable task is thought of as the gold standard for detection of motor impairment. It has been shown previously that wasted mice perform significantly worse than wildtype controls on the accelerating rotarod from 21 days (Newbery *et al.,* 2005). The grip strength meter was investigated to establish if this test could categorize wasted mice earlier than the rotarod. Newbery *et al* (Newbery *et al.,* 2005) showed that the sequence of events in wasted mice begins with gliosis in the spinal cord, followed by retraction of motor nerve terminals in muscle and finally motor neuron pathology and death. As retraction of motor nerve terminals precedes motor neuron pathology in wasted mice it would be possible that the grip strength meter may detect any deficit before the rotarod. In the test of forelimbs only and all four limbs combined, wasted mice had significantly lower grip strength than controls by 20 days. This is a day earlier than detection by rotarod. The difference between groups was more significant when analysing forelimbs only compared to all four limbs. This supports previous data from our group (Newbery *et al.,* 2005) which indicated that the disease severity of spinal cord pathology shows a rostrocaudal gradient. To complete this data it would be interesting to see the results of measuring hindlimbs only however this proved too difficult to conduct.

The results of the first ageing study show no statistically significant differences between wildtype and heterozygote animals of either gender in either rotarod performance or grip-strength. However, female heterozygotes from around 12 months of age do perform slightly worse than wildtype controls on the rotarod. The study was limited by numerous factors and presents many possible avenues for future investigations.

Firstly the tests themselves have limitations. A common problem with the rotarod test is that mice may cling to the beam and rotate instead of falling when they lose balance. If this occurred in this study, mice were permitted to rotate 360^{o} while

clinging to the beam only once. If they then began to walk again the test was allowed to continue. If however the mouse rotated more than once the test was terminated and the time measurement taken immediately following the first rotation. Another factor that can affect rotarod performance is weight, with smaller, lighter mice performing better than overweight animals. To account for this variable, data was also analysed with normalisation to body weight (data not shown). No significant differences were observed in either data set. Finally, susceptibility to fatigue may contribute to poor performance. A maximum time on the rotarod was set to 180 seconds as in Barneoud *et al* (Barneoud *et al.,* 1997) to try and limit fatigue that could be caused by allowing mice to continue indefinitely. Significant breaks were also given between tests on a given day to minimize this, and tests were not conducted on consecutive days to allow sufficient recovery time. It is possible that higher rotation rates at a fixed speed in future tests may ensure that falls are attributable to motor coordination and less to fatigue. Despite these problems the rotorod still remains the gold standard for measuring motor function in mice and so is still believed to be the best test for this study and future studies of this kind.

The grip strength meter has less confounding variables. The only variable that must be taken into account is weight, thus normalising the meter reading to body weight is required and was conducted in this study

Other tests could be considered in future studies. In some studies such as Barneoud *et al* (Barneoud *et al.,* 1997), the balance beam has shown to detect deficits in mouse models of neurodegeneration prior to the age at which motor neuron death is observed. Mice are trained to cross an elevated beam and the time taken to cross and/or the number of rear foot slips are recorded. This test that challenges fine motor balance and coordination was attempted in this study, however all mice (wildtypes and heterozygotes) performed poorly and thus it was deemed unsuitable. Mice displayed "hind limb dragging" where their abdomen were flattened against the upper surface of the beam and their hind limbs and tail were wrapped around the beam. They would therefore use their forelimbs to drag themselves across the beam instead of walking therefore measuring foot slips became an impossible task.

In future studies, further tests where training is not required could be used, such as gait abnormality using footprint tests, although previous attempts of this method in our lab have been problematic and often inconclusive. In a recent study Knippenberg *et al* compared several behavioural assessments to select the most appropriate methods for detecting motor symptom onset in the G93A SOD1 mouse model (Knippenberg *et al.,* 2010). This study states that deficits were observed first by rotarod and around a week later, by step length analyses. They concluded that while the rotarod detected the earliest signs of disease, the footprint test has the major advantages of being far less time consuming and costly and also is less stressful to the animals. Thus both assays should perhaps be considered for future studies. In the Barneoud *et al* study an inclined plane test was the first to detect any deficit in the G1H SOD1 transgenic mice (Barneoud *et al.,* 1997). Mice were scored based on their ability to remain on a wooden board which was set at varying angles between 70^{o}-$85.^{o}$

There are many options for further behavioural analysis of these animals in future however as previously mentioned the rotarod is known as the gold standard for this type of study and therefore should continue to be used in future studies. Other test could also be beneficial but mostly to further untangle the behavioural aspect of disease, not to replace the rotarod.

The more important issue that needs to be addressed for future studies is to understand why there was a statistically significant difference between heterozygotes and wildtypes in the pilot study but not in this ageing study.

There were some differences between these studies. The first of these was that the pilot mice had not been subjected to the rotarod repeatedly throughout their lives (as in the first ageing study described here). The difference in results could therefore be explained in terms of learning capability or differences in the amount of exercise the animals received during the course of the study. In a study comparing various behaviour testing methods in G1H mutant SOD1 transgenic mice, it was noted that the age at which animals are first tested was important in determining the age at which significant deficits could be observed (Barneoud *et al.,* 1997). This may be due to the differing abilities of the groups to learn and habituate to a given task. In

these studies both wildtypes and heterozygotes demonstrated learning behaviour in the rotarod test as when they only had 1 month between tests, performance in all groups increased compared to when tests were conducted every 3 months. This was also true of the Barneoud study(Barneoud *et al.,* 1997), in that both wildtypes and transgenics showed evidence of learning. Kirkinezos *et al* published a studying showing the beneficial effects of exercise on the G93A model of ALS (Kirkinezos *et al.,* 2003). Regular treadmill exercise over a 10 week period significantly expanded the lifespan of the diseased animals. Another study demonstrated that exercise delayed the onset of disease in females but not in males and had no affect on lifespan of either sex (Veldink *et al.,* 2003). This data suggested that regular exercise could potentially mask any differences between the wildtypes and heterozygotes in this study and therefore may explain why the pilot study showed statistical difference whereas the ageing cohort didn't. The affect of exercise on ALS patients has always been controversial with numerous studies implicating various exercise activities as risk factors in ALS and others identifying exercise as beneficial resulting in increased quality of life. Dalbello-Haas *et al* review current data on the subject and conclude that current data is inconclusive due to the small numbers of subjects in the studies (Dalbello-Haas *et al.,* 2008). In the United States, ALS is referred to as Lou Gehrigs disease after the famous baseball player who succumbed to the disease in the late 1930s. Numerous other famous athletes including boxer Ezzard Charles, baseball player Jim Hunter and the more local Don Levie of Leicester city football club to name a few who all suffered with the disease. While so many cases of athletes with the disease may suggest exercise as a risk factor many specific neurological advantages to exercise have also been identified. These include increasing neurogenesis (van Praag *et al.,* 1999) and hindering age-related neuronal loss (Larsen *et al.,* 2000) (which is of particularly relevance here).

Exercise and learning behaviour could certainly explain the differing results between the pilot study and first ageing study. A new pilot study cohort of ageing mice was then gathered which had not been exposed to behavioural tests in the past. Limited animals were available for this study. An 18 month old cohort of male and female wildtypes and heterozygotes were analysed but no statistically significant differences

were observed between any of these groups. A 12 month cohort of females also showed no significant difference between wildtypes and heterozygotes. However there is a definite trend for females heterozygotes to perform worse than wildtype females. The mean difference between female wildtypes and heterozygotes appears more dramatic in the pilot study and in the 12 month old female cohort described here than in the larger ageing cohort. This supports the theory that exercise may be masking any difference in the ageing cohort. The next study to be undertaken should include larger groups of animals that should be tested once at 18 months of age.

Another interesting avenue for future investigations is to address what is happening at 12 months that causes this decline in female heterozygotes but not in males. The importance of gender differentiation when analysing behaviour data is becoming increasingly recognised. As such analysing animals separately by gender has been recommended in the recently updated guidelines for preclinical animal research in ALS (Ludolph *et al.,* 2010)

Studies of SOD1 G93A transgenic mice have shown that disease onset is significantly earlier in males than in females (Veldink *et al.,* 2003; Choi *et al.,* 2008). Studies have also shown that overactomy accelerates the progression of motor neuron disease symptoms in female SOD1 G93A transgenic animals suggesting that female sex hormones are neuroprotective (Groeneveld *et al.,* 2004; Choi *et al.,* 2008). 17β-estradiol treatment of these ovarectomised females also reversed the reduced survival rate. These studies suggest that oestrogen is a key player in the female advantage of lifespan in these animals. Up until menopause oestrogen may be providing a selective advantage to females but when they reach the age of menopause they lose this advantage. Interestingly the age of onset of menopause for mice is thought to be between 12-14 months of age (Silver 1995). This coincides with the age at which a difference is first observed between female wildtypes and heterozygotes. Therefore it is possible that on approaching menopause the decline in oestrogen normally associated with menopause could account for the increased difference between the female groups in this project. Investigating ovarectomised females would be an interesting tactic for investigating the apparent difference between males and females in this study. Veldink *et al* also demonstrated that

exercising female hSOD1 mice had a higher uterus weight and less irregular estrous cycles than non-exercising females which they conclude to mean that exercising females have a higher exposure to oestrogen (Veldink *et al.,* 2003). This supports the results of this project in that a smaller difference is observed between female groups when animals received regular exercise. A possible hypothesis could be that the poorer performance observed in female heteorzygotes could be attributed to lower eEF1A2 expression combined with an additional effect caused by menopause (such as a change in oestrogen level). This may account for why female heterozygotes and not male heterozygotes show a decrease in rotaord performance (compared to wildtypes controls) even though male heterozygotes show a greater reduction in eEF1A2 expression by western blot.

Another consideration for future work will be the genetic background of the animals as this could have an effect on both behavioural testing and on any disease phenotype. Whilst the onset of wasted disease is unaffected by genetic background (unpublished observations described in Abbott *et al* (Abbott *et al.,* 1994)) genetic background has been shown to influence disease onset in transgenic mouse models. Studies have shown that crossing the SOD1 transgenic mice onto different backgrounds resulted in differences in disease severity (Kunst *et al.,* 2000; Heiman-Patterson *et al.,* 2005). The degree of difference between survival of males and females was also affected by different genetic backgrounds (Heiman-Patterson *et al.,* 2005). Messer *et al* demonstrated that outcrossing of motor neuron degeneration *(mnd/mnd)* mice from a C57BL/6J genetic background to a AKR/J background advances symptom onset (Messer *et al.,* 1999). Modifier genes in different genetic backgrounds must therefore play an important role in disease pathology and thus genetic background should certainly be a consideration in any future studies. Although in this study all mice were of the same stock, genetic background was mixed and so could possibly lead to difference between groups and certainly between individuals. Furthermore some wildtype C56BL/6J males were also tested during the pilot study. These males far outperformed all of the mice (wildtypes included) from the wasted stock (data not shown). Perhaps breeding the mice onto a purer C57BL/6J background might result in wildtypes reaching 100% performance more quickly and

thus maybe any difference between wildtypes and heterozygotes may become more evident.

Behavioural differences between groups can be attributable to many things and thorough pathological analysis is therefore crucial in studies such as this. In this study no significant differences were seen in the spinal cord pathology between any of the groups examined using GFAP and neurofilament antibodies as markers of neurodegeneration. Levels of GFAP in the mouse CNS have been shown to increase with age (O'Callaghan and Miller 1991; Kohama *et al.,* 1995; Mouton *et al.,* 2002; Hartman *et al.,* 2007) and therefore may explain the high level of staining in older wildtypes that made analysis difficult. Moulton *et al* also demonstrated that aged females have an increased number of microglia and astrocytes compared to males of the same age (Mouton *et al.,* 2002). The heavy staining in the samples made this difficult to ascertain in this study. Motor neuron counts also demonstrated no significant difference between groups, however the small number of animals at the endpoint of the study combined with the crude counting method could account for this. Furthermore the choice of marker may not have been ideal given the difference in expression of eEF1A2 the spinal cord of wildtype and heterozygous animals. In future more sophisticated methods should be adopted for this such as the fractionator method and image analysis software used in Fishcer *et al* (Fischer *et al.,* 2004) and Weber *et al* (Weber *et al.,* 1997). It would also been useful to measure neuron size as 12 months old ZPR1 heterozygotes show decreased neuron size compared to wildtypes (Doran *et al.,* 2006).

Gene dosage has a direct effect on ZPR1 causing decreased ZPR1 protein levels in heterozygous ZPR1 mice compared to wildtype controls (Doran *et al.,* 2006). This decrease became more extensive with age. Whilst 6 week old heterozygote mice showed no marked decrease in motor neuron number compared to wild type controls, by 12 months of age heterozygote mice displayed reduced cell density and loss of anterior horn motor neurons compared to wildtypes. This correlates directly with the decrease in ZPR1 protein with age. ZPR1 has been shown to preferentially bind to GDP bound eEF1A (Mishra *et al.,* 2007). As eEF1A2 has a slower disassociation rate than eEF1A1 it is possible that ZPR1 preferentially binds eEF1A2. It is therefore

plausible that in ageing wasted heterozygotes the reduced levels of eEF1A2 result in insufficient ZPR1-eEF1A complexes which may decrease motor neuron viability. An interesting avenue for future work would be to examine whether any changes occur in the levels or localization of ZPR1 and SMN in older heterozygote animals, which would contribute to further our understanding of the interaction between these three proteins.

By examining eEF1A2 protein levels in various tissues it became apparent that while heterozygotes would be expected to have approximately 50% of eEF1A2 protein of wildtypes (Newbery 2003) this is not always the case for older animals. It appears that with age the amount of eEF1A2 in brain, spinal cord and muscle of heterozygotes decreases. These data also suggest that in brain tissue the decrease is more dramatic in males than in females. This result must be viewed with caution as ensuring the exact region of the brain is taken in each sample was very difficult. Analysing eEF1A2 expression in tissues from mice of varying ages would be interesting to identify when any decrease in protein expression first appears.

This information is extremely useful as in this study it shows that 26% of eEF1A2 protein in muscle for example is sufficient for normal motor function. Having a reduction to only a quarter of wildtype eEF1A2 expression does not result in a significant behavioural deficits or pathology. This information is essential if eEF1A2 were ever used for gene therapy, for example.

3.5. Conclusion

The aim of this study was to assess whether wasted heterozygotes develop any signs of motor neuron degeneration later in life. The results of the project are still inconclusive to some extent. Given that the pilot study showed statistically significant difference in the performance of wildtypes and heterozygotes on the rotarod and the same pattern appears in both of these ageing studies they do provide an interesting model for future investigation. As there is little evidence of any pathological differences between heterozygotes and wildtypes their value as a model for motor neuron degeneration however is limited.

4. Chapter 4: Investigating the primary cause of the pathology in wasted mice

4.1. Aim

The main aim of this study was to investigate the primary cause of the pathology of wasted mice. To address this aim, transgenic animals expressing eEF1A2 under the control of a neuronal specific promoter were generated to attempt to investigate the effect of only neuronal eEF1A2 expression (i.e. loss of muscle eEF1A2) on wasted mice.

4.2. Introduction

The wasted mouse model (*wst*) arose from the spontaneous deletion of the promoter region and first non-coding exon of eEF1A2. This 15.8kb deletion completely abolishes eEF1A2 protein expression (Chambers *et al.,* 1998). Mice homozygous for this deletion develop symptoms of neuromuscular disease such as weight loss (largely attributed to loss of muscle bulk), tremors and gait abnormalities from 21 days of age. Mice deteriorate rapidly from this point resulting in death by 28 days (Shultz *et al.,* 1982). The onset of these neuromuscular symptoms in wasted mice coincides with a developmental switch in eEF1A variants in muscle. eEF1A1 expression is normally highly expressed in muscle at birth and then gradually declines to become undetectable by 21 days. By this point in wildtype animals, eEF1A2 expression would normally have taken over (Khalyfa *et al.,* 2001). A similar expression pattern of eEF1A variants is also seen in motor neurons (Newbery *et al.,* 2005; Newbery *et al.,* 2007). Wasted mice at 21 days therefore have neither eEF1A1 or eEF1A2 expression in muscle or motor neurons. Motor neuron pathology similar to that seen in human motor neuron degeneration is also observed in wasted mice from around 21 days (Chambers *et al.,* 1998; Newbery *et al.,* 2005)

Previous transgenic studies in our lab imply that *Eef1a2* is the only gene responsible for the wasted phenotype (Loh 2003; Newbery *et al.,* 2007). However it is currently

unknown whether the muscle degeneration in wasted mice is a primary myopathy due to the loss of eEF1A2 in muscle or is due to denervation atrophy caused by the loss of eEF1A2 in the motor neurons.

This question was previously approached by generating transgenic animals expressing eEF1A2 under the control of the human specific actin promoter (HSA (Dharmasaroja 2007)). Homozygous wasted mice (*wst/wst*) carrying the muscle-specific transgene died at the same age as those without the transgene, despite significant levels of eEF1A2 protein expression in muscle. The muscle specific transgene therefore failed to rescue the wasted phenotype. These results suggest that the loss of eEF1A2 in neurons is the primary cause of the muscle pathology, but it is critical to test this experimentally, especially given that only one line expressing eEF1A2 under the control of the HSA promoter was generated in the previous study. In this project a construct containing the human *EEF1A2* gene under the control of the rat Neuronal Specific Enolase (NSE) promoter was generated to test this. A 1.8kb fragment of the promoter region of NSE has been previously shown to contain all the regulatory elements required for driving neuronal specific expression in transgenic mice (Forss-Petter *et al.,* 1990). Numerous studies have demonstrated neuronal specific transgene expression using this promoter region (Maddatu *et al.,* 2004; de Luca *et al.,* 2005) and this was therefore the reason for its use in this study.

These experiments will aid in our understanding of the pathology of wasted mice in addition to improving our understanding of motor neuron degeneration.

4.3. Results

4.3.1. The NSE-EEF1A2 construct

To meet the aim of this study a construct containing the human *EEF1A2* gene under the control of the rat neuronal specific promoter Neuronal Specific Enolase (NSE*)* was generated.

4.3.1.1. eEF1A2

A pUC19-EEF1A2 plasmid was created by subcloning the 18,891bp human *EEF1A2* gene from the P1-derived artificial chromosome (PAC) previously constructed by Dawn Loh (Loh 2003). The gene (including its promoter) was cloned into the multiple cloning site of the pUC19 plasmid, between the *Hind*III and *Kpn*I sites by Dr Julia Boyd. Thie pUC19-EEF1A2 was used for the generation of the transgenic construct.

An *Age*I site located 102bp upstream of the second exon (the first coding exon) of *EEF1A2* was identified as a suitable unique site for insertion of the new promoter (Dharmasaroja 2007). The aim was to remove the promoter region of *EEF1A2* by digestion with *Hind*III and *Age*I. The NSE promoter (flagged with *Hind*III and *Age*I sites) could then be inserted into this site.

4.3.1.2. The Promoter

A 1946bp fragment from the Rat NSE promoter region was amplified by polymerase chain reaction (PCR) from a cell pellet from the RAT2 cell line. Primers were designed to span the required region and also to attach restriction sites to the ends of the fragment. Nested PCR was then performed with primers targeting the newly added restriction sites, resulting in the correct product flanked with the desired restriction sites. The 5' end of the promoter contained a *Hind*III site and the 3' end contained an *Age*I site. The use of different restriction sites decreased the probability of the promoter being inserted in the incorrect orientation.

4.3.1.3. Cloning

Following PCR amplification of the promoter region, a double restriction digest was performed with *Hind*III and *Age*I restriction enzymes on the nested PCR promoter product (flanked with *Hind*III and *Age*I restriction sites). Simultaneously, a restriction digest was also performed on the pUC19-EEF1A2 vector which removed the 7.7kb promoter region of *EEF1A2*. Attempts were made to gel extract the required fragment of *EEF1A2* (and eliminate the unrequired *EEF1A2* promoter region) however the gel extraction purification seemed to hinder ligation. The digested promoter and vector were therefore purified by a PCR purification kit (Qiagen) and ligated with a T4 ligase. Diagramatic representation of the cloning strategy can be seen in figure 4.1. Ligation was optimally achieved at 25^{o}C for four hours using a 4:1 promoter:vector ratio. Ligated products were then transformed into TOP10 competent cells (Invitrogen). Positive colonies were screened by colony PCR using primers which would produce a product that bridged the 3' end of the NSE promoter and the 5' of the *EEF1A2* gene (this ensured that the original *EEF1A2* promoter had not re-ligated into the backbone vector). Details of the primers used can be seen in Chapter 2: Materials and Methods. A Maxi-prep kit (Qiagen) was used to prepare large scale preparations of the NSE-EEF1A2 construct. Restriction digests were performed on these preparations to ensure the correct construct was present (figure 4.2, table 4.1). Further PCR analysis was also performed using multiple primer pairs to confirm the correct orientation of the promoter. The NSE promoter region, exons 2-7 of *EEF1A2* and the region between the promoter and exon 2 of *EEF1A2* were sequenced to check for any mutations. No mutations were found in any of these regions. As such the construct was deemed suitable for microinjection.

The 13Kb construct was excised from the vector by a double restriction digest with *Hind*III and *Kpn*I, separated from the plasmid backbone on a gel and purified by elutrap electroelution in preparation for microinjection.

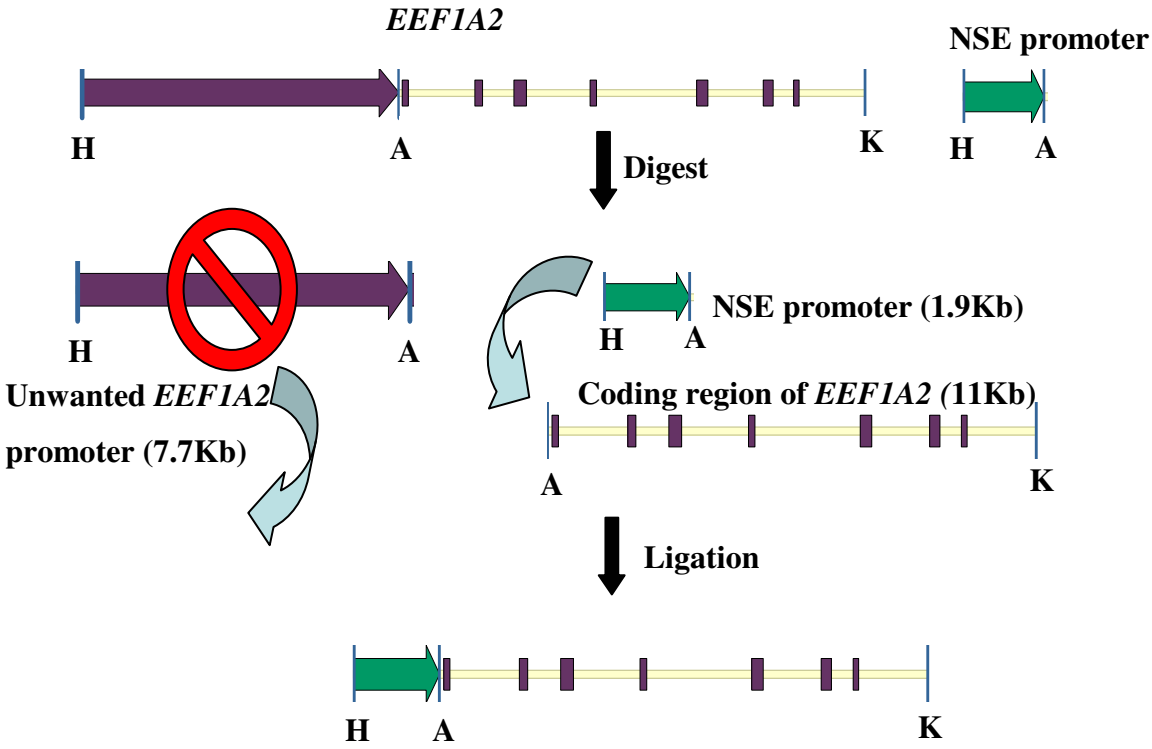

Figure 4.1. NSE-EEF1A2

Diagramatic representation of the generation of the NSE-EEF1A2 construct. H indicates a *Hind*III restriction site, A indicates an *Age*I restriction site and K indicates a *Kpn*I restriction site.

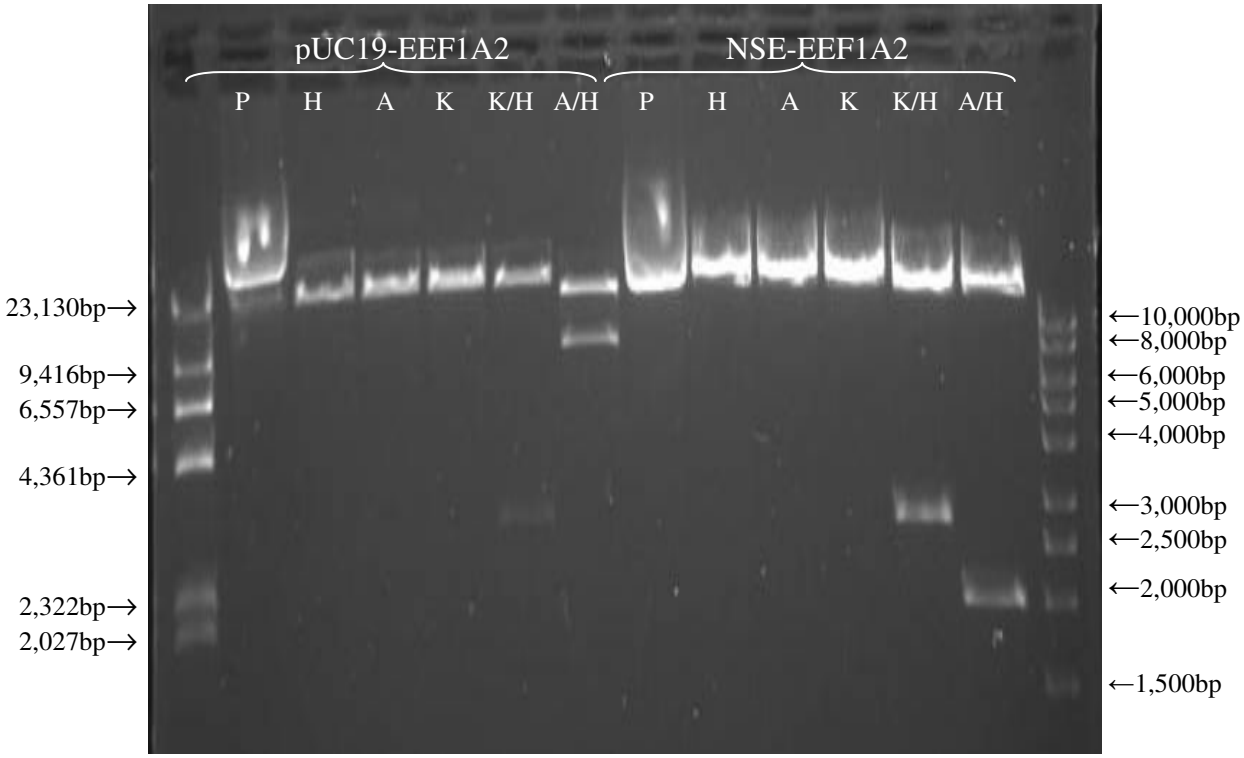

Figure 4.2. Restriction digests of NSE-EEF1A2

Agarose gel (0.6%) showing restriction digest products from pUC19-EEF1A2 and NSE-EEF1A2 construct. Single digests with *Hind*III (H), *Age*I (A) and *Kpn*I (K) are shown which all linearise the plasmid. A double digest with *Age*I and *Hind*III (A/H) removes the promoter region and a double digest with *Kpn*I and *Hind*III (K/H) removes the entire construct from the vector. Expected product sizes can be seen in table 4.1 below.

Enzyme/s	pUC19-EEF1A2	NSE-EEF1A2
Hind III	21528bp	15,729bp
*Age*I	21528bp	15,729bp
*Kpn*I	21528bp	15,729bp
Hind III & *Kpn*I	18,881bp, 2647bp	13082bp, 2647bp
Hind III & *Age*I	13,783bp, 7745bp	13,783bp, 1946bp

Table 4.1. Expected product sizes from restriction digests of NSE-EEF1A2

Expected product sizes from restriction digests of the NSE-EEF1A2 and pUC19-EEF1A2 constructs.

4.3.2. Generating NSE-EEF1A2 transgenic mice

Microinjection of the NSE-EEF1A2 construct into fertilised embryos, and subsequent embryo transfer into pseudo-pregnant females was performed by Emma Murdoch. Ninety seven embryos at the two cell stage were transplanted across three pseudo-pregnant females of which thirty six live pups were born. Positive offspring were identified by PCR of genomic DNA extracted using the DNeasy extraction kit (Qiagen). Two primer pairs (as shown in figure 4.3) were used; the forward primers were both located within the NSE promoter region and the reverse primers located within the *EEF1A2* gene. Three animals were identified that were positive for the transgene (two male and one female).

Figure 4.3. Location of transgenic primers.

Target regions of primers used to identify the presence of the NSE-EEF1A2 transgene in mice. Two primer pairs were used: NSE-EEF1A2 F1 paired with NSE-EEF1A2 R1 results in a PCR product with an expected size of 671bp, NSE-EEF1A2 F2 paired with NSE-EEF1A2 R2 results in a PCR product with an expected size of 387bp. The *Age*I site is also highlighted (pink), which marks the end of the NSE promoter region and the beginning of the *EEF1A2* gene. Underlined text denotes the location of the first coding exon of *EEF1A2* (exon 2).

4.3.3. Maintaining transgenic lines

The three founders were separately mated to wasted heterozygote mice (+/*wst*). All three founders transmitted the transgene through the germline resulting in transgenic offspring. The three separate lines were then designated NSE-EEF1A2-A, NSE-EEF1A2-B and NSE-EEF1A2-C. Lines containing wasted homozygous animals carrying the NSE-EEF1A2 transgene (+*/tg*, *wst/wst*), were generated by mating wasted heterozygote animals carrying the NSE-EEF1A2 transgene (+*/tg*, +*/wst*) with heterozygote animals without the transgene (+/+, +*/wst,*). All transgenic mice were therefore hemizyous for the transgene. The strategy for generating wasted homozygous animals carrying the NSE-EEF1A2 transgene (+*/tg*, *wst/wst*) is shown in figure 4.4.

Wasted homozygous animals carrying the NSE-EEF1A2 transgene (+/*tg*, *wst/wst*) were identified by genoptyping with four primer sets. Genotyping primers routinely used to identify the wildtype *Eef1a2* allele and separately the wasted *Eef1a2* allele were used as well as two separate primer pairs to identify the NSE-EEF1A2 transgene. Further details of the genotyping assay for the wasted mutation can be found in Chapter 2: Materials and methods. The target region of the transgene specific primers used for genotyping can be seen in figure 4.3. Examples of genotyping results can be seen in figure 4.5.

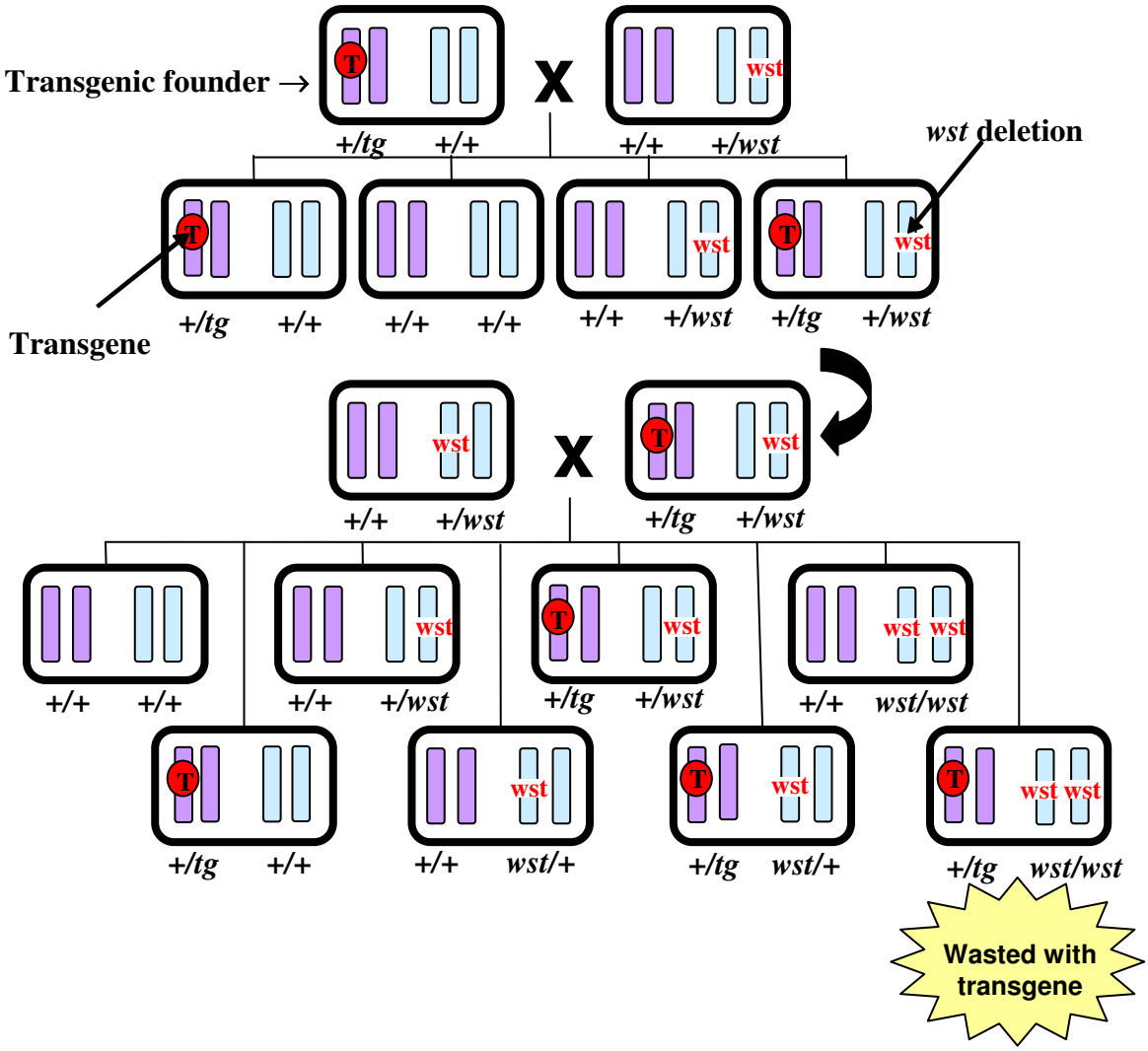

Figure 4.4. Diagramatic representation of the strategy for generating wasted mice carrying the NSE-EEF1A2 transgene (*+/tg wst/wst*).

Transgenic founders (*+/tg,+/+*) were initially mated to non-transgenic wasted heterozygotes (*+/+,+/wst*). One in four offspring were expected to be wasted heterozygotes carrying the transgene (*+/tg,+/wst*). Wasted heterozygotes carrying the transgene (*+/tg,+/wst*) were then mated to wasted heterozygotes without the transgene (*+/+,+/wst*). One in 8 of the offspring from these matings are expected to be both homozygous for the wasted deletion and be carriers of the transgene (*+/tg, wst/wst*).

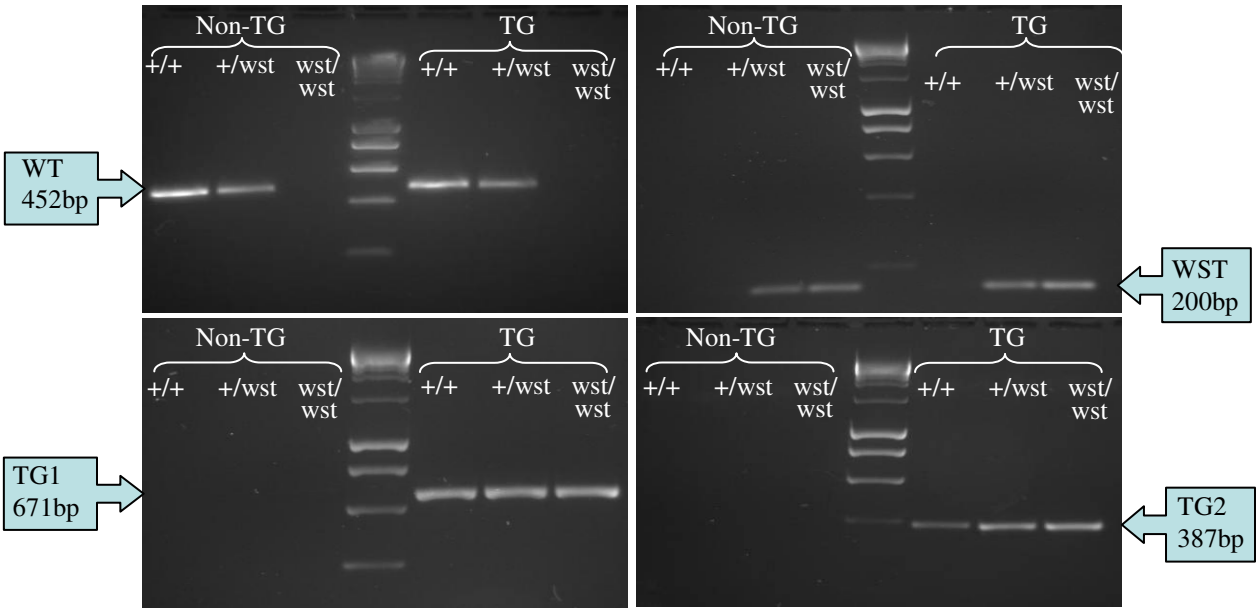

Figure 4.5. Genotyping of transgenic NSE-EEF1A2 animals.

Examples of genotyping results from NSE-EEF1A2 transgenic (TG) animals and non-transgenic controls (Non-TG). PCR results from a non transgenic and a transgenic wildtype (+/+), heterozygote *(+/wst*) and wasted (*wst/wst*) animals. Gel (a) shows PCR products that correspond to the wildtype *Eef1a2* (WT) allele (expected size of product: 452bp). Gel (b) shows PCR products that correspond to the wasted *Eef1a2* (WST) allele (expected size of product: 200bp). Gels (c) and (d) show PCR products from 2 sets of NSE-EEF1A2 transgene specific primers: TG1 (NSE-EEF1A2 F1 and NSE-EEF1A2 –R1 (expected size 671bp)) and TG2 (NSE-EEF1A2 F2 and NSE-EEF1A2 R2 (expected size 387bp)).

4.3.4. Analysis of transgenic mice

4.3.4.1. NSE-EEF1A2-A

Wasted mice (*wst/wst*) usually begin to develop symptoms of neuromuscular disease at around 21 days. Wasted mice carrying the transgene (*+/tg, wst/wst*) in the NSE-EEF1A2-A line showed symptoms of neuromuscular disease including weight loss and tremors at a similar age to wasted mice without the transgene (+/+*, wst/wst*).

Body weight

As wasted mice show a dramatic decrease in body weight from 21 days until death, mice from the NSE-EEF1A2-A line were weighed at 25 days (end stage) to assess whether this disease phenotype was corrected. Wasted mice carrying the transgene (*+/tg, wst/wst*) showed no significant difference in body weight compared to wasted animals without the transgene (+/+, *wst/wst*). Wasted mice, both with and without the transgene, weighed significantly less than wildtype littermates (figure 4.6, table 4.2). This indicates that this aspect of the disease phenotype is not corrected in these animals.

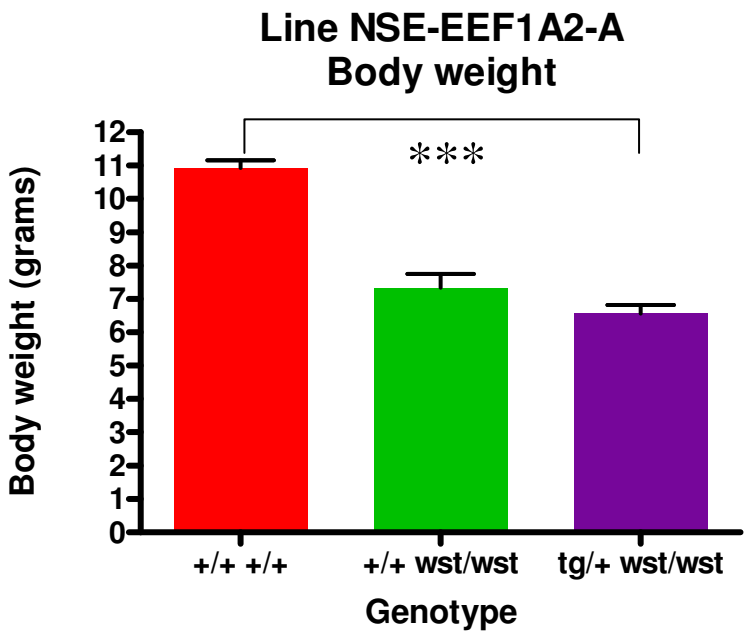

Figure 4.6. Body weights of 25 day old mice from the NSE-EEF1A2-A line.

Body weights of wildtype animals (+/+, +/+), wasted animals without the transgene (*+/+, wst/wst*) and wasted animals with the transgene (*+/tg, wst/wst*) are shown. Animals were weighed at 25 days (end stage). *** indicates a p value <0.001

Genotype	N	Mean	Min	Max	S.D	S.E.M
+/+ +/+	3	10.1	9.1	11.3	1.1	0.6
+/+ wst/wst	3	7.3	6.5	7.9	0.7	0.4
+/tg wst/wst	3	6.6	6.1	7.0	0.5	0.3

Table 4.2. Body weights of 25 day old mice from the NSE-EEF1A2-A line.

Statistical analysis of body weights from wildtype animals (+/+, +/+), wasted animals without the transgene (*+/+, wst/wst*) and wasted animals with the transgene (*+/tg, wst/wst*) are shown. Animals were weighed at 25 days (end stage). Number of animals (N), mean, minimum (Min) and maximum (Max) bodyweight for each genotype are shown. S.D indicates the standard deviation across each genotype and S.E.M is a measure of the standard error of the mean.

Grip strength analysis

Wasted mice demonstrate poor grip strength from around 20 days (Chapter 3). At 25 days of age, analysis of both forelimb and all four limb grip strength showed that wasted mice carrying the transgene (*+/tg, wst/wst*) were indistinguishable from wasted mice without the transgene (+/+, *wst/wst*). It therefore appears that the transgene does not rescue the poor grip strength phenotype of wasted mice (figure 4.7, Table 4.3).

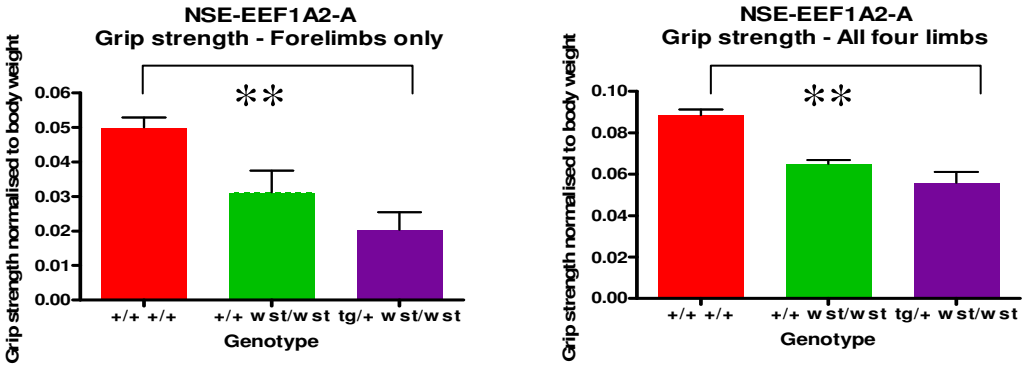

Figure 4.7. Grip strength analysis of 25 day old mice from the NSE-EEF1A2-A line.

Mean grip strength analysis from 25 day old wildtype animals (+/+,+/+), wasted animals without the transgene *(+/+, wst/wst)* and wasted animals with the transgene (*+/tg, wst/wst*) from the NSE-EEF1A2 line A are shown. Forelimb (left graph) and all four limb (right graph) grip strength readings from 3 tests (measured in Newtons) were normalised to body weight (measured in grams). ** indicates a p value <0.01 when comparing wildtype mice to wasted mice carrying the transgene (*+/tg, wst/wst).*

(a) Forelimbs only

Genotype	N	Mean	Min	Max	S.D	S.E.M
(+/+, +/+)	3	0.050	0.044	0.054	0.005	0.003
(+/+, *wst/wst*)	3	0.031	0.021	0.042	0.011	0.006
(+/tg, *wst/wst*)	3	0.020	0.014	0.030	0.009	0.005

(b) All four limbs

Genotype	N	Mean	Min	Max	S.D	S.E.M
(+/+, +/+)	3	0.088	0.083	0.091	0.005	0.003
(+/+, *wst/wst*)	3	0.065	0.062	0.068	0.003	0.002
(+/tg, *wst/wst*)	3	0.056	0.045	0.062	0.009	0.005

Table 4.3. Grip strength analysis of 25 day old mice from the NSE-EEF1A2-A line.

Statistical analysis of grip strength measurements from 25 day old wildtype animals (+/+,+/+), wasted animals without the transgene *(+/+, wst/wst*) and wasted animals with the transgene (*+/tg, wst/wst*) from the NSE-EEF1A2 line A. Animals were tested three times at 25 days (end stage) and an average per animal calculated. Number of animals (N), mean, minimum (Min) and maximum (Max) bodyweight for each genotype are shown. S.D indicates the standard deviation across each genotype and S.E.M is a measure of the standard error of the mean.

Protein expression.

Whilst it was shown that the founder of NSE-EEF1A2-A successfully transmitted the transgene through the germline, Western blot analysis of wasted mice carrying the transgene (*+/tg wst/wst)* indicated that the transgene was not being expressed at the protein level (figure 4.8). Brain, spinal cord and muscle tissues were analysed for protein expression from three wildtype animals (+/+, +/+), three wildtype mice carrying the trangene (*+/tg*, +/+), three wasted animals (+/+, *wst/wst*) and three wasted animals carrying the transgene (*+/tg, wst/wst*), all at 25 days of age. Wasted mice carrying the transgene showed no expression of eEF1A2 in any of the tissues examined. As it appears the transgene is not expressed in these animals, no further analysis was carried out on the NSE-EEF1A2-A line.

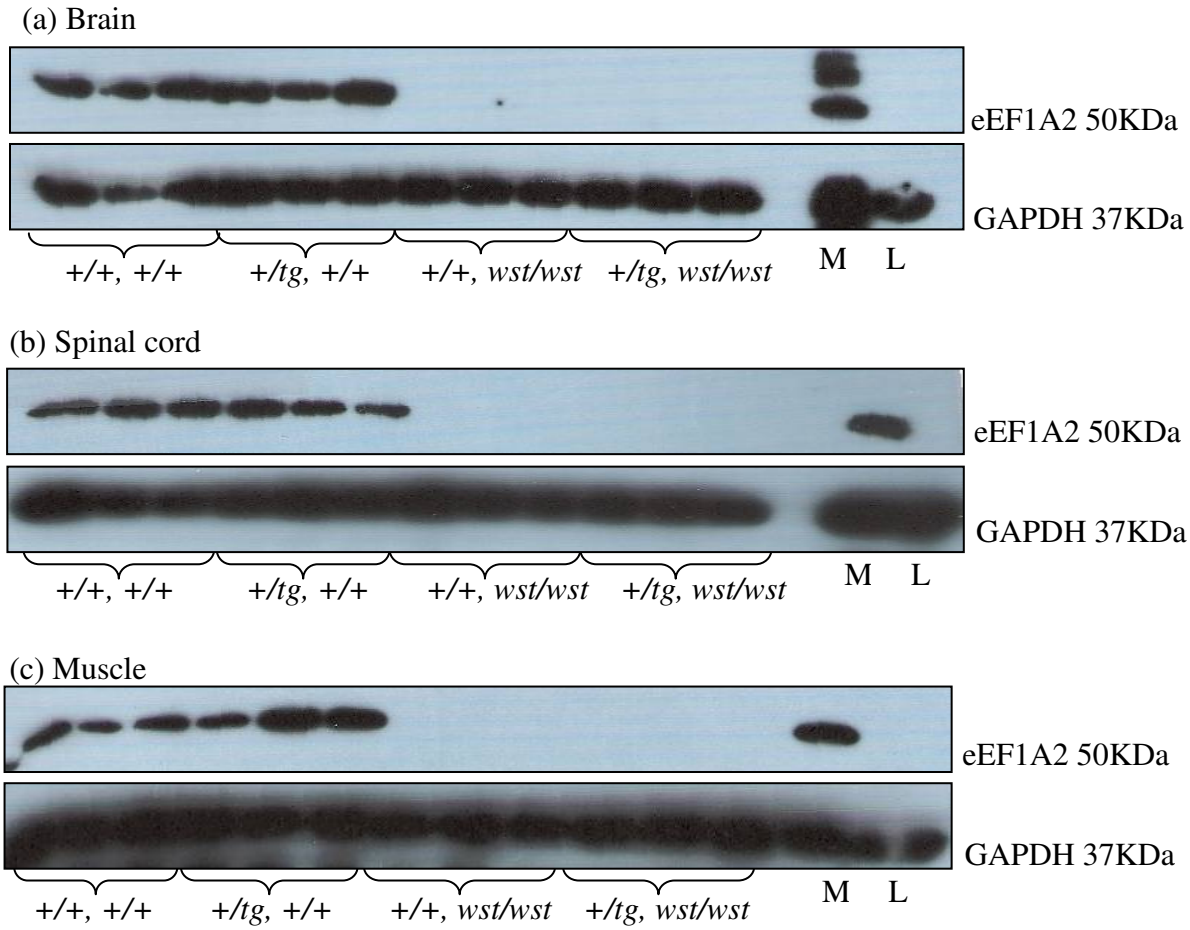

Figure 4.8. eEF1A2 protein expression in tissues from NSE-EEF1A2-A line animals.

Western blots showing expression of eEF1A2 and GAPDH (as a loading control) of animal tissue from the transgenic line NSE-EEF1A2-A. Expression from three animals from each group (wildtype (+/+,+/+), wildtype with the transgene (*+/tg*, +/+,) wasted animals without the transgene *(+/+, wst/wst*) and wasted animals with the transgene (*+/tg, wst/wst*)) are shown. M indicates a muscle sample (as an eEF1A2 positive control) and L indicates a liver sample (an eEF1A2 negative control).

4.3.4.2. NSE-EEF1A2-B

Unlike the NSE-EEF1A2-A line, wasted mice carrying the transgene (*+/tg, wst/wst*) from the NSE-EEF1A2-B line showed no observable signs of neuromuscular disease at 25 days. Wasted mice carrying the transgene were indistinguishable from wildtype mice at 25 days of age (figure 4.9 panels (a) and (b)). At the anatomical level, tissues from wasted mice carrying the transgene (*+/tg, wst/wst*) were also indistinguishable from wildtype littermate controls. The splenic and thymic atrophy (figure 4.9) normally seen in wasted mice (+/+, *wst/wst*) was not observed in wasted mice carrying the transgene (*+/tg, wst/wst*). It therefore appears that some aspects of the wasted phenotype have been corrected by the NSE-EEF1A2 transgene in this line.

Body weight

As wasted mice show a dramatic decrease in body weight from 21 days until death, mice from the NSE-EEF1A2-B line were weighed at 25 days (end stage) to assess whether this aspect of the disease phenotype was corrected (figure 4.10). As expected wasted mice showed a significant decrease in body weight compared to littermate controls. Wasted mice carrying the transgene *(+/tg, wst/wst*) showed a significant increase in body weight compared to the wasted animals without the transgene (+/+, *wst/wst*). No significant difference was observed between wasted mice with the transgene and the wildtype and heterozygote controls. It would therefore appear that the transgene has therefore rescued this aspect of the wasted phenotype.

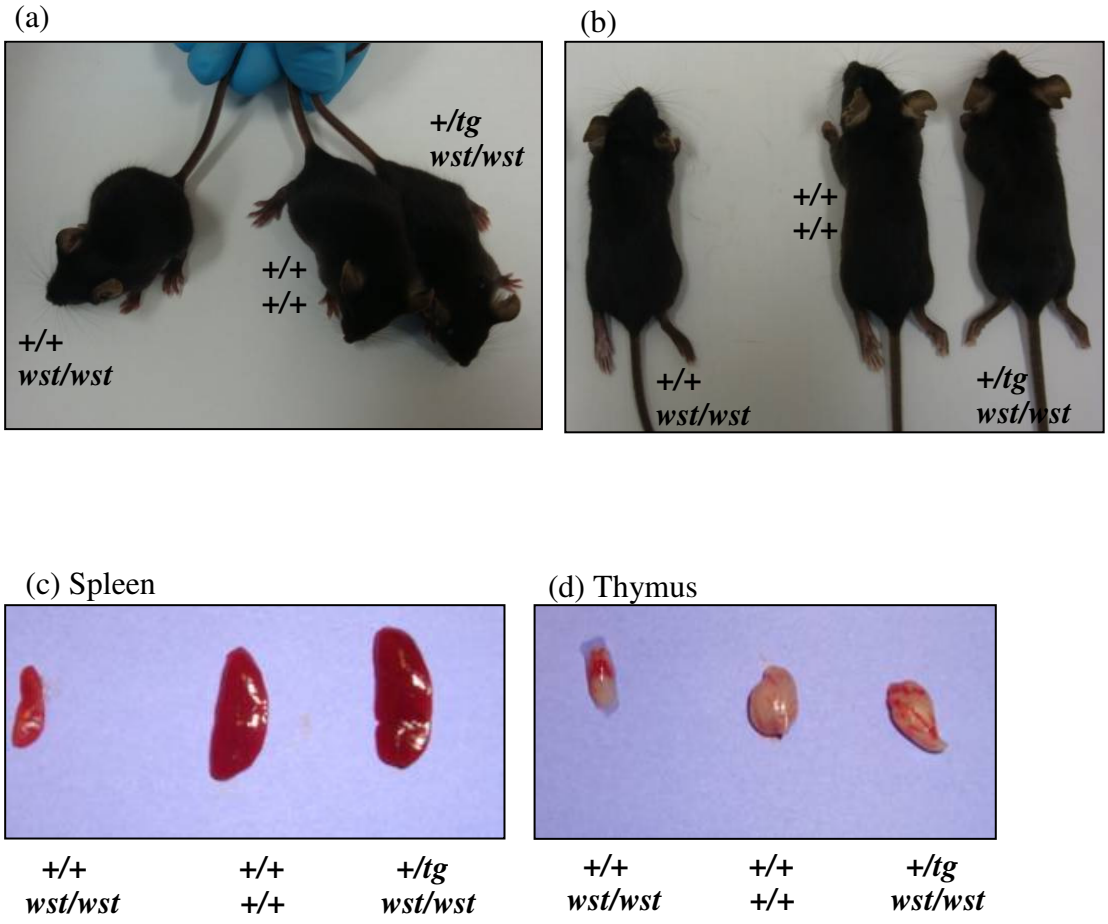

Figure 4.9. Photographs of animals from the NSE-EEF1A2-B line.

Photographs of animals from the NSE-EEF1A2-B line. Panels (a) and (b) show a wildtype animal (+/+,+/+) a wasted animal (+/+, *wst/wst*) and a wasted animal carrying the transgene (*+/tg, wst/wst*). Panels (c) (spleen) and (d) (thymus) show tissues from the animals pictured in (a) and (b).

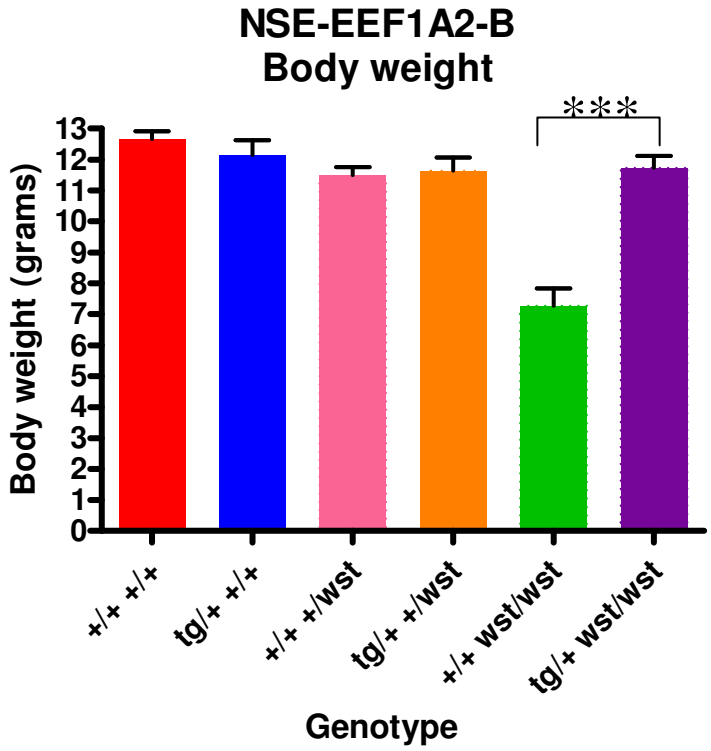

Figure 4.10. Body weights of 25 day old mice from the NSE-EEF1A2-B line.

Body weight measurements (in grams) from wildtype animals (+/+,+/+), wildtype animals with the transgene (+/*tg*, +/+), heterozygote animals without the transgene (+/+, +/*wst*), heterozygote animals with the transgene (+/*tg*, +/*wst*) wasted animals without the transgene (+/+, *wst/wst*) and wasted animals with the transgene (+/*tg*, *wst/wst*) are shown. Animals were weighed at 25 days (end stage). *** indicates a p value <0.01

Genotype	N	Mean	Min	Max	S.D	S.E.M
(+/+, +/+)	13	12.7	11.0	14.1	0.9	0.3
(+/tg, +/+)	13	12.1	7.6	15.2	1.7	0.5
(+/+, +/wst)	15	11.5	9.5	12.9	1.0	0.3
(+/tg, +/wst)	9	11.6	9.9	13.9	1.3	0.4
(+/+, wst/wst)	8	7.3	5.1	9.9	1.6	0.6
(+/tg, wst/wst)	6	11.7	10.7	12.8	0.9	0.4

Table 4.4. Body weights of 25 day old mice from the NSE-EEF1A2-B line.

Statistical analysis of body weights from mice of the NSE-EEF1A2-B line. Animals were weighed at 25 days (end stage). Number of animals (N), mean, minimum (Min) and maximum (Max) bodyweight for each genotype are shown. S.D indicates the standard deviation across each genotype and S.E.M is a measure of the standard error of the mean.

Grip strength analysis

At 25 days of age, analysis of grip strength in both forelimbs only and all four limbs showed that wasted mice carrying the transgene (*+/tg, wst/wst*) were indistuinguishable from wildtype animals (+/+,+/+) and had significantly higher grip strength than wasted mice without the transgene (+/+, *wst/wst*). It appears that the poor grip strength normally seen in wasted mice is therefore corrected upon expression of the transgene.

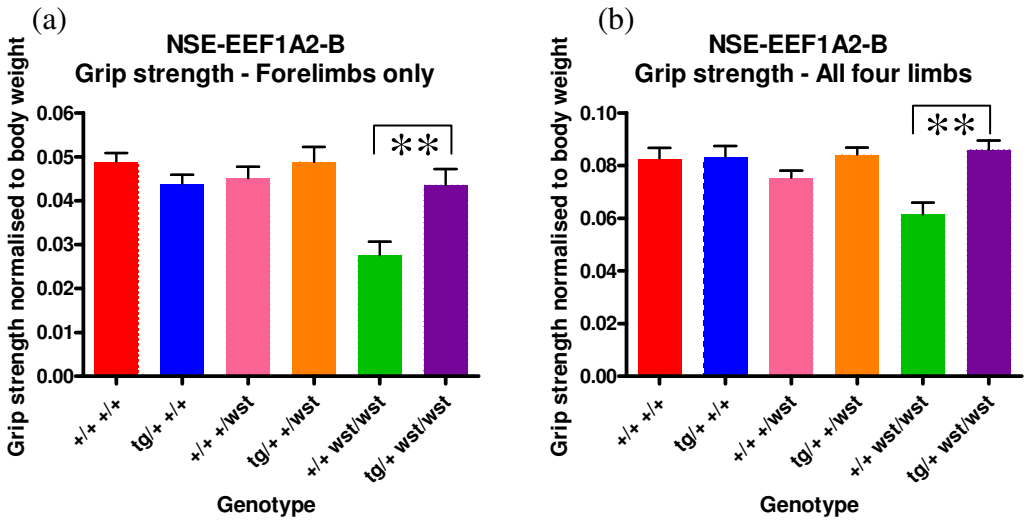

Figure 4.11. Grip strength analysis of 25 day old mice from the NSE-EEF1A2-B line.

Mean grip strength analysis from 25 day old wildtype animals (+/+,+/+), wildtype animals with the transgene (*+/tg,* +/+), heterozygote animals without the transgene (+/+, +/*wst*), heterozygote animals with the transgene (*+/tg, +/wst*), wasted animals without the transgene *(+/+, wst/wst*) and wasted animals with the transgene (*+/tg, wst/wst*) from the NSE-EEF1A2 line B are shown. Forelimb (left graph) and all four limb (right graph) grip strength readings from 3 tests (measured in Newtons) were normalised to body weight (measured in grams). ** indicates a p value <0.01.

(a) Forelimbs only

Genotype	N	Mean	Min	Max	S.D	S.E.M
(+/+, +/+)	13	0.049	0.038	0.060	0.007	0.002
(+/tg, +/+)	13	0.044	0.031	0.059	0.007	0.002
(+/+, +/wst)	15	0.045	0.031	0.060	0.010	0.003
(+/tg, +/wst)	9	0.049	0.032	0.060	0.010	0.003
(+/+, wst/wst)	8	0.028	0.017	0.040	0.009	0.003
(+/tg, wst/wst)	6	0.044	0.034	0.060	0.009	0.004

(b) All four limbs

Genotype	N	Mean	Min	Max	S.D	S.E.M
(+/+, +/+)	13	0.083	0.062	0.121	0.015	0.004
(+/tg, +/+)	13	0.083	0.065	0.112	0.016	0.004
(+/+, +/wst)	15	0.075	0.055	0.095	0.010	0.003
(+/tg, +/wst)	9	0.084	0.073	0.101	0.009	0.003
(+/+, wst/wst)	8	0.061	0.046	0.085	0.013	0.004
(+/tg, wst/wst)	6	0.086	0.076	0.097	0.008	0.003

Table 4.5. Grip strength analysis of 25 day old mice from the NSE-EEF1A2-B line.

Statistical analysis of grip strength from 25 day old wildtype animals (+/+,+/+), wildtype animals with the transgene (*+/tg*, +/+), heterozygote animals without the transgene (*+/+, +/wst*), heterozygote animals with the transgene (*+/tg, +/wst*) wasted animals without the transgene *(+/+, wst/wst*) and wasted animals with the transgene (*+/tg, wst/wst*) from the NSE-EEF1A2 line B. Animals were weighed at 25 days (wasted end stage). Number of animals (N), mean, minimum (Min) and maximum (Max) grip strength reading for each genotype are shown. S.D indicates the standard deviation across each genotype and S.E.M is a measure of the standard error of the mean.

Protein expression

Western blots indicate that the transgene is expressed at the protein level in animals from NSE-EEF1A2 line B (Figure 4.12). Expression is not however restricted to the central nervous system. Brain, spinal cord, muscle, heart and liver samples were analysed for protein expression from 25 day old animals. Three wildtype animals (+/+, +/+), three wildtype animals carrying the transgene (+*/tg,* +/+), three wasted animals (+/+, *wst/wst*) and three wasted animals carrying the transgene (+*/tg, wst/wst*) were analysed. Results show that the transgene is expressed in brain and spinal cord as expected but also in muscle and heart tissue (figure 4.12). Panels of tissues from six week old wasted animals carrying the transgene were also examined (an example can be seen in figure 4.13). No expression of eEF1A2 was seen in any other tissues examined. The protein expression pattern in wasted animals carrying the transgene (+*/tg, wst/wst*) is therefore as is seen in wildtype animals at the level of detection of the whole tissue by Western blotting.

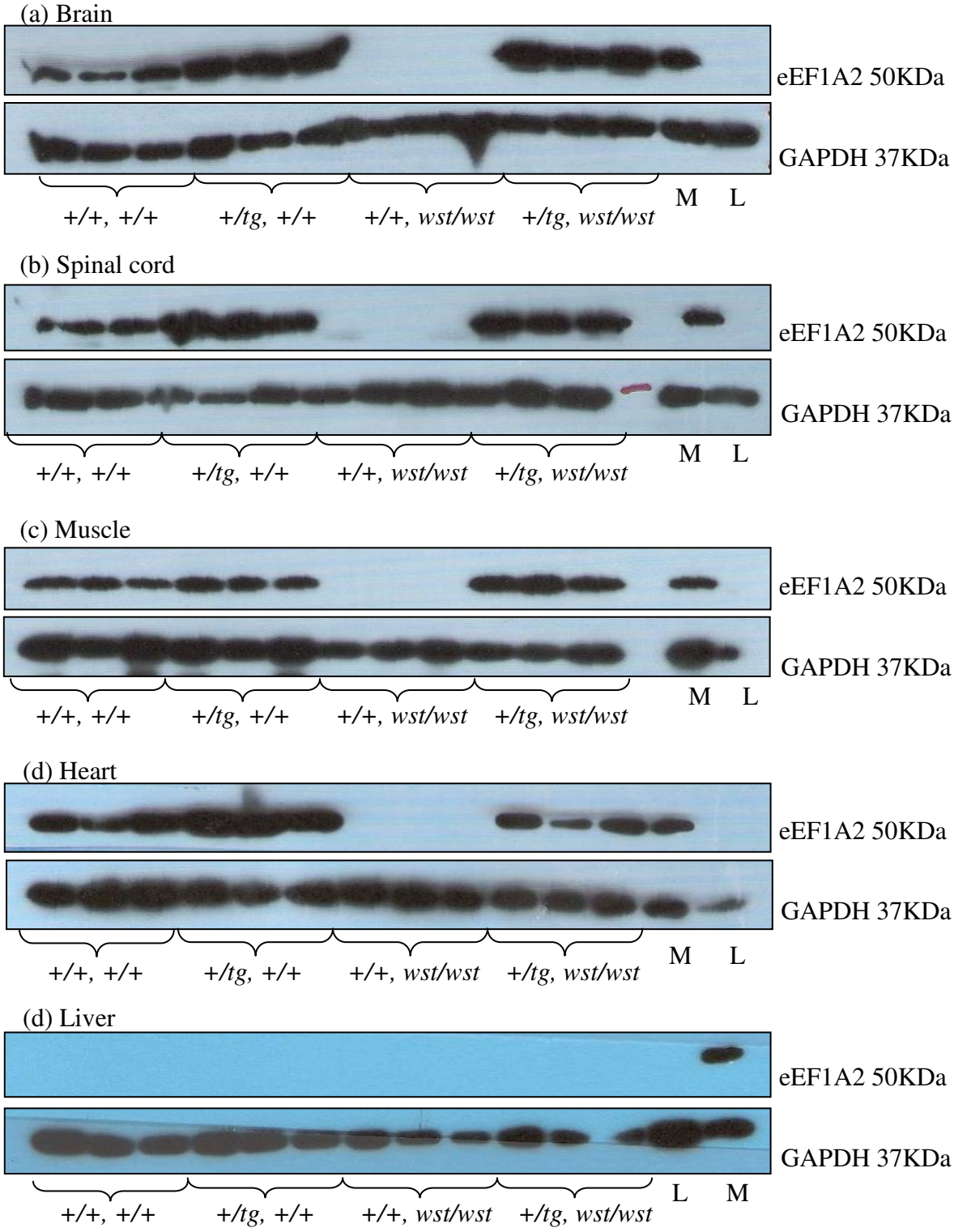

Figure 4.12. eEF1A2 protein expression in tissues from NSE-EEF1A2-B line animals.

Western blots showing expression of eEF1A2 and GAPDH (as a loading control) of animals from the transgenic line NSE-EEF1A2-B. Expression from three animals from each group (wildtype (+/+,+/+), wildtype with the transgene (+/+, *+/tg*,) wasted animals without the transgene *(+/+, wst/wst*) and wasted animals with the transgene (*+/tg, wst/wst*)) are shown. M indicates a muscle sample (as an eEF1A2 positive control) and L indicates a liver sample (an eEF1A2 negative control).

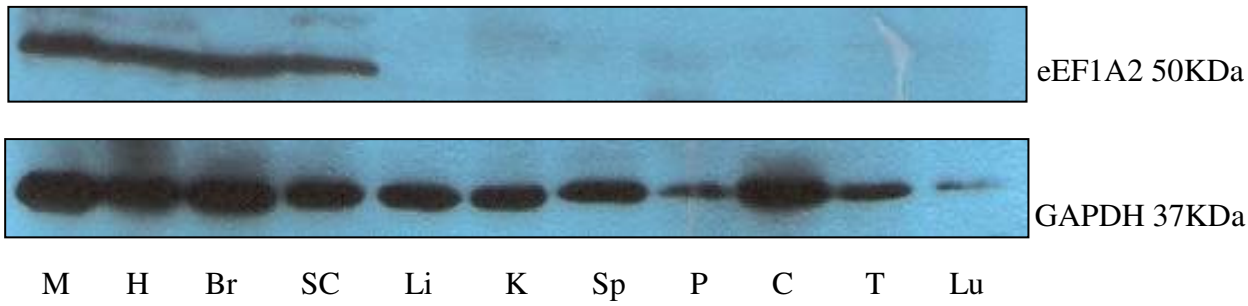

Figure 4.13. eEF1A2 protein expression in a panel of tissues from NSE-EEF1A2-B line animals.

Western blots showing expression of eEF1A2 and GAPDH (as a loading control) on an expanded panel of tissues from a wasted animal carrying the transgene (*+/tg, wst/wst*) from the transgenic line NSE-EEF1A2-B. M=Muscle, H=Heart, Br=Brain, SC= Spinal cord, Li=Liver, K=Kidney, Sp = Spleen, P=Pancreas, C=Colon, Lu=Lung. This Western was performed by Jennifer Doig.

Immunohistochemistry

Spinal cord and brain sections of animals from the NSE-EEF1A2 line B were stained by immunohistochemistry using an eEF1A2 specific antibody. This was to investigate whether the same patterns of eEF1A2 expression was seen at the cellular level between wildtype mice (+/+, +/+) and wasted animals carrying the transgene (*+/tg, wst/wst*). In the spinal cord, wasted animals carrying the transgene showed similar staining patterns compared to wildtype controls (figure 4.14). Staining was observed in the motor neurons as expected but also some additional staining was seen in non-motor neuron cells in the white matter. This ectopic expression of eEF1A2 in smaller neurons appears not be deleterious in terms of survival but may warrant further examination.

Brain expression of eEF1A2 was again similar between wildtype animals (+/+, +/+) and wasted animals carrying the transgene (*+/tg, wst/wst*) including positive staining of the Purkinjie cells of the cerebellum (figure 4.15) and also in the cells of the hippocampus (figure 4.16). This is the same expression pattern as that seen in wildtype mice.

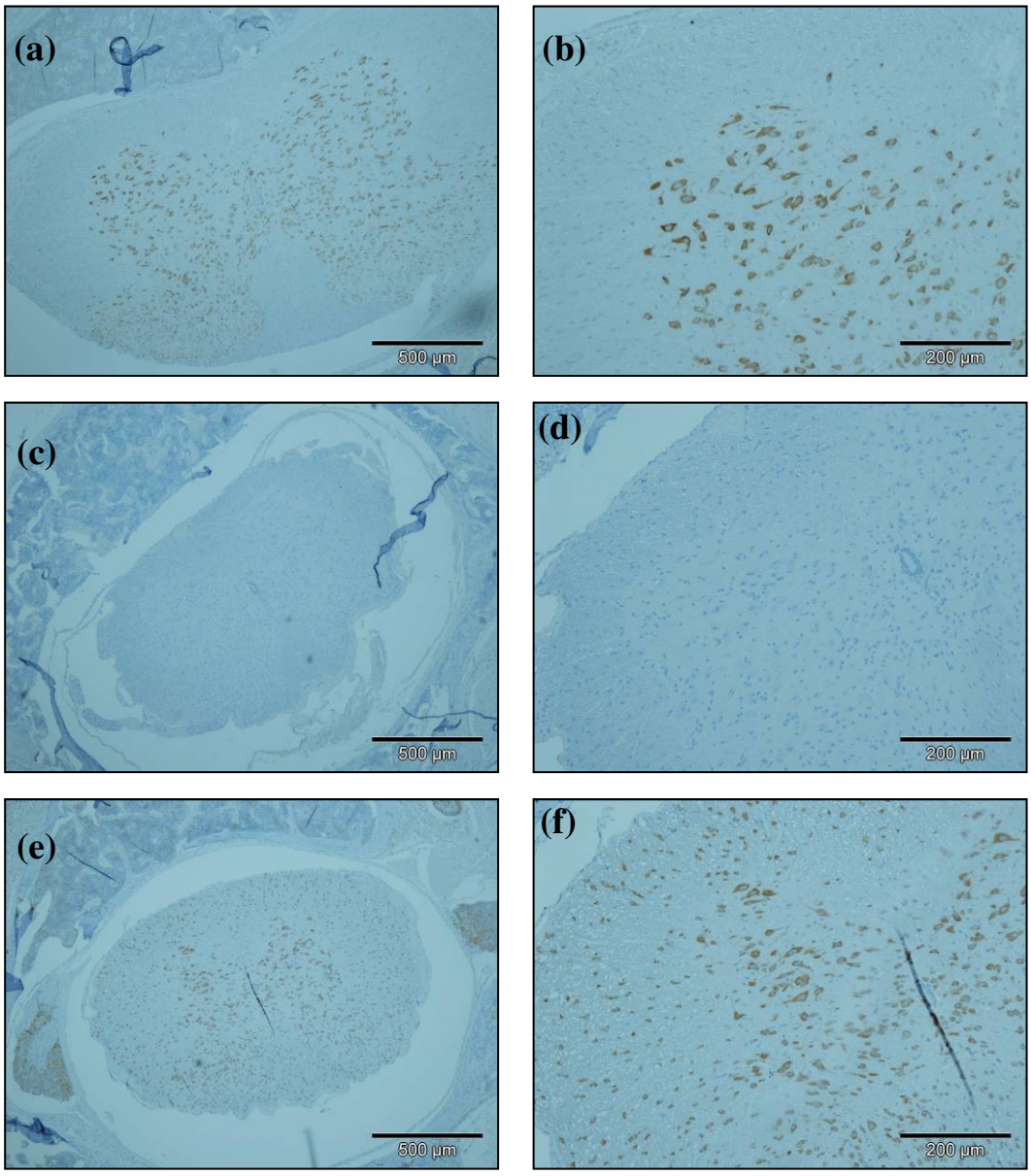

Figure 4.14. eEF1A2 expression in the spinal cord of animals from NSE-EEF1A2 line B.

Cervical spinal cord sections from animals from the NSE-EEF1A2-B line stained with an antibody recognising eEF1A2. Panels (a) and (b) are from a wildtype animal (+/+, +/+), panels (c) and (d) are from a wasted animal (+/+, *wst/wst*) and panels (e) and (f) are from a wasted animal carrying the transgene (*+/tg, wst/wst*). Panels (a), (c) and (e) are at 4x magnification while panels (b), (d) and (f) are at 10x magnification.

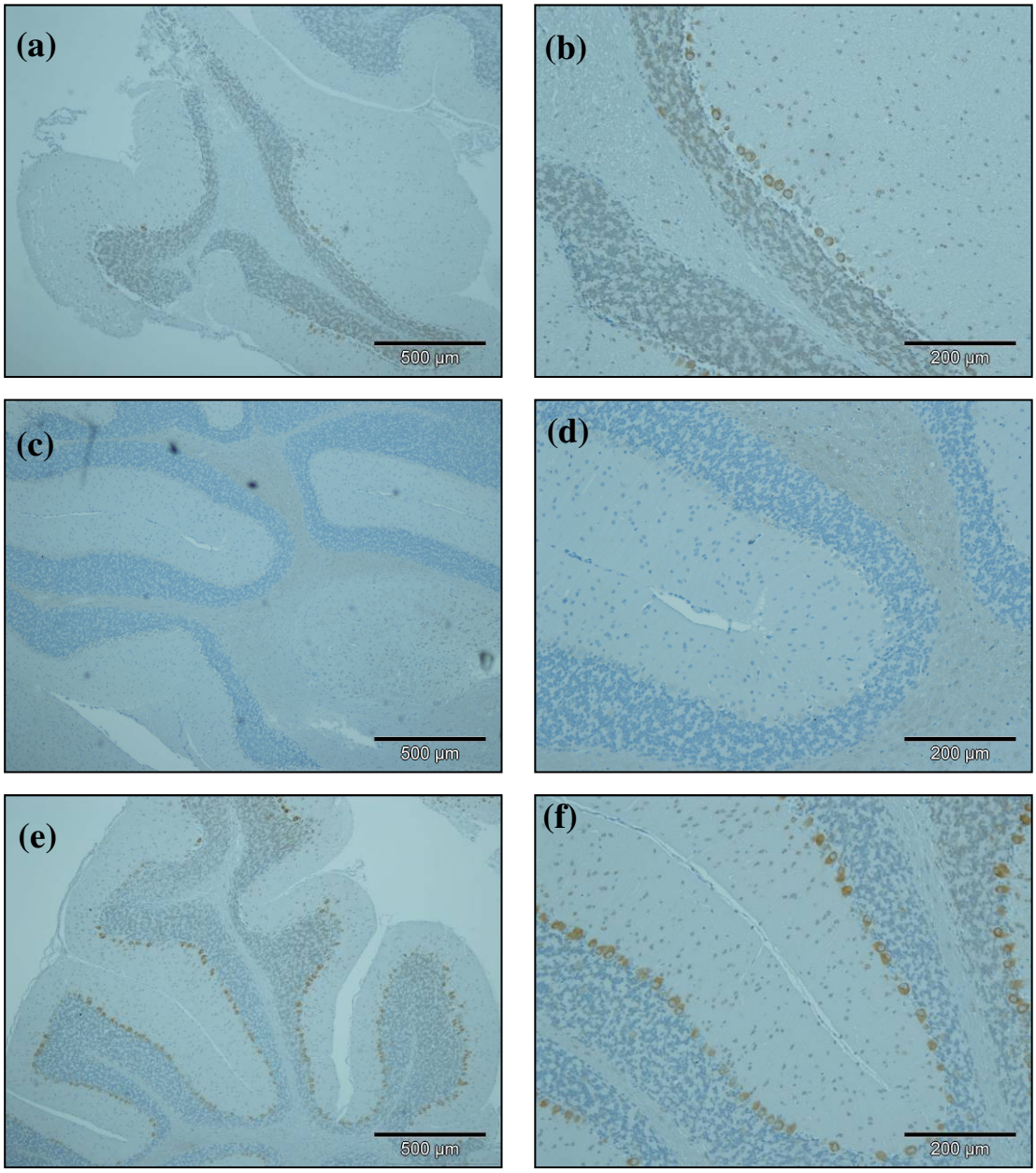

Figure 4.15. eEF1A2 expression in the cerebellum of animals from NSE-EEF1A2 line B.

Cerebella sections of animals from the NSE-EEF1A2-B line stained with an antibody recognising eEF1A2. Panels (a) and (b) are from a wildtype animal (+/+, +/+), panels (c) and (d) are from a wasted animal (+/+, *wst/wst*) and panels (e) and (f) are from a wasted animal carrying the transgene (*+/tg, wst/wst*). Panels (a), (c) and (e) are at 4x magnification while panels (b), (d) and (f) are at 10x magnification.

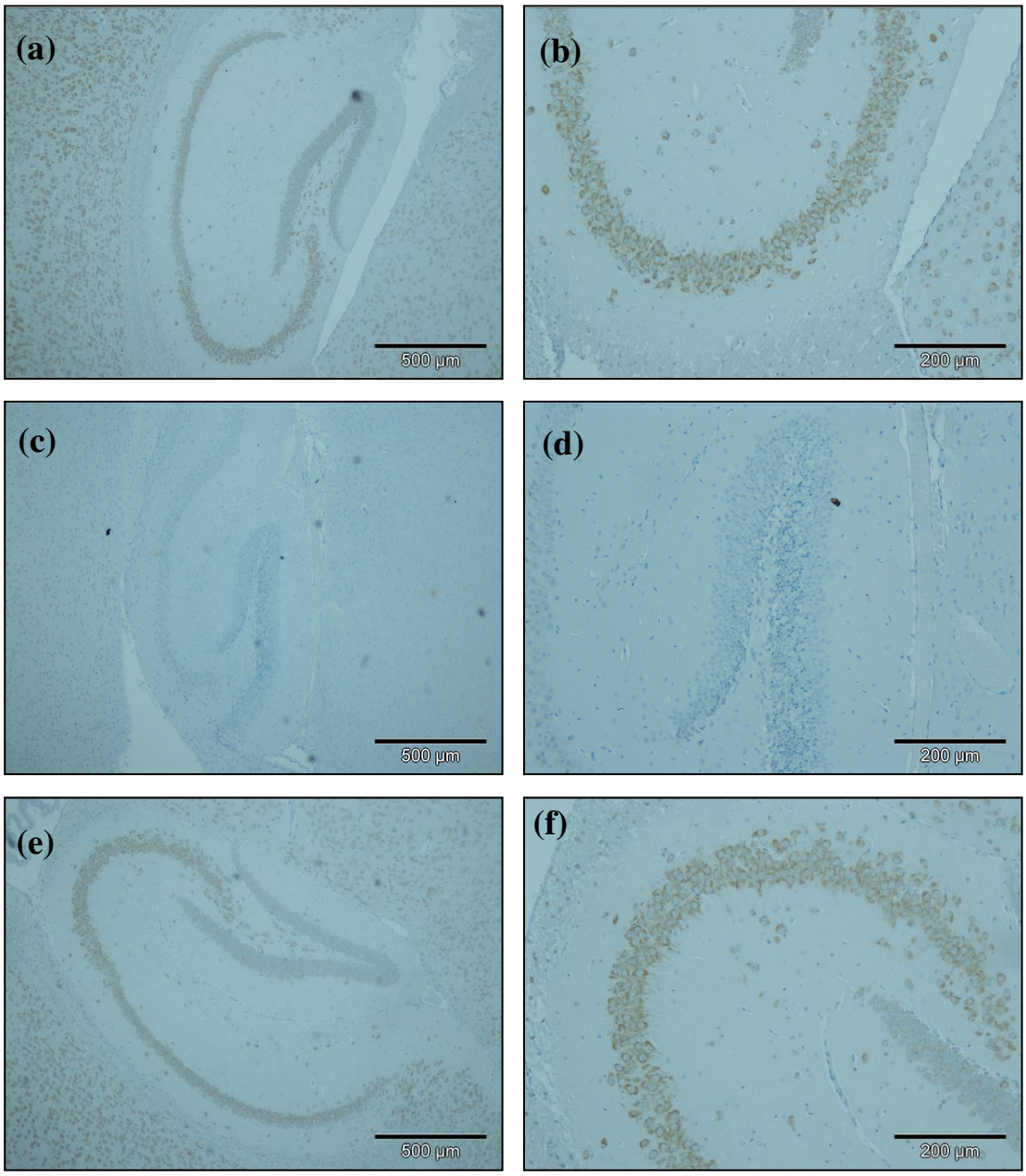

Figure 4.16. eEF1A2 expression in the hippocampus of animals from NSE-EEF1A2 line B.

Hippocampal sections from animals from the NSE-EEF1A2-B line stained with an antibody recognising eEF1A2. Panels (a) and (b) are from a wildtype animal (+/+, +/+), panels (c) and (d) are from a wasted animal (+/+, *wst/wst*) and panels (e) and (f) are from a wasted animal carrying the transgene (*+/tg, wst/wst*). Panels (a), (c) and (e) are at 4x magnification while panels (b), (d) and (f) are at 10x magnification.

eEF1A2 expression in the pancreas

Wasted animals with the transgene (*+/tg, wst/wst*) appear indistinguishable from wildtype mice at the protein level in all tissue and the cellular level in brain and spinal cord. Previously, immunohistochemistry experiments have revealed that eEF1A2 is also expressed in specialised cells in other tissues (not detected by Western blotting) including cells within the Islets of Langerhans in the pancreas (Newbery *et al.,* 2007).

Immunohistochemistry was performed on sections of pancreas from NSE-EEF1A2-B animals at 6 weeks of age to investigate eEF1A2 expression. Unlike wildtype animals no expression of eEF1A2 was observed in the islet cells of wasted animals carrying the transgene (*+/tg, wst/wst*). In conclusion wasted animals carrying the transgene (*+/tg, wst/wst*) from NSE-EEF1A2 line B are indistinguishable from wildtype animals in terms of protein expression at the level of whole tissue but maybe not at the level of specific cell types.

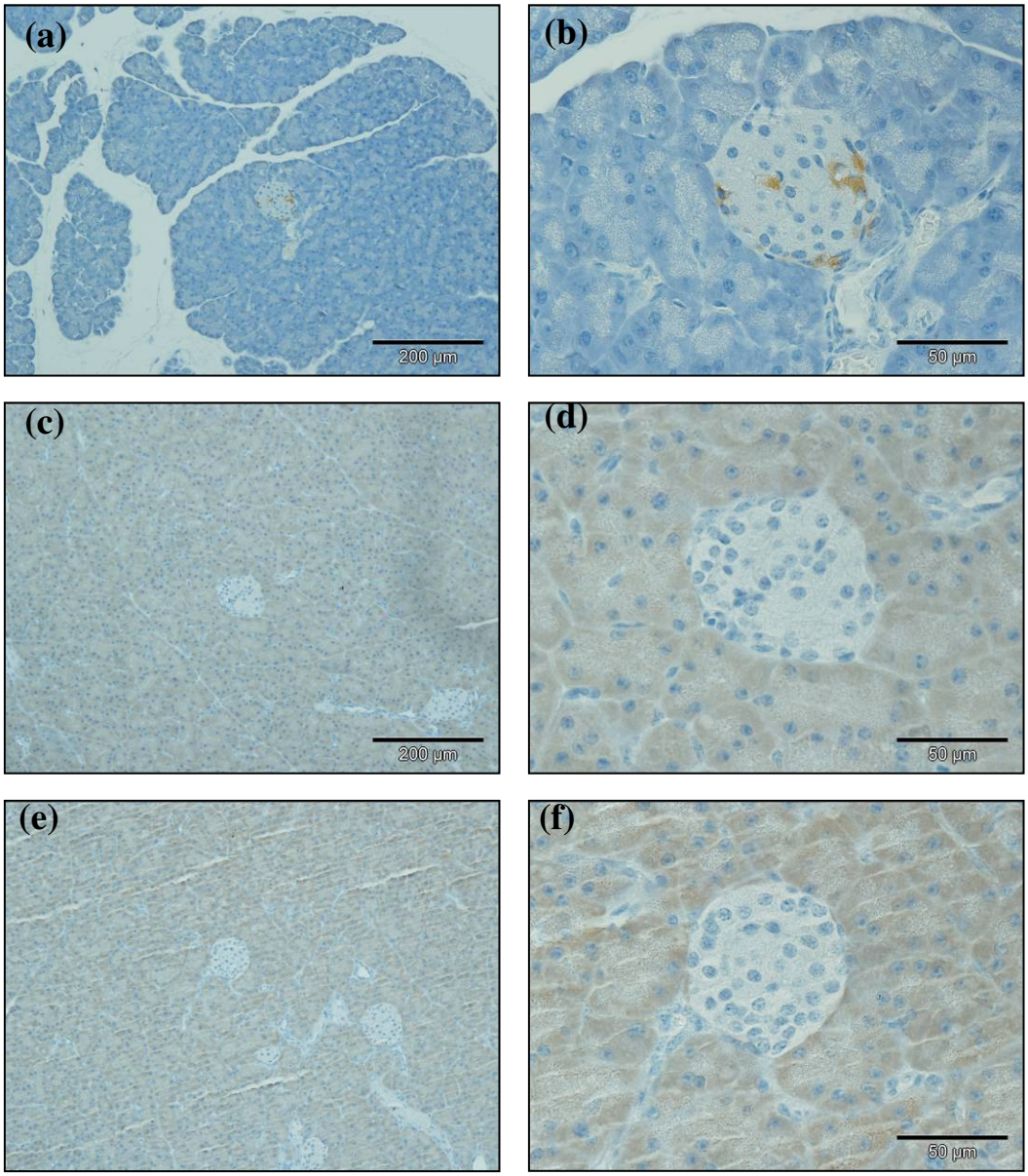

Figure 4.17. eEF1A2 expression in the pancreas of animals from NSE-EEF1A2 line B.

Pancreas sections of animals from the NSE-EEF1A2-B line stained with an antibody recognising eEF1A2. Panels (a) and (b) are from a wildtype animal (+/+, +/+), panels (c) and (d) are from a wasted animal (+/+, *wst/wst*) and panels (e) and (f) are from a wasted animal carrying the transgene (*+/tg, wst/wst*). Panels (a), (c) and (e) are at 10x magnification while panels (b), (d) and (f) are at 40x magnification.

4.3.4.3. NSE-EEF1A2-C

As with the NSE-EEF1A2 line B, the NSE-EEF1A2-C line wasted mice carrying the transgene (*+/tg, wst/wst*) showed no observable signs of neuromuscular disease at 25 days. Wasted mice carrying the transgene (*+/tg, wst/wst*) were indistinguishable from wildtype mice (+/+, +/+) at 25 days of age (figure 4.18). The splenic and thymic atrophy normally seen in wasted mice (*+/+, wst/wst*) was not observed in wasted mice carrying the transgene (*+/tg, wst/wst*). It therefore appears that the NSE-EEF1A2 transgene has corrected some aspects of the wasted phenotype in line C.

Body weight

As wasted mice show a dramatic decrease in body weight from 21 days until death, mice from the NSE-EEF1A2-C line were weighed at 25 days (end stage) to assess whether this disease phenotype was corrected (figure 4.19, Table 4.6). Wasted mice carrying the transgene (*+/tg, wst/wst*) showed a significant difference in body weight compared to wasted animals without the transgene (+/+, *wst/wst*). No significant difference was observed between wasted mice with the transgene and wildtype controls. As expected wasted mice showed a significant decrease in body weight compared to littermate controls. It would appear that the transgene has therefore rescued this aspect of the wasted phenotype.

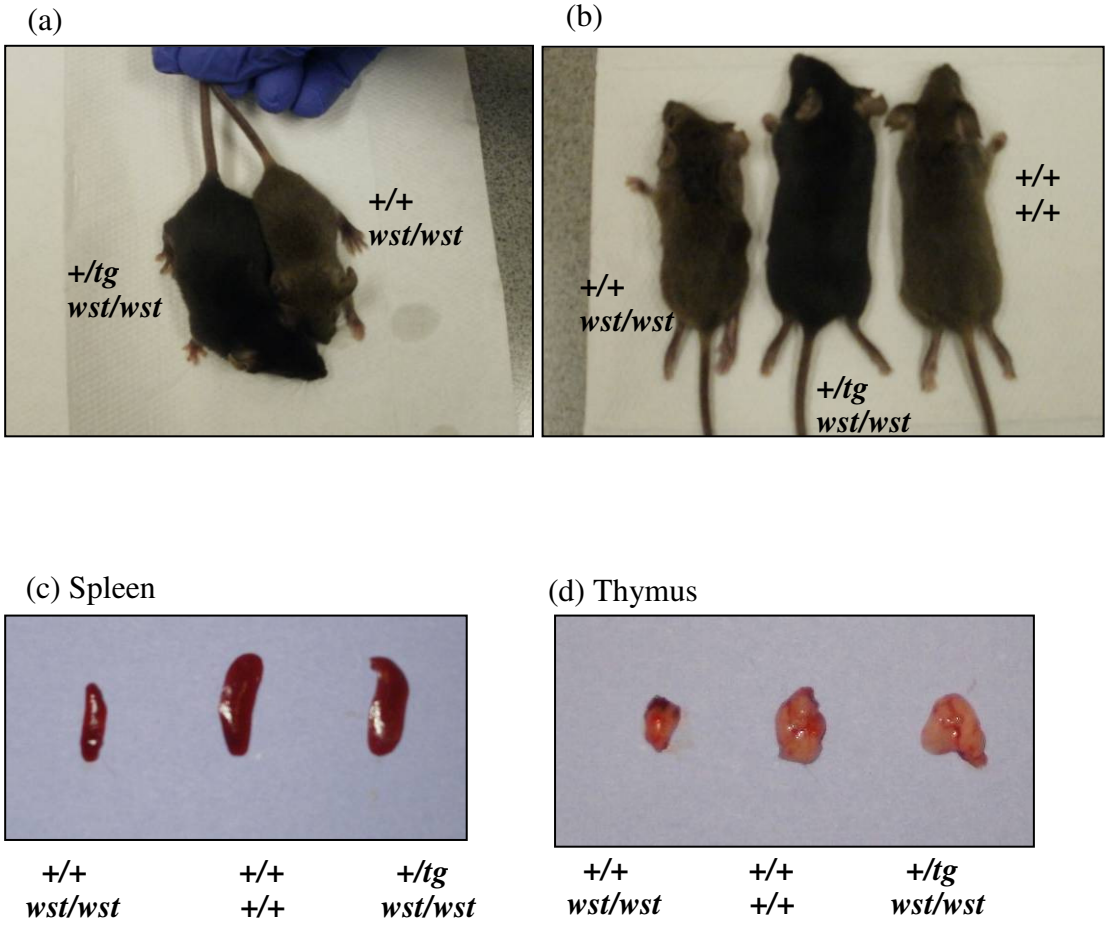

Figure 4.18. Photographs of animals from the NSE-EEF1A2-C line.

Photographs of animals from the NSE-EEF1A2-C line. Panels (a) and (b) show a wildtype animal (+/+,+/+) a wasted animal (+/+, *wst/wst*) and a wasted animal carrying the transgene (*+/tg, wst/wst*). Panels C (spleen) and D (thymus) show tissues from the animals in panel (b)

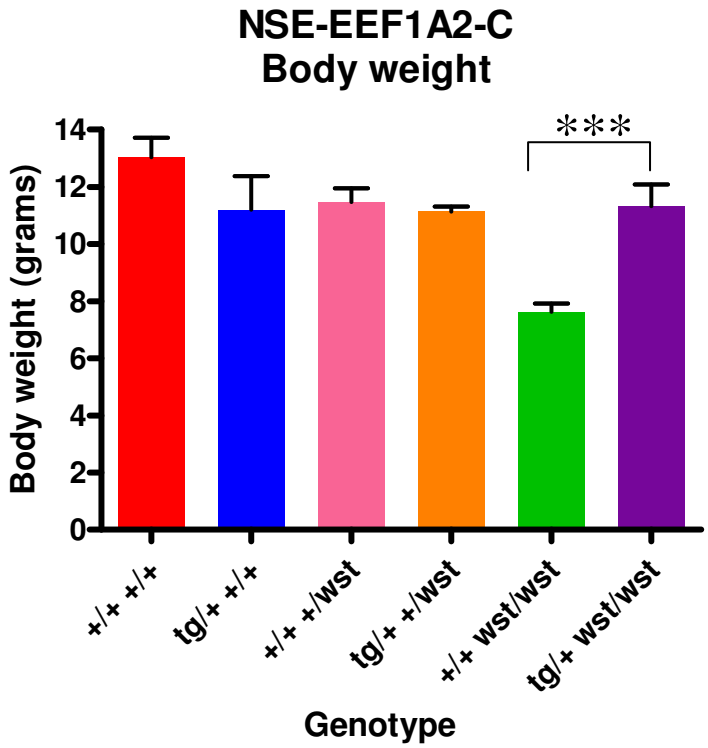

Figure 4.19. Body weights of 25 day old mice from the NSE-EEF1A2-C line.

Body weight measurements from wildtype animals (+/+, +/+), wildtype animals with the transgene (+/tg, +/+), heterozygote animals without the transgene (+/+, *+/wst*), heterozygote animlas with the transgene (*+/tg, +/wst*), wasted animals without the transgene *(+/+, wst/wst*) and wasted animals with the transgene (*+/tg, wst/wst*) are shown. Animals were weighed at 25 days (end stage). *** indicates a p value <0.01

Genotype	N	Mean	Min	Max	S.D	S.E.M
(+/+, +/+)	6	13	10.9	14.6	1.7	0.7
(+/tg, +/+)	5	11.2	9	15.4	2.6	1.2
(+/+, +/wst)	8	11.5	10.1	14.6	1.4	0.5
(+/tg, +/wst)	6	11.1	10.4	11.7	0.4	0.2
(+/+, wst/wst)	9	7.6	6.6	8.9	0.9	0.3
(+/tg, wst/wst)	10	11.3	8	14.6	2.4	0.8

Table 4.6. Body weights of 25 day old mice from the NSE-EEF1A2-C line.

Statistical analysis of body weights of mice from the NSE-EEF1A2-C line. Animals were weighed at 25 days (disease end stage). Number of animals (N), mean, minimum (Min) and maximum (Max) bodyweight for each genotype are shown. S.D indicates the standard deviation across each genotype and S.E.M is a measure of the standard error of the mean.

Grip strength analysis

Analysis of both forelimb and all four limb grip strength (figure 4.20, table 4.7) showed that wasted mice carrying the transgene (*+/tg, wst/wst*) were indistinguishable from wildtype animals (+/+,+/+) and had significantly higher grip strength than wasted mice without the transgene (+/+, *wst/wst*). It appears that the poor grip strength normally seen in wasted mice is therefore corrected by the expression of the transgene in this line.

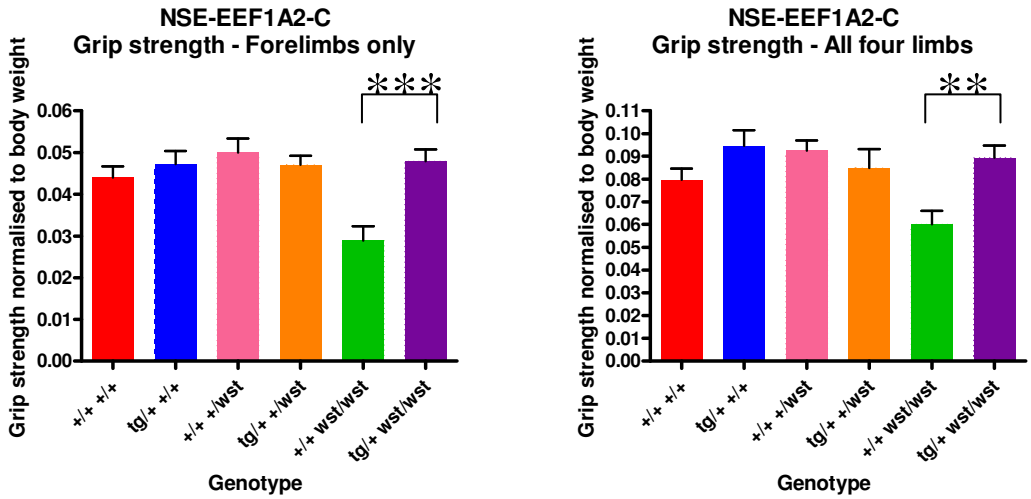

Figure 4.20. Grip strength analysis of 25 day old mice from the NSE-EEF1A2-C line.

Mean grip strength analysis from 25 day old wildtype animals (+/+,+/+), wildtype animals with the transgene (+/*tg*, +/+), heterozygote animals without the transgene (+/+, +/*wst*), heterozygote animals with the transgene (+/*tg, +/wst*), wasted animals without the transgene *(+/+, wst/wst*) and wasted animals with the transgene (+/*tg, wst/wst*) from the NSE-EEF1A2 line C are shown. Forelimb (left graph) and all four limb (right graph) grip strength readings from 3 tests (measured in Newtons) were normalised to body weight (measured in grams). *** indicates a p value <0.001 and ** indicates a p value <0.01.

(a) Forelimbs only

Genotype	N	Mean	Min	Max	S.D	S.E.M
(+/+, +/+)	6	0.044	0.033	0.052	0.007	0.003
(+/tg, +/+)	5	0.047	0.041	0.058	0.007	0.003
(+/+, +/wst)	8	0.050	0.034	0.061	0.010	0.003
(+/tg, +/wst)	6	0.047	0.040	0.054	0.005	0.002
(+/+, wst/wst)	9	0.029	0.014	0.044	0.010	0.003
(+/tg, wst/wst)	10	0.048	0.032	0.064	0.009	0.003

(b) All four limbs

Genotype	N	Mean	Min	Max	S.D	S.E.M
(+/+, +/+)	6	0.080	0.063	0.097	0.012	0.005
(+/tg, +/+)	5	0.094	0.069	0.107	0.016	0.007
(+/+, +/wst)	8	0.092	0.075	0.114	0.013	0.004
(+/tg, +/wst)	6	0.085	0.060	0.115	0.020	0.008
(+/+, wst/wst)	9	0.060	0.040	0.091	0.017	0.006
(+/tg, wst/wst)	10	0.048	0.032	0.064	0.009	0.003

Table 4.7. Grip strength analysis of 25 day old mice from the NSE-EEF1A2-C line.

Statistical analysis of grip strength from 25 day old wildtype animals (+/+,+/+), wildtype animals with the transgene (*+/tg*, +/+), heterozygote animals without the transgene (+/+, *+/wst*), heterozygote animals with the transgene (*+/tg, +/wst*) wasted animals without the transgene *(+/+, wst/wst*) and wasted animals with the transgene (*+/tg, wst/wst*) from the NSE-EEF1A2 line C. Animals were tested at 25 days (wasted end stage). Number of animals (N), mean, minimum (Min) and maximum (Max) bodyweight for each genotype are shown. S.D indicates the standard deviation across each genotype and S.E.M is a measure of the standard error of the mean.

Protein expression

Western blots indicate that the transgene is expressed at the protein level. As in The NSE-EEF1A2-B line, expression is not restricted to the central nervous system (figure 4.21). Brain, spinal cord, muscle, heart and liver samples were analysed for protein expression from 25 day old animals. Three wildtype animals (+/+, +/+), three wildtypes carrying the transgene (*+/tg,* +/+), three wasted animals (+/+, *wst/wst*) and three wasted animals carrying the transgene (*+/tg, wst/wst*) were analysed. Results show that the transgene is expressed in brain and spinal cord as expected but again also in muscle (figure 4.21). Unlike NSE-EEF1A2-B however, it initially appeared that there was no eEF1A2 expression in heart (figure 4.21 panel (d)). Further investigation of the hearts of more animals actually showed variable expression of eEF1A2 (figure 4.26, table 4.8). Panels of tissues from six week old wasted animals carrying the transgene were also examined (an example can be seen in figure 4.22). No expression of eEF1A2 was seen in any other tissues examined.

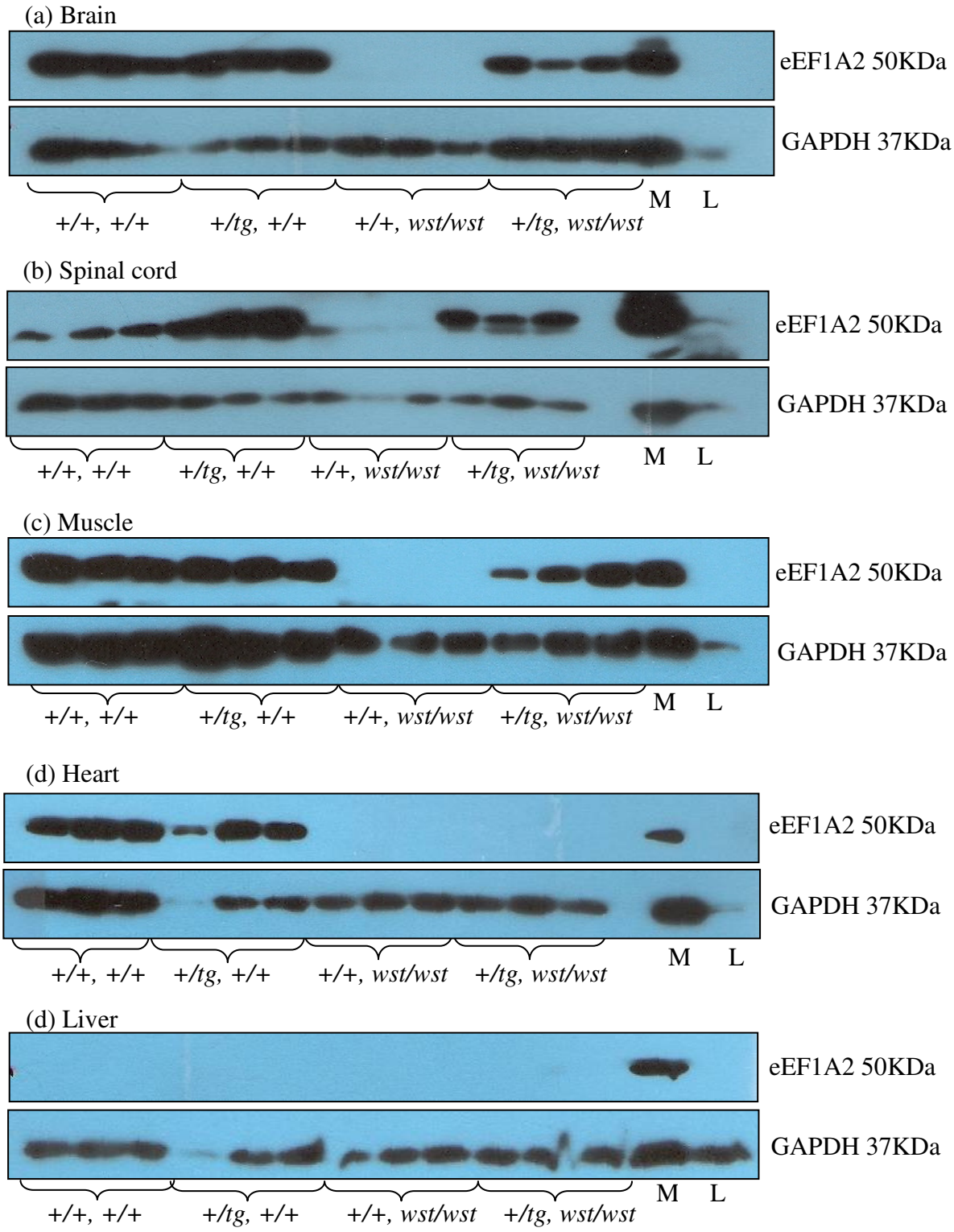

Figure 4.21. eEF1A2 protein expression in tissues from NSE-EEF1A2-C line animals.

Western blots showing expression of eEF1A2 and GAPDH (as a loading control) of animals from the transgenic line NSE-EEF1A2-C. Expression from three animals from each group (wildtype (+/+,+/+), wildtype with the transgene *(+/+, +/tg*), wasted animals without the transgene *(+/+, wst/wst*) and wasted animals with the transgene (*+/tg, wst/wst*)) are shown. M indicates a muscle sample (as an eEF1A2 positive control) and L indicates a liver sample (an eEF1A2 negative control).

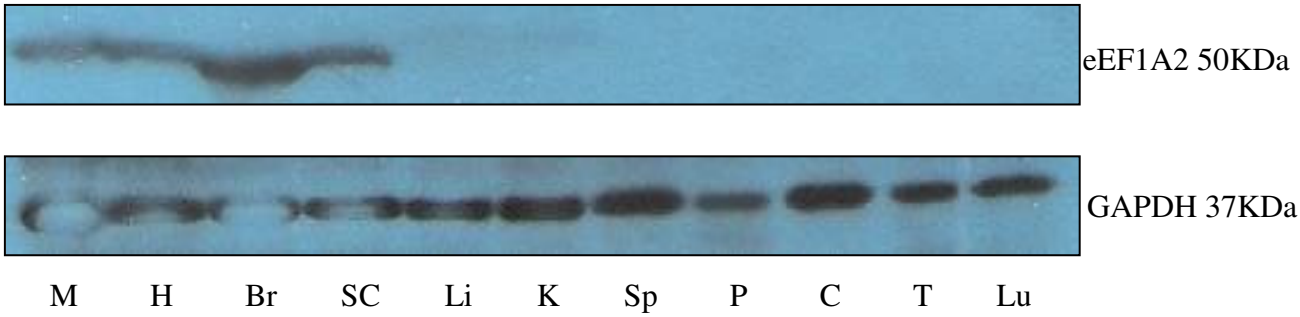

Figure 4.22. eEF1A2 protein expression in a panel of tissues from NSE-EEF1A2-C line animals.

Western blots showing expression of eEF1A2 and GAPDH (as a loading control) on an extended tissue panel from a wasted animal carrying the transgene (*+/tg, wst/wst*) from the transgenic line NSE-EEF1A2-B. M=Muscle, H=Heart, Br=Brain, SC= Spinal cord, Li=Liver, K=Kidney, Sp = Spleen, P=Pancreas, C=Colon, Lu=Lung. This Western was performed by Jennifer Doig.

Immunohistochemistry

Spinal cord and brain sections of animals from the NSE-EEF1A2 line C were stained by immunohistochemistry using an eEF1A2 specific antibody. This was to investigate whether the same patterns of eEF1A2 expression was seen at the cellular level between wildtype mice (+/+, +/+) and wasted animals carrying the transgene (*+/tg, wst/wst*). The staining pattern in the spinal cord from wasted animals carrying the transgene was indistinguishable from that seen in wildtype controls (figure 4.23). Brain expression of eEF1A2 was again similar between wildtype animals (+/+, +/+) and wasted animals carrying the transgene (*+/tg, wst/wst*) including positive staining of the Purkinjie cells of the cerebellum (figure 4.24) and also in the cells of the hippocampus (figure 4.25), in keeping with wildtype expression.

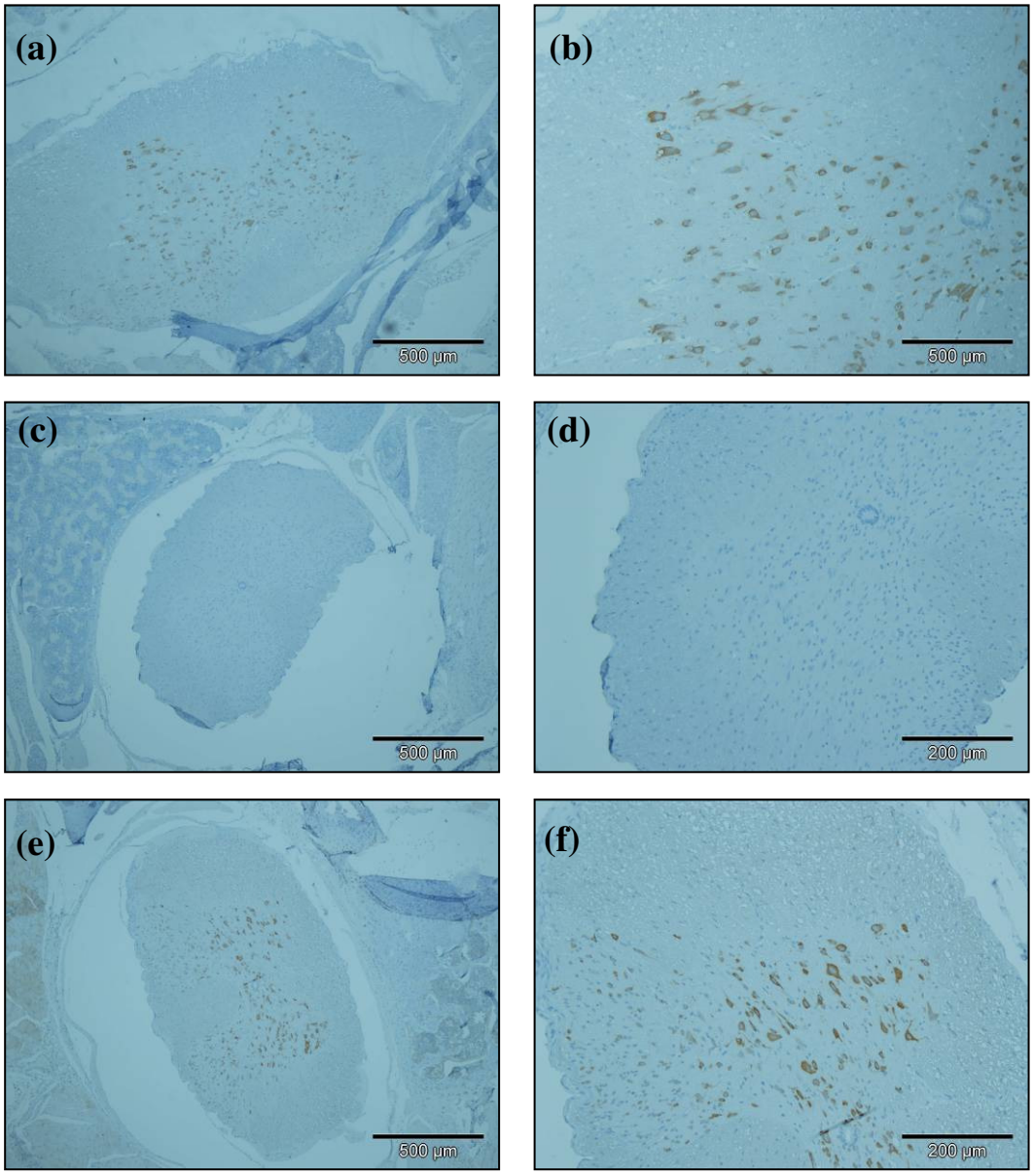

Figure 4.23. eEF1A2 expression in the spinal cord of animals from NSE-EEF1A2 line C.

Cervical spinal cord sections from animals from the NSE-EEF1A2-C line stained with an antibody recognising eEF1A2. Panels (a) and (b) are from a wildtype animal (+/+, +/+), panels (c) and (d) are from a wasted animal (+/+, *wst/wst*) and panels (e) and (f) are from a wasted animal carrying the transgene (*+/tg, wst/wst*). Panels (a), (c) and (e) are at 4x magnification while panels (b), (d) and (f) are at 10x magnification. These results were obtained using the POLINK method.

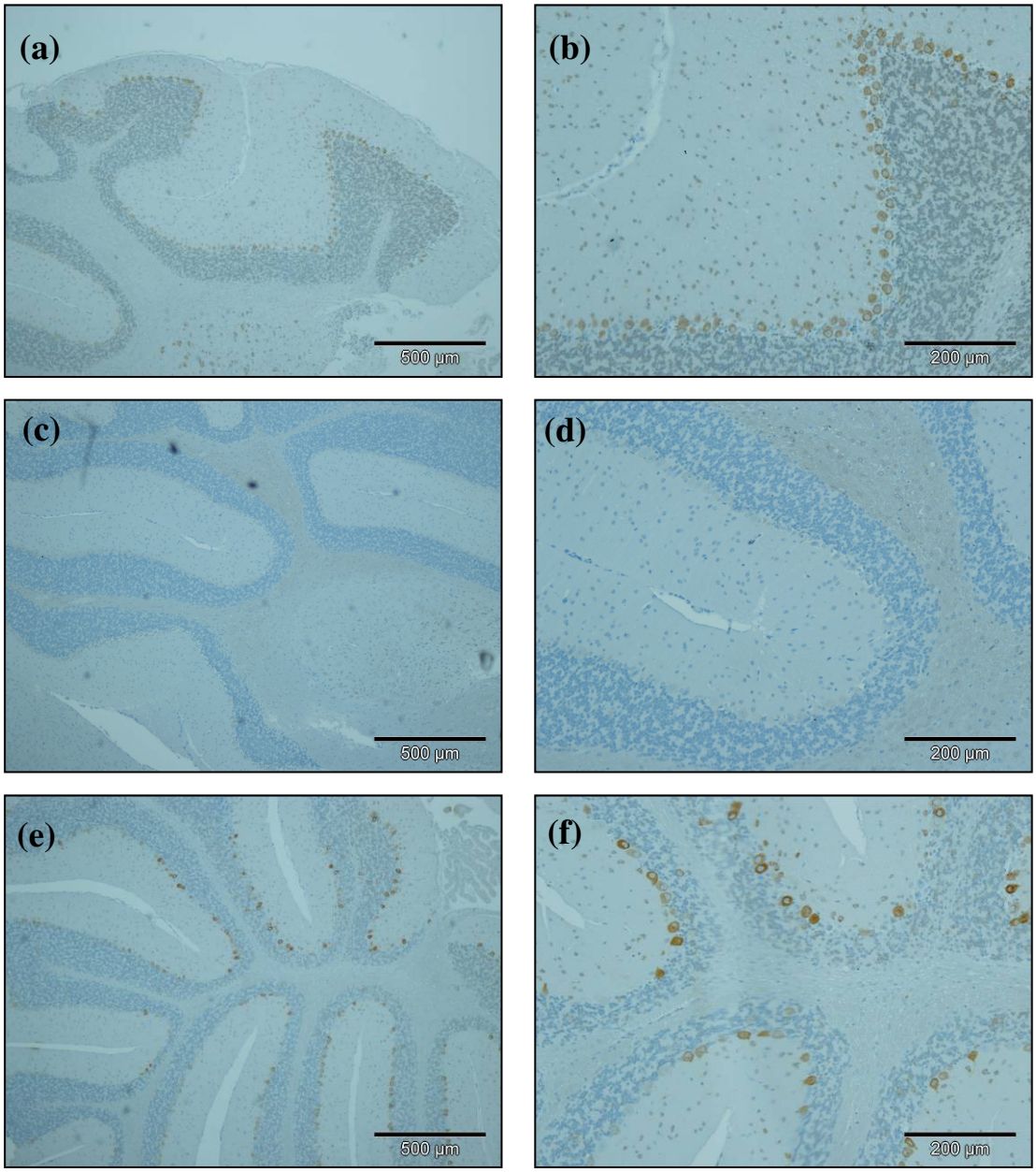

Figure 4.24. eEF1A2 expression in the cerebellum of animals from NSE-EEF1A2 line C.

Cerebella sections from animals from the NSE-EEF1A2-C line stained with an antibody recognising eEF1A2. Panels (a) and (b) are from a wildtype animal (+/+, +/+), panels (c) and (d) are from a wasted animal (+/+, *wst/wst*) and panels (e) and (f) are from a wasted animal carrying the transgene (*+/tg, wst/wst*). Panels (a), (c) and (e) are at 4x magnification while panels (b), (d) and (f) are at 10x magnification. These results were obtained using the POLINK method.

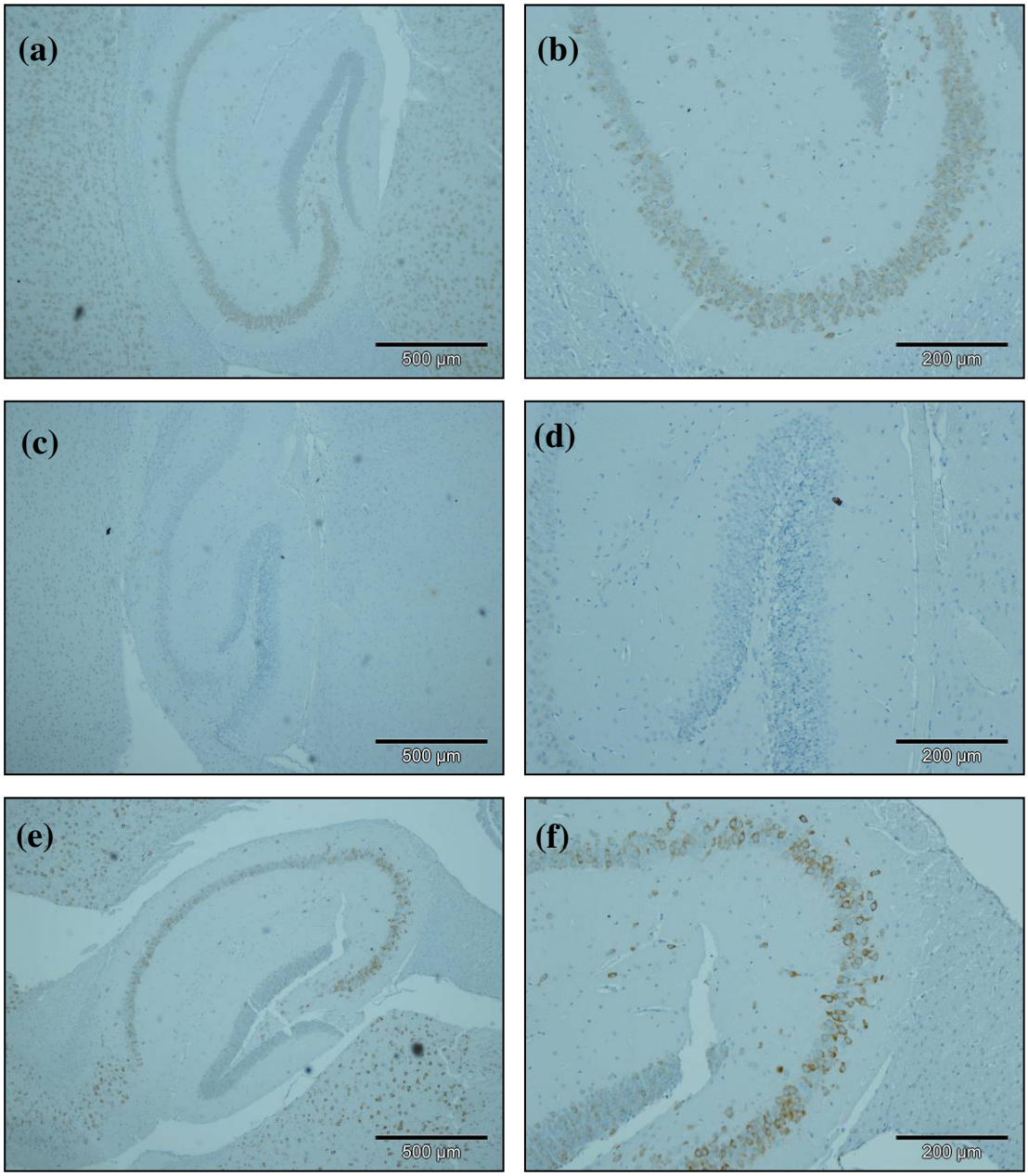

Figure 4.25. eEF1A2 expression in the hippocampus of animals from NSE-EEF1A2 line C.

Hippocampal sections from animals from the NSE-EEF1A2-C line stained with an antibody recognising eEF1A2. Panels (a) and (b) are from a wildtype animal (+/+, +/+), panels (c) and (d) are from a wasted animal (+/+, *wst/wst*) and panels (e) and (f) are from a wasted animal carrying the transgene (*+/tg, wst/wst*). Panels (a), (c) and (e) are at 4x magnification while panels (b), (d) and (f) are at 10x magnification. These results were obtained using the POLINK method.

A possible heart phenotype.

Prior to the knowledge of the variable expression of eEF1A2 in heart, a cohort of animals from the NSE-EEF1A2 line C were aged to six months to further investigate any phenotype caused by this transgene in animals of adult mice. A proportion (5 out of 9) of the wasted animals with the transgene in this ageing cohort failed to survive to 6 months. Animals would die suddenly between 6 weeks and 4 months of age. On observation of two of these animals, hearts appeared enlarged. This initiated a further study into the heart phenotype of these animals.

Initially it appeared that wasted mice carrying the transgene from line C had no expression of eEF1A2 in heart (even though it was expressed everywhere else that eEF1A2 would be seen in wildtype animals) on a Western blot as shown in figure 4.21, but this was not the case for all animals (figure 4.26). Further wasted animals carrying the transgene (*+/tg, wst/wst*) of around 6 weeks of age were analysed for heart eEF1A2 expression by Western blotting (figure 4.26). As can be seen in figure 4.26 expression was highly variable. Table 4.8 displays data from all animals so far investigated for heart eEF1A2 expression to attempt to identify any correlations between heart eEF1A2 expression and sex and/or genetic lineage. No obvious correlation was seen but this is further elaborated on in the discussion section of this chapter.

In the animals where no eEF1A2 expression was observed in the heart (figure 4.21), eEF1A1 expression was also investigated in the hearts of these animals to identify whether a compensatory mechanism was in place. As is shown in figure 4.27, no expression of eEF1A1 was observed in these samples thus eEF1A1 is not compensating for the loss of eEF1A2 in these animals.

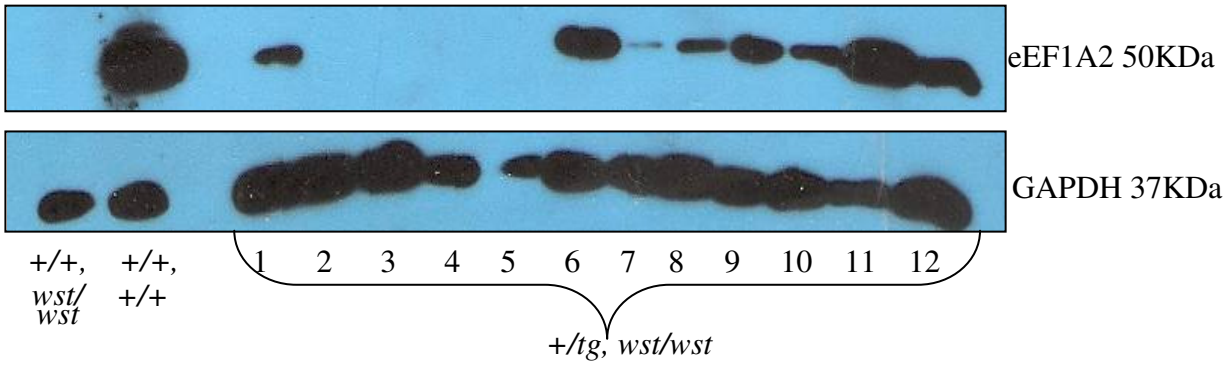

Figure 4.26. eEF1A2 expression in heart tissue of wasted animals carrying the transgene from the NSE-EEF1A2 line C.

eEF1A2 and GAPDH expression in heart tissue from 12 wasted animals carrying the transgene (*+/tg, wst/wst*).

Number	Age at death	Cause of death	Sex	eEF1A2 Expression	Breeding Pair	Transgenic Parent
1	4 weeks	Culled	Female	Yes (weak)	Two	Male
2	4 weeks	Culled	Female	No	Two	Male
3	6 weeks	Culled	Male	No	Two	Male
4	6 weeks	Unknown	Male	No	Two	Male
5	7 weeks	Unknown	Male	No	Two	Male
6	6 weeks	Culled	Male	Yes (strong)	Four	Female
7	6 weeks	Culled	Male	Yes (weak)	Four	Female
8	6 weeks	Culled	Male	Yes (weak)	Four	Female
9	7 weeks	Culled	Female	Yes (strong)	Four	Female
10	7 weeks	Culled	Male	Yes (weak)	Four	Female
11	6 weeks	Culled	Female	Yes (strong)	Six	Male
12	6 weeks	Culled	Male	Yes (weak)	Five	Female

Table 4.8. eEF1A2 expression in heart tissue of wasted animals carrying the transgene from the NSE-EEF1A2 line C.

Details of 12 wasted animals carrying the transgene (*+/tg*, *wst/wst*) including age and cause of death, sex, the degree of eEF1A2 expression (as shown in figure 4.26), breeding pair (to display which mice are from the same parental line) and an indication of which parent the transgene was inherited from.

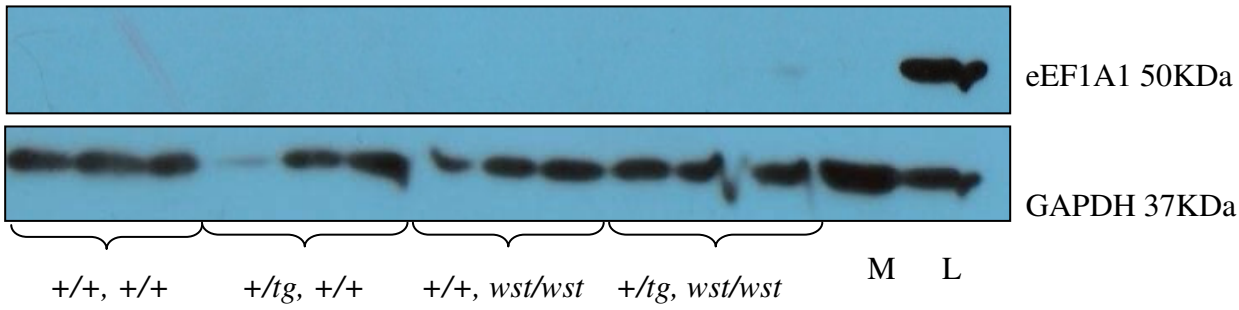

Figure 4.27. eEF1A1 expression in heart tissue of animals from the NSE-EEF1A2-C line

Western blots showing expression of eEF1A1 and GAPDH (as a loading control) of animals from the transgenic line NSE-EEF1A2-C. Expression from three animals from each group (wildtype (+/+,+/+), wildtype with the transgene (+/+, +/tg,}wasted animals without the transgene *(+/+, wst/wst*) and wasted animals with the transgene (*+/tg, wst/wst*)) are shown. M indicates a muscle sample (as an eEF1A1 negative control) and L indicates a liver sample (an eEF1A1 positive control).

4.4. Discussion

The nature of the primary cause of the pathology of wasted mice is still to be confirmed. It remains to be established whether the loss of eEF1A2 in muscle leading to a primary muscle myopathy is the primary cause of the muscle pathology, or whether it is the loss of neuronal eEF1A2 causing denervation of muscle that leads to muscle atrophy.

As mentioned, Permphan Dharmasaroja's work addressed one half of this important question. It was shown that expression of eEF1A2 exclusively in muscle, did not appear to rescue the wasted phenotype, despite significant levels of eEF1A2 protein expression in muscle tissue. Only one transgenic line that expressed muscle specific eEF1A2 was generated. Further lines should be investigated, to eliminate the possibility of the results observed being due solely to the integration site of the transgene. Four additional transgenic lines were generated within this project by microinjection of the construct used previously (Dharmasaroja 2007). Unfortunately restrictions in animal movements imposed by the Biological Research Facility resulted in the generation of wasted mice carrying the transgene being significantly delayed. This in turn prevented expression analysis from being conducted on wasted mice carrying the muscle specific transgene within the time scale of the project. Preliminary results generated by Jennifer Doig suggests that two of the four lines express eEF1A2 specifically in muscle tissue and this expression does not correct the wasted phenotype (unpublished data). These results are consistent with those of the previous line generated (Dharmasaroja 2007) and as such further support the notion that the loss of neuronal eEF1A2 is the primary cause of the muscle pathology. To complete the picture, rescue by neuronal eEF1A2 only, needs to be demonstrated, which was the primary aim of this study.

To directly compare the two halves of this experiment, the same methodology was used in this study as was used by Permphan (Dharmasaroja 2007). The same eEF1A2 construct was used to isolate the gene and the same restriction sites were used to insert the promoter (neuronal specific enolase (NSE) promoter) as was used in the generation of the muscle specific promoter used previously. One deviation from the

previous protocol was required; the method of purification of the eEF1A2 fragment. In his thesis Permphan describes how using gel purification he was able to separate the unwanted eEF1A2 promoter region from the required fragment (Dharmasaroja 2007). Although the same protocol was followed here, the gel purification protocol appeared to hinder ligation. Thus it was deemed necessary to simply purify the entire digest with a purification kit (rather than separate out the fragments on a gel) and then add promoter at a higher ratio than was used previously. This resulted in an increased number of colonies requiring screening due to the competition between the *EEF1A2* promoter and the new NSE promoter. Positive colonies were eventually identified by PCR and confirmed by restriction digest, however this did result in a delay in the cloning of the construct.

As previously described, three transgenic lines were generated in the first round of injection of which all three transmitted through the germline. It quickly became apparent that two of the three transgenic lines were rescuing the wasted phenotype. The third line NSE-EEF1A2-A failed to rescue any aspect of the wasted phenotype. Expression analysis quickly showed that although the construct was present in the genomic DNA, it was not being expressed at the protein level or the RNA level (data not shown). The reason for this is undetermined however it is likely to be due to the site of integration. For example the transgene may have integrated into an area of the genome which is transcriptionally inactive or is strongly repressed.

At first it appeared the other two lines (NSE-EEF1A2-B and NSE-EEF1A2-C) were completely rescuing the wasted phenotype. Unfortunately expression analysis showed undesired, non-specific expression in muscle tissue. As a result the aims of the project could not be addressed, as expression was not exclusively neuronal.

NSE-EEF1A2-B showed the same expression pattern on a Western blot as is seen in wildtype animals. In wasted animals carrying the transgene (*+/tg, wst/wst*) eEF1A2 expression was observed in brain, spinal cord, muscle and heart but in no other tissue examined. Non-specific promoter expression of transgenes is commonly seen and is often due to the site of integration. One possibility in this study is that the transgene has integrated into the genome adjacent to a muscle specific promoter/enhancer element, resulting in non-specific muscle expression.

This is not the first study using this promoter to see non-specific expression. In Shim *et al* expression of the transgene was found to be expressed at high levels in the brain and lower levels of expression was observed in kidney and liver but none in muscle (Shim *et al.,* 2007). Hwang *et al* (Hwang *et al.,* 2002) also used this promoter and presented two transgenic lines, one of which had very non-specific expression across multiple tissue types and the other showed expression in brain, muscle and heart (like our study). Many investigations using the rat NSE promoter region described by Forss-Petter *et al* (Forss-Petter *et al.,* 1990) had directly received a plasmid containing the promoter from the authors of the paper. It is possible that there may be slight discrepancies between the sequence of the promoter cloned here and the one cloned in other studies. The NSE promoter-containing-plasmid was therefore kindly donated by Dr Forss-Petter. This promoter was sequenced and compared to that obtained from the RAT2 cell line that was used in this study. A single discrepancy was identified; the promoter used in this study contained an additional 20bp upstream of the NSE promoter. This additional sequence was investigated and the only sequence found to match this 20bp region was that of NSE. It is therefore unlikely that this additional 20bp is the cause of the non-specific muscle expression seen in this study. To remove any doubt, in future studies a direct PCR of the promoter construct received from the Forss-Petter lab should be used to correspond exactly with the experiments previously reported. Other neuronal specific promoters such as the Thy1.2 expression cassette (Caroni 1997) should also be investigated.

The cell specific expression of eEF1A2 in pancreas of NSE-EEF1A2-B wasted mice carrying the transgene (*+/tg, wst/wst*) was also investigated. In addition to expression of eEF1A2 in the CNS and muscle tissue, some specialized cell types in other tissues also express eEF1A2. The Islets of Langerhan cells, some neuroendocrine cells in the base of the gut and retinal ganglion cells are examples (Newbery *et al.,* 2007). The Islets of Langerhans were investigated in these transgenic animals to assess whether there is any difference in expression between wildtype animals (+/+, +/+) and wasted animals carrying the transgene (*+/tg, wst/wst*). Results showed no eEF1A2 expression in the Islets of Langerhans in wasted mice carrying the transgene (*+/tg, wst/wst*). While this loss appears not to influence any of the observable symptoms in

wasted mice, it will be interesting to investigate whether these animals display any abnormalities in the pancreas because of this lack of eEF1A2 in the islets. A cohort of animals were aged to >6months of age to examine this. Pathological analysis of the pancreas showed no observable differences between wasted mice carrying the transgene (*+/tg, wst/wst*) and wildtype controls (data not shown). However, the pancreas should be analysed biochemically in these animals, to elucidate whether eEF1A2 is required for nomal pancreatic function. At the time of completion of the project the necessary licence was not in place to conduct such experiments but these will be conducted in the future.

The non-specific expression of eEF1A2 has prevented the aims of this project from being addressed, however overexpression of eEF1A2 in muscle is of interest to Dr Bernard Jasmin's group (Miura *et al.,* 2010). They are now investigating tissue samples from wildtype animals carrying the transgene as they appear to express eEF1A2 above the level observed in wildtype animals. Any results from this investigation have yet to be reported.

Inititally, NSE-EEF1A2 line C appeared to have the same limitations as the NSE-EEF1A2-B line. Like in NSE-EEF1A2 line B, wasted mice carrying the transgene (*+/tg, wst/wst*) in NSE-EEF1A2 line C showed no observable signs of neuromuscular disease. Initial expression analysis suggested that protein expression in the NSE-EEF1A2-C line was again not restricted to the central nervous system (CNS). In the panel of mice investigated, expression was observed in brain, spinal cord and muscle of wasted mice carrying the transgene (*+/tg, wst/wst*). Unlike in the NSE-EEF1A2-B line no expression of EEF1A2 was initially observed in hearts of wasted mice carrying the transgene (*+/tg, wst/wst*). Thus it appeared that eEEF1A2 expression had been corrected in the CNS and muscle but not heart. At this time a cohort of mice were being aged to 6 months to undertake similar studies as the NSE-EEF1A2-B line. Many mice in the cohort however, didn't survive to six months of age. Of the 9 wasted mice carrying the transgene (*+/tg, wst/wst*) in this cohort only 4 survived to 6 months of age. The mice appeared to die spontaneously between 6 weeks and 4 months of age. Two mice were examined after death and on observation appeared to have enlarged hearts. These two mice also showed no expression of eEF1A2 in heart

tissue (figure 4.26, animals 4 and 5). The mice that did survive to 6 months were sacrificed and either sent for pathological analysis (conducted by David Brownstein) or tested for heart eEF1A2 expression. No abnormal pathology was observed in the hearts of any of the animals investigated. The hearts of the remaining animals were examined by Western blot for eEF1A2 expression. eEF1A2 expression was observed in the hearts of these animals. Thus it appears the phenotype of these animals is highly variable. To attempt to address this issue the hearts of more wasted animals carrying the transgene (*+/tg, wst/wst*) were investigated. Results were highly variable. Some mice expressed no eEF1A2 in heart and others expressed varying levels. Many possibilities could account for this outcome and multiple factors were considered while attempting to solve this complex issue. No correlation was observed between eEF1A2 expression and the sex of the animals suggesting the variability was not linked to a single variant on a sex chromosome. Imprinting may play a role i.e. the variation could be linked to sex of the transmitting parent, however this also appears not to be the case. Multiple integration sites remain one of the more likely possibilities. It is possible that an expressing variant and a non-expressing variant exist within this line. One variant may have integrated into a site where heart expression is inhibited for example. Copy number analysis by Real-Time PCR could be used to attempt to address whether there are more than one integration sites, or better still Fluorescence *In Situ* Hybridisation (FISH) could be used to identify the integration site/s of the transgene. Generating mouse lines and the subsequent breeding steps required to generate sufficient mice of the desired phenotype involves unavoidable delays. As such the complex inheritance of the transgene remains unresolved. Current studies are focusing on trying to determine the inheritance pattern but this is proving very complex. Wasted transgenic males (*+/tg*, *wst/wst*) are being mated to heterozygous females (+/+, *+/wst*) to attempt to increase the numbers of wasted animals carrying the transgene (*+/tg, wst/wst*). As wasted mice carrying the transgene (*+/tg,wst/wst*) potentially suffer from a heart-related disorder, female wasted mice carrying the transgene (*+/tg,wst/wst*) are not being used for breeding because pregnancy may put too much pressure on the heart. One breeding pair in particular, breeding pair two, produced the most wasted mice carrying the transgene (*+/tg, wst/wst*) without eEF1A2 expression in the heart.

However not all wasted transgenic animals from this pair have no eEF1A2 expression in the heart. Offspring of this breeding pair are the main focus of current breeding strategies. At the time of submitting this thesis this issue had not been resolved. An additional point to be considered is that in the work by Permphan Dharmasroja on the muscle specific transgenic line, some wasted mice carrying the muscle specific transgene had expression in both heart and muscle and some only in muscle. In the data shown (Dharmasaroja 2007), two animals that express eEF1A2 in heart are females and the two animals that only express eEF1A2 in muscle are male. The significance of this is unclear with such small numbers but the new muscle specific lines may further help to clarify the significance of these findings.

While the NSE-EEF1A2 line C cannot be used to address the initial aims of this experiment they still may prove to be a very interesting model for future studies investigating the loss of eEF1A2 in the hearts of wasted mice. Once the inheritance of the transgene can be confirmed, a line expressing eEF1A2 in all tissues where it is normally expressed with the exception of the heart could be generated. An alternative strategy would be to produce a heart-specific conditional knockout of eEF1A2. Such lines could address many important questions regarding the pathology of wasted mice. An important question that needs to be addressed is how animals with no expression of eEF1A2 in heart can survive to at least 6 weeks of age (the earliest age at which sudden death occurred in wasted mice carrying the transgene). In wasted mice, eEF1A1 expression is observed in heart until 21 days (Khalyfa *et al.,* 2001) after which time, in wildtype animals, expression of eEF1A2 takes over. Therefore in mice from line C where no expression of eEF1A2 is seen in heart it is presumed that by 21 days the hearts of these animals will express neither eEF1A1 or eEF1A2. This has been shown in some of these animals (figures 4.21 and 4.27). The crucial question is how these animals survive without this essential translation factor. An interesting avenue of investigation is to assess how much protein synthesis is taking place in the hearts of these animals before and after the eEF1A variant switch.. A recently publish technique named SUnSET (Surface Sensing of Translation) uses an analogue of aminoacyl tRNAs, (puromycin) to achieve this (Schmidt *et al.,* 2009). The incorporation of puromycin into proteins directly reflects the rate of mRNA

translation. Antibodies to puromycin are then used to directly monitor translation using immunofluorescence. This non-radioactive method is currently being investigated by our lab.

4.5. Conclusion

In conclusion the main aim of this project could not be achieved due to the non-specific expression of the transgene. However interesting transgenic lines have been generated which with some further work could; potentially yield a line suitable for investigating the pathology of the hearts of wasted animals (NSE-EEF1A2-C) and investigate the role of eEF1A2 in the pancreas (NSE-EEF1A2-B). The questions that were intended to be addressed are still of crucial importance for our understanding of the wasted phenotype. These experiments should certainly be pursued, with some modification. Injection of a modified construct will hopefully yield wasted animals with transgenic expression of eEF1A2 exclusively in the CNS which will be able to answer the questions set out in this project.

5. Chapter 5: Investigating the role of eEF1A2 in motor neuron degeneration

5.1. Aim

The first aim of this study was to investigate whether eEF1A2 has a role in human motor neuron degeneration. The second aim was to investigate whether recently identified candidate genes in human motor neuron disease have disrupted protein expression in the wasted mouse model. These data could further validate the wasted mouse model as a model for human motor neuron degeneration.

5.2. Introduction

5.2.1. Animal models of motor neuron degeneration

Identifying links between animal models and human disease is essential to increase our understanding of various diseases and to aid in the development of appropriate disease treatments. Animal models are crucial for increasing our understanding of diseases as they give a whole biological system with which to work. The links between mouse models and human disease are usually uncovered in one of two ways. Often studies use information from human disease patients to identify candidate genes that are then used to develop animal models to further investigate the role of said genes. An example of this is seen with the discovery of SOD1 as a gene involved in familial amyotrophic lateral sclerosis (ALS) by linkage analysis (Rosen *et al.,* 1993). This discovery has resulted in the generation of numerous SOD1 mutant animal models. Alternatively, existing animal models or models generated by spontaneous mutation sometimes illuminate genes or biological pathways that are then investigated in human disease cases.

For many years mutations in SOD1 and the subsequent SOD1 mutant models have dominated research in ALS. However in recent years numerous new candidate genes have come to light as having important roles in the disease. The most prominent of

these is the 43KDa TAR DNA binding protein TDP-43. TDP-43 was identified in 2006 as the major component of ubiquitinated inclusions in the motor neurons of sporadic ALS patients (Neumann *et al.,* 2006).

Since the identification of TDP-43 as a component of motor neuron inclusions in ALS, TDP-43 expression has been thoroughly investigated in numerous models of ALS and other neurodegenerative diseases to attempt to find further associations between mouse models and human disease. In this project TDP-43 expression is investigated in the wasted mouse model.

The wasted mouse model is an example of a spontaneous mutation in a gene (*Eef1a2*) leading to a neuromuscular disorder in mice. The wasted mouse model was initially thought to be a model for ataxia telangiectasia (Shultz *et al.,* 1982), but on further investigation of the pathology of wasted mice it became apparent that it was more appropriate as a model for early onset motor neuron degeneration. Wasted mice show many similar pathological features of the human disease including vacuolar degeneration of motor neurons, reactive gliosis as shown by enhanced GFAP expression, neurofilament accumulation in neuronal cell bodies and loss of anterior horn motor neurons (Lutsep and Rodriguez 1989; Newbery 2003; Newbery *et al.,* 2005).

5.2.2. eEF1A2 in human disease

Positional cloning identified *Eef1a2* as the mutated gene in the wasted mouse model (Chambers *et al.,* 1998), however little is known about the role of eEF1A2 in human disease. To date eEF1A2 has not been identified in any screens such as genome wide association studies for genes involved in ALS. In 2009 however a genome wide association study identified eEF1D (otherwise known as eEF1Bδ) as a new locus demonstrating ALS specific copy number variation (Wain *et al.,* 2009). eEF1B is thought to be the guanine exchange factor for eEF1A and thus this finding has very interesting implications for understanding the role of eEF1A2 in human motor neuron degeneration.

In 2006 Bakay *et al* used microarray technology to analyse gene expression in several muscle disorders including nine cases of ALS (Bakay *et al.,* 2006). eEF1A2 was shown to be downregulated in muscle samples from ALS patients as shown in figure 5.1. Groups of samples from other muscle disorders including Duchenne muscular dystrophy and Becker muscular dystrophy among others were also investigated. Of the disorders analysed eEF1A2 was most significantly decreased in samples from ALS patients. This is the first evidence of eEF1A2 being disrupted in human motor neuron disease. To our knowledge, eEF1A2 has never been investigated in the spinal cord of motor neuron disease patients and so this was the starting point of this project.

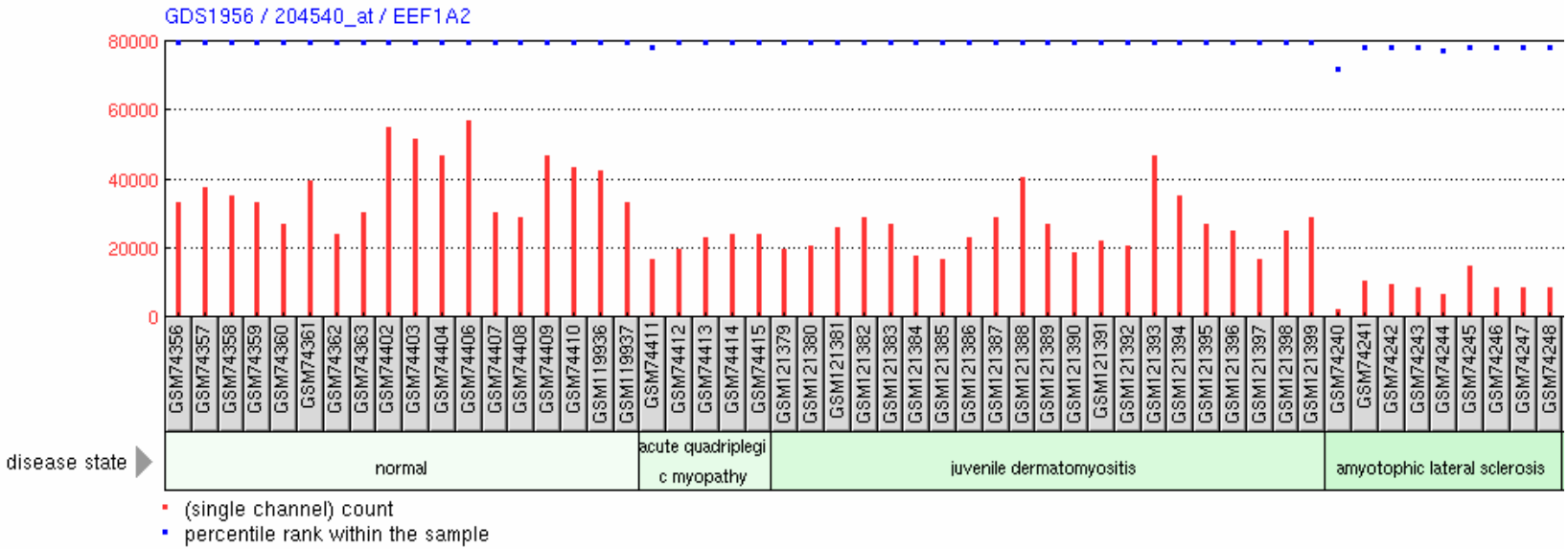

Figure 5.1. eEF1A2 is downregulated in muscle samples from patients with ALS.

A snapshot of expression profiling of eEF1A2 in muscle biopsies from ALS patients (and other muscle disorders) compared to healthy controls. The image was prepared using "Genome expression omnibus profiles" on NCBI http://www.ncbi.nlm.nih.gov/sites/geo. The red bars represent the measured level of abundance of eEF1A2 in the muscle samples (as measured by Affymetrix Microarray (Bakay et al., 2006)).

5.3. Results

5.3.1. Tissue samples

Spinal cord sections from ten motor neuron disease (MND) patients and ten controls without any known neurological disease were investigated in this study. Samples were kindly provided by Dr Colin Smith from the Edinburgh Brain Bank. Details of the samples can be seen in table 5.1.

Spinal cord samples from low copy number G93A SOD1 mutant mice were also examined in this study. These samples were kindly donated by Dr Abraham Acevedo-Arozena of MRC Harwell. Spinal cords from three end-stage (33 weeks of age) SOD1 mutant mice were received together with spinal cords from three age-matched controls, all of which were investigated in this study.

(a) MND cases

ID	Age	Duration	Family history	Diagnosis
MND-1	72	6 months	No	MND
MND-2	77	Months (respiratory illness only)	No	MND
MND-3	71	Unknown, clinically PSP	No	MND
MND-4	81	Less than 12 months	No	MND
MND-5	77	12 months	No	MND
MND-6	70	Unknown	No	Distal neuropathy
MND-7	52	3-4 years	Yes	MND
MND-8	72	6 months	No	MND
MND-9	70	unknown	No	MND
MND-10	58	12 months	?	MND

(b) Controls

ID	Age	Cause of death
Control-1	55	Ischaemic heart disease
Control-2	37	Internal haemorrhage
Control-3	35	Unascertained
Control-4	53	Ischaemic heart disease
Control-5	53	Ischaemic heart disease
Control-6	78	Bronchopneumonia
Control-7	89	Perforated duodenal ulcer
Control-8	24	Acute alcohol poisoning
Control-9	28	Hanging
Control-10	43	Ischaemic heart disease

Table 5.1. Patient data from MND patients and controls

Diagnosis, age of onset, disease duration and family history of MND patient samples used in this study (table (a)). Cause of death and age at death of control samples used in this study (b).

5.3.2. eEF1A2 expression in motor neurons

Expression of eEFIA2 was examined in the human sections by immunohistochemistry (IHC) using an eEF1A2-specific antibody, generated by Helen Newbery in our laboratory (Newbery 2003). Results showed that in the spinal cord sections from all ten of the control samples examined, all showed consistently high levels of eEF1A2 expression in the motor neurons (an example is shown in figure 5.2 panel (c)). The spinal cord sections from MND patients showed varying results. Of the ten MND patient samples examined only two sections showed levels of eEF1A2 expression in motor neurons similar to the levels seen in control samples (an example is shown in figure 5.1 panel (d)). Four out of the ten displayed variable degrees of staining between motor neurons (an example is shown in figure 5.1 panel (e)), although overall staining was weaker than control samples. The remaining four samples showed no eEF1A2 expression in motor neurons (an example is shown in figure 5.1 panel (f)). This is the first evidence of eEF1A2 downregulation in motor neurons in MND patients and thus warrants further investigation. To assess whether this downregulation in eEF1A2 was simply a result of dying motor neurons, eEF1A2 expression was also examined in spinal cord sections from end stage SOD1 mutant mice. This model has no known mutation in eEF1A2 but mutant mice display severe motor neuron pathology, comparable to that seen in human MND patients. As seen in figure 5.3. results show that eEF1A2 is not downregulated in motor neurons from the SOD1 mutant mice spinal cords. This would suggest that the downregulation of eEF1A2 in human MND patients is not simply the result of damaged motor neurons.

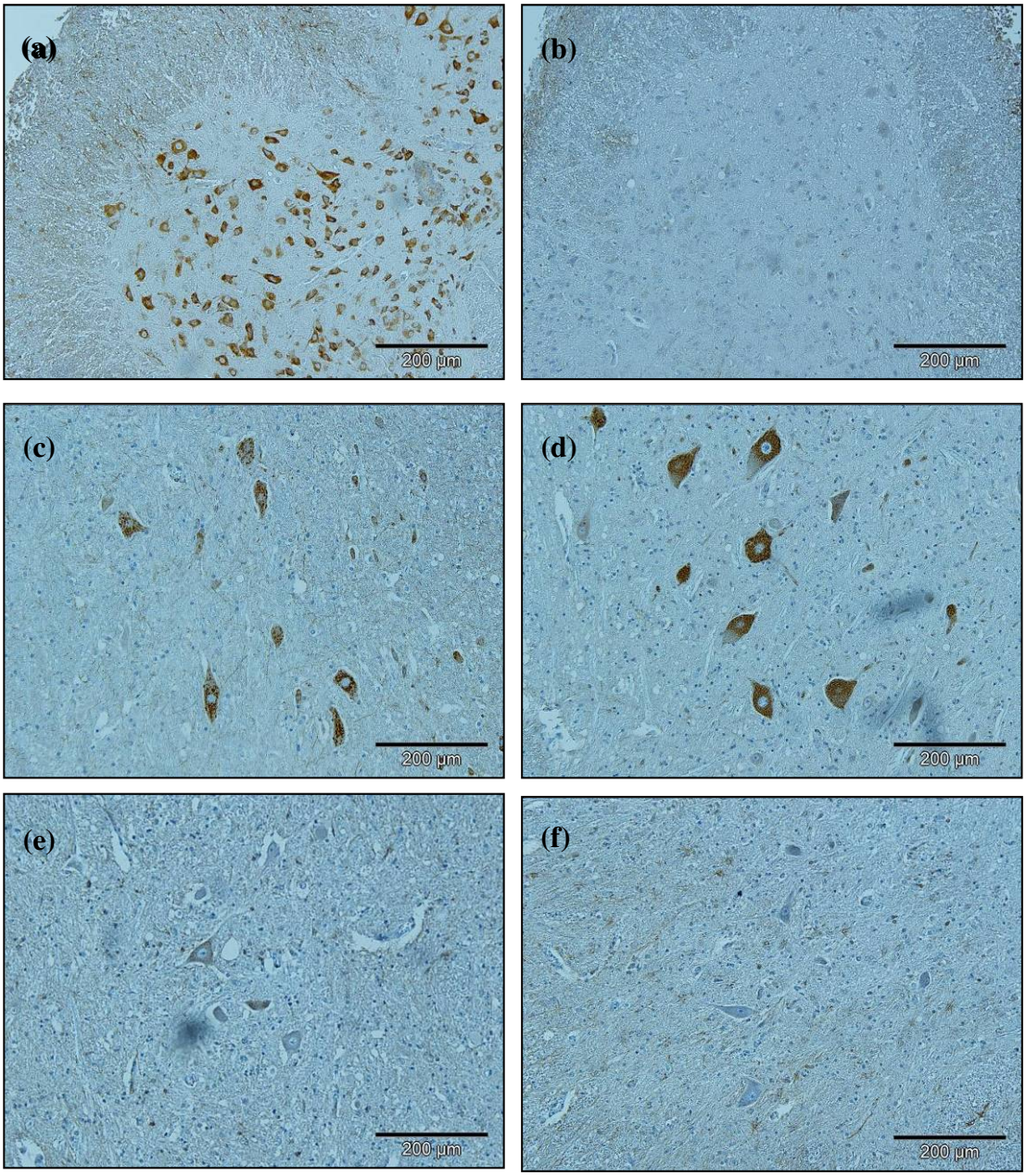

Figure 5.2. eEF1A2 expression in human MND spinal cords.

Examples of spinal cord sections from human MND patients and controls stained with an antibody recognising eEF1A2. Panel (a) shows a section from a wildtype mouse (positive control) and panel (b) shows a section from a wasted (*wst/wst*) mouse (negative control). Panel (c) is an example of a human control section and panels (d), (e) and (f) are examples from MND patients. All images were taken at 10x magnification. These results were obtained using the EnVision method.

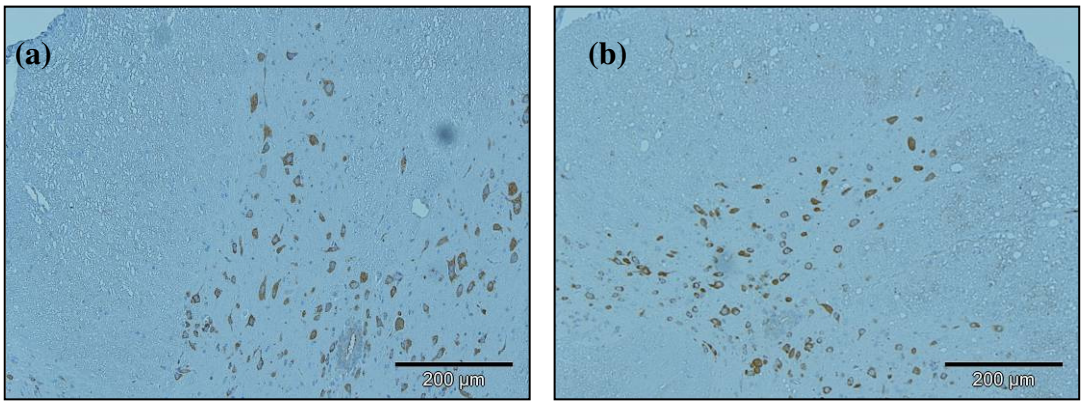

Figure 5.3. eEF1A2 expression in mutant SOD1 mice

Examples of a cervical spinal cord section from a wildtype (a) and a mutant SOD1 (b) mouse stained with an antibody recognising eEF1A2. Images were taken at 10x magnification. These results were obtained using the EnVision method.

5.3.3. eEF2 expression in motor neurons.

To confirm the results from the expression analysis of eEF1A2 in spinal cord sections of MND patients, it was necessary to find a suitable control that would stain motor neurons in both MND patient and control samples equally. Such a control would confirm that the downregulation of eEF1A2 is specific to this protein, and not a more general decrease in overall protein expression in damaged motor neurons.

The first of those investigated was the eukaryotic elongation factor 2 (eEF2). As can be seen in figure 5.4 the expression of eEF2 was weaker in MND patient samples (an example is seen in panel (b)) than control samples (an example is seen in panel (a)). Another control was therefore required as this data suggests that perhaps the downregulation observed in eEF1A2 may not be specific, and it was possible that a general downregulation of either elongation factors or factors involved in protein synthesis was being observed. Figure 5.4 also shows that a decrease in expression of eEF2 was also seen in SOD1 mutant mice (an example is seen in panel (d)) compared to age matched wildtype controls (as example is seen in panel (c)) and also in wasted (*wst/wst*) mice (an example is seen in panel (f)) compared to wildtype controls. eEF2 was therefore deemed an unsuitable control for this experiment but yielded some potentially interesting results.

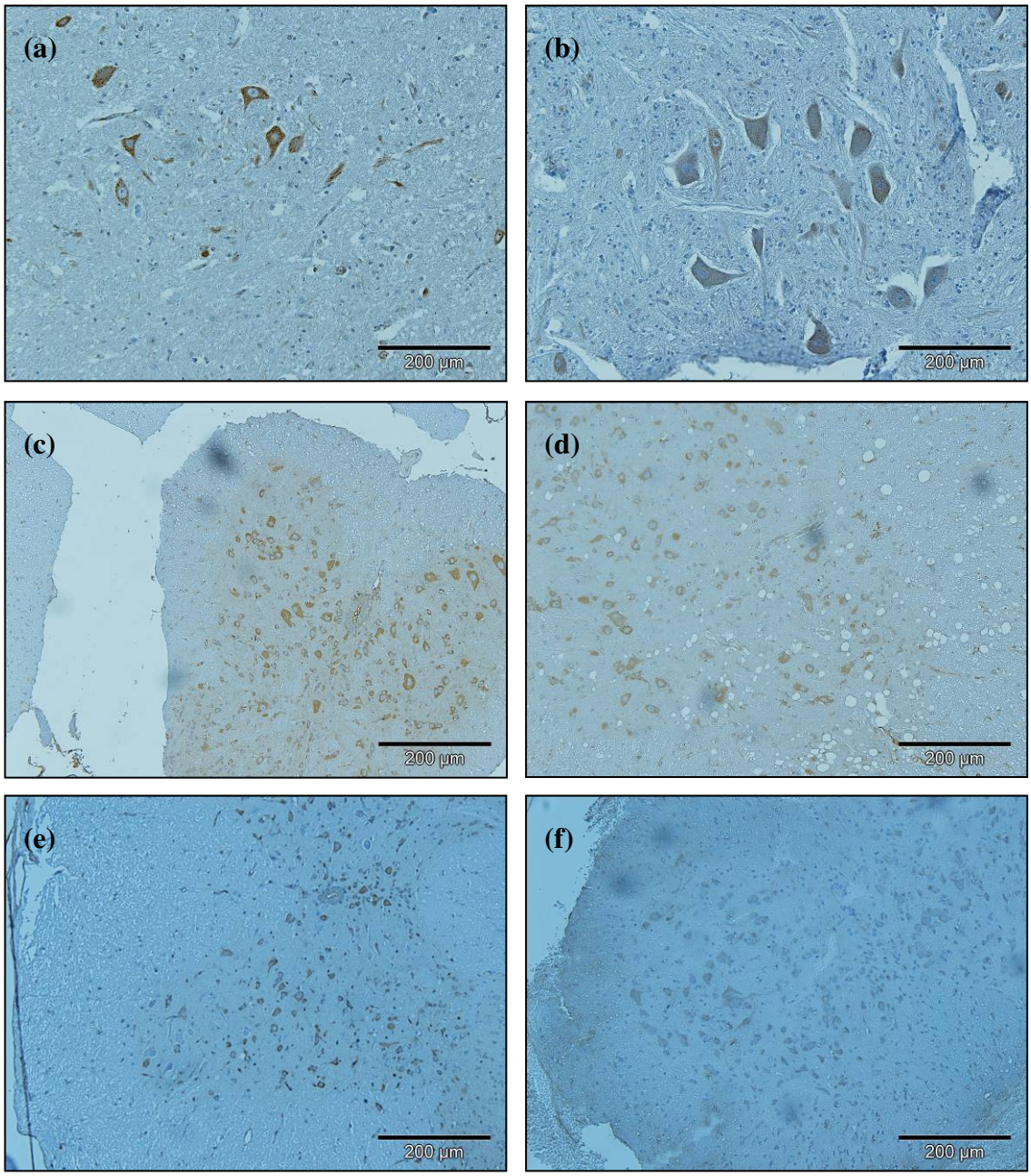

Figure 5.4. eEF2 expression in human and mouse spinal cord sections

Examples of spinal cord sections from human MND patients and controls stained with an antibody recognising eEF2. Panel (a) and (b) show human spinal cord sections from an MND patient (b) and a control (a). Panels (c)-(f) show cervical spinal cord sections from a SOD1 (d) mutant mouse along with an age matched control (c) and a wasted (*wst/wst*) mouse (f) along with an age matched control (e). All images were taken at 10x magnification. These results were obtained using the POLINK method.

5.3.4. NeuN expression in motor neurons

The next control to be investigated was an antibody that detects the neuron specific protein NeuN (Neuronal Nuclei). As can be seen in figure 5.5 this antibody has proved to be a useful marker of neuronal cells in spinal cords from wildtype (panels (c) and (e)), wasted (panel (f)) and SOD1 (panel (d)) mice. However no NeuN expression was observed in neuronal cells in the spinal cords of MND patients. Some detection was observed in human control samples but staining was highly variable and sometimes undetectable thus it was also deemed an unsuitable control antibody for this investigation.

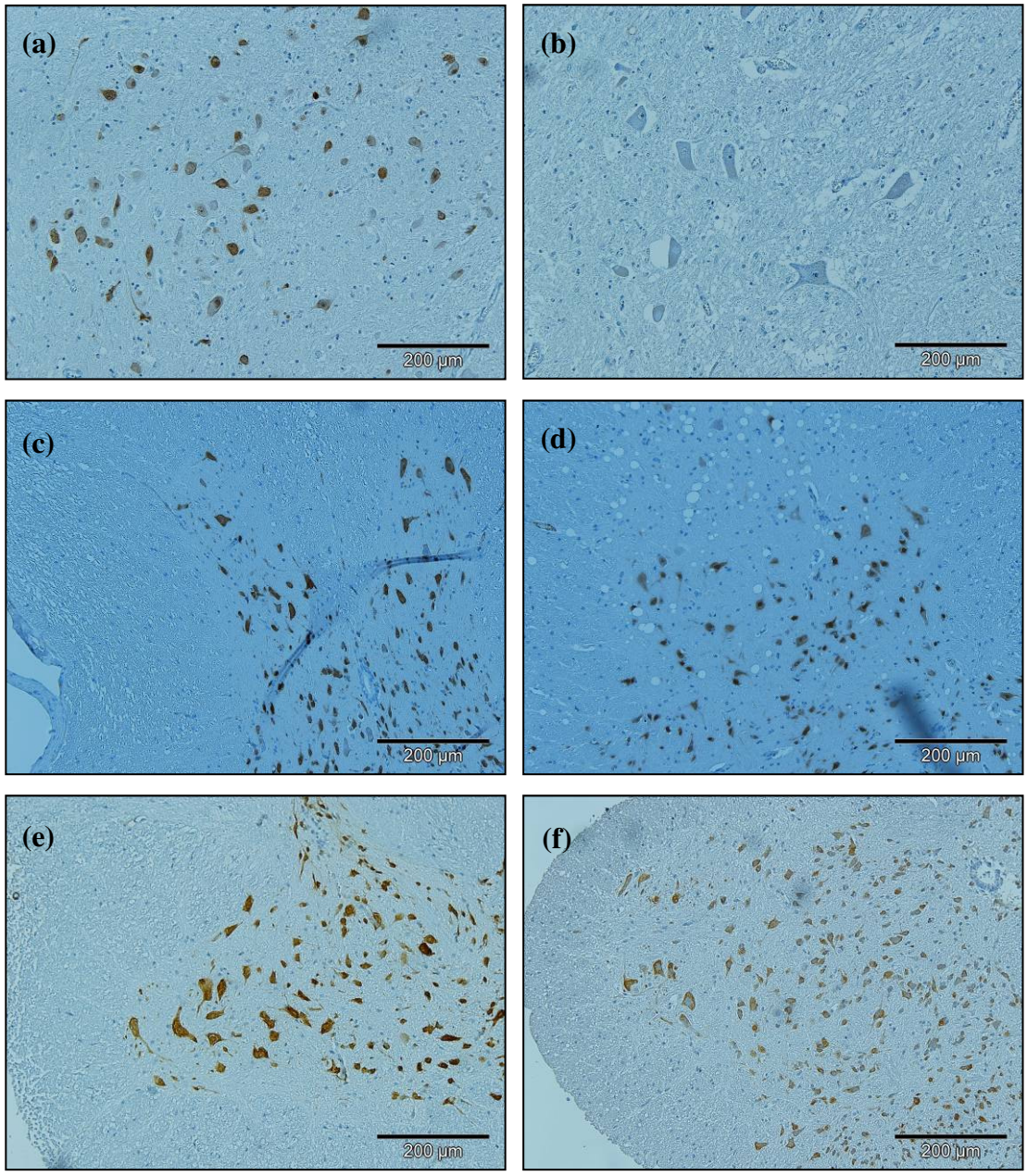

Figure 5.5. NeuN expression in human and mouse spinal cord sections

Examples of spinal cord sections from human MND patients and controls stained with an antibody recognising NeuN. Panel (a) and (b) show human spinal cord sections from an MND patient (b) and a control (a). Panels (c)-(f) show cervical spinal cord sections from a SOD1(d) mutant mouse along with an age matched control (c) and a wasted (*wst/wst*) mouse (f) along with an age matched control (e). All images were taken at 10x magnification. These results were obtained using the POLINK method.

5.3.5. GRP78 expression in motor neurons

The next question was to address whether there may be a more fundamental problem with the sections from the MND patient samples, which may explain why motor neurons in these samples remain largely unstained with multiple antibodies. All samples, while processed on different occasions, were all processed using exactly the same protocol. Thus in order to establish whether staining in the motor neurons from these MND patient samples could be achieved a protein which has previously shown to be overexpressed in motor neurons from MND patients was next examined. The protein selected was the stress response chaperone Glucose Regulated Protein 78 (GRP78). Using an antibody that binds a protein overexpressed in motor neurons from ALS patients should indicate whether the motor neurons in these sections are capable of staining. If no staining is observed in the patient samples this would indicate a more fundamental problem with the sections.

Motor neurons in spinal cord sections from all ten MND patient samples showed strong staining for GRP78, an example is shown in figure 5.6 panel (b). This indicates that immunolabelling of motor neurons is achievable in these samples and there is no apparent problem with the MND patient samples. The level of staining in the MND patients was indistinguishable from the control samples. This therefore supports the finding that eEF1A2 expression is truly downregulated in motor neurons from some MND patients.

As can be seen in figure 5.6 no overexpression of GRP78 was observed in spinal cords from wasted mice (panel (f)) or SOD1 (panel(d)) mutant mice compared to wildtype controls (panels (c) and (e)).

Identifying a suitable control antibody that detects protein in motor neurons from both ALS patient samples and control samples equally is still important. Whilst GRP78 appears to stain both ALS patient and control samples equally in this study GRP78 has been shown previously to be upregulated in motor neurons from ALS patients and as such is not an ideal control.

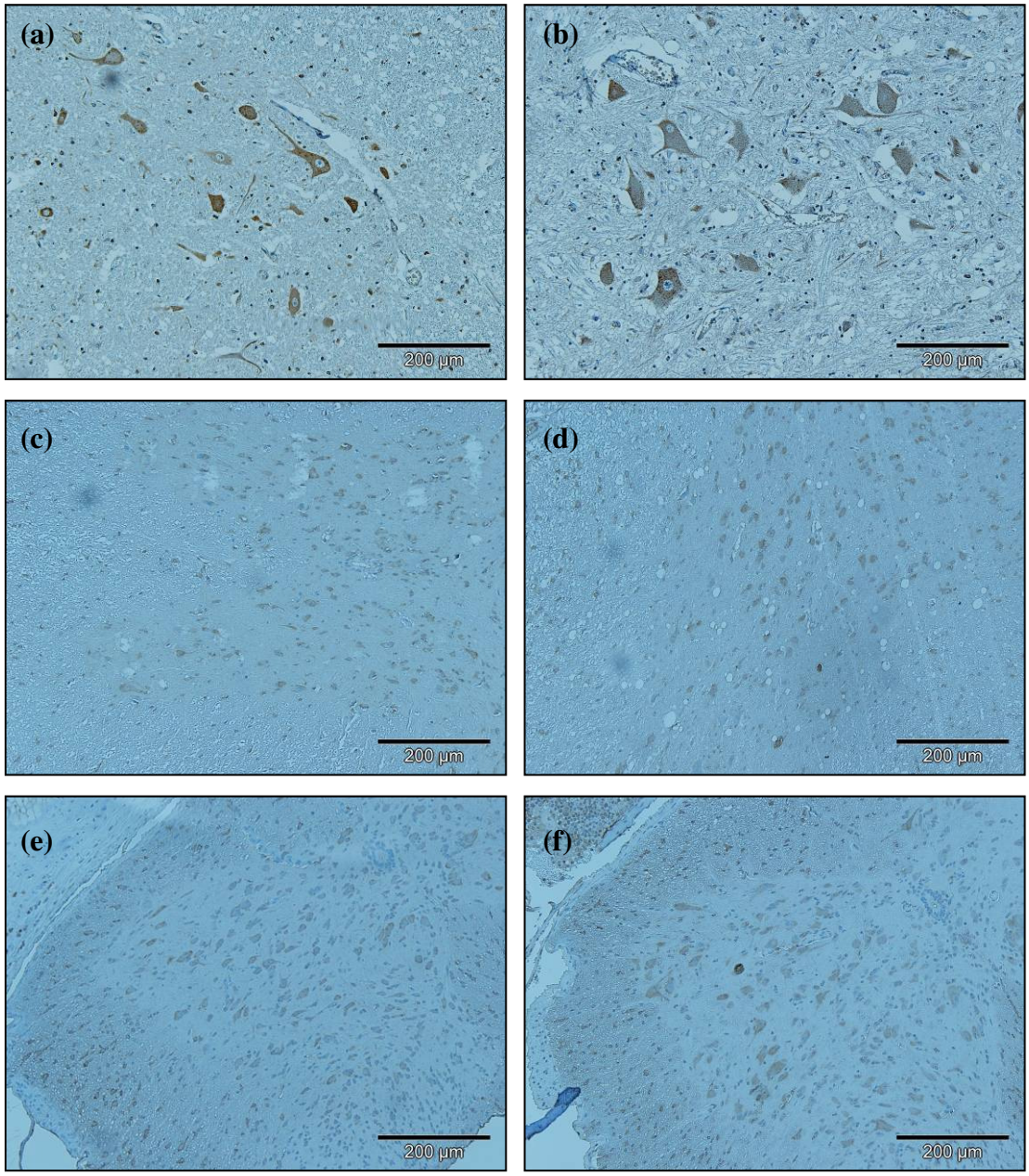

Figure 5.6. GRP78 expression in human and mouse spinal cord sections

Examples of spinal cord sections from a human MND patient and controls stained with an antibody recognising GRP78. Panel (a) and (b) show human spinal cord sections from an MND patient (b) and a control (a). Panels (c)-(f) show cervical spinal cord sections from a SOD1(d) mutant mouse along with an age matched control (c) and a wasted (*wst/wst*) mouse (f) along with an age matched control (e). All images were taken at 10x magnification. These results were obtained using the POLINK method.

5.3.6. eEF1Bδ expression in motor neurons

As eEF1Bδ has recently been implicated in ALS, the expression of eEF1Bδ was also examined in the spinal cord sections from MND patients. All control samples showed similar expression levels of eEF1Bδ, an example is shown in figure 5.7 panel (b). Eight of the ten MND patients showed a similar level of eEF1Bδ expression in the motor neurons compared to control samples (an example is shown in figure 5.7 (d)). The remaining two samples showed a decrease in eEF1Bδ expression in motor neurons although this was variable between cells as shown in figure 5.7 panel (c). Therefore overall there was no significant decrease in eEF1Bδ expression between spinal cord sections from controls and MND patients although this was not the case for all samples.

eEF1Bδ expression was also examined in spinal cord sections of SOD1 mutant mice. Results show that there is no significant difference in the expression of eEF1Bδ between control animals (figure 5.7 panel (e)) and SOD1 mutant animals (figure 5.7 panel (f)).

5.3.6.1. eEF1A2 and eEF1Bδ

The expression of eEF1A2 and eEF1Bδ is summarised in table 5.2. Data shows some correlation between these two translation factors. Whilst a decrease in eEF1A2 does not consistently result in a decrease in eEF1Bδ expression, it appears that those samples with lower expression of eEF1Bδ have little or no expression of eEF1A2.

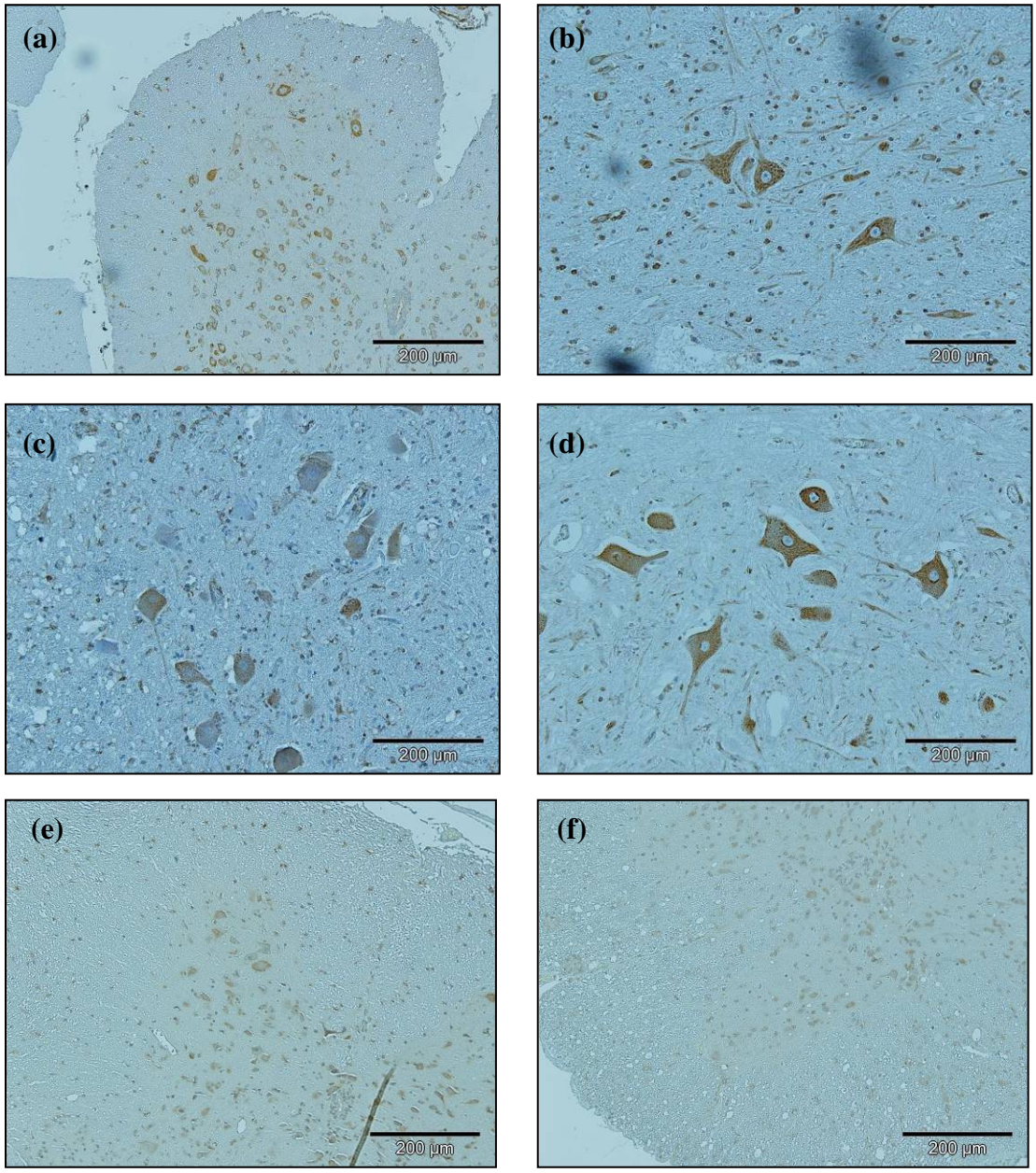

Figure 5.7. eEF1Bδ expression in human and mouse spinal cord sections.
Examples of spinal cord sections from human and mouse spinal cord stained with an antibody recognising eEF1Bδ. Panel (a) shows a section from a wildtype mouse (positive control), panel (b) is an example of a human control section and panels (c) and (d) are examples from MND patients. Sections from the cervical spinal cord of a SOD1(f) mouse and an age matched control (e) are also shown. All images were taken at 10x magnification. These results were obtained using the EnVision method.

ID	Age	Duration	Family history	Diagnosis	eEF1A2	eEF1Bδ
MND-1	72	6 months	No	MND	–	*
MND-2	77	Months (respiratory illness only)	No	MND	*	**
MND-3	71	Unknown, clinically PSP	No	MND	**	**
MND-4	81	Less than 12 months	No	MND	*	**
MND-5	77	12 months	No	MND	–	**
MND-6	70	Unknown	No	Distal neuropathy	–	**
MND-7	52	3-4 years	Yes	MND	–	**
MND-8	72	6 months	No	MND	*	**
MND-9	70	unknown	No	MND	*	*
MND-10	58	12 months	?	MND	**	**

Table 5.2. Analysis of eEF1A2 and eEF1Bδ expression in motor neurons of ALS patients.

Expression levels of eEF1A2 and eEF1Bδ in motor neurons from spinal cord sections of ALS patients. ** indicates strong antibody staining throughout the section (similar to control samples), * indicates weak and variable staining and – indicates no observable staining.

5.3.7. From human disease to wasted mice: TDP-43

As previously mentioned many new genes have recently come to light as having roles in human motor neuron degeneration. The most prominent of these is the 43KDa Tar DNA binding Protein (TDP-43). In human disease the normally nuclear TDP-43 expression is disrupted and the protein accumulates in ubiquitinated inclusions in the cell body (Neumann *et al.,* 2006). An example of such inclusions can be seen in the motor neuron from an MND patient in figure 5.9 panel (b). Of the ten MND samples examined here, seven showed evidence of TDP-43 inclusions. Spinal cords from wasted mice together with age matched controls were investigated for any abnormal TDP-43 protein localisation. Sections from post-symptomatic wasted mice (25 days – 28 day old) and pre-symptomatic (15 day old) mice together with age matched controls were examined. Immunohistochemistry results showed that in spinal cords from control animals, TDP-43 protein is found as expected in the nucleus of motor neurons (as shown in figure 5.10 panel (a), (c) and (e)). In spinal cords from both pre-symptomatic and post-symptomatic wasted (*wst/wst*) animals, the normal nuclear TDP-43 staining pattern appears disrupted in motor neurons. The cytoplasm of some motor neurons appears to show diffuse staining with the TDP-43 antibody and no nuclear staining. No inclusions were observed in the cell body of the motor neuron as is seen in human disease. SOD1 mice show no disrupted TDP-43 expression which supports previous investigations of TDP-43 expression in SOD1 mice (Robertson *et al.,* 2007; Turner *et al.,* 2008).

5.3.7.1. eEF1A2 and TDP-43

There appears to be no direct correlation between the level of expression of eEF1A2 and the presence of TDP-43 inclusions (table 5.3).

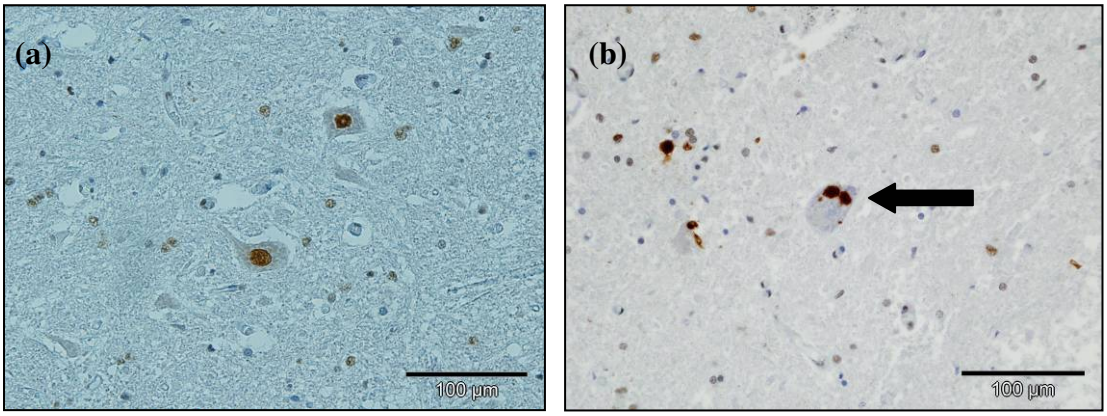

Figure 5.8. TDP-43 expression in human spinal cord.

Examples of spinal cord sections from a human MND patient (panel (b)) and a control (panel (a)) stained with an antibody recognising TDP-43. TDP-43 inclusions are seen in motor neurons of the MND patient (indicated by the black arrow). Images were taken at 20x magnification. These results were obtained using the EnVision method.

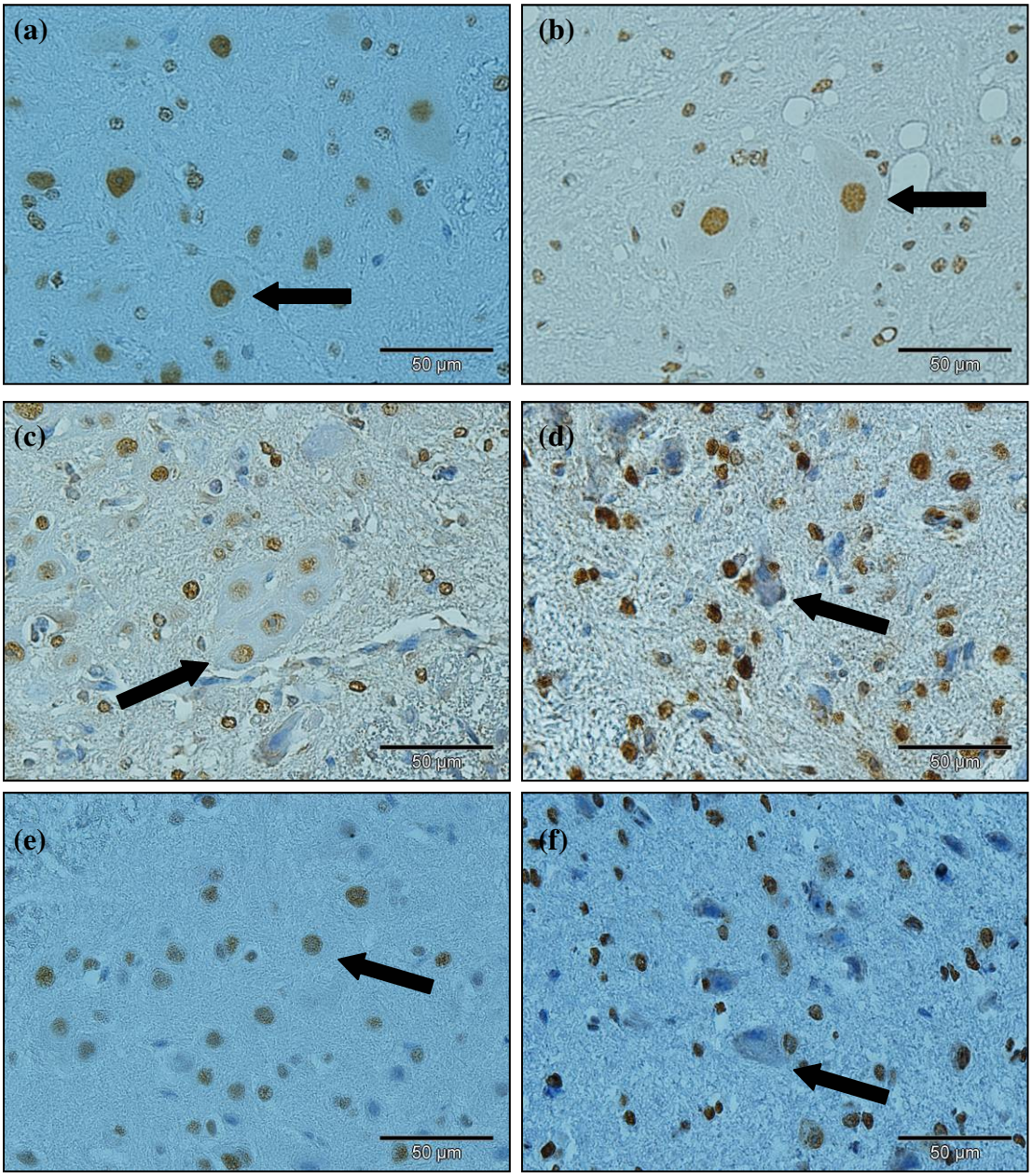

Figure 5.9. TDP-43 expression in wasted and SOD1 mouse spinal cord. Examples of spinal cord sections from wasted (panel (d) and (f)), SOD1 (panel b) and age matched control mice ((a), (c), (e)). Panels (c) and (d) show cervical sections from 15 day old, pre-symptomatic mice while panels (e) and (f) show cervical sections from 24 day old, symptomatic mice. Arrows show examples of motor neurons with either strong nuclear staining (controls and SOD1 sections) or disrupted TDP-43 expression as indicated by the presence of a blue nucleus (wasted mice). Images were taken at 40x magnification. These results were obtained using the EnVision method.

ID	Age	Duration	Family history	Diagnosis	eEF1A2	TDP-43
MND-1	72	6 months	No	MND	–	Inclusions
MND-2	77	Months (respiratory illness only)	No	MND	*	Inclusions
MND-3	71	Unknown, clinically PSP	No	MND	**	Inclusions
MND-4	81	Less than 12 months	No	MND	*	Inclusions
MND-5	77	12 months	No	MND	–	Inclusions
MND-6	70	Unknown	No	Distal neuropathy	–	No inclusions
MND-7	52	3-4 years	Yes	MND	–	Inclusions
MND-8	72	6 months	No	MND	*	Inclusions
MND-9	70	unknown	No	MND	–	Inclusions
MND-10	58	12 months	?	MND	**	No inclusions

Table 5.3. Analysis of eEF1A2 and TDP-43 expression in motor neurons of ALS patients.

Expression of eEF1A2 together with TDP-43 inclusion analysis in spinal cord sections from ALS patients. ** indicates strong antibody staining throughout the section (similar to control samples), * indicates weak and variable staining and – indicates no observable staining. The presence of any observable TDP-43 inclusions is also noted.

5.4. Discussion

Here is shown the first study investigating eEF1A2 in spinal cords from MND patients and controls (with no known neurological disease). The results indicate that eEF1A2 is downregulated to varying degrees in the motor neurons of eight out of the ten patient samples examined. The key to determining if this downregulation is specific to eEF1A2 is finding a suitable control antibody that detects neuronal proteins in motor neurons of ALS patients and normal controls equally. Various antibodies were tested in this project, however only the GRP78 antibody (which has previously been shown to be upregulated in motor neurons from ALS patients (Sasaki 2010) detected equal protein levels in motor neurons from all ALS patients and normal controls.

eEF2 was downregulated in spinal cord sections from ALS patients, SOD1 mutant mice and wasted mice compared to healthy controls. This suggests that damaged motor neurons fail to express eEF2. It was therefore necessary to investigate a protein with no known role in translation such as Neuronal Nuclei (NeuN). NeuN expression is observed in the nuclei of neurons (Mullen *et al.,* 1992) and has been shown to be a useful neuronal marker for diagnostic histopathology (Wolf *et al.,* 1996). This antibody however showed variable staining in both MND patient samples and normal controls. This indicates that this antibody is not suitable for use on these human spinal cord sections despite appearing to work effectively on mouse spinal cord sections. As the NeuN antibody was raised in mouse it is possible that the antibody is detecting some other neuronal protein in mouse tissue which makes it appear to be working effectively on mouse but not on human tissue. The observation that neuron cytoplasm as well as the nucleus is also stained in mouse spinal cord supports this. Other NeuN antibodies could perhaps be investigated to see if this is a specific antibody problem.

Immunohistochemistry using an antibody to detect proteins that are overexpressed in motor neurons from MND patients such as GRP78 showed motor neuron staining in MND patient samples. This showed that the samples themselves could be stained with some antibodies and therefore remain suitable for the project. Unusually GRP78

expression was also observed in all control samples. This contradicts previous data from a study investigating GRP78 in ALS patients and controls which showed very little expression of GRP78 in the motor neurons of control sample (Sasaki 2010). No observable difference in GRP78 expression was observed between spinal cord sections from MND patients and controls. Ideally a control antibody that should detect protein in motor neurons from both MND patient samples and controls equally should continue to be investigated i.e. a protein unaffected by neuronal degeneration. This could prove difficult as findings suggest that some neuronal proteins such as NeuN and Neuronal specific enolase (NSE) may decrease during neurodegenerative disease (Sarnat and Trevenen 2007). Perhaps staining motor neurons from MND patients will always be problematic due to motor neuron damage. An antibody to another protein upregulated in ALS should also be tested such as calcium binding protein S100β (Migheli *et al.,* 1999) to confirm that the motor neurons in the MND patient samples can stain with multiple proteins.

Expression of the delta subunit of the eEF1B complex (eEF1Bδ) was also examined. eEF1Bδ showed similar expression between motor neurons from MND patients and controls. Only two MND patient samples showed any obvious decrease in eEF1Bδ expression in motor neurons, thus eEF1Bδ could be involved in a subset of ALS cases. This is in agreement with study the by Wain *et al* who implicating copy number variation of eEF1Bδ in ALS samples (Wain *et al.,* 2009). Little difference was observed in eEF1Bδ expression between motor neurons in SOD1 mutant mice and wildtype controls. Determining eEF1Bδ expression in wasted mice is now crucial and is currently being investigated by another PhD student in the lab.

In recent years numerous new genes have been found to have roles in human motor neuron degeneration. The most intensely studied of these is TDP-43. Studies investigating TDP-43 expression in ALS and Frontotemporal Lobar Dementia (FTLD) have found ubiquitinated TDP-43 inclusions in nearly all sporadic and SOD1-negative familial ALS samples (Neumann *et al.,* 2006; Mackenzie *et al.,* 2007; Tan *et al.,* 2007). TDP-43 expression has been investigated in numerous

mouse models of motor neuron degeneration with varying results. SOD1 mutant animals show no abnormal distribution of TDP-43 (Robertson *et al.,* 2007; Turner *et al.,* 2008) as is confirmed here. This supports the data from human ALS samples which suggests that motor neurons cases with SOD1 mutations have ubiquitin positive but TDP-43 negative inclusions, (Mackenzie *et al.,* 2007). Other models however such as the wobbler mouse model (Dennis and Citron 2009) and the mutant Vesicle-Associated Membrane Protein-associated ProteinB (VAPB) model (Tudor *et al.,* 2010) both show mislocalisation of TDP-43. TDP-43 positive inclusions are also found in the motor neurons of mutant animals. It was therefore important to investigate whether any changes in TDP-43 expression are observed in wasted mice compared to controls. In human disease the normal neuronal localisation of TDP-43 is disrupted resulting in the formation of inclusions in motor neurons. Wasted mice showed little neuronal TDP-43 in motor neurons of the spinal cord and some diffuse cytoplasmic staining, however no inclusions were observed in any sample. A change in the localisation of TDP-43 from its normal nuclear location to the cytoplasm has been described in motor neurons in tissue sections from patients with ALS (Brandmeir *et al.,* 2008) and these are thought to be "pre-inclusion" motor neurons. The absence of inclusions in wasted mice was unsurprising as motor neurons from wasted mice do not develop ubiquitinated inclusions (Newbery 2003). This could be due to the rapid disease progression and early age of death in these animals resulting in little time for inclusion development. Wasted mice could therefore provide a useful model for investigating neuronal degeneration prior to inclusion development.

Interestingly TDP-43 has been shown to interact with SMN (Wang *et al.,* 2002) which is also known to form a complex with eEF1A (Gangwani *et al.,* 1998; Gangwani *et al.,* 2001). Disruption of TDP-43 could therefore affect eEF1A2 protein expression and vice-versa. In addition eEF1A has been implicated in the nuclear export pathway (Khacho *et al.,* 2008). An attractive hypothesis would be that disruption of eEF1A could lead to a disruption in transport across the nuclear membrane which may account for the mislocalisation of proteins such as TDP-43. Firstly however, distinguishing the separate roles of eEF1A1 and eEF1A2 in nuclear transport would need to be addressed.

This is the first account of spinal cord eEF1A2 expression being altered in human motor neuron degeneration. Further analysis with increased sample numbers (and more closely age-matched controls) should be performed to confirm this finding. In addition the expression of the eEF1A1 variant should also be examined in these sections. Unfortunately problems with the specificity of the eEF1A1 antibodies for IHC prevented this from being addressed in this study. Previous studies have shown that in injured rat muscle there is a switch in the expression of eEF1A variants. eEF1A2 expression is downregulated and eEF1A1 expression is upregulated until recovery at which time the expression is switched back (Carlson *et al.,* 2002; Khalyfa *et al.,* 2003). It would therefore be very interesting to investigate if this also happens in damaged motor neurons. While problems were encountered with the specificity of the eEF1A1 antibody using IHC the antibody has proven to be variant specific on Western blots therefore looking at variant specific expression from tissues on a Western blot could be investigated should samples become available. Also examining levels of RNA expression by Real-Time PCR in spinal cord samples from MND patients would be beneficial to asses whether changes seen in eEF1A2 expression are at the RNA level as well as the protein level.

If eEF1A2 is truly downregulated in a proportion of MND patients further investigation into the cause of this will be required. In her PhD thesis, Helen Newbery analysed 40 familial ALS and 64 sporadic cases of MND for mutations in the exons of eEF1A2 (Newbery 2003). No MND specific mutations were found in the protein coding regions of *EEF1A2*. It is therefore unlikely that mutations in *EEF1A2* are responsible for common cases of MND. Only seven of the eight exons of *EEF1A2* were investigated as exon 8 is a particularly GC rich region and thus amplifying the region by PCR is extremely problematic. Therefore mutations in exon 8 of *EEF1A2* have not been currently detectable. At the time this initial sequencing was undertaken it was not deemed practical or cost effective to sequence the promoter region, however given the results of this study, this should now be thoroughly investigated. Examples of the importance of variability in promoter regions of various genes have been implicated in motor neuron degeneration. A mutation in the promoter region of Vascular Endothelial Growth Factor (VEGF), for

example leads to late onset motor neuron degeneration in an ALS mouse model (Oosthuyse *et al.,* 2001). An ALS specific promoter haplotype in the paraoxonase 1 (PON1) gene has also been identified (Landers *et al.,* 2008). Copy number variation in *EEF1A2* should also be investigated in MND patients and controls to try and determine if a decrease in copy number is the cause of the decrease in protein expression of eEF1A2.

eEF1A2 expression should also be analysed in samples from patients with other neurodegenerative conditions such as Spinal Muscular Atrophy (SMA) or Frontotemporal dementia (FTD). SMA is caused by mutations in the Survival Motor Neuron (*SMN*) gene resulting in decreased full length SMN protein (Lefebvre *et al.,* 1995; Lefebvre *et al.,* 1997). Given that SMN and eEF1A both interact with ZPR1 (Gangwani *et al.,* 1998; Gangwani *et al.,* 2001) it would be interesting to observe if levels of eEF1A are changed in samples from patients with SMA. Significant overlap is observed between ALS and FTD and therefore investigating whether downregulation of eEF1A2 is common to both disorders, could possibly identify another pathological similarity between the two.

In addition, other mouse models of motor neurodegeneration such as the wobbler mouse model, Legs at odd angles (Loa) and other SOD1 mutant models should also be investigated for eEF1A2 expression in the spinal cord. While the spinal cords from SOD1 mutant mice investigated here show little change in eEF1A2 this may not be the case for all models. Investigating other models may help to uncover whether the loss of eEF1A2 observed in the patient samples in this study is an early onset and possible contributory event to motor neuron degeneration or if it is simply a result of motor neuron degeneration. Such information is crucial in identifying potential therapeutic targets.

The initial findings shown here indicating that TDP-43 is disrupted in the wasted model without the development of inclusions requires further investigation. A thorough time course experiment with increased numbers of samples at each age should now be investigated to confirm these initial findings. Ideally counting the number of motor neurons with nuclear and with cytoplasmic staining should also be conducted. Immunofluorescence should also be considered as a clearer method of

identifying motor neurons with mislocalisation of TDP-43. TDP-43 RNA expression in the spinal cords of wasted mice and wildtype controls of various ages could be investigated to see if expression increases (as in seen with the wobbler mouse model (Dennis and Citron 2009)). In addition to immunohistochemistry, TDP-43 expression in the spinal cord from protein extracts of nuclear and cytoplasmic fractions could be measured by Western blotting. This would aid in confirming whether TDP-43 localisation is truly disrupted in the wasted mouse model. A phosphorylated TDP-43 antibody should also be investigated as it is thought that the inclusions seen in ALS patients contain phosphorylated TDP-43. An antibody specific for phosphorylated TDP-43, which has been shown to detect inclusions present in ALS samples, and not normal nuclear TDP-43 (Hasegawa *et al.,* 2008; Inukai *et al.,* 2008) may result in a clearer indication of TDP-43 pathology in sections from wasted mice spinal cord. This would confirm whether wasted mice are positive for TDP-43 inclusions in addition to purely mislocalised TDP-43.

An interesting avenue of future research would be to identify whether eEF1A2 has a role in nuclear export and also to investigate whether eEF1A2 interacts with TDP-43 as this could have important implications for our understanding of the mislocalisation of TDP-43.

The wasted mouse model has been shown to be a useful model for motor neuron degeneration. As such, continuing to investigate whether protein expression of other, recently identified candidate genes in ALS, are disrupted in wasted mice is important. In her thesis Helen Newbery searched for ubiquitinated incusions and also for decreased expression of Microtubule Associated Protein MAP2 in wasted mice, both of which are pathological features observed in the spinal cord from ALS patients (Leigh *et al.,* 1988; Leigh *et al.,* 1991; Kikuchi *et al.,* 1999). No ubiquitinated inclusions were observed in wasted mice and no difference in MAP2 protein expression between spinal cord sections of wasted mice and controls was seen. Other recently identified ALS candidates could also be considered for future investigation such as Fused in Sarcoma (FUS) or Translocation in Liposarcoma (TLS), which like TDP-43, display a shift in expression of protein from the nucleus to cytoplasmic inclusions (Kwiatkowski *et al.,* 2009; Vance *et al.,* 2009). It is to be

expected that not all candidate genes will have an effect in the wasted model, but identifying ones that do increases our knowledge of commonly disrupted proteins across different animal models and will increase our understanding of motor neuron degeneration.

5.5. Conclusion

These data show for the first time that downregulation of eEF1A2 is observed in motor neurons from patients with motor neuron disease. This interesting finding should now be expanded to include increased sample numbers and further expression analysis. This could result in eEF1A2 being investigated as a therapeutic target in motor neuron degeneration. The data presented also show abnormal distribution of the TDP-43 protein in wasted mice without the formation of inclusions. Given the high incidence of TDP-43 pathology in ALS, additional investigation of TDP-43 expression in the wasted mouse model may further validate it as a useful model for motor neuron degeneration.

6. Chapter 6: Investigating the role of eEF1A in the heat shock response

6.1. Aim

The aim of this project was to determine if eEF1A1 and eEF1A2 have similar or different roles in the heat shock response. To attempt to address this aim, the intention was to knock down eEF1A1 and eEF1A2 separately in cells and to assess the effect this has on the cells ability to mount a heat shock response. The different abilities of eEF1A1 and eEF1A2 to participate in the heat shock response could show a key difference between the two variants. A difference in their roles in the heat shock response may explain in part why motor neurons, which only express eEF1A2, are vulnerable to heat shock.

6.2. Introduction

Many examples of the diverse roles of eEF1A have been documented, but in almost all cases the specific variant involved is not identified. This is largely due to commercially available eEF1A antibodies recognizing both variants equally. One example of a proposed non-canonical function for eEF1A was published by Shamovsky *et al* in 2006. This study found that eEF1A is involved in the heat shock response (or stress response) by its interaction with heat-shock transcription factor 1 (HSF1, (Kugel and Goodrich 2006; Shamovsky *et al.,* 2006).

Heat shock proteins (or stress proteins) produced during a heat shock response are part of the cells integral repair mechanism. Their levels are increased in response to numerous environmental stresses including (but not limited to) elevated temperature, oxygen deprivation and exposure to toxins. They act as molecular chaperones aiding in refolding proteins that have misfolded during the stress period.

While the exact role of eEF1A in the heat shock response is unclear, a model (shown in figure 6.1) has been proposed (Kugel and Goodrich 2006). It is thought that following heat shock, HSF1 monomers are released from their inactive conformation and localise in the nucleus as a homotrimer (Shi *et al.,* 1998). These trimers then bind heat shock elements (HSEs), found in the promoter regions of genes up-regulated during the heat shock response (Morimoto 1998; Voellmy 2004; Kugel and Goodrich 2006).

Shamovsky *et al* searched for factors in mammalian cell extracts that associate with HSF1 and found eEF1A (Shamovsky *et al.,* 2006). It was also shown that heat shock enhanced the association between these two proteins. It is believed that eEF1A together with a previously unknown RNA named heat shock RNA 1 (HSR1) are involved in the trimerisation of HSF1, although their exact mechanism of action is unknown. eEF1A purified from rat liver was shown to activate HSF1 in this study and this must therefore be eEF1A1, as eEF1A2 is not expressed in liver. The study failed to address directly whether eEF1A2 can also play a part in the heat-shock response.

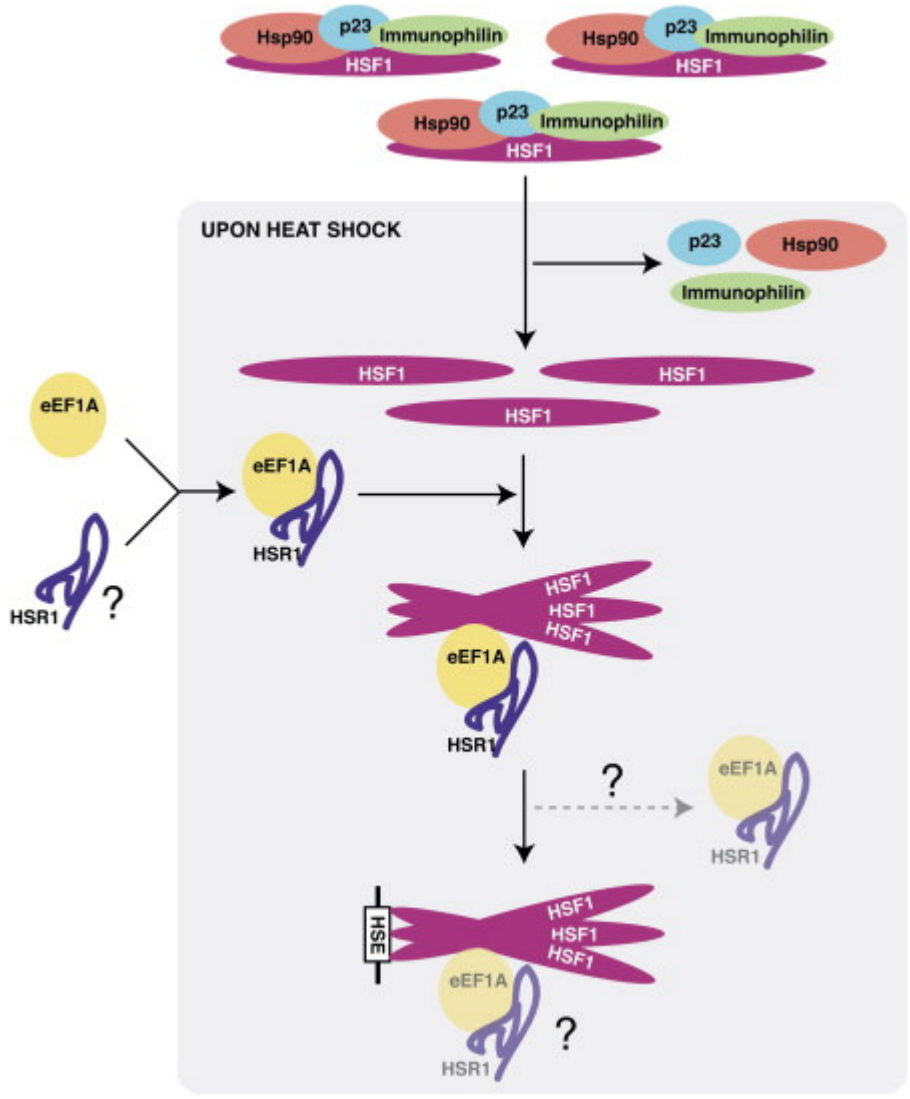

Figure 6.1. A model for the role of eEF1A in the heat shock response.

The current model as suggested by Kugel and Goodrich (Kugel and Goodrich 2006). On heat shock HSF1 is released from its inhibitors. These monomeric HSF1 molecules trimerise in the presence of eEF1A and HSF1. The HSF1 trimers bind promoter regions of heat shock proteins and function in transcriptional activation. Figure taken from Kugel and Goodrich 2006.

Distinguishing the roles of these two variants in the heat shock response is particularly relevant to the study of motor neuron degeneration. As motor neurons have been shown to express eEF1A2 and not eEF1A1 (Newbery *et al.,* 2007) and have a poor heat shock response (Batulan *et al.,* 2003).

Numerous examples of the important neuroprotective roles of heat shock proteins have been reported (Brown 2007), for example SOD-1 toxicity has been shown to be delayed by gene transfer of HSP70 in cultured motor neurons (Bruening *et al.,* 1999). Overexpression studies of HSP70, HSP40 and HSP27 in animal models of neurodegenerative disease have also demonstrated their neuroprotective properties (Muchowski and Wacker 2005). For example, crossing mice overexpressing HSP27 to mice overexpressing mutant SOD1 results in a decrease in disease severity, including a reduced rate of motor deterioration and increased motor neuron survival (Sharp *et al.,* 2008). These investigations suggest that an insufficient stress response in motor neurons increases their vulnerability to toxic insult.

Batulan *et al* demonstrated that while heat shock failed to induce HSP70 expression in cultured motor neurons, injection of a constituitively active form of HSF1 resulted in high levels of HSP70 (Batulan *et al.,* 2003). This suggests that the most likely cause of failure of motor neurons to induce a stress response involves the HSF1 activation pathway, a key player of which has now be shown to be eEF1A1 (Kugel and Goodrich 2006; Shamovsky *et al.,* 2006). As motor neurons express eEF1A2 and not eEF1A1, addressing whether eEF1A2 also has an important role in the heat shock response, and can substitute for eEF1A1 is now vital.

The availability of eEF1A1 and eEF1A2 specific antibodies, which have been generated and optimised in our lab, has allowed experiments to be conducted to address this question. Dr Vicky Tomlison (Tomlinson 2007) began investigating this question by studying the roles of eEF1A1 and eEF1A2 in the heat shock response using HeLa cells. HeLa cells are known to express both eEF1A1 and eEF1A2. siRNAs designed to target human eEF1A1 and eEF1A2 were used to knockdown eEF1A1 and eEF1A2 respectively in HeLa cells. Cells were heat shocked following transfection and the protein expression of the heat shock protein HSP70 was measured as a readout of the heat shock response. HSP70 (or HSP72) is one of the

inducible HSPs i.e. it should only be present under cell stress. While successful knockdown was achieved for eEF1A1 and eEF1A2, HeLa cells proved unsatisfactory for the addressing the aims of this project because this cell line was found to express HSP70 constitutively. They are therefore an inappropriate cell line for the investigation of the induction of heat shock due to their already disrupted heat shock response.

Following this work the baby hamster kidney (BHK) cell line was investigated as this cell line was used successfully by Shamovsky *et al* (Shamovsky *et al.,* 2006).

This work formed part of a MSc by research rotation project conducted by myself in the Abbott group. During this project siRNAs were designed to target hamster eEF1A1. At this time the complete hamster genome sequence including the sequence for eEF1A2 was unavailable.

The results of this project showed that BHK cells express both eEF1A1 and eEF1A2 but not constitutive HSP70, making them an ideal candidate cell line to address this research question. Two siRNAs for eEF1A1 were designed based on homologous regions between hamster, mouse and human eEF1A1 that were different from mouse and human eEF1A2. The results of this project showed that ablating eEF1A1 in BHK cells inhibited the induction of the heat shock response. This preliminary data required further validation and as such was the starting point of this project.

6.3. Results

6.3.1. RNAi: BHK cells

The first aim of this project was to replicate the RNAi experiments conducted previously in BHK cells and to test the specificity of the eEF1A1 siRNAs used. The two hamster eEF1A1 (Ham1a1-1 and Ham1a1-2) siRNAs were transfected separately into BHK cells using a Nucleofector (Lonza). The effect of decreasing eEF1A1 expression on the heat shock response was determined by measuring protein expression of HSP70. Samples were transfected, and allowed to recover for 24hrs before being subjected to heat shock. Some samples were pelleted immediately following heat shock and some were left to recover overnight at 37^{o}C (approximately 16 hours) before pelleting. This recovery period proved essential to allow protein synthesis to occur, resulting in the expression of measurable HSP70 protein. Protein extracts from cells that had not had a recovery period following heat shock expressed no observable HSP70 protein (figure 6.2). Both Western blots in figure 6.2 represent samples from the same experiment. The "Untransfected " samples have the same protein extracts used in both Westerns so that both blots are directly comparable. As can be seen in figure 6.2, both eEF1A1 siRNAs successfully decreased levels of eEF1A1. Due to the large degree of homology between eEF1A1 and eEF1A2 it is critical to test that the siRNA's are specific for one variant. These samples were therefore also examined for the expression of eEF1A2 protein to test the specificity of the RNA interference. As can be seen in figure 6.2, eEF1A2 expression is also decreased in cells transfected with both eEF1A1 targetting siRNAs. These siRNAs are therefore unsuitable to address the aims of this project as they disrupt both eEF1A1 and eEF1A2 expression. Although the siRNAs are not specific for eEF1A1, the Western blots show that this decrease in eEF1A completely ablates the heat shock response (indicated by red stars in figure 6.2). This highlights the crucial role that eEF1A plays in the heat shock response, as without it no HSP70 is induced. As can be seen in figure 6.2 panel (a), the presence of a scrambled non-targetting siRNA also appears to have disrupted the heat shock response and so it is possible that the transfection of any siRNA is enough to block HSP70 induction. However this aliquot

of scrambled siRNA was very old and when other scrambled non-targetting controls were tested they had no effect on the induction of HSP70 (data not shown). Thus an alternative scrambled siRNA was used in all future experiments.

As previously mentioned designing specific eEF1A1 siRNAs was difficult due to the hamster eEF1A2 sequence being unavailable. Numerous attempts were made to sequence regions of hamster eEF1A2 from BHK cells. RT-PCR primers based on homologous regions of eEF1A2 from mouse and human (but that were different from hamster eEF1A1) were designed to amplify a region of hamster eEF1A2 for sequencing. A region of approximately 500bp of hamster eEF1A2 was sequenced from RNA extracted from BHK cells. Sequencing of this fragment confirmed it to be eEF1A2.

Two hamster eEF1A2 specific siRNAs were designed to target this region however following transfection by Nucleofector neither siRNA resulted in any observable knockdown of eEF1A2 protein (data not shown). The numerous problems encountered as a result of not knowing the sequence of hamster eEF1A2 led to the investigation of other candidate cell lines.

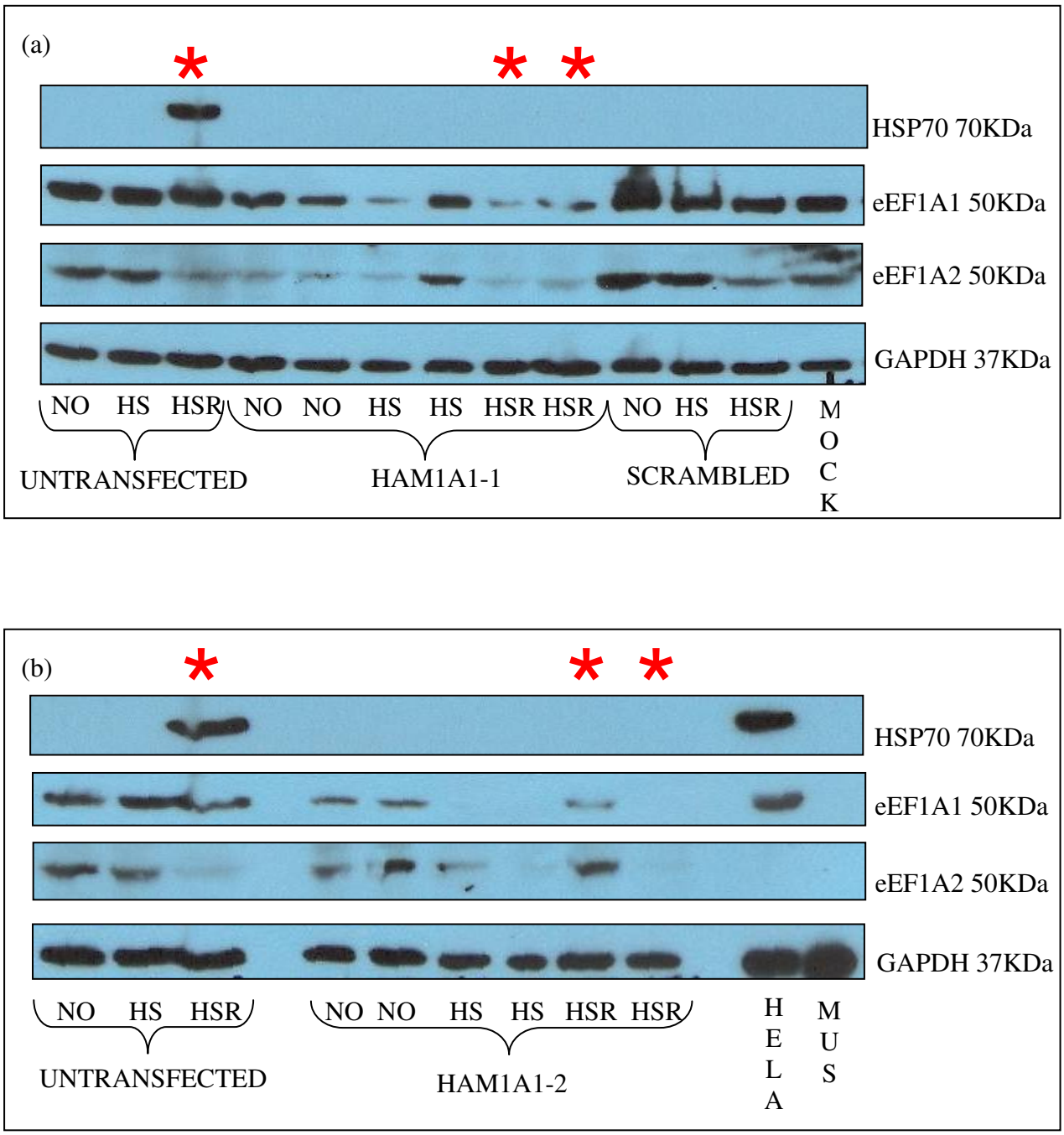

Figure 6.2. Knocking down eEF1A in BHK cells inhibits HSP70 induction.

Western blots showing protein expression from BHK cells transfected with eEF1A1 siRNAs; HAM1A1-1 (panel (a)) and HAM1A1-2 (panel (b)), and also a non-targeting scrambled control (panel (a)). NO indicates untreated cells, HS indicates heat shock with no recovery, HSR indicates heat shock followed by recovery, MOCK indicates a mock transfection, MUS indicates mouse muscle (negative for eEF1A1), HELA indicates HeLa cells (positive control for eEF1A and HSP70). Red stars mark samples that were heat shocked and allowed to recover, highlighting the dfference in HSP70 expression between control cells and those transfected with siRNAs

6.3.2. RNAi: NSC-34 cells

Whilst trying to overcome the problems encountered while investigating BHK cells, another cell line was investigated. NSC-34 (Neuroblastoma Spinal Cord) is a hybrid cell line produced by fusion of motor neuron enriched, embryonic mouse spinal cord cells and mouse neuroblastoma (Cashman *et al.,* 1992). A project student in our lab, Corinne Krommer, showed that NSC-34 cells express both eEF1A1 and eEF1A2 and thus satisfy some of the criteria required for this experiment. The cells were subsequently tested for constitutive HSP70 expression. Initially NSC-34 cells were subjected to 42^{o}C heat shock for two hours (as was sufficient for BHK cells) followed by a 16 hour recovery at 37^{o}C. However, as can be seen from figure 6.3 panel (a), 2 hours at 42^{o}C followed by a 16 hour recovery period was not sufficient to induce HSP70 expression in NSC-34 cells. Subjecting cells to 43^{o}C heat shock for two hours was then tested. As can be seen in figure 6.3 panel (b), HSP70 expression was detectable following two hours at 43^{o}C and 16 hours recovery at 37^{o}C. Therefore HSP70 expression is only detectable in NSC-34 cells following heat shock at 43^{o}C. At this point it was decided in future experiments, all heat shocked cells would be placed at 37^{o}C for 16 hours following heat shock, therefore all other experiments described in this chapter do not include samples that were heat shocked and pelleted immediately.

In addition to being a far more biologically relevant cell line for this investigation than BHK cells, NSC-34 cells express both eEF1A variants and show no constitutive HSP70 expression and are therefore an ideal candidate for these experiments. Since NSC-34 cells are derived from mouse, and mouse eEF1A1 and eEF1A2 sequences are readily available, designing variant specific siRNAs was less problematic than for BHKs.

Mouse specific siRNAs were designed to target mouse eEF1A1 and eEF1A2 separately. Two eEF1A1 specific siRNAs (named m1A1-a and m1A1-b) and two eEF1A2 specific siRNAs (named m1A2-a and m1A2-b) were investigated. Similarly to the BHK cell line experiments, a Nucleofector was used initially to transfect the siRNAs into NSC-34 cells. This technique proved very difficult with this cell line; the procedure resulted in high levels of cell death in NSC-34 cells.

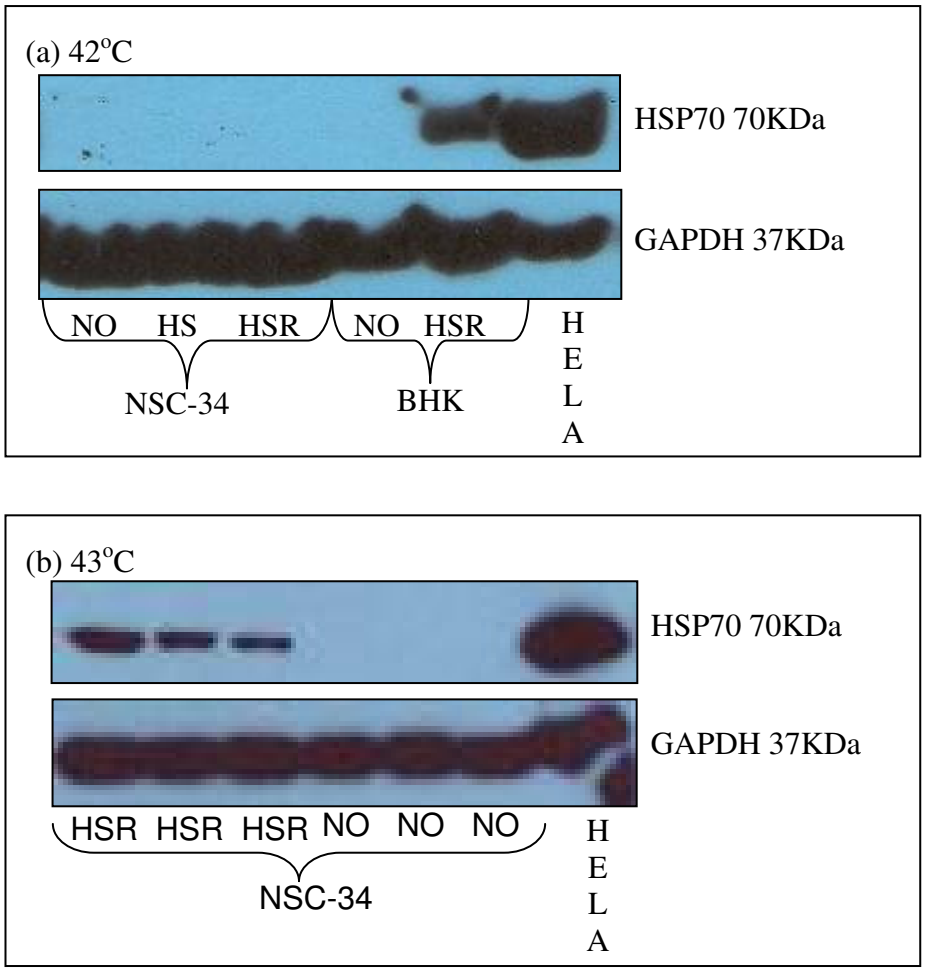

Figure 6.3. NSC-34 cells do not constitutively express HSP70.

Western blots showing the expression of HSP70 in NSC-34 cells following heat shock. Panel (a) shows heat shock at 42°C and panel (b) shows heat shock at 43°C. HELA indicates HeLa cells which are a positive control for HSP70 expression. NO indicates no heat shock (cells remained at 37°C), HS indicates cells were subjected to heat shock and not allowed to recover, HSR indicates cells were subjected to heat shock followed by 16 hour recovery at 37°C.

Numerous attempts were made to optimise the procedure but these were unsuccessful. Lipid transfection using siLentFect (Biorad) was therefore tested. Preliminary mock transfection reactions resulted in little cell death in NSC-34 cells and therefore siLentFect was deemed a suitable reagent for transfection of these cells. Experiments to assess the affect of knocking down eEF1A1 and eEF1A2 could now commence. Cells were transfected with the separate siRNAs, allowed to recover for 24 hours, incubated at 43^{o}C for 2 hours and allowed to recover overnight. Control cells remained at 37^{o}C for the duration of the experiment.

Preliminary results indicate that decreasing eEF1A1 disrupts the cells' ability to mount a heat shock response, as measured by HSP70 expression (figure 6.4). Both eEF1A1 siRNAs decreased the level of eEF1A1 expression and subsequently blocked HSP70 induction. The eEF1A2 siRNAs decreased eEF1A2 protein expression, however this did not dramatically reduce the level of HSP70 in heat shocked cells (figure 6.5). These preliminary data suggests that eEF1A1 is necessary for the induction of the heat shock response whereas eEF1A2 has a less important role. The graphs in figures 6.4 and 6.5 display the expression of eEF1A1 (figure 6.4), eEF1A2 (figure 6.5) and HSP70 in the samples subjected to heat shock normalised to GAPDH (as a loading control). These are compared to the cells transfected with the non-targeting scrambled siRNA and subjected to heat shock. This control is the most appropriate for comparison given that experimental conditions are identical between the samples transfected with a non-targetting siRNA and those transfected with the eEF1A siRNAs. This ensures that any knockdown is due to the specific siRNA and not to the presence of any siRNA molecule. The expression of each protein was measured using the GeneGnome image analysis software.

These experiments were replicated numerous times. The level of knockdown of eEF1A1 and eEF1A2 varied dramatically between and within experiments. Due to this variability, data from multiple experiments was combined in the following way. For the eEF1A1 knockdown experiments, levels of eEF1A1 expression was first normalised to GAPDH in all samples where cells had been subjected to heat shock. To measure the amount of knockdown, the levels of eEF1A1 expression (normalised to GAPDH) from cells transfected with siRNAs and heat shocked were then

normalised to the cells transfected with scrambled siRNA and subjected to heat shock. This gave a measurement for knockdown for each well with an siRNA and subjected to heat shock as compared to the non-targetting scrambled control. If the expression of the eEF1A1 was reduced by 10% or more compared to the scrambled control, this sample was counted in the analysis.

For each experiment, the expression data from all wells with a knockdown of greater than 10% were pooled. The mean of these pooled samples gave a mean knockdown of eEF1A1 by eEF1A1 siRNAs (compared to transfection with a scrambled control) for that experiment. As seen in the table in figure 6.6. the combined results of three separate experiments were then pooled to give a combined knockdown measurement of eEF1A1 in all three experiments. HSP70 expression was measured in the same selected samples in the same way i.e. normalised to scrambled then pooled. The same method was also used to measure eEF1A2 knockdown and subsequent HSP70 expression in the eEF1A2 siRNA experiments.

The specificity of the siRNAs was confirmed by examining protein expression of the variant not being targeted by the siRNA; i.e eEF1A1 expression was checked in samples with eEF1A2 siRNAs and vice versa. No significant problems with specificity were observed as shown in figures 6.4 and 6.5. While it may appear in figure 6.4 that cells transfected with the eEF1A1 siRNA m1a1-a and then heat shocked have decreased levels of eEF1A2, this is not the case. The Western blot showing eEF1A1 and eEF1A2 are in fact from different gels and GAPDH was undetectable in this lane also (data not shown) and this result is thus thought to be due to a loading error. All four siRNAs have been shown to be specific for their target variant in multiple experiments (data not shown).

The results of multiple RNAi experiments are represented by graphs in figure 6.6. These combined data indicate that significantly reducing eEF1A1 by approximately 50% results in a significant decrease of around 60% in the expression of HSP70. The results also suggest that significantly reducing levels of eEF1A2 by approximately 70% has no significant efffect on HSP70 expression.

Taken together these data suggest a crucial role for eEF1A1 and not eEF1A2 in the heat shock response.

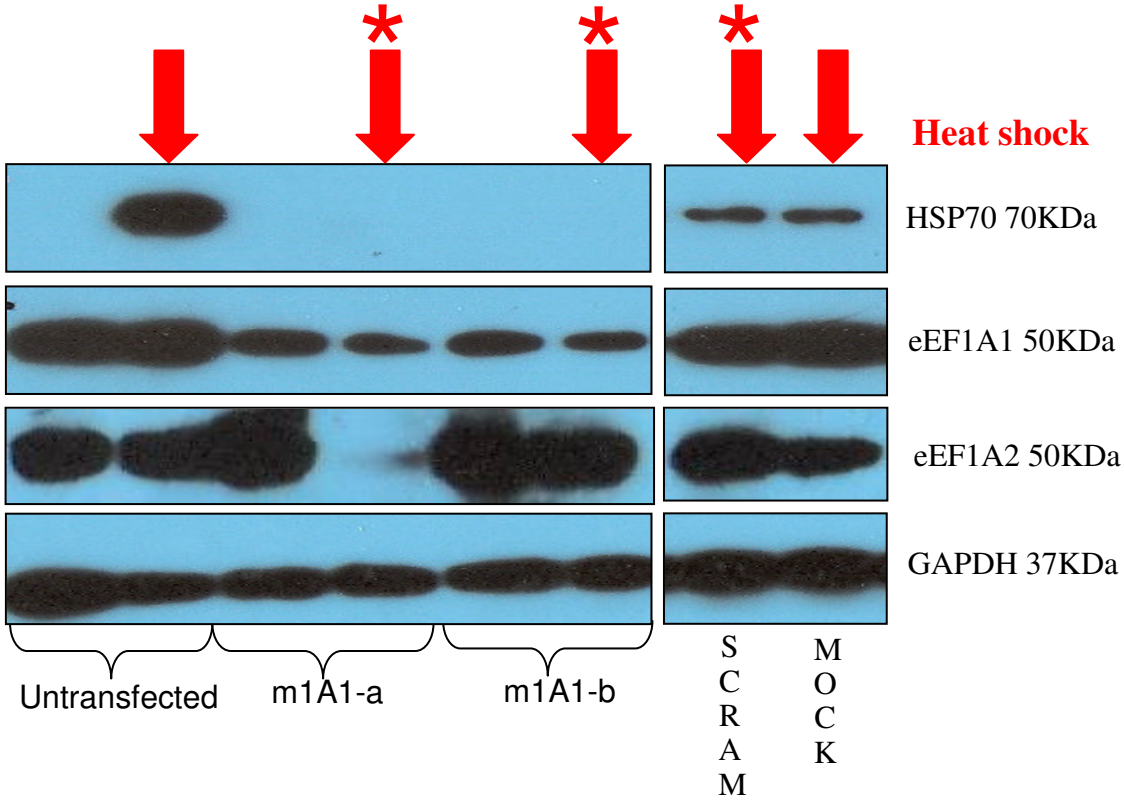

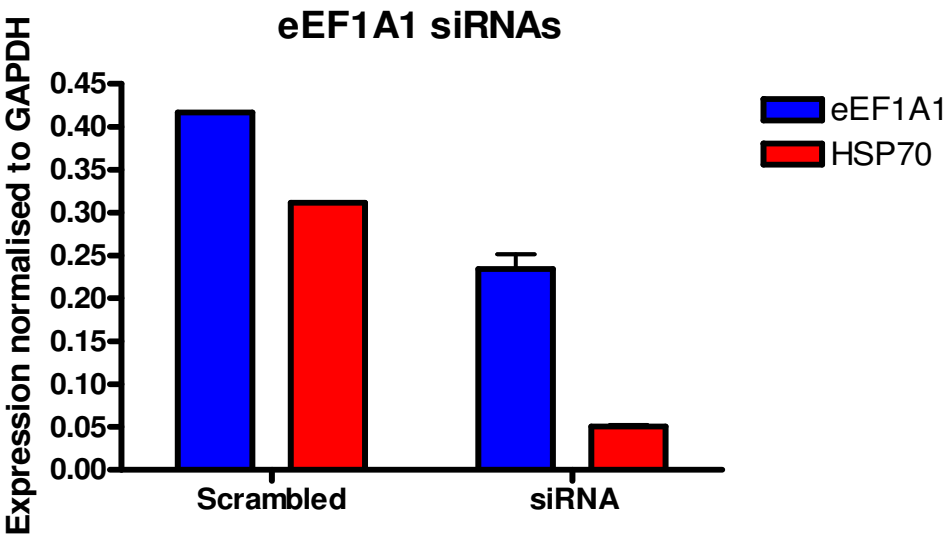

Figure 6.4. Knocking down eEF1A1 ablates the heat shock response.

Protein expression from NSC-34 cells transfected with eEF1A1 siRNAs. Western blots showing expression of eEF1A1, eEF1A2, HSP70 and GAPDH (loading control) in cells transfected with two eEF1A1 siRNAs (m1a1-a and m1a1-b). Scram indicates a scrambled non-targeting negative control, Mock indicates a mock transfection (no siRNA). Red arrows highlight lanes with samples subjected to heat shock. Red stars highlight samples used in the analysis (graph). The graph indicates expression of eEF1A1 and HSP70 normalised to GAPDH in heat shocked samples transfected with eEF1A1 siRNAs and the scrambled non-targeting negative control.

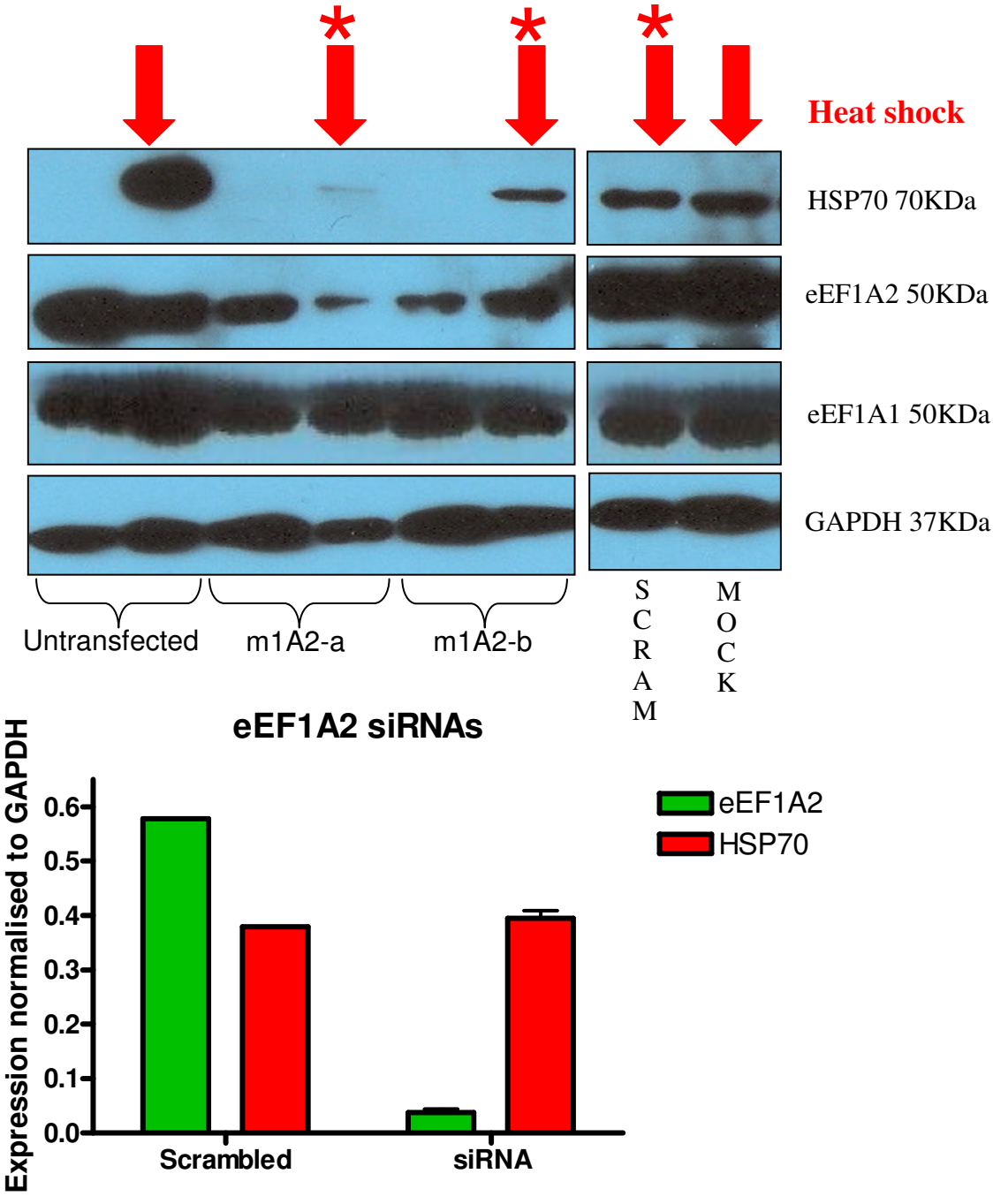

Figure 6.5. Knocking down eEF1A2 has little effect on the heat shock response. Protein expression from NSC-34 cells transfected with eEF1A2 siRNAs. Western blots showing expression of eEF1A2, eEF1A1, HSP70 and GAPDH (as a loading control) in cells transfected with two eEF1A2 siRNAs (m1a2-a and m1a2-b). Scram indicates a scrambled non-targeting negative control, Mock indicates a mock transfection (no siRNA). Red arrows highlight lanes with samples subjected to heat shock. Red stars highlight samples used in the analysis (graph). The graph indicates expression of eEF1A2 and HSP70 normalised to GAPDH in heat shocked samples transfected with eEF1A2 siRNAs and the scrambled non-targeting negative control.

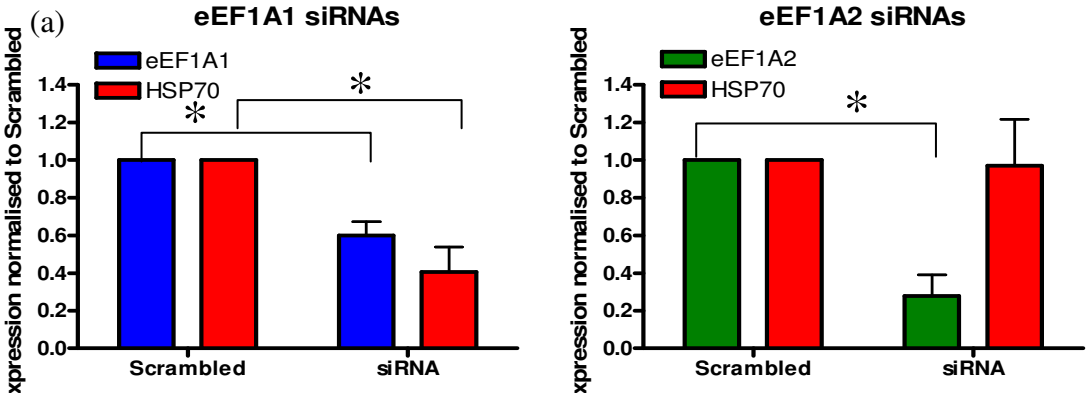

Figure 6.6. Combined RNAi data.

(a) Expression of eEF1A1 and HSP70 from heat shocked cells transfected with eEF1A1 siRNAs, normalised to heat shocked cells transfected with a scrambled non-targetting siRNA. (b) Expression of eEF1A2 and HSP70 from heat shocked cells transfected with eEF1A2 siRNAs , normalised to heat shocked cells transfected with a scrambled non-targetting siRNA. * indicates a p value<0.05.

(a) eEF1A1 siRNAs

Remaining expression	Experiment 1 (n=2)	Experiment 2 (n=5)	Experiment 3 (n=2)	Mean	S.D	S.E.M
eEF1A1	0.56	0.50	0.74	0.60	0.13	0.07
HSP70	0.17	0.42	0.63	0.41	0.23	0.13

(b) eEF1A2 siRNAs

Remaining expression	Experiment 1 (n=2)	Experiment 2 (n=6)	Experiment 3 (n=8)	Mean	S.D	S.E.M
eEF1A2	0.06	0.43	0.35	0.28	0.20	0.11
HSP70	1.45	0.63	0.84	0.97	0.43	0.25

Table 6.1. Combined RNAi data.

(a) Expression of eEF1A1 and HSP70 from heat shocked cells transfected with eEF1A1 siRNAs, normalised to heat shocked cells transfected with a scrambled non-targetting siRNA. (b) Expression of eEF1A2 and HSP70 from heat shocked cells transfected with eEF1A2 siRNAs , normalised to heat shocked cells transfected with a scrambled non-targetting siRNA. S.D indicates standard deviation, S.E.M indicates standard error of the mean, n indicates the number of wells analysed.

6.4. Discussion

Although the importance of the trimerisation of heat shock factor 1(HSF1) in the heat shock response has been known for some time, the importance of the co-operation of eEF1A and a previously unknown RNA named heat shock RNA 1 (HSR1) in this chain of events has only recently been found (Shamovsky *et al.,* 2006). We know that eEF1A1 can fulfil this role from the previous study (Shamovsky *et al.,* 2006) as they found eEF1A purified from liver is involved in HSF1 activation. Liver only expresses eEF1A1 and not eEF1A2. We hypothesised that eEF1A2 is not able to fulfil the same role in the heat shock response as eEF1A1.

In this project, RNAi in various cell lines was used to investigate the separate rolls of eEF1A1 and eEF1A2 in the heat shock response. The criteria for a cell line to be suitable for this project, was firstly that the cells express both eEF1A1 and eEF1A2 and second that cells do not constitutively express the inducible heat shock protein HSP70. The first cell line to be investigated was the baby hamster kidney (BHK) cell line. This cell line expresses eEF1A1 and eEF1A2 and only expresses HSP70 when subjected to heat shock at 42^{o}C, thus making it an ideal candidate for this experiment. The hamster eEF1A2 sequence is currently unavailable which made designing variant specific siRNAs very difficult. While it appeared initially as though knocking down eEF1A1 ablates the heat shock response in BHK cells, analysis of eEF1A2 in these same samples showed a similar pattern of protein expression. The two most logical explanations for this are firstly that the siRNAs are not specific and second that one or both of the variant specific antibodies are not specific in hamster. Given that the panel of antibodies used have been shown to be variant specific in mouse, human and also xenopus, it is unlikely that this is the cause of the problem. It is therefore more likely that the problem lies with the specificity of the siRNAs. More efforts could have been spent attempting to further sequence hamster eEF1A2 and designing more siRNAs however it was deemed more practical to investigate an alternative cell line. The mouse NSC-34 cell line was investigated as an alternative and proved to be a more suitable and convenient cell line to work with than BHK cells. NSC-34 cells also express both eEF1A variants and don't constitutively express HSP70. Interestingly, here is shown that NSC-34 cells have a

slightly higher threshold for heat shock than BHKs. This is shown by the fact that 42^{o}C is not enough to induce the heat shock response as in BHK cells and that a minimum temperature of 43^{o}C is required to induce HSP70 expression in NSC-34 cells. This may be due to NSC-34 cells being a neuronal cell line as neurons are thought to have a higher threshold for heat shock than other cell types

Preliminary data from RNAi in NSC-34 cells suggests that ablating eEF1A1 results in the inhibition of heat shock induction while ablating eEF1A2 has little effect on the cells ability to mount a heat shock response. However the RNAi experiments have been very problematic and as such some replication and optimisation is still required to confirm these findings.

The first problem faced was an unreliable negative control. A scrambled control from Ambion was used alongside the eEF1A1 siRNAs in the initial experiments in BHK cells. Western blots showed that although the scrambled siRNA was not affecting the expression of eEF1A1 in the cells, the level of HSP70 was reduced by the presence of this apparent negative control (Figure 6.2). It was therefore possible that the presence of any siRNA would reduce HSP70 expression. Other scrambled controls were investigated and it transpired that only this aliquot of the Ambion scrambled control affected HSP70 expression. A new scrambled control was used in all future experiments thus eliminating this problem. A positive actin siRNA was also tested in BHK cells which had no observable affect on eEF1A1, eEF1A2 or HSP70 expression. In NSC-34 cells the actin siRNA had little effect on the expression of eEF1A1, eEF1A2 or HSP70. However problems with the actin antibody prohibited the effect of the actin siRNA on the levels of actin from being confirmed in NSC-34 cells. While scrambled is used as a negative control its efficiency as a positive control cannot be measured. An siRNA with a known target which has no influence on the gene of interest is thus more useful as its functional capabilities can be confirmed. An actin siRNA may not be ideal for this as actin has been shown to interact with eEF1A (Ejiri 2002). This should be investigated in future experiments. The nucleofection procedure also proved problematic for NSC-34 cells (although not for BHK cells). Numerous attempts were made to transfect siRNAs into NSC-34 cells using a Nucelofector but these often resulted in large amounts of cell death.

Various experimental conditions as recommended by the manufacturer were tested but all were unsuccessful. SiLentFect was then tested, which resulted in very little cell death. There are multiple reagents available for transfection of siRNAs and these should be thoroughly investigated to try and optimise knockdown of the eEF1A variants in NSC-34 cells. For these experiments a GFP plasmid was transfected into cells to measure transfection efficiency but this is of limited use as a plasmid is very different from an siRNA. Confirmation of effective transfection should be determined using a fluorescently labelled siRNA in future experiments which may help with the optimisation procedures.

The siRNAs produced variable results both within and between experiments. The eEF1A1 siRNAs in particular resulted in often poor knockdown. The effectiveness of the eEF1A1 siRNAs appeared to decrease with time and usage. This could simply be a result of degradation of the siRNAs which in the past have proved to be vulnerable to repetitive freeze-thawing. Ordering new siRNAs and aliquoting on arrival may eliminate this problem from future experiments. However numerous attempts in the past to reduce eEF1A1 expression have also proved unsuccessful or not reproducible. Attempts have been made in our laboratory by multiple researchers using multiple methods, all of which have been problematic. This could be due to the importance of eEF1A1 for cell survival. Important compensatory mechanisms could be in place to prohibit reduction of this crucial elongation factor. Using eEF1A2 siRNAs was less problematic. Successful knockdown of eEF1A2 was achieved consistently on multiple occasions.

For future experiments many replicate wells for each siRNA and also for the scrambled controls should be used to try to reduce the variability between experiments.

As mentioned, numerous technical problems were encountered in this project and much work is still required to eliminate these difficulties and optimise experimental conditions. In addition many other avenues of research have become apparent of which time restraints prohibited these from being investigated in this project.

One important aspect of this research area that has yet to be fully addressed is whether heat shock itself has any affect on levels of expression eEF1A1 and

eEF1A2. Shamovsky *et al* suggest that the shut down of translation caused by heat shock releases eEF1A from its translational role so that it is freely available to participate in the heat shock response (Shamovsky *et al.,* 2006). This suggests no change in the total expression of eEF1A. Lucy Mallins (under my supervision) began to investigate whether eEF1A1 and/or eEF1A2 expression levels changed during heat shock. Lucy showed that heat shock has no significant affect on eEF1A1 expression in NSC-34, PC12 (dervived from a rat pheochromocytoma (Greene and Tischler 1976)) and SHY5Y (derived from a neuroblastoma (Biedler *et al.,* 1973; Biedler *et al.,* 1978) cells. However it was observed that eEF1A2 protein expression was sometimes decreased upon heat shock in these cell lines. This can also be observed in figure 6.2 where eEF1A2 levels in untransfected cells appear reduced in cells that were subjected to heat shock and recovery compared to cells that were not heat shocked. This result however is variable between experiments and a more detailed time course investigation is required to confirm these findings.

Lucy also investigated other cell lines as potential candidates for the RNAi experiments. It was shown that SHY5Y and PC12 cells express both eEF1A1 and eEF1A2 however only PC12 cells showed no constitutive HSP70. At the beginning of the project only BHK cells had shown expression of both eEF1A1 and eEF1A2 without constitutive expression of HSP70. It has now been shown that NSC-34 cells and PC12 cells both also meet these criteria. Other cell lines such as SHY5Y, HeLa, COS7, OVCAR5 and MO6 all have constitutive HSP70 (data not shown) but there may be other cell lines yet to be investigated that would be appropriate for the experiments. Stable cell lines expressing both variants could also be studied.

The differentiation state of neuronal cell lines has also been shown to affect heat shock induction. The ability of the rat neuronal PC12 cell line to induce HSP70 on heat shock is diminished when differentiated (Hatayama *et al.,* 1997). While the NSC-34 cells in these experiments were all undifferentiated, it is possible to differentiate them to a more neuronal state (Cashman *et al.,* 1992). It would be interesting to assess the affect of differentiating these cells and other neuronal cell lines on the heat shock response and to investigate whether any changes are observed in eEF1A1 and eEF1A2 expression between undifferentiated and differentiated cells.

Other heat shock proteins should also be investigated , as a possible compensatory role in the absence of HSP70 cannot be ruled out. These could include HSP25/27 which has been shown to rescue motor neurons following nerve injury (Sharp *et al.,* 2006) and also has been found to be up-regulated in cell lines with mutant SOD1 (Batulan *et al.,* 2003).

Differences in the protein interactions of eEF1A1 and eEF1A2 with HSF1 during heat shock should also be investigated. To address this, methods such as Biomolecular florescence complementation (BiFC) or Proximity ligation assay (PLA) could be attempted. BiFC is a relatively new method, which is used to directly visualise protein-protein interactions in living cells (Hu *et al.,* 2002). Two fragments of a split fluorescent protein are fused to the two proteins of interest. An interaction between these proteins of interest allows association between the two fragments of the fluorescent protein to produce a biomolecular fluorescent complex. This has been used by a group here in Edinburgh (Gkogkas *et al.,* 2008). Another method which is currently being optimised in our lab is PLA. In brief, this technique involves the use of two PLA probes which consist of a secondary antibody with an attached oligonucleotide. When two proteins and thus their primary antibodies are in close proximity, these PLA probes bind and the oligonucleotides attached to them come into close enough proximity to be amplified by PCR. This results in a fluorescent PCR product that can be visualised down the microscope as a dot (Gustafsdottir *et al.,* 2005). This technique can be used to assess protein-protein interactions in cells and also in tissue sections.

If the preliminary data from this study is validated and shows that only eEF1A1 has a role in the heat shock response, the effect of transfecting an eEF1A1 expression construct into cultured motor neurons could be assessed. This would address whether the ability of the motor neurons to respond to stress is improved by the presence of eEF1A1. This study in itself would be problematic as motor neurons have shown to be very difficult to culture.

This question could also be addressed at the whole animal level. Transgenic studies in our laboratory are currently investigating the affect of expressing eEF1A1 under the control of the eEF1A2 promoter in mice. These animals will be crossed to the

wasted line to generate wasted mice (*wst/wst*, which lack eEF1A2 expression) with the eEF1A1 transgene to assess whether eEF1A1 under the control of the eEF1A2 promoter can rescue the wasted phenotype. If this proved to be the case, these animals expressing neuronal eEF1A1 could also be crossed to other models of motor neuron degeneration such as a mutant SOD1 line to see if the presence of neuronal eEF1A1 can provide any protection agains motor neuron degeneration in these animals.

6.5. Conclusion

The results of this project suggest a crucial role for eEF1A1 in the heat shock response, specifically by its effect on HSP70 expression. eEF1A2 appears to have a less crucial role and is unable to compensate for the loss of eEF1A1 in the heat shock response. The different abilities of eEF1A1 and eEF1A2 in participating in the heat shock response show a key difference between the two and may explain in part why motor neurons are vulnerable to heat shock (Batulan *et al.,* 2003). This is important not only for our understanding of the selective vulnerability of motor neurons in motor neuron disease/amyotrophic lateral sclerosis but also in other neurodegenerative disorders such as Alzheimers and Parkinsons disease. Disrupted stress pathways in these neurodegenerative diseases are thought to lead to aggregate formation in neurons. Once confirmed, these results could lead to the investigation of eEF1A1 as a potential therapeutic target for treatment of motor neuron degeneration.

7. Chapter 7: Discussion

7.1. Project aims

In this project the role of eEF1A in motor neuron degeneration was studied. The main aims of this project were to increase our understanding of the importance of this crucial elongation factor by further studying the wasted (*wst*) mouse model and also by investigating what role it has (if any) in human motor neuron disease. Within this research area there were four main aims. Firstly, to ascertain whether there is a gene dosage effect of eEF1A2 by examining ageing heterozygote animals for any signs of motor neuron degeneration. Secondly, to understand further the pathology of wasted mice, tissue specific transgenic animals were examined. Thirdly, human spinal cord sections from ALS patients were examined for any changes in eEF1A2, which would further validate the wasted mouse model as a model of human motor neuron degeneration. Finally, a possible role of eEF1A in the heat shock response was investigated. Together, these four projects aimed to improve our understanding of the wasted mouse model and to increase our knowledge of the mechanisms involved in motor neuron degeneration both in mouse and human disease.

7.2. Gene dosage of eEF1A2

Ageing mice heterozygous for a mutation in the ZPR1 gene have shown to be a useful model for studying motor neuron degeneration (Doran *et al.,* 2006). This, combined with the finding that eEF1A (the specific variant was not identified) is found in a complex with ZPR1 and SMN (Gangwani *et al.,* 1998), led to the investigation of wasted heterozygotes (+/*wst*) as a possible model for motor neuron degeneration. This study is the first to examine ageing heterozygote wasted mice (+/*wst*) for signs of motor neuron degeneration. The grip strength meter proved to be an effective tool for measuring disease in wasted mice and so was used in combination with the accelerating rotarod to assess any physical differences in the ageing cohort. The study showed no statistical difference between wildtype (+/+) and heterozygote (+/*wst*) animals in either male or female mice. However there was

a trend for female heterozygous (+/*wst*) animals to perform slightly worse than female wildtype animals (+/+) on the accelerating rotarod. In addition no significant pathological differences were observed between the groups. These results suggest that ageing heterozygote wasted mice (+/*wst*) are not a useful model for studying motor neuron degeneration, and that 50% of wild-type levels of eEF1A2 are sufficient for normal function. This study does however raise some interesting issues regarding the impact of gender, age and also exercise/training regimes on the results of behavioural studies (as dicussed in chapter 3).

Although wasted heterozygotes may not be a valuable model for studying motor neuron degeneration the important link between eEF1A and ZPR1 should however continue to be investigated. The main aim in this regard should be to establish which of the eEF1A variants is found to complex with ZPR1. The observation that wasted mice have reduced ZPRI (Murray *et al.,* 2008), leads to the possibility that shared disease pathways may exist between the wasted model and models of spinal muscular atrophy. Results from this study however should be viewed with caution as it is possible that ZPR1 may simply be reduced due to disrupted protein synthesis resulting from the loss of eEF1A2. Further investigating the function of ZPR1 in wasted mice may therefore shed light on our understanding of common pathologies between models of motor neuron degeneration and thus improve our understanding of the vulnerability of motor neurons in these conditions.

7.3. Tissue specific eEF1A2 expression

A key question yet to be answered in the wasted mouse is whether the reduction of eEF1A2 in muscle has a direct effect on muscle pathology, or whether muscle pathology occurs indirectly due to the loss of eEF1A2 in motor neurons. The aim of this part of the project was to investigate whether it is the loss of neuronal eEF1A2 leading to denervation of muscle or the loss of eEF1A2 in muscle, is the primary cause of the muscle atrophy in wasted animals. Unfortunately, this could not be fully addressed in this study due to the common problem of non-specific transgene expression. Transgenic animals expressing only neuronal eEF1A2 were therefore not

achieved. The study did, however uncover some potentially interesting findings. The generation of a mouse line with normal expression of eEF1A2 in all tissues except the heart will allow the role of eEF1A2 in the heart to be studied. The transgenic animals generated also offer the opportunity to investigate the so-far unknown role of eEF1A2 in other tissues such as the pancreas. While no gross pancreatic dysfunction has yet been seen in wasted mice, this may take longer than 28 days (the approximate lifespan of a wasted mouse) to manifest. Transgenic animals which survive beyond the 28 day stage (such as the NSE-EEF1A2 line B described in this study) may therefore be of interest. A diabetes susceptibility locus has been mapped to 20q13.3 (Rotimi *et al.,* 2004) which is in a similar region to *EEF1A2*. Expression of eEF1A1 in the eEF1A2 positive cells should first be investigated, as co-expression cannot yet be ruled out which may reduce the impact of the loss of eEF1A2.

The investigation of mice expressing only neuronal eEF1A2 (i.e no muscle eEF1A2) together with the mice expressing only muscle eEF1A2 (i.e. no neuronal eEF1A2 - currently under investigation) will increase our understanding of the primary cause of the muscle pathology seen in wasted mice. Transgenic animals could also be used to investigate the role of eEF1A2 in the heart of wasted mice. In addition to using the transgenic line created here (line C), conditional knockouts of eEF1A2 could also be generated. These could potentially address the crucial timing of the loss of eEF1A2 in all tissues and also whether the pathology caused by the loss of eEF1A2 is reversible. This may also aid in our understanding of the ultimate cause of death of wasted mice. Likely hypotheses for the cause of death currently centre around the loss of eEF1A2 in muscle. The lack of eEF1A in skeletal muscle of wasted animals for example may eventually lead to respiratory failure. The transgenic animals generated in our lab, which show that muscle specific eEF1A2 do not rescue the wasted phenotype begin to contradict this opinion. Alternatively the loss of eEF1A in heart may ultimately lead to a cardiac failure. Further tissue specific transgenic models together with an investigation into *de-novo* protein synthesis in the affected tissues in wasted mice may help us to address these hypotheses.

7.4. eEF1A2 in human disease

While animal models provide a relatively easy way to investigate the roles of protein in human disease, they are limited in their use. Continuing to investigate human samples is therefore of fundamental importance. This study highlights a possible role for eEF1A2 in human motor neuron disease and is the first (to our knowledge) of eEF1A2 being investigated in human spinal cord of patients with motor neuron disease. 80% of spinal cords from MND patients studied here showed a decrease in the expression of eEF1A2 in their motor neurons. This, combined with previous findings (Bakay *et al.,* 2006) showing decreased eEF1A2 expression in muscle samples from MND patients highlights the need to further investigate the role of eEF1A2 in human motor neuron degeneration. Expanding the findings shown here to include larger sample numbers is crucial to gain a more accurate understanding of the extent to which eEF1A2 is involved in human disease. Collaborations are currently underway to expand this study.

The recently identified role of TDP-43 (Arai *et al.,* 2006; Neumann *et al.,* 2006) in ALS demonstrates the importance of studying pathological samples from human disease patients. Animal models are currently being developed to further understand its role in the disease process. While these are being developed, mouse models which show abnormal TDP-43 expression are now key for furthering our understanding of its role in motor neuron degeneration. As shown here wasted mice may be one such model. A detailed understanding of TDP-43 in the wasted mouse model should now be investigated. While studying inclusions is not possible in the wasted model due to the absence of ubiquitinated inclusions, wasted mice may offer insights into the role of TDP-43 prior to the formation of inclusions. Understanding the role of eEF1A variants in nuclear transport may also strengthen this study.

To begin to understand the function of eEF1A2 in human disease copy number variation could be investigated in MND patients. In addition the promoter region of eEF1A2 should be sequenced, to assess whether any rare mutations in the promoter region may be responsible for any ALS cases. Investigating eEF1A2 in other animal

models of motor neuron degeneration and also possibly other neurodegenerative diseases may uncover whether eEF1A2 has roles in these.

The results of this study further emphasise the importance of the wasted mouse model for studying human disease. In addition it demonstrates the necessity for investigating all possible models of motor neuron degeneration and not just those with known mutations in human disease. Collectively information from sporadic mouse models may uncover common pathogenic pathways and previously unknown factors in human disease. This study has also highlighted some of the difficulties of analysing degenerating motor neurons and the importance of understanding how protein expression in motor neurons changes during degeneration.

7.5. eEF1A in the heat shock response

One possible mechanism for the involvement of eEF1A variants in motor neuron disease could be through the stress response pathways as shown here in the investigation of eEF1A1 and eEF1A2 in the heat shock response. Results show that eEF1A1 has a crucial role in the heat shock response and that eEF1A2 does not fully share this role. Ablating eEF1A1 disrupted the heat shock response in NSC-34 cells while the remaining eEF1A2 was unable to compensate for this loss. This study has therefore potentially identified a functional difference between the two variants which further expands on our understanding of why we have two variants with almost indistinguishable roles in translation. One possible hypothesis might be that the role of eEF1A1 in cytoskeletal remodelling is detrimental to motor neurons. They therefore express eEF1A2, with the shortcoming of having a poor heat shock response as a result. The expression of eEF1A2 rather than eEF1A1 in motor neurons may in part explain the vulnerability of motor neurons to heat shock (Batulan *et al.,* 2003) and may also prove an interesting link between eEF1A and motor neuron degeneration.

The potential therapeutic benefit of eEF1A1 should be investigated further. Ideally eEF1A1 would be introduced into cell lines expressing only eEF1A2, to assess for any changes in the cells ability to mount a heat shock response. Motor neurons have

proven to be very difficult to culture, and to our knowledge, no cell lines expressing only eEF1A2 and no eEF1A1 have yet been identified. Many labs are attempting to generate motor neuron-like cell lines which, once validated, could be considered for this study. For example subsets of motor neurons have been generated from human embryonic stem cells in a recent study by Patani *et al* (Patani *et al.,* 2011). Cells such as these could be investigated to determine the expression pattern of eEF1A variants to determine if they may be utilised for studies investigating the functional differnces between the two variants.

Further animal models may be also be considered for this investigation. Current work in the laboratory is attempting to generate transgenic animals expressing eEF1A1 under the control of the eEF1A2 promoter which will investigate the potential of eEF1A1 (in motor neurons and muscle) to rescue the wasted phenotype.

Pharmacological compounds which induce the expression of heat shock proteins are being investigated as potential therapeutic agents for neurodegenerative disease. Arimolcolol, a co-inducer of the heat shock response has been shown to delay disease progression and reduce both neuronal loss and aggregate formation in SOD1 transgenic mice (Kieran *et al.,* 2004; Kalmar *et al.,* 2008). It would be beneficial to test compounds such as these on other mouse models that do not arise from SOD1 mutations, to observe what affect (if any) they may have. It has also been shown that targeting multiple HSPs has a greater effect on the reduction in aggregate formation in cells (Takeuchi *et al.,* 2002) and has a greater effect on the rescue of SOD1 mutant mice than individual HSPs (Patel *et al.,* 2005). Thus targeting factors which may be involved in the regulation of multiple HSPs such as HSF1 might be of more therapeutic benefit and might also reduce the detrimental side affects of overexpression of individual HSPs such as alterations in cell cycle regulation and cancer (Mosser and Morimoto 2004). Manipulating the entire heat shock pathway as opposed to individual HSPs may therefore achieve greater neuroprotection. Arimochol for example acts by prolonging the activity of HSF1 (Kieran *et al.,* 2004), resulting in the upregulation of HSP70 and HSP90 resulting in prolonged survival. Transgenic expression of HSP70 alone however, does not slow disease progression in these mice (Liu *et al.,* 2005). Given that eEF1A1 appears to act on HSF1 which

then regulates multiple heat shock factors, it now warrants further investigation as a possible therapeutic target for motor neuron degeneration.

7.6. Conclusion

The main aim of the project has been achieved; it has improved our understanding of the role of eEF1A2 in motor neuron degeneration and has uncovered multiple avenues for future research.

On of the key questions that remain to be answered is; why is eEF1A2 only expressed in terminally differentiated cells such as motor neurons. Many functions of eEF1A1 have been previously uncovered including cytoskeletal rearrangement and nuclear transport. Studies examining the differing roles of the two variants are therefore key to an understanding of the parts they may play in disease processes.

The separate roles of the two variants in nuclear transport for example is of particular interest. Findings that eEF1A has been found in a complex with SMN which in turn has been found to complex with TDP-43 may provide a link between eEF1A and TDP-43. Investigating which variant/s complex with SMN and are involved in nuclear transport may therefore be important for our understanding of eEF1A in motor neuron degeneration. The wasted mouse is therefore crucial for not only improving our understanding of the biology of eEF1A but also the various pathways involved in motor neuron degeneration.

In order to fully understand theses disease processes, multiple avenues of research including mouse models, cell models and human samples should be fully investigated. All three have been utilised in this study and together are essential for the progression of the field. While human tissue shows us the most accurate portrayal of what is occurring in tissues of the body during disease, this is usually at the end-stage of disease. It therefore offers us little insight into the early stages of disease progression, where therapeutic intervention may still be a possibility. Models of disease are therefore essential for our understanding of the initiation and development of disease processes.

Cell models provide us with an inexpensive view into proteins of interest. Findings in cells can then be extended to the whole animal models to investigate their role in a whole biological system. In the past, animal models have allowed further investigation of factors identified in human disease and (as demonstrated here) they also have the potential to uncover new factors and pathways that may be involved in human disease which have yet to be examined. They are of utmost importance in multifactorial diseases such as ALS as they allow us to tease apart the complex network of events and to investigate the roles of single factors and pathways of interest. They also offer the opportunity to investigate and test therapeutic agents. With the development of high throughput, detailed genetic analysis such as next generation sequencing which in time may uncover a plethora of disease associated genes, animal models will be crucial in teasing apart the individual roles of these genes. Continuing to investigate and improve animal models is therefore paramount for our understanding of neurodegenerative conditions.

With the prevalence of neurodegenerative disease on the rise, it is now more important than ever to understand these conditions. Even with the recent discovery of some key players in ALS, the cause of the vast majority of ALS remains unknown. There are still many crucial unanswered questions such as; why ubiquitously expressed proteins such as SOD1 and TDP-43 cause selective vulnerability of motor neurons, and what role do protein aggregates play in disease processes? To address these fundamental questions, investigating common features of different neurodegenerative disease such as aggregate formation, RNA processing and the stress response is crucial. Understanding the normal functions of proteins involved in ALS and the identification of shared pathological pathways is vital for the development of effective treatments for these debilitating conditions.

8. References

Abbott, C.*, et al.* (1994). Linkage mapping around the ragged (Ra) and wasted (wst) loci on distal mouse chromosome 2. *Genomics* **20**(1): 94-8.

Abbott, C. M. and C. G. Proud (2004). Translation factors: in sickness and in health. *Trends Biochem Sci* **29**(1): 25-31.

Aghajanian, G. K. and F. E. Bloom (1967). The formation of synaptic junctions in developing rat brain: a quantitative electron microscopic study. *Brain Res* **6**(4): 716-27.

Anand, N.*, et al.* (2002). Protein elongation factor EEF1A2 is a putative oncogene in ovarian cancer. *Nat Genet* **31**(3): 301-5.

Ann, D. K.*, et al.* (1991). Isolation and characterization of the rat chromosomal gene for a polypeptide (pS1) antigenically related to statin. *J Biol Chem* **266**(16): 10429-37.

Arai, T.*, et al.* (2006). TDP-43 is a component of ubiquitin-positive tau-negative inclusions in frontotemporal lobar degeneration and amyotrophic lateral sclerosis. *Biochem Biophys Res Commun* **351**(3): 602-11.

Ayala, Y. M.*, et al.* (2008). Structural determinants of the cellular localization and shuttling of TDP-43. *J Cell Sci* **121**(Pt 22): 3778-85.

Bakay, M.*, et al.* (2006). Nuclear envelope dystrophies show a transcriptional fingerprint suggesting disruption of Rb-MyoD pathways in muscle regeneration. *Brain* **129**(Pt 4): 996-1013.

Barneoud, P.*, et al.* (1997). Quantitative motor assessment in FALS mice: a longitudinal study. *Neuroreport* **8**(13): 2861-5.

Batulan, Z.*, et al.* (2003). High threshold for induction of the stress response in motor neurons is associated with failure to activate HSF1. *J Neurosci* **23**(13): 5789-98.

Bechtold, D. A.*, et al.* (2000). Localization of the heat-shock protein Hsp70 to the synapse following hyperthermic stress in the brain. *J Neurochem* **74**(2): 641-6.

Biedler, J. L.*, et al.* (1973). Morphology and growth, tumorigenicity, and cytogenetics of human neuroblastoma cells in continuous culture. *Cancer Res* **33**(11): 2643-52.

Biedler, J. L.*, et al.* (1978). Multiple neurotransmitter synthesis by human neuroblastoma cell lines and clones. *Cancer Res* **38**(11 Pt 1): 3751-7.

Boillee, S.*, et al.* (2006). ALS: a disease of motor neurons and their nonneuronal neighbors. *Neuron* **52**(1): 39-59.

Brandmeir, N. J.*, et al.* (2008). Severe subcortical TDP-43 pathology in sporadic frontotemporal lobar degeneration with motor neuron disease. *Acta Neuropathol* **115**(1): 123-31.

Brown, I. R. (2007). Heat shock proteins and protection of the nervous system. *Ann N Y Acad Sci* **1113**: 147-58.

Bruening, W.*, et al.* (1999). Up-regulation of protein chaperones preserves viability of cells expressing toxic Cu/Zn-superoxide dismutase mutants associated with amyotrophic lateral sclerosis. *J Neurochem* **72**(2): 693-9.

Bruijn, L. I.*, et al.* (1997). ALS-linked SOD1 mutant G85R mediates damage to astrocytes and promotes rapidly progressive disease with SOD1-containing inclusions. *Neuron* **18**(2): 327-38.

Bruijn, L. I.*, et al.* (2004). Unraveling the mechanisms involved in motor neuron degeneration in ALS. *Annu Rev Neurosci* **27**: 723-49.

Buratti, E.*, et al.* (2004). Nuclear factor TDP-43 binds to the polymorphic TG repeats in CFTR intron 8 and causes skipping of exon 9: a functional link with disease penetrance. *Am J Hum Genet* **74**(6): 1322-5.

Buratti, E.*, et al.* (2001). Nuclear factor TDP-43 and SR proteins promote in vitro and in vivo CFTR exon 9 skipping. *Embo J* **20**(7): 1774-84.

Cai, H.*, et al.* (2005). Loss of ALS2 function is insufficient to trigger motor neuron degeneration in knock-out mice but predisposes neurons to oxidative stress. *J Neurosci* **25**(33): 7567-74.

Carlson, B. M.*, et al.* (2002). Effects of long-term denervation on skeletal muscle in old rats. *J Gerontol A Biol Sci Med Sci* **57**(10): B366-74.

Caroni, P. (1997). Overexpression of growth-associated proteins in the neurons of adult transgenic mice. *J Neurosci Methods* **71**(1): 3-9.

Cashman, N. R.*, et al.* (1992). Neuroblastoma x spinal cord (NSC) hybrid cell lines resemble developing motor neurons. *Dev Dyn* **194**(3): 209-21.

Chambers, D. M.*, et al.* (1998). The lethal mutation of the mouse wasted (wst) is a deletion that abolishes expression of a tissue-specific isoform of translation elongation factor 1alpha, encoded by the Eef1a2 gene. *Proc Natl Acad Sci U S A* **95**(8): 4463-8.

Chen, Y. Z.*, et al.* (2004). DNA/RNA helicase gene mutations in a form of juvenile amyotrophic lateral sclerosis (ALS4). *Am J Hum Genet* **74**(6): 1128-35.

Choi, C. I.*, et al.* (2008). Effects of estrogen on lifespan and motor functions in female hSOD1 G93A transgenic mice. *J Neurol Sci* **268**(1-2): 40-7.

Chuang, S. M.*, et al.* (2005). Proteasome-mediated degradation of cotranslationally damaged proteins involves translation elongation factor 1A. *Mol Cell Biol* **25**(1): 403-13.

Condeelis, J. (1995). Elongation factor 1 alpha, translation and the cytoskeleton. *Trends Biochem Sci* **20**(5): 169-70.

Coovert, D. D.*, et al.* (1997). The survival motor neuron protein in spinal muscular atrophy. *Hum Mol Genet* **6**(8): 1205-14.

Cottrelle, P.*, et al.* (1985). Either one of the two yeast EF-1 alpha genes is required for cell viability. *Curr Genet* **9**(8): 693-7.

Cozzolino, M.*, et al.* (2008). Amyotrophic lateral sclerosis: from current developments in the laboratory to clinical implications. *Antioxid Redox Signal* **10**(3): 405-43.

Dal Canto, M. C. and M. E. Gurney (1995). Neuropathological changes in two lines of mice carrying a transgene for mutant human Cu,Zn SOD, and in mice overexpressing wild type human SOD: a model of familial amyotrophic lateral sclerosis (FALS). *Brain Res* **676**(1): 25-40.

Dalbello-Haas, V.*, et al.* (2008). Therapeutic exercise for people with amyotrophic lateral sclerosis or motor neuron disease. *Cochrane Database Syst Rev*(2): CD005229.

de Luca, C.*, et al.* (2005). Complete rescue of obesity, diabetes, and infertility in db/db mice by neuron-specific LEPR-B transgenes. *J Clin Invest* **115**(12): 3484-93.

Dennis, J. S. and B. A. Citron (2009). Wobbler mice modeling motor neuron disease display elevated transactive response DNA binding protein. *Neuroscience* **158**(2): 745-50.

Derventzi, A.*, et al.* (1993). Phorbol ester PMA stimulates protein synthesis and increases the levels of active elongation factors EF-1 alpha and EF-2 in ageing human fibroblasts. *Mech Ageing Dev* **69**(3): 193-205.

Dharmasaroja, P. (2007). The Role of eEF1A2 in the Pathogenesis of Motor Neurone Disease in Wasted Mice. *PhD Thesis*.

DiBernardo, A. B. and M. E. Cudkowicz (2006). Translating preclinical insights into effective human trials in ALS. *Biochim Biophys Acta* **1762**(11-12): 1139-49.

Dion, P. A.*, et al.* (2009). Genetics of motor neuron disorders: new insights into pathogenic mechanisms. *Nat Rev Genet* **10**(11): 769-82.

Doran, B.*, et al.* (2006). Deficiency of the zinc finger protein ZPR1 causes neurodegeneration. *Proc Natl Acad Sci U S A* **103**(19): 7471-5.

Duttaroy, A.*, et al.* (1998). Apoptosis rate can be accelerated or decelerated by overexpression or reduction of the level of elongation factor-1 alpha. *Exp Cell Res* **238**(1): 168-76.

Ejiri, S. (2002). Moonlighting functions of polypeptide elongation factor 1: from actin bundling to zinc finger protein R1-associated nuclear localization. *Biosci Biotechnol Biochem* **66**(1): 1-21.

Evgrafov, O. V.*, et al.* (2004). Mutant small heat-shock protein 27 causes axonal Charcot-Marie-Tooth disease and distal hereditary motor neuropathy. *Nat Genet* **36**(6): 602-6.

Fischer, L. R.*, et al.* (2004). Amyotrophic lateral sclerosis is a distal axonopathy: evidence in mice and man. *Exp Neurol* **185**(2): 232-40.

Forss-Petter, S.*, et al.* (1990). Transgenic mice expressing beta-galactosidase in mature neurons under neuron-specific enolase promoter control. *Neuron* **5**(2): 187-97.

Fujita, K.*, et al.* (1998). Increases in fragmented glial fibrillary acidic protein levels in the spinal cords of patients with amyotrophic lateral sclerosis. *Neurochem Res* **23**(2): 169-74.

Gangwani, L.*, et al.* (1998). Interaction of ZPR1 with translation elongation factor-1alpha in proliferating cells. *J Cell Biol* **143**(6): 1471-84.

Gangwani, L.*, et al.* (2001). Spinal muscular atrophy disrupts the interaction of ZPR1 with the SMN protein. *Nat Cell Biol* **3**(4): 376-83.

Gkogkas, C.*, et al.* (2008). VAPB interacts with and modulates the activity of ATF6. *Hum Mol Genet* **17**(11): 1517-26.

Greene, L. A. and A. S. Tischler (1976). Establishment of a noradrenergic clonal line of rat adrenal pheochromocytoma cells which respond to nerve growth factor. *Proc Natl Acad Sci U S A* **73**(7): 2424-8.

Greenway, M. J.*, et al.* (2006). ANG mutations segregate with familial and 'sporadic' amyotrophic lateral sclerosis. *Nat Genet* **38**(4): 411-3.

Groeneveld, G. J.*, et al.* (2004). Ovariectomy and 17beta-estradiol modulate disease progression of a mouse model of ALS. *Brain Res* **1021**(1): 128-31.

Gurney, M. E.*, et al.* (1994). Motor neuron degeneration in mice that express a human Cu,Zn superoxide dismutase mutation. *Science* **264**(5166): 1772-5.

Gustafsdottir, S. M.*, et al.* (2005). Proximity ligation assays for sensitive and specific protein analyses. *Anal Biochem* **345**(1): 2-9.

Hadano, S.*, et al.* (2001). A gene encoding a putative GTPase regulator is mutated in familial amyotrophic lateral sclerosis 2. *Nat Genet* **29**(2): 166-73.

Hall, T. A. (1999). BioEdit: a user-friendly biological sequence alignment editor and analysis program for Windows 95/98/NT *Nucleic Acids Symposium Series* **41**: 95-98.

Hartman, T. K.*, et al.* (2007). Mutant mice with small amounts of BubR1 display accelerated age-related gliosis. *Neurobiol Aging* **28**(6): 921-7.

Hasegawa, M.*, et al.* (2008). Phosphorylated TDP-43 in frontotemporal lobar degeneration and amyotrophic lateral sclerosis. *Ann Neurol* **64**(1): 60-70.

Hatayama, T.*, et al.* (1997). Reduced induction of HSP70 in PC12 cells during neuronal differentiation. *J Biochem* **122**(5): 904-10.

Heiman-Patterson, T. D.*, et al.* (2005). Background and gender effects on survival in the TgN(SOD1-G93A)1Gur mouse model of ALS. *J Neurol Sci* **236**(1-2): 1-7.

Helmken, C.*, et al.* (2003). Evidence for a modifying pathway in SMA discordant families: reduced SMN level decreases the amount of its interacting partners and Htra2-beta1. *Hum Genet* **114**(1): 11-21.

Hershey, J. W. (1991). Translational control in mammalian cells. *Annu Rev Biochem* **60**: 717-55.

Hu, C. D.*, et al.* (2002). Visualization of interactions among bZIP and Rel family proteins in living cells using bimolecular fluorescence complementation. *Mol Cell* **9**(4): 789-98.

Hwang, D. Y.*, et al.* (2002). Alterations in behavior, amyloid beta-42, caspase-3, and Cox-2 in mutant PS2 transgenic mouse model of Alzheimer's disease. *Faseb J* **16**(8): 805-13.

Inukai, Y.*, et al.* (2008). Abnormal phosphorylation of Ser409/410 of TDP-43 in FTLD-U and ALS. *FEBS Lett* **582**(19): 2899-904.

Irobi, J.*, et al.* (2004). Hot-spot residue in small heat-shock protein 22 causes distal motor neuropathy. *Nat Genet* **36**(6): 597-601.

Kahns, S.*, et al.* (1998). The elongation factor 1 A-2 isoform from rabbit: cloning of the cDNA and characterization of the protein. *Nucleic Acids Res* **26**(8): 1884-90.

Kalmar, B.*, et al.* (2008). Late stage treatment with arimoclomol delays disease progression and prevents protein aggregation in the SOD1 mouse model of ALS. *J Neurochem* **107**(2): 339-50.

Khacho, M.*, et al.* (2008). eEF1A is a novel component of the mammalian nuclear protein export machinery. *Mol Biol Cell* **19**(12): 5296-308.

Khalyfa, A.*, et al.* (2001). Characterization of elongation factor-1A (eEF1A-1) and eEF1A-2/S1 protein expression in normal and wasted mice. *J Biol Chem* **276**(25): 22915-22.

Khalyfa, A.*, et al.* (2003). Changes in protein levels of elongation factors, eEF1A-1 and eEF1A-2/S1, in long-term denervated rat muscle. *Restor Neurol Neurosci* **21**(1-2): 47-53.

Kieran, D.*, et al.* (2004). Treatment with arimoclomol, a coinducer of heat shock proteins, delays disease progression in ALS mice. *Nat Med* **10**(4): 402-5.

Kirkinezos, I. G.*, et al.* (2003). Regular exercise is beneficial to a mouse model of amyotrophic lateral sclerosis. *Ann Neurol* **53**(6): 804-7.

Knippenberg, S.*, et al.* (2010). Significance of behavioural tests in a transgenic mouse model of amyotrophic lateral sclerosis (ALS). *Behav Brain Res*.

Knudsen, S. M.*, et al.* (1993). Tissue-dependent variation in the expression of elongation factor-1 alpha isoforms: isolation and characterisation of a cDNA encoding a novel variant of human elongation-factor 1 alpha. *Eur J Biochem* **215**(3): 549-54.

Kohama, S. G.*, et al.* (1995). Increases of glial fibrillary acidic protein in the aging female mouse brain. *Neurobiol Aging* **16**(1): 59-67.

Kugel, J. F. and J. A. Goodrich (2006). Beating the heat: A translation factor and an RNA mobilize the heat shock transcription factor HSF1. *Mol Cell* **22**(2): 153-4.

Kunst, C. B., *et al.* (2000). Genetic mapping of a mouse modifier gene that can prevent ALS onset. *Genomics* **70**(2): 181-9.

Kwiatkowski, T. J., Jr., *et al.* (2009). Mutations in the FUS/TLS gene on chromosome 16 cause familial amyotrophic lateral sclerosis. *Science* **323**(5918): 1205-8.

Lagier-Tourenne, C. and D. W. Cleveland (2009). Rethinking ALS: the FUS about TDP-43. *Cell* **136**(6): 1001-4.

Laird, F. M., *et al.* (2008). Motor neuron disease occurring in a mutant dynactin mouse model is characterized by defects in vesicular trafficking. *J Neurosci* **28**(9): 1997-2005.

Landers, J. E., *et al.* (2008). A common haplotype within the PON1 promoter region is associated with sporadic ALS. *Amyotroph Lateral Scler* **9**(5): 306-14.

Larsen, J. O., *et al.* (2000). Does long-term physical exercise counteract age-related Purkinje cell loss? A stereological study of rat cerebellum. *J Comp Neurol* **428**(2): 213-22.

Le Sourd, F., *et al.* (2006). Cellular coexistence of two high molecular subsets of eEF1B complex. *FEBS Lett* **580**(11): 2755-60.

Lee, S., *et al.* (1994). Cloning of human and mouse brain cDNAs coding for S1, the second member of the mammalian elongation factor-1 alpha gene family: analysis of a possible evolutionary pathway. *Biochem Biophys Res Commun* **203**(3): 1371-7.

Lee, S., *et al.* (1992). Tissue-specific expression in mammalian brain, heart, and muscle of S1, a member of the elongation factor-1 alpha gene family. *J Biol Chem* **267**(33): 24064-8.

Lee, S., *et al.* (1995). Terminal differentiation-dependent alteration in the expression of translation elongation factor-1 alpha and its sister gene, S1, in neurons. *Exp Cell Res* **219**(2): 589-97.

Lee, S., *et al.* (1993). Differential expression of S1 and elongation factor-1 alpha during rat development. *J Biol Chem* **268**(32): 24453-9.

Leegwater, P. A., *et al.* (2001). Subunits of the translation initiation factor eIF2B are mutant in leukoencephalopathy with vanishing white matter. *Nat Genet* **29**(4): 383-8.

Lefebvre, S., *et al.* (1995). Identification and characterization of a spinal muscular atrophy-determining gene. *Cell* **80**(1): 155-65.

Lefebvre, S., *et al.* (1997). Correlation between severity and SMN protein level in spinal muscular atrophy. *Nat Genet* **16**(3): 265-9.

Leigh, P. N., *et al.* (1988). Ubiquitin deposits in anterior horn cells in motor neurone disease. *Neurosci Lett* **93**(2-3): 197-203.

Leigh, P. N., *et al.* (1991). Ubiquitin-immunoreactive intraneuronal inclusions in amyotrophic lateral sclerosis. Morphology, distribution, and specificity. *Brain* **114 (Pt 2)**: 775-88.

Li, X., *et al.* (2009). Mutant copper-zinc superoxide dismutase associated with amyotrophic lateral sclerosis binds to adenine/uridine-rich stability elements in the vascular endothelial growth factor 3'-untranslated region. *J Neurochem* **108**(4): 1032-44.

Liu, J., *et al.* (2005). Elevation of the Hsp70 chaperone does not effect toxicity in mouse models of familial amyotrophic lateral sclerosis. *J Neurochem* **93**(4): 875-82.

Loh, D. (2003). Analysis of the role of eukaryotic elongation factor 1 alpha-2 (eEF1A-2) in the Wasted mouse mutant. *PhD Thesis*.

Lowenstein, D. H., *et al.* (1991). The stress protein response in cultured neurons: characterization and evidence for a protective role in excitotoxicity. *Neuron* **7**(6): 1053-60.

Lu, L., *et al.* (2007). Mutant Cu/Zn-superoxide dismutase associated with amyotrophic lateral sclerosis destabilizes vascular endothelial growth factor mRNA and downregulates its expression. *J Neurosci* **27**(30): 7929-38.

Ludolph, A. C., *et al.* (2010). Guidelines for preclinical animal research in ALS/MND: A consensus meeting. *Amyotroph Lateral Scler* **11**(1-2): 38-45.

Ludolph, A. C. and A. D. Sperfeld (2005). Preclinical trials--an update on translational research in ALS. *Neurodegener Dis* **2**(3-4): 215-9.

Lund, A., *et al.* (1996). Assignment of human elongation factor 1alpha genes: EEF1A maps to chromosome 6q14 and EEF1A2 to 20q13.3. *Genomics* **36**(2): 359-61.

Lutsep, H. L. and M. Rodriguez (1989). Ultrastructural, morphometric, and immunocytochemical study of anterior horn cells in mice with "wasted" mutation. *J Neuropathol Exp Neurol* **48**(5): 519-33.

Mackenzie, I. R., *et al.* (2007). Pathological TDP-43 distinguishes sporadic amyotrophic lateral sclerosis from amyotrophic lateral sclerosis with SOD1 mutations. *Ann Neurol* **61**(5): 427-34.

Maddatu, T. P., *et al.* (2004). Transgenic rescue of neurogenic atrophy in the nmd mouse reveals a role for Ighmbp2 in dilated cardiomyopathy. *Hum Mol Genet* **13**(11): 1105-15.

Mansilla, F., *et al.* (2002). Mapping the human translation elongation factor eEF1H complex using the yeast two-hybrid system. *Biochem J* **365**(Pt 3): 669-76.

Markowitz, J. A., *et al.* (2004). Spinal muscular atrophy in the neonate. *J Obstet Gynecol Neonatal Nurs* **33**(1): 12-20.

Mercado, P. A., *et al.* (2005). Depletion of TDP 43 overrides the need for exonic and intronic splicing enhancers in the human apoA-II gene. *Nucleic Acids Res* **33**(18): 6000-10.

Merrick, W. C., Nyborg, J. (2000). The protein biosynthesis elongation cycle. In Translational Control of Gene Expression. Cold Sping Harbor Laboratory Press, Cold Spring Harbor, NY.**:** 89-125.

Messer, A., *et al.* (1999). An early-onset congenic strain of the motor neuron degeneration (mnd) mouse. *Mol Genet Metab* **66**(4): 393-7.

Migheli, A., *et al.* (1999). S-100beta protein is upregulated in astrocytes and motor neurons in the spinal cord of patients with amyotrophic lateral sclerosis. *Neurosci Lett* **261**(1-2): 25-8.

Mishra, A. K., *et al.* (2007). Structural insights into the interaction of the evolutionarily conserved ZPR1 domain tandem with eukaryotic EF1A, receptors, and SMN complexes. *Proc Natl Acad Sci U S A* **104**(35): 13930-5.

Mitsumoto, H. and W. G. Bradley (1982). Murine motor neuron disease (the wobbler mouse): degeneration and regeneration of the lower motor neuron. *Brain* **105 (Pt 4)**: 811-34.

Miura, P., *et al.* (2010). The utrophin A 5'-UTR drives cap-independent translation exclusively in skeletal muscles of transgenic mice and interacts with eEF1A2. *Hum Mol Genet* **19**(7): 1211-20.

Moisse, K., *et al.* (2009a). Cytosolic TDP-43 expression following axotomy is associated with caspase 3 activation in NFL-/- mice: support for a role for TDP-43 in the physiological response to neuronal injury. *Brain Res* **1296**: 176-86.

Moisse, K., *et al.* (2009b). Divergent patterns of cytosolic TDP-43 and neuronal progranulin expression following axotomy: implications for TDP-43 in the physiological response to neuronal injury. *Brain Res* **1249**: 202-11.

Morimoto, R. I. (1998). Regulation of the heat shock transcriptional response: cross talk between a family of heat shock factors, molecular chaperones, and negative regulators. *Genes Dev* **12**(24): 3788-96.

Mosser, D. D. and R. I. Morimoto (2004). Molecular chaperones and the stress of oncogenesis. *Oncogene* **23**(16): 2907-18.

Mouton, P. R., *et al.* (2002). Age and gender effects on microglia and astrocyte numbers in brains of mice. *Brain Res* **956**(1): 30-5.

Muchowski, P. J. and J. L. Wacker (2005). Modulation of neurodegeneration by molecular chaperones. *Nat Rev Neurosci* **6**(1): 11-22.

Mullen, R. J., *et al.* (1992). NeuN, a neuronal specific nuclear protein in vertebrates. *Development* **116**(1): 201-11.

Munoz, D. G., *et al.* (1988). Accumulation of phosphorylated neurofilaments in anterior horn motoneurons of amyotrophic lateral sclerosis patients. *J Neuropathol Exp Neurol* **47**(1): 9-18.

Murray, J. W., *et al.* (1996). Bundling of actin filaments by elongation factor 1 alpha inhibits polymerization at filament ends. *J Cell Biol* **135**(5): 1309-21.

Murray, L. M., *et al.* (2008). Loss of translation elongation factor (eEF1A2) expression in vivo differentiates between Wallerian degeneration and dying-back neuronal pathology. *J Anat* **213**(6): 633-45.

Nagy, D.*, et al.* (1994). Reactive astrocytes are widespread in the cortical gray matter of amyotrophic lateral sclerosis. *J Neurosci Res* **38**(3): 336-47.

Neumann, M.*, et al.* (2006). Ubiquitinated TDP-43 in frontotemporal lobar degeneration and amyotrophic lateral sclerosis. *Science* **314**(5796): 130-3.

Newbery, H. J. (2003). The role of eEF1A-2 in the pathogenesis of Motor Neuron Disease. *PhD Thesis*.

Newbery, H. J.*, et al.* (2005). Progressive loss of motor neuron function in wasted mice: effects of a spontaneous null mutation in the gene for the eEF1 A2 translation factor. *J Neuropathol Exp Neurol* **64**(4): 295-303.

Newbery, H. J.*, et al.* (2007). Translation elongation factor eEF1A2 is essential for post-weaning survival in mice. *J Biol Chem* **282**(39): 28951-9.

Nishimura, A. L.*, et al.* (2004). A mutation in the vesicle-trafficking protein VAPB causes late-onset spinal muscular atrophy and amyotrophic lateral sclerosis. *Am J Hum Genet* **75**(5): 822-31.

O'Callaghan, J. P. and D. B. Miller (1991). The concentration of glial fibrillary acidic protein increases with age in the mouse and rat brain. *Neurobiol Aging* **12**(2): 171-4.

Oosthuyse, B.*, et al.* (2001). Deletion of the hypoxia-response element in the vascular endothelial growth factor promoter causes motor neuron degeneration. *Nat Genet* **28**(2): 131-8.

Ou, S. H.*, et al.* (1995). Cloning and characterization of a novel cellular protein, TDP-43, that binds to human immunodeficiency virus type 1 TAR DNA sequence motifs. *J Virol* **69**(6): 3584-96.

Pan, J.*, et al.* (2004). Immuno-characterization of the switch of peptide elongation factors eEF1A-1/EF-1alpha and eEF1A-2/S1 in the central nervous system during mouse development. *Brain Res Dev Brain Res* **149**(1): 1-8.

Pape, T.*, et al.* (1998). Complete kinetic mechanism of elongation factor Tu-dependent binding of aminoacyl-tRNA to the A site of the E. coli ribosome. *Embo J* **17**(24): 7490-7.

Pasinelli, P. and R. H. Brown (2006). Molecular biology of amyotrophic lateral sclerosis: insights from genetics. *Nat Rev Neurosci* **7**(9): 710-23.

Patani, R.*, et al.* (2011). Retinoid-independent motor neurogenesis from human embryonic stem cells reveals a medial columnar ground state. *Nat Commun* **2**: 214.

Patel, Y. J.*, et al.* (2005). Hsp27 and Hsp70 administered in combination have a potent protective effect against FALS-associated SOD1-mutant-induced cell death in mammalian neuronal cells. *Brain Res Mol Brain Res* **134**(2): 256-74.

Pellizzoni, L.*, et al.* (1998). A novel function for SMN, the spinal muscular atrophy disease gene product, in pre-mRNA splicing. *Cell* **95**(5): 615-24.

Puls, I.*, et al.* (2003). Mutant dynactin in motor neuron disease. *Nat Genet* **33**(4): 455-6.

Robertson, J.*, et al.* (2007). Lack of TDP-43 abnormalities in mutant SOD1 transgenic mice shows disparity with ALS. *Neurosci Lett* **420**(2): 128-32.

Rodnina, M. V.*, et al.* (1997). Hydrolysis of GTP by elongation factor G drives tRNA movement on the ribosome. *Nature* **385**(6611): 37-41.

Rosen, D. R.*, et al.* (1993). Mutations in Cu/Zn superoxide dismutase gene are associated with familial amyotrophic lateral sclerosis. *Nature* **362**(6415): 59-62.

Rotimi, C. N.*, et al.* (2004). A genome-wide search for type 2 diabetes susceptibility genes in West Africans: the Africa America Diabetes Mellitus (AADM) Study. *Diabetes* **53**(3): 838-41.

Ruest, L. B.*, et al.* (2002). Peptide elongation factor eEF1A-2/S1 expression in cultured differentiated myotubes and its protective effect against caspase-3-mediated apoptosis. *J Biol Chem* **277**(7): 5418-25.

Sasaki, S. (2010). Endoplasmic reticulum stress in motor neurons of the spinal cord in sporadic amyotrophic lateral sclerosis. *J Neuropathol Exp Neurol* **69**(4): 346-55.

Saxena, S. K.*, et al.* (1992). Angiogenin is a cytotoxic, tRNA-specific ribonuclease in the RNase A superfamily. *J Biol Chem* **267**(30): 21982-6.

Schmidt, E. K.*, et al.* (2009). SUnSET, a nonradioactive method to monitor protein synthesis. *Nat Methods* **6**(4): 275-7.

Selkoe, D. J. (2001). Alzheimer's disease results from the cerebral accumulation and cytotoxicity of amyloid beta-protein. *J Alzheimers Dis* **3**(1): 75-80.

Shamovsky, I.*, et al.* (2006). RNA-mediated response to heat shock in mammalian cells. *Nature* **440**(7083): 556-60.

Sharp, P.*, et al.* (2006). Heat shock protein 27 rescues motor neurons following nerve injury and preserves muscle function. *Exp Neurol* **198**(2): 511-8.

Sharp, P. S.*, et al.* (2008). Protective effects of heat shock protein 27 in a model of ALS occur in the early stages of disease progression. *Neurobiol Dis* **30**(1): 42-55.

Shaw, P. J. and C. J. Eggett (2000). Molecular factors underlying selective vulnerability of motor neurons to neurodegeneration in amyotrophic lateral sclerosis. *J Neurol* **247 Suppl 1**: I17-27.

Shi, Y.*, et al.* (1998). Molecular chaperones as HSF1-specific transcriptional repressors. *Genes Dev* **12**(5): 654-66.

Shim, S. B.*, et al.* (2007). Tau overexpression in transgenic mice induces glycogen synthase kinase 3beta and beta-catenin phosphorylation. *Neuroscience* **146**(2): 730-40.

Shultz, L. D.*, et al.* (1982). 'Wasted', a new mutant of the mouse with abnormalities characteristic to ataxia telangiectasia. *Nature* **297**(5865): 402-4.

Silver, L. M. (1995). Mouse genetics: concepts and applications.

Slobin, L. I. (1980). The role of eucaryotic factor Tu in protein synthesis. The measurement of the elongation factor Tu content of rabbit reticulocytes and other mammalian cells by a sensitive radioimmunoassay. *Eur J Biochem* **110**(2): 555-63.

Smeitink, J. A.*, et al.* (2006). Distinct clinical phenotypes associated with a mutation in the mitochondrial translation elongation factor EFTs. *Am J Hum Genet* **79**(5): 869-77.

Spillantini, M. G.*, et al.* (1997). Alpha-synuclein in Lewy bodies. *Nature* **388**(6645): 839-40.

Strong, M. J.*, et al.* (2007). TDP43 is a human low molecular weight neurofilament (hNFL) mRNA-binding protein. *Mol Cell Neurosci* **35**(2): 320-7.

Takeuchi, H.*, et al.* (2002). Hsp70 and Hsp40 improve neurite outgrowth and suppress intracytoplasmic aggregate formation in cultured neuronal cells expressing mutant SOD1. *Brain Res* **949**(1-2): 11-22.

Tan, C. F.*, et al.* (2007). TDP-43 immunoreactivity in neuronal inclusions in familial amyotrophic lateral sclerosis with or without SOD1 gene mutation. *Acta Neuropathol* **113**(5): 535-42.

Thompson, J. D.*, et al.* (1994). CLUSTAL W: improving the sensitivity of progressive multiple sequence alignment through sequence weighting, position-specific gap penalties and weight matrix choice. *Nucleic Acids Res* **22**(22): 4673-80.

Tomlinson, V. (2007). The putative oncogene *EEF1A2* and its role in breast and ovarian cancer. *PhD Thesis*.

Tomlinson, V. A.*, et al.* (2005). Translation elongation factor eEF1A2 is a potential oncoprotein that is overexpressed in two-thirds of breast tumours. *BMC Cancer* **5**: 113.

Tovar, Y. R. L. B.*, et al.* (2009). Experimental models for the study of neurodegeneration in amyotrophic lateral sclerosis. *Mol Neurodegener* **4**: 31.

Tudor, E. L.*, et al.* (2010). Amyotrophic lateral sclerosis mutant vesicle-associated membrane protein-associated protein-B transgenic mice develop TAR-DNA-binding protein-43 pathology. *Neuroscience* **167**(3): 774-85.

Turner, B. J.*, et al.* (2008). TDP-43 expression in mouse models of amyotrophic lateral sclerosis and spinal muscular atrophy. *BMC Neurosci* **9**: 104.

van Praag, H.*, et al.* (1999). Running increases cell proliferation and neurogenesis in the adult mouse dentate gyrus. *Nat Neurosci* **2**(3): 266-70.

Vance, C.*, et al.* (2009). Mutations in FUS, an RNA processing protein, cause familial amyotrophic lateral sclerosis type 6. *Science* **323**(5918): 1208-11.

Veldink, J. H.*, et al.* (2003). Sexual differences in onset of disease and response to exercise in a transgenic model of ALS. *Neuromuscul Disord* **13**(9): 737-43.

Voellmy, R. (2004). On mechanisms that control heat shock transcription factor activity in metazoan cells. *Cell Stress Chaperones* **9**(2): 122-33.

Wain, L. V.*, et al.* (2009). The role of copy number variation in susceptibility to amyotrophic lateral sclerosis: genome-wide association study and comparison with published loci. *PLoS One* **4**(12): e8175.

Wang, I. F.*, et al.* (2002). Higher order arrangement of the eukaryotic nuclear bodies. *Proc Natl Acad Sci U S A* **99**(21): 13583-8.

Wang, I. F.*, et al.* (2008a). TDP-43, the signature protein of FTLD-U, is a neuronal activity-responsive factor. *J Neurochem* **105**(3): 797-806.

Wang, X.*, et al.* (2008b). Induced ncRNAs allosterically modify RNA-binding proteins in cis to inhibit transcription. *Nature* **454**(7200): 126-30.

Watanabe, M.*, et al.* (2001). Histological evidence of protein aggregation in mutant SOD1 transgenic mice and in amyotrophic lateral sclerosis neural tissues. *Neurobiol Dis* **8**(6): 933-41.

Weber, U. J.*, et al.* (1997). Total number and size distribution of motor neurons in the spinal cord of normal and EMC-virus infected mice--a stereological study. *J Anat* **191 (Pt 3)**: 347-53.

Wong, P. C.*, et al.* (1995). An adverse property of a familial ALS-linked SOD1 mutation causes motor neuron disease characterized by vacuolar degeneration of mitochondria. *Neuron* **14**(6): 1105-16.

Xu, Z. P.*, et al.* (2002). The nuclear function of angiogenin in endothelial cells is related to rRNA production. *Biochem Biophys Res Commun* **294**(2): 287-92.

Yang, L.*, et al.* (1998). Oncoprotein TLS interacts with serine-arginine proteins involved in RNA splicing. *J Biol Chem* **273**(43): 27761-4.

Yang, Y.*, et al.* (2001). The gene encoding alsin, a protein with three guanine-nucleotide exchange factor domains, is mutated in a form of recessive amyotrophic lateral sclerosis. *Nat Genet* **29**(2): 160-5.

Yeo, G.*, et al.* (2004). Variation in alternative splicing across human tissues. *Genome Biol* **5**(10): R74.

Zinszner, H.*, et al.* (1997). TLS (FUS) binds RNA in vivo and engages in nucleo-cytoplasmic shuttling. *J Cell Sci* **110 (Pt 15)**: 1741-50.